POLITECNICO DI MILANO

Scuola di Ingegneria Edile - Architettura
Corso di Laurea in Ingegneria dei Sistemi Edilizi

Self-Healing Capacity of Fiber Reinforced Concretes with Different Additions

Relatore: Prof. Ing. Liberato FERRARA
Co-Relatore: Prof. Ing. Ravindra GETTU

Tesi di Laurea Specialistica di:

Isaia ALBERTINI
Matricola 783907

Anno Accademico 2013/2014

Summary

Abstract 12
1. Introduction 13
1.1. Background of the work 13
1.2. Aim of the research 14
1.3. Summary of the contents 15
2. Background of research 16
2.1. Introduction 16
2.2. Deterioration of concrete structures 16
2.3. Self-healing properties of concrete 20
2.4. Terminology 20
2.5. Mechanisms 22
2.5.1. Crystallization of calcium carbonate 22
2.5.2. Continuing hydration 23
2.5.3. Sedimentation of particles 24
2.5.4. Swelling of the cement matrix 25
2.5.5. Factors influencing self-healing 25
2.5.6. Mix constituents 25
2.5.7. Presence of water and water type 25
2.5.8. Water pressure 26
2.5.9. Water pH 27
2.5.10. Water temperature 27
2.5.11. Crack width 28
2.5.12. Stability of the crack 29
2.6. Mechanical properties of healed cracks 29
2.7. Concrete incorporating admixtures 31
2.7.1. Concrete incorporating fly ash 31
2.7.2. Concrete incorporating chemical admixtures, expansive agents and geomaterials 32
2.7.3. Pros and cons 34

2.8. Bioconcrete ... *35*
2.8.1. Degradation of urea ... 35
2.8.2. Calcium lactate-based bacteria ... 37
2.8.3. Effect of bacteria cells and walls on concrete strength ... 39
2.8.4. Pros and cons ... 40
2.9. Fiber reinforced concretes ... *41*
2.9.1. Self-healing capacity of FRC ... 42
2.9.2. Self-healing capacity of ECC and HPFRCC ... 43
2.9.3. Natural fibers to enhance the performances and healing capacities of concrete ... 45
2.9.4. Pros and cons ... 47
2.10. Concretes employing polymers ... *48*
2.10.1. Concretes with the addition of polymers in emulsion ... 48
2.10.2. Sap-modified concrete ... 50
2.10.3. Pros and cons ... 53
2.11. Concrete with capsules ... *54*
2.11.1. Autonomic healing in encapsulated materials ... 55
2.11.2. Survival to the mixing process ... 55
2.11.3. Influence on mechanical properties and workability ... 56
2.11.4. Compatibility with the healing agent and the cement matrix ... 56
2.11.5. Probability and release efficiency of the capsules and healable crack volume ... 57
2.11.6. Classification of encapsulated materials ... 59
2.11.7. Vascular systems: engineered healing systems ... 61
2.11.8. Vascular systems: engineered activated-repairing systems ... 63
2.11.9. Pros and cons ... 65
2.12. Conclusions ... *66*
3. Experimental Program ... 67
3.1. Introduction ... *67*
3.2. Summary of the experimentation ... *68*
3.2.1. Application of compressive stress ... 71
3.3. Characteristics of the employed materials ... *72*
3.3.1. Constituents of concrete ... 72
3.3.2. Characteristics and effect of steel fibers ... 73
3.3.3. Characteristics and effect of Penetron ... 73
3.3.4. Characteristics and effect of SBR-latex ... 74
3.4. Fabrication of the specimens ... *75*

3.4.1. Standard properties of the concrete ... 76
3.5. Performed tests ... 77
3.5.1. Compressive test ... 77
3.5.2. Three point bending test ... 77
3.5.3. UPV tests ... 80
3.5.4. Permeability test ... 82
3.6. Conclusions ... 83
4. Discussion of Results ... 84
4.1. Introduction ... 84
4.2. Material characterization ... 84
4.2.1. Compressive test results ... 84
4.2.2. Bending test results ... 87
4.3. Bending behaviour and self-healing properties of the specimens ... 89
4.3.1. precracking phase ... 89
4.3.2. CMOD 600 µm - reloading after 30 days ... 91
4.3.3. CMOD 600 µm - reloading after 90 days ... 95
4.3.4. CMOD 600 µm - reloading after 270 days ... 98
4.3.5. CMOD 4000 µm: reloading after 30 days ... 101
4.3.6. CMOD 4000 µm: reloading after 90 days ... 104
4.3.7. CMOD 4000 µm: reloading after 270 days ... 107
4.3.8. Choosing a measure for self-healing ... 108
4.3.9. Evaluation of self-healing: CMOD 600 µm ... 110
4.3.10. Evaluation of self healing: CMOD 4000 µm ... 122
4.4. Conclusions ... 128
4.4.1. Discussion of some critical points ... 130
5. Conclusions ... 131
5.1. Recommendations for the future ... 134
5.1.1. Improvement of the present work ... 134
5.1.2. Different concrete admixtures ... 134
5.1.3. Other properties of healed cracks ... 134
Bibliography ... 135
A. Appendix ... A-1
A.1. Compressive tests result ... A-1
A.2. Design of the compressive setup ... A-5
A.3. Design of the bending-tensile setup ... A-9

A.4. Three point bending test results: 600 µm A-14

A.5. Three point bending test results: 4000 µm A-17

A.6. Weather conditions in Chennai A-20

A.7. Weather conditions in Milan A-25

List of figures

Figure 1: performance (on the left) and cost (on the right) with elapse of time for normal (A) and high quality (B) structures by Van Breugel. Direct cost of repair included. Interests and inflation ignored. 18
Figure 2: performance (on the left) and cost (on the right) with elapse of time for a structure made of self-healing concrete by Van Breugel. Direct cost of repair included. Interests and inflation ignored. 18
Figure 3: computed service life (a) and life cycle cost (b) showing the effect of self-healing by Li. The "construction cost" here, refers to mainly the initial material cost..... 19
Figure 4: definition of self-healing/repairing concrete by JCI..... 21
Figure 5: definition of self-healing/repairing concrete by Mihashi and Nishiwaki..... 21
Figure 6: possible causes of self-healing: (a) formation of calcium carbonate or calcium hydroxyde, (b) sedimentation of particles, (c) continued hydration, (d) swelling of the cement matrix by Ter Heide 22
Figure 7: interfaces and reactions in $CaCo_3$ - CO_2 - H_2O system by Edvardsen 23
Figure 8: *permeability versus extent of hydration by Hearn and Morley*..... 23
Figure 9: *Glanville's permeanility curves from Hearn and Morley showing the effect of flow reversal on sandstone and concrete: a) effect of reversal direction of flow in a sandstone specime: permeability increases after each reversaln; b) effect of reversal flow direction in a concrete specimen: there is only a slight increase of permeability after the reversal; physical clogging is not responsible of permanent healing* 24
Figure 10: example of flow-through quantities after a 2 years test period by Ramm and Biscoping..... 27
Figure 11: decrease of the normalized flow rate because of the self-healing of the crack for HPC at various temperatures and a pressure gradient of 1 MPa/m and a crack width of 0.05 m, by Rehinardt and Jooss... 28
Figure 12: relationship between water flow and time for different crack widths by Edvardsen..... 28
Figure 13: relationship between flow and time for active cracks by Edvardsen 29
Figure 14: SEM cross-section picture for concrete after self-healing: (a) normal cement concrete; (b) concrete specimen with 30% slag; (c) concrete specimen with 40% fly ash by Zhou et al. 32
Figure 15: self-healed re-hydration products in crack by hydrogarnet phases C-A-H and calcite phases by kishi and Ahn 33
Figure 16: developing of calcite crystals at higher magnification by Siddique and Chahal. Rod-shaped objects, consistent with the dimensions of Bacillus Pasteurii are spread around the crystals...... 37
Figure 17: cement stone specimens with incorporating healing agent by Jonkers (B. Cohnii spores plus calcium lactate), cracked after 7 (panels A: 250x and B: 1000x) and 28 days curing (panels C: 500x and D: 2000x). the large mineral precipitatesvisible on the surface of the younger specimens seem to be due to the conversion of calcium lactate by bacteria. The small precipitates on older specimens surface resemble those produced by abiotic specimens..... 38
Figure 18: at the left: type of failure in cementicious materials; at the right: typical behaviour of ECC. Picture by Antonopoulos..... 41

Figure 19: at the left: partial crack healing in an ECC with PVA fibers by Antonopoulos. The scale bar has a height of 20 µm; at the right: bridging effect of PVA fibers by Antonopoulos 45
Figure 20: self-repairing by modification of concrete using an epoxy resin without hardener 49
Figure 21: cross-linking of epoxy resin in presence of calcium hydroxide by Lukowski and Adamczewski 49
Figure 22: polymer film in epoxy cement composite by Lukowski and Adamczewski 50
Figure 23: schematic showing potential mechanisms of self-sealing cracks using SAP by Lee 51
Figure 24: formation of $CaCO_3$ domes on the sample surface after shrinking of SAPs by Snoeck. The height of the scale bar is 500 µm 51
Figure 25: (a) basic method of the microcapsule approach: (i) cracks form in the matrix; (ii) the cracks rupture the microcapsules, releasing the healing agent through capillary action; (iii) the healing agent contract the catalyst, triggering polymerization thus ensuring the closure of the nearby cracks and (b) ESEM image showing a ruptured microcapsule. Image by Van Tittelboom and D Belie 54
Figure 26: (a) hollow glass fibers and (b) damage visual enhancement in composite laminate by the bleeding action of a fluorescent dye from hollow glass fibers. Image by Van Tittelboom and De Belie 55
Figure 27: schematic illustration of the forces acting on an internally encapsulated healing agent 58
Figure 28: calculated average released volume as function of the capsules concentration for different values of aspect ratio 59
Figure 29: morphology of the diatomaceous earth powders 60
Figure 30: vascular based self-healing approache, reported by Van Tittelboom. Leakage of the healing agent from the tank via the vascular into the crack due to gravitational and capillary forces and eventual (hydrostatic) pressure. One channel (A) and multiple channel vascular systems (B). 61
Figure 31: general concept proposed by Sangadji and Schlangen, which make use of porous network concrete 62
Figure 32: schematic diagram of self-diagnosis composite structure by Mihashi and Nishiwaki 63
Figure 33: schematic illustration of activated repairing system by Nishiwaki and Mihashi 64
Figure 34: resume of the specimens casted in India. For each of them three point bending, UPV and low permeability tests were performed. Three samples per batch were tested after different conditioning periods 69
Figure 35: resume of the specimens casted in Italy. For each of them three point bending tests were performed. Three samples per batch were tested after different conditioning periods 70
Figure 36: setup designed for the application of compression 71
Figure 37: three-point bending test set up 78
Figure 38: different locations considered in performing the UPV tests 80
Figure 39: new location considered in performing the UPV test 81
Figure 40: water leakage test setup by Schlangen 82
Figure 41: water leakage setup realized 82
Figure 42: representation of the obtained results in comparison with the EC2 hardening law of concrete ... 86
Figure 43: average flexural behaviour of the samples of each tested batch of specimens, subjected to three point bending test 28 days after casting. After the first softening branch, a hardening is performed by Indian FRC samples both with and without crystallizing agent. 89
Figure 44: level of crack sealing after 30 days of conditioning for specimens precracked up to 600 µm 91
Figure 45: average behaviour during precracking up to 600 µm of virgin FRC specimens casted in India and reloading after 30 days. The residual load of precracking is recovered only at CMOD 1500 µm 92
Figure 46: average behaviour during precracking up to 600 µm of virgin Indian FRC specimens containing Penetron and reloading after 30 days. The residual load of precracking is recovered only at CMOD 1500 µm, but load bearing capacity increases up to 2000-2500 µm 92

Figure 47: average behaviour during precracking up to 600 µm of virgin latex-modified FRC specimens and reloading after 30 days. Any hardening behaviour is highlighted..... 93
Figure 48: average behaviour during precracking up to 600 µm of virgin FRC specimens casted in Italy and reloading after 30 days. The reloading curve seems a natural prosecution of the precracking curve..... 93
Figure 49: behaviour during precracking up to 600 µm of virgin Italian FRC specimens containing Penetron and reloading after 30 days. The peak load of reloading overtakes significantly the residual load of precracking, in contrast with the average softening behaviour performed by the samples..... 94
Figure 50: level of crack sealing after 90 days of conditioning for specimens precracked up to 600 µm 95
Figure 51: average behaviour of plain concrete samples subjected to three point bending test after 90 days. Any particular recovery happened, but samples were strong enough to be tested..... 96
Figure 52: average behaviour during precracking up to 600 µm of virgin FRC specimens casted in India and reloading after 90 days. The graph highlights a slight increase in stiffness and strength in comparison with the tests at 30 days..... 96
Figure 53: average behaviour during precracking up to 600 µm of virgin FRC Indian specimens containing Penetron and reloading after 90 days. The graph highlights a slight increase in stiffness and strength in comparison with the tests at 30 days..... 97
Figure 54: average behaviour during precracking up to 600 µm of virgin latex-modified FRC specimens and reloading after 90 day . The graph highlights an increase in initial stiffness in comparison with the tests at 30 days. A slight hardening is showed..... 97
Figure 55: average behaviour during precracking up to 600 µm of virgin FRC specimens casted in India and FRCreloading after 270 days. 99
Figure 56: average behaviour during precracking up to 600 µm of virgin FRC specimens casted in India with Penetron and reloading after 270 days 99
Figure 57: average behaviour during precracking up to 600 µm of virgin latex-modified FRC specimens and reloading after 270 days..... 100
Figure 58: level of crack sealing after 30 days of conditioning for specimens precracked up to 4000 µm ... 101
Figure 59: average behaviour during precracking up to 4000 µm of virgin FRC specimens casted in India and reloading after 30 days...... 102
Figure 60: average behaviour during precracking up to 4000 µm of virgin FRC specimens casted in India with crystallizing agent and reloading after 30 days. 102
Figure 61: average behaviour during precracking up to 4000 µm of virgin latex-modified FRC specimens casted in India and reloading after 30 days. 103
Figure 62: level of crack sealing after 90 days of conditioning for specimens precracked up to 4000 µm .. 104
Figure 63: average behaviour during precracking up to 4000 µm of virgin FRC specimens casted in India and reloading after 90 days...... 105
Figure 64: average behaviour during precracking up to 4000 µm of virgin FRC specimens casted in India with crystallizing agent and reloading after 90 days. 106
Figure 65: average behaviour during precracking up to 4000 µm of virgin latex-modified FRC specimens casted in India and reloading after 90 days. 106
Figure 66: average behaviour during precracking up to 4000 µm of virgin FRC specimens casted in India and reloading after 270 days...... 107
Figure 67: Precracking and reloading after 30 days of an Indian FRC sample. By comparing the precracking and reloading curves, the self-healing can be evaluated. If any healing takes place, the peak load of reloading is higher than the residual load of precracking. 108
Figure 68: self-healing is evaluated as difference between the load corresponding to CMOD 1500 µm during reloading and the residual load of precracking. To this latter is added the contribution of softening (or

hardening), calculated on the average curve of precracking. Global self-healing is expressed by the green line 109
Figure 69: percentage strength recovery of FRC samples precracked at CMOD 600 µm and reloaded after 30 days of conditioning 111
Figure 70: evaluation of the self-healing after 30 days of conditioning on FRC samples casted in India without the addition of crystallizing agent. 112
Figure 71: evaluation of the self-healing after 30 days of conditioning on FRC samples casted in India with the addition of crystallizing agent. 112
Figure 72: evaluation of the self-healing after 30 days of conditioning on latex-modified FRC samples casted in India 113
Figure 73: percentage strength recovery of FRC samples casted in Italy and precracked at CMOD 600 µm and reloaded after 30 days of conditioning, in comparison with the corresponding Indian results 114
Figure 74: evaluation of the self-healing after 30 days of conditioning on FRC samples casted in Italy without the addition of crystallizing agent. 115
Figure 75: evaluation of the self-healing after 30 days of conditioning on FRC samples casted in Italy with the addition of crystallizing agent. 115
Figure 76: percentage strength recovery of FRC samples precracked at CMOD 600 µm after 90 days of conditioning 116
Figure 77: evaluation of the self-healing after 90 days of conditioning on FRC samples casted in India without the addition of crystallizing agent. 117
Figure 78 evaluation of the self-healing after 90 days of conditioning on FRC samples casted in India with the addition of crystallizing agent. 118
Figure 79 evaluation of the self-healing after 90 days of conditioning on latex-modified FRC samples casted in India 118
Figure 80: percentage strength recovery of FRC samples precracked at CMOD 600 µm after 270 days of conditioning 119
Figure 81 *evaluation of the self-healing after 270 days of conditioning on FRC samples casted in India without the addition of crystallizing agent.* 120
Figure 82: evaluation of the self-healing after 270 days of conditioning on FRC samples casted in India with the addition of crystallizing agent. 121
Figure 83: evaluation of the self-healing after 270 days of conditioning on latex-modified FRC samples casted in India 121
Figure 84 percentage strength recovery of FRC samples precracked at CMOD 4000 µm after 30 days of conditioning 122
Figure 85: evaluation of the self-healing after 30 days of conditioning on FRC samples casted in India without the addition of crystallizing agent 123
Figure 86: evaluation of the self-healing after 30 days of conditioning on FRC samples casted in India with the addition of crystallizing agent 124
Figure 87: *evaluation of the self-healing after 30 days of conditioning on latex-modified FRC samples casted in India* 124
Figure 88: percentage strength recovery of FRC samples precracked at CMOD 4000 µm after 90 days of conditioning 125
Figure 89: evaluation of the self-healing after 90 days of conditioning on FRC samples casted in India without the addition of crystallizing agent 126
Figure 90: evaluation of the self-healing after 90 days of conditioning on FRC samples casted in India with the addition of crystallizing agent 127

Figure 91: evaluation of the self-healing after 90 days of conditioning on latex-modified FRC samples casted in India 127
Figure 92: percentage recovery of the different batches along with time, calculated on the reference CMOD 1500 µm (precracking 600 µm) 128
Figure 93: percentage recovery of the various mixes along with time, calculated on the reference CMOD 1500 µm (precracking 4000 µm) 129
Figure A-1: compressive setup A-5
Figure A-2: plate modeling in sap2000 ..... A-6
Figure A-3: stresses on the plate in sap2000 ..... A-6
Figure A-4: geometry of the plate and the cross stiffener A-7
Figure A-5: simplified modeling of plate and cross in sap2000 ..... A-7
Figure A-6: stress on plate and cross in sap2000 ..... A-8
Figure A-7: distribution of the forces A-9
Figure A-8: central support A-9
Figure A-9: bending-tensile setup A-9
Figure A-10: main parameters which determine the choice of a spring A-10
Figure A-11: catalogue from www.prontomolle.it A-11
Figure A-12: calculation of the stress induced by three point bending test A-18

List of tables

Table 1: summary of the employed mixes 72
Table 2: components of the basic concrete matrix 73
Table 3: characteristics of the steel fibers 73
Table 4: standard properties of the employed mixes 76
Table 5: compressive strength of plain concrete after 28 days 84
Table 6: compressive strength of FRC (India) samples after 28 days 84
Table 7: compressive strength of FRC + Penetron samples after 28 days 84
Table 8: compressive strength of FRC + Latex samples after 28 days 84
Table 9: compressive strength of FRC (Italy) samples at 7, 14 and 28 days 85
Table 10: compressive strength of FRC + Penetron (Italy) samples at 7, 14 and 28 days 85
Table 11: flexural characterization of plain concrete samples casted in India 88
Table 12: flexural characterization of FRC samples casted in India for CMOD = 600 µm and CMOD = 4000 µm 88
Table 13: flexural characterization of FRC samples containing Penetron for CMOD = 600 µm and CMOD = 4000 µm 88
Table 14: flexural characterization of latex-modified FRC samples for CMOD = 600 µm and CMOD = 4000 µm 88
Table 15: flexural characterization of FRC samples casted in Italy for CMOD = 600 µm and CMOD = 4000 µm 88
Table 16: characteristic values obtained for plain FRC specimens casted in India and reloaded after 30 days 110
Table 17: characteristic values obtained for FRC specimens with the addition of Penetron casted in India and reloaded after 30 days 110
Table 18: characteristic values obtained for latex-modified specimens reloaded after 30 days 110
Table 19: characteristic values obtained for FRC specimens without crystallizing agent reloaded after 30 days 113
Table 20: characteristic values obtained for FRC specimens containing the crystallizing agent reloaded after 30 days 113
Table 21: characteristic values obtained for FRC specimens casted in India reloaded after 90 days 116
Table 22: characteristic values obtained for FRC specimens casted in India reloaded after 90 days 116
Table 23: characteristic values obtained for latex-modified FRC specimens reloaded after 90 days 116
Table 24: characteristic values obtained for FRC specimens casted in India and reloaded after 270 days .. 119
Table 25 characteristic values obtained for FRC specimens casted in India with the addition of crystalizing agent and reloaded after 270 days 119
Table 26: characteristic values obtained for latex-modified FRC specimens reloaded after 270 days 119
Table 27: values of peak load and residual load of precracking, peak load of reloading and quantification of recovery for FRC specimens casted in India and reloaded after 30 days 122

Table 28: values of peak load and residual load of precracking, peak load of reloading and quantification of recovery for FRC samples casted in India with the addition of crystallizing agent and reloaded after 30 days 122
Table 29: values of peak load and residual load of precracking, peak load of reloading and quantification of recovery for latex-modified FRC specimens reloaded after 30 days 122
Table 30: values of peak load and residual load of precracking, peak load of reloading and quantification of recovery for FRC specimens casted in India and reloaded after 90 days 125
Table 31: values of peak load and residual load of precracking, peak load of reloading and quantification of recovery for FRC specimens casted in India with the addition of Penetron and reloaded after 90 days 125
Table 32: values of peak load and residual load of precracking, peak load of reloading and quantification of recovery for latex-modified FRC specimens reloaded after 90 days 125
Table A-1: compressive strength on plain concrete samples A-1
Table A-2: compressive strength on FRC samples casted in India A-2
Table A-3: compressive strength on FRC samples casted in India with Penetron A-2
Table A-4: compressive strength on latex-modified FRC samples A-2
Table A-5: compressive strength at 7, 14 and 28 days of FRC samples casted in Italy A-3
Table A-6: compressive strength at 7, 14 and 28 days of FRC samples casted in Italy with Penetron A-4
Table A-7: three point bending test results strength on plain concrete samples: CMOD 600µm A-13
Table A-8: three point bending test results strength on FRC samples (India): CMOD 600µm A-13
Table A-9: three point bending test results strength on FRC samples containing Penetron (India): CMOD 600µm A-14
Table A-10: three point bending test results strength on latex-modified FRC samples: CMOD 600µm A-14
Table A-11: three point bending test results strength on FRC samples (Italy): CMOD 600µm A-15
Table A-12: three point bending test results strength on FRC samples containing Penetron (Italy): CMOD 600µm A-15
Table A-13: three point bending test results strength on FRC samples (India): CMOD 4000µm A-16
Table A-14: three point bending test results strength on FRC samples containing Penetron (India): CMOD 4000µm A-16
Table A-15: three point bending test results strength on latex-modified FRC samples: CMOD 4000µm A-17
Table A-16: weather conditions in Chennai, December 2013 ..... A-19
Table A-17: weather conditions in Chennai, January 2014 ..... A-20
Table A-18: weather conditions in Chennai, February 2014 ..... A-21
Table A-19: weather conditions in Chennai, March 2014 ..... A-22
Table A-20: weather conditions in Chennai, April 2014 ..... A-23
Table A-21: weather conditions in Milan, September 2014 ..... A-24
Table A-22: weather conditions in Milan, October 2014 ..... A-25
Table A-23: weather conditions in Milano, November 2014 ..... A-26

Abstract

The improvement of service life of concrete structures has become essential for both economical and environmental reasons: nowadays cement industry produces about 8% of global CO2 emissions and 50% of the annual construction budget is spent for rehabilitation and maintenance of existing structures.

Self-healing materials opens the way to a new structure concept, characterized by an enhanced longevity, thanks to the provided capacity of self-repairing and recovering the original performances after being damaged.

Concrete is suitable to be employed with this aim, thanks to its reactivity under suitable environmental conditions. Its self-healing capacity depends on many factors, such as the presence of additions, width of crack, type and duration of exposure to several external conditions.

In this work, the problem of self-healing of concrete will be investigated with reference to a normal strength fiber reinforced concrete. The effect of different widths of crack, exposure times to wet/dry cycles, application of a through-crack compressive stress and the ability of different additions to trigger the self-healing ability of material will be considered.
A methodology for the assessment and quantification of mechanical recovery will also be proposed.

1. Introduction

1.1. Background of the work

Reinforced concrete structures are naturally subjected to a deterioration process, due to aging and the action of aggressive agents. Deterioration can be induced by alkali-aggregate reactions, freeze and thaw cycles, fire and abrasion, but the most common cause of degradation of structures is the corrosion of steel bars.

Corrosion of steel bars is an electro-chemical reaction, which acts when a difference in potential exists along the steel bar embedded in concrete. This system is set up as an electro-chemical cell, where an electrolyte solution, such as of pore solution, connects the cathodic and anodic regions. Positively charged Fe^{++} ions pass in the pore solution and negatively charged electrons pass in the cathode through the steel. There electrons are absorbed by the pore solution and react with water and oxygen to form hydroxyl ions OH^-, which react with ferrous ions in the electrolyte solution to form ferrous hydroxide $Fe(OH)_2$. Ferrous hydroxide is then converted in rust by further oxidation.
The effect of corrosion is the formation of rust, whose density, which is lower than the density of steel, leads to an increase in volume of the bars. This expansion results in cracking and spalling of the concrete cover along with the advancing of the process. Once the phenomenon has started, the rate increases because of the facility of aggressive agents to ingress the fractured or delaminated concrete and react with the steel bars.

The presence of an intact concrete cover prevents the steel bars from corrosion for a long period.
However, concrete-based structures naturally presents the inconvenience of cracks. Cracks are unavoidable in non pre-stressed concrete, due to the natural process of shrinkage in the early ages; moreover, during its life-cycle the structure is subjected to loads that induce stresses, which can result in cracks if tensile.

The occurrence of a crack establishes a weak zone, where the aggressive agents can flow.
During its service life, the structure can cumulate cracks, that can compromise the durability. Because of that, for infrastructures, repairing actions may be needed after only 10 to 15 years; additionally, after the first intervention, further rehabilitations are in general needed in shorter times.
In developed countries, many of the existing infrastructures have been built in the years immediately after the Second World War. Material deterioration due to aging and the growth of urban population which uses these structure, is increasing their maintenance costs exponentially.
A study published by the Strategic Development Council (SDC) in 2004 estimated the maintenance cost of American concrete structures between 18 and 21 billion dollars per year, 8 of which would be spent to repair bridges and 4 of which are employed for the reparation of pavements [1].
Similar costs are foreseen in UK, where, as reported by Dunn [2], 80 billion Pounds are annually spent to repair and maintain existing structures, many of which are concrete-made.
In Europe, about 50% of the annual construction budget is spent for rehabilitation of existing buildings [3].

These costs are going to increase: the American Society of Civil Engineers estimates that in the next 5 years 2.2 trillion dollars will be needed to repair structures and the same amount of money will be required for Asian's infrastructures [4].
Besides the direct costs of maintenance, indirect costs due to the traffic jam result in a loss of productivity. These have been estimated 10 times higher than the direct costs [3].
In addition, in 2008, 8% of world CO_2 emissions were generated by cement industry and construction, which turned out to be the most pollutant human activity.

So, for both economical and environmental reasons, the goal of enhancing the service life of structures and infrastructures has become popular. A longer life could lessen the demand of new infrastructure and, on the other hand, reduce the energy consumption and the related emission of CO_2.

The idea of self-healing in concrete comes from the concept of structures that do not need maintenance at all. In this case, the occurrence of a crack would activate the automatic process of reparation of the material that would regain the initial level of performance, in terms of both mechanical properties and permeability.

The employment of such a kind of material would be justified since its costs, higher at the beginning, should not increase and finally would be lower than the costs of other solutions, when projected on the life-cycle of the structure.

1.2. Aim of the research

The aim of this research is to investigate the capacity of different additions of enhancing the self-healing abilities of fiber reinforced concrete with medium-high water to cement ratios, subjected to wide cracks.

In literature a large amount of studies focused on the self healing capacities of high performance fiber reinforced concretes (HPFRC) or engineered cementicious composites (ECC). These materials are characterized by high cement and fiber content and low water to cement ratio and so their employment is nowadays still confined to a few particular applications, due to their cost.
On the other hand, about no studies have concentrated on the self-healing capacities of ordinary fiber reinforced concretes featuring a lower cement content and medium-high water to cement ratio, which can be employed in several applications, such as the construction of industrial floors, road pavements, tunnels and bridge desks, thanks to their lower cost and good performances.

Often, these materials are also combined with chemical additions that improve their waterproofing capacities and, consequently, their durability in aggressive environments.
Quite common is the use of latex-modified concrete for bridge desks or road pavements, to enhance either the abrasiveness and the pore structure.
Also, crystalline admixtures are becoming really popular to protect concrete structures against the penetration of water and chloride agents. In particular they are largely employed for underground works.

This study proposes an analysis of the self healing capacities of the above mentioned materials in terms of mechanical performance.
The effect of the addition of respectively a commercial latex and a crystalline admixtures to the mix will be also studied.

The goal is definitely to determine if self healing takes place in these materials and the influence of time, width of crack, additions and the application of through-crack stresses on this process.

1.3. Summary of the contents

This work have been conducted in part at Indian Institute of Technology of Madras (India), in part at Politecnico di Milano (Italy), within an exchange program.

The first part of the study has been carried out in India.
There, the investigation of the scientific background has been concluded , resulting in the second chapter of this thesis, which contains a review of the literature on self-healing of concrete.
Moreover, the experimental programme has been organized and mechanical tests have been performed on different concrete mixes, in order to study the effects of different additions, widths of crack and time of conditioning on self-healing.

In Italy, the experimental work conducted in India has been completed with the investigation of the effects of a through-crack compressive stress applied during conditioning.

The third chapter of this thesis summarizes the experimental programme and its organization during the whole project.
As well, the procedures of the performed tests are explained, by referring to the corresponding standards.
The fourth chapter covers the collection of results and their interpretation.
There, the behaviour of the employed materials will be described and a method to calculate self-healing effects will be presented.
Then, the results in term of self-healing will be discussed, along with the effect of the parameters affecting the process. Results achieved in India and Italy will be compared.
The fifth and last chapter consists of the conclusions of the work and, referring to the aim presented in the first chapter , will argue around the objectives that have been satisfied.
Finally, suggestions for the future works will be given.

2. Background of research

2.1. Introduction

The objective of this chapter is an analysis of the background of research of the self-healing phenomena in concrete based materials.

The first section briefly describes the main mechanisms of deterioration of concrete structures and the related economic costs of their reparation. This section is aimed at introducing the motivations which lead to the study of self-healing of concrete and to show how its knowledge can be useful both in economical and environmental terms.

The second section focuses on the chemical reactions that naturally occur in reparation of concrete and on the engineered methods that have been performed to enhance the self-repairing properties of the material.

2.2. Deterioration of concrete structures

Reinforced concrete structures are naturally subjected to a deterioration process, which is commonly caused by the corrosion of steel bars.

Corrosion of steel bars acts as an electro-chemical reaction, where the cathodic and anodic regions are connected by the electrolyte solution in form of pore solution. Positively charged Fe^{++} ions pass in the pore solution and negatively charged electrons pass in the cathode through the steel. Here electrons are absorbed by the pore solution and react with water and oxygen in order to form hydroxyl ions OH^-.
The reaction of these latter with ferrous ions leads to the formation of ferrous hydroxide $Fe(OH)_2$ that is then converted into rust by further oxidation.

The reactions which represent the entire process are the following:

Anodic:

$$\mathbf{Fe \rightarrow Fe^{++} + 2e^-}$$

$$\mathbf{Fe^{++} + 2OH^- \rightarrow Fe(OH)_2}$$

$$\mathbf{4Fe(OH)_2 + 2H_2O + O_2 \rightarrow 4Fe(OH)_3}$$

Cathodic:

$$\mathbf{4e^- + O_2 + 2H_2O \rightarrow 4OH^-}$$

The formation of rust leads essentially to a volume increase, which results in cracking and spalling of the cover because of the induced stresses.

Essential conditions for the activation of corrosion mechanism are the presence of water and oxygen. Due to this, dry concrete generally does not show corrosion, just like concrete totally immersed in water is protected by the lack of oxygen. The optimal relative humidity for activation of corrosion is 70 to 80%. For higher values the diffusion of the oxygen is in fact reduced.

Even if these conditions are satisfied, steel can resist to degradation, thanks to the presence of a protective layer of oxide which forms in the hydrating paste and coats the bars. This phenomenon is called *passivation* and is active with pH values in a range from 12.6 to 13.5, which are normal for the hardened cement paste in young concrete.

However*, de-passivation* can take place if the pH drops, with the consequent loss of the protective layer. Essentially this phenomenon can be due to two main causes: *carbonation* and *chloride attack.*

Carbonation is due to the presence of carbon dioxide in the air and it's the most common form of concrete degradation. Carbon dioxide reacts with air moisture or water, to form carbon acid, which reacts with lime in the pore solution in order to form calcium carbonate. These reactions lead to a decrease in pH level, which is reduced to below 10, with the consequent disappearing of the passivation layer. Unprotected steel bars can degrade in presence of water and oxygen.

Concerning the chloride attack, in contact with steel bars, chloride ions activate the surface of steel to form an anode, while the passivated surface acts as a cathode. Further induced reactions result in the formation of ferrous hydroxide, which can, as previously exposed, form rust for further oxidation.

$$Fe^{++} + 2Cl^{-} \rightarrow FeCl_2$$

$$FeCl_2 + 2H_2O \rightarrow Fe(OH)_2 + 2HCl$$

When the concrete layer is intact, durability is determined by mainly two characteristics of the paste: permeability and diffusivity.
Permeation and diffusion of aggressive agent through the concrete cover and carbonation, deeply depend on the concrete pore structure and on time, influenced also by many other parameters, such as the water to cement ratio and the presence of mineral admixtures.
However, it can be said that many years are needed to carbonate a 15 mm thick layer of concrete (100 years when the water to cement ratio is 0.45 for a normal concrete[5]).
Similarly, chloride agents act from external environment (today it is strictly forbidden to employ in concrete structures chloride-based products) and consequently, infrastructures such as highways treated with de-icing salts and marine structures are the most sensible to this kind of aggression.
Chloride ions penetrate the concrete layer by transport of the water containing them or by diffusion. If the structure is subjected to wet/dry cycles with marine water, the eventual presence of oxygen activates the corrosion mechanism.

Concrete structures are subjected to the formation of cracks during their life cycle. If not repaired, these cracks weaken the structure by creating spots where the aggressive agents can penetrate and compromise the integrity of the reinforcing bars. This is why essentially a maintenance is periodically necessary.
Structures performance depending on time can be described as in **Figure 1**

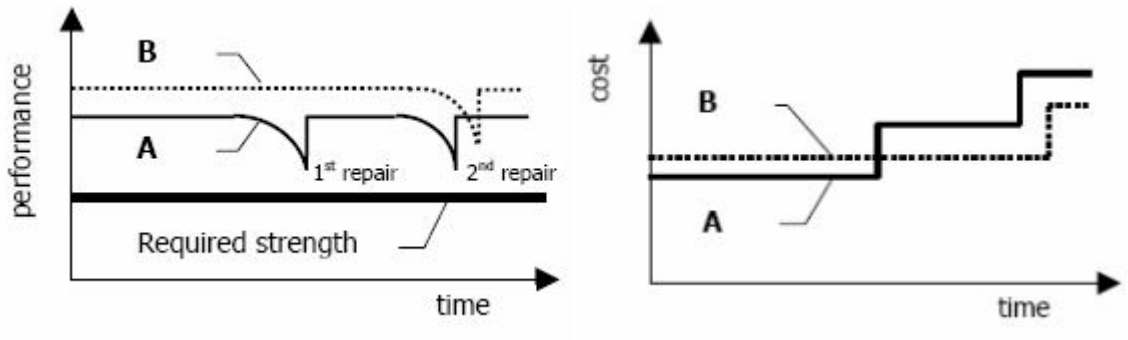

Figure 1: performance (on the left) and cost (on the right) with elapse of time for normal (A) and high quality (B) structures by Van Breugel. Direct cost of repair included. Interests and inflation ignored.

Traditional structures (curve A) normally need a first repair after 10 to 15 years from casting. These repairing operations lead to an increase of the cost represented by the steps in the graph on the right. It is matter of fact and experience that the use of a better performing material (curve B) at the beginning of the process will require higher initial investments, but will result in a decrease of the life-cycle cost of the structure, due to the lower number of maintenance actions.

In the case of self-healing structures, the occurrence of a crack would activate the automatic process of reparation of the material that would regain the initial level of performance. The employment of such a kind of material would be justified since its costs, higher at the beginning, would be fixed and lower than the costs of other solutions, when split on the life-cycle of the structure (**Figure 2**).

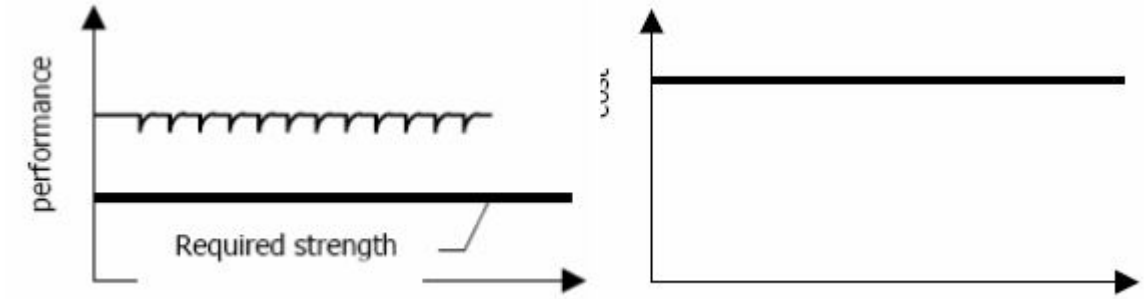

Figure 2: performance (on the left) and cost (on the right) with elapse of time for a structure made of self-healing concrete by Van Breugel. Direct cost of repair included. Interests and inflation ignored.

In the practice, self-healing has never been taken into consideration in the design of concrete structures, but for the case of some water reservoir; only a few studies are concentrated on the benefits given by a self-healing concrete on the life-cycle costs of structures.

Li *et al.* [4] proposed the study of the life-cycle of a reinforced concrete bridge deck in a chloride environment.

In his model, Li studied the cost of construction and maintenance of the bridge deck, by varying the employed materials (reinforced concrete or reinforced ECC) and the conditions of these materials (uncracked RC and ECC, cracked RC with a width of crack of 200 and 400 µm, cracked ECC up to tensile strains of 0.3 and 0.5%, ECC with self healing and without self-healing).

The results of his simulation showed a life cycle cost of the best performing ECC much lower (about half) than the life cycle cost of normal concrete on an estimated service life of 100 years, in comparison to a three times higher initial cost. Self-healing could perform a further cost reduction of about 25% by cost in comparison with the same material unable to self-heal.

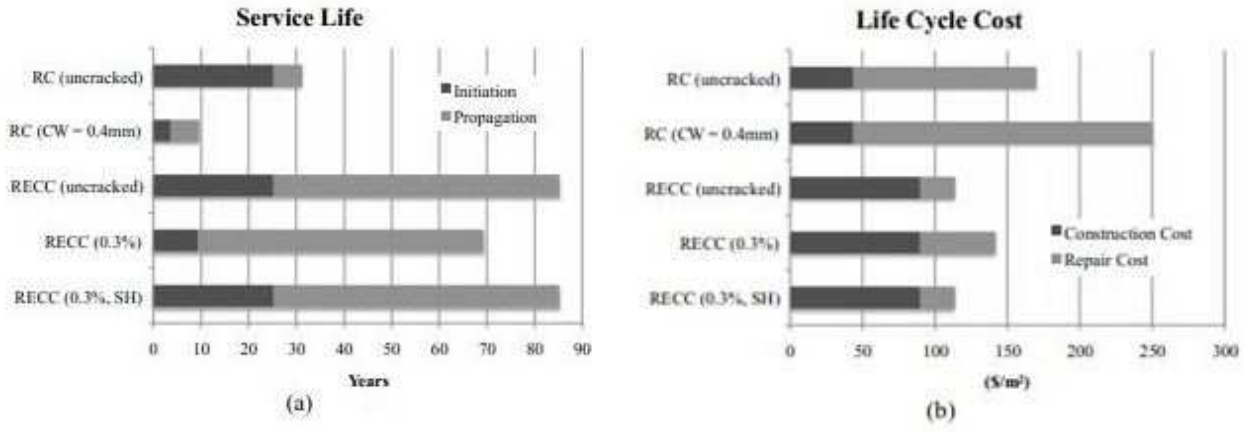

Figure 3: computed service life (a) and life cycle cost (b) showing the effect of self-healing by Li. The "construction cost" here, refers to mainly the initial material cost

As van Breugel [6] hypothesizes, owners might be interested in a product that does not show any decay. Unfortunately, today's knowledge of self-healing phenomena in concrete is not enough enhanced to develop structures presenting such a characteristic, but engineered approaches to self-healing already exist. These have followed essentially four ways: inclusion of bacteria, encapsulation of chemical agents, use of mineral additions and stimulation of self-healing under self-controlled crack width.

In the next paragraph, the mechanisms of self-healing and the methods so far employed will be described in detail.

2.3. Self-healing properties of concrete

It is quite well assessed that concrete, under certain circumstances, exhibits the capacity of self-healing small cracks. This propriety is known as autogenous healing, since it depends only on the material constituents, without any artificial repairing action.

Ferrara reports [7] that healing of cracks in fractured concrete structures was noticed by the French Academy of Science in 1836, in water retaining structures, culverts and pipes. This phenomenon was attributed to the convection of calcium hydroxide exuded from hydrated cement and converted into calcium carbonate on exposure to the atmosphere.

In 1913 Abrams [8]described the autogenous healing of concrete as a "group of phenomena which were brought out in the tests of pull-out specimens loaded one or more time, after having been previously testing to their maximum resistance".

Further evidences [7] were noted and reported in the following years by Loving, who in 1936 observed the formation of calcium carbonate inside the cracks of concrete culverts, and by Whitehurst, who observed the variation of the elastic modulus and strength in concrete structures after a natural cycle of freeze and thaw.
In 1956 Lauer and Slate provided the most complete investigation and explication about autogenous healing. They described the reactions that conduce to the formation of calcium carbonate in cracked concretes, explaining what in 19th century the French had already sensed and showing a direct correlation between the fractured area and the size of calcium carbonate crystals deposited.

Several studies had been conducted after the milestone work by Lauer and Slate. The most part of these focused on tightness of healed concretes (especially [9][10][11]) and only a few of them concentrated on the mechanical recovery [12][13][14][15] .

2.4. Terminology

The development of this research field in the last decades led different scientific committees and scientists to define self-healing. This paragraph will refer to the definitions of JCI (Japanese Concrete Institute) TC-075B and RILEM (Reunion Internationale des Laboratoires et Experts des Materiaux, Systemes de Construction et Ouvrages) Ex221-SHC.

As Schlangen *et al*. [16] report in their book, one first classification can be the following:

- ***Autogenous Healing:*** a natural process of filling and sealing cracks without any external operations and works;
- ***Engineered Healing or repairing:*** artificial and intentional methods for filling and sealing cracks. The healing materials or devices are introduced as a designed function into concrete in advance;
- ***Self-Healing or repairing:*** process of filling and sealing cracks that automatically take place in situ without any practical works by workers; this point can be interpreted as the sum of the previous points: self-healing or repairing can automatically happen due to the autogeneous healing processes or the action of an engineered healing.
- ***Natural healing:*** natural phenomena of filling and sealing cracks that results from some chemical reactions, such as further hydration and carbonation, or mechanical blocking at crack faces.

- ***Autonomic healing:*** involuntary healing of cracks that are provided by admixtures. The admixtures such as fly ash and a specific expansive agent are intentionally incorporated into concrete in advance.
- ***Activated repairing:*** automatic repairing using some artificial devices, which usually consist of sensors and actuators. Repairing function is given by different substances from original constitutions of concrete. This may be considered as "intelligent materials" or "smart systems".
- ***Repairing:*** general repairing which needs practical works and treatments in situ by workers.

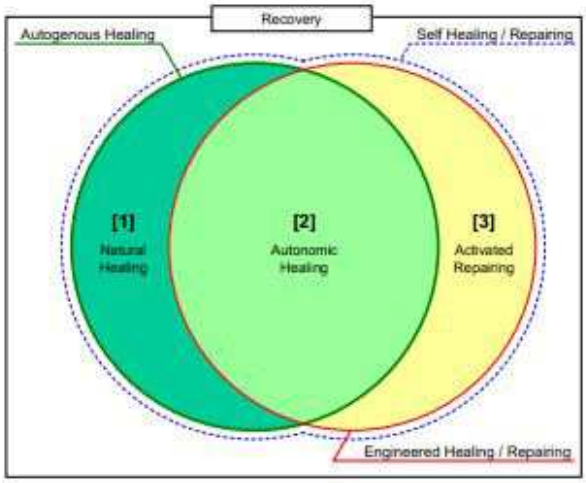

Figure 4: definition of self-healing/repairing concrete by JCI

These definition were used by RILEM to further develop a classification of self-repairing [17]:

- ***Passive self-repairing:*** repairing that occurs due to the reaction to external stimulus without the need of human intervention;
- ***Active self-repairing:*** repairing that occurs due to the reaction to external stimulus with the need of human intervention;

RILEM took the JCI subdivision between autogenous and autonomic self-healing, operating a further classification based on the process and the result of self-healing:

- Autogenic self-closing: own generic material closes cracks;
- Autogenic self healing: own generic materials restores properties;
- Autonomic self closing: engineered additions close cracks;
- Autonomic self-healing: engineered additions restore properties.

Figure 5: definition of self-healing/repairing concrete by Mihashi and Nishiwaki

In literature, for example in Hearn [10], sometimes self-sealing is used synonymously as self-closing.

2.5. Mechanisms

Different researches recognized four mechanisms (**Figure 6**) which would determine the sealing of cracks:

- Crystallization of calcium carbonate
- Continuing hydration
- Sedimentation of particles
- Swelling of the cement matrix

Among them, only the first two are permanent and determine the healing [10].

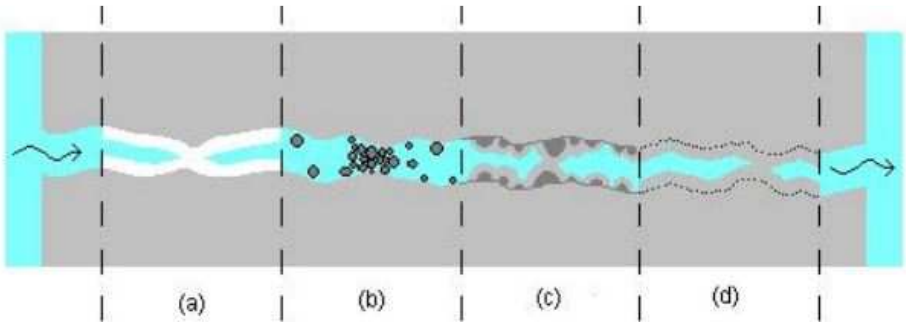

Figure 6: possible causes of self-healing: (a) formation of calcium carbonate or calcium hydroxyde, (b) sedimentation of particles, (c) continued hydration, (d) swelling of the cement matrix by Ter Heide

2.5.1. Crystallization of calcium carbonate

Calcium hydroxide is a reaction product of hydration of concrete. In presence of water, it forms a precipitate on the crack surface (**Figure 7**).

- $Ca(OH)_2 \leftrightarrow Ca^{2+} + 2OH^-$
  Water (as well as air) usually contains dissolved carbon dioxide:
- $CO_2 + H_2O \leftrightarrow CO_3^{2-} + H^{2+}$
  Calcium carbonate is a product of the reaction between calcium ions, obtained from calcium hydroxide dissolution and carbonate ions obtained from the reaction between water and carbon dioxide:
- $Ca^{2+} + CO_3^{2-} \leftrightarrow CaCO_3$
  As long as calcium hydroxide and water are present, calcium carbonate crystals precipitate on the free surfaces of the crack and fill it.

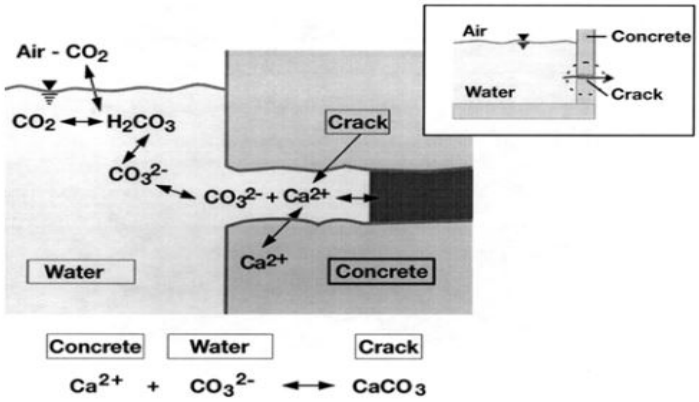

Figure 7: interfaces and reactions in $CaCo_3$ - CO_2 - H_2O system by Edvardsen

2.5.2. Continuing hydration

Continuing hydration of concrete is, with the formation of calcium carbonate, the main reaction conducing to the crack sealing.

As early as in 1913 by Abrams [8], this phenomenon was recognised, but only in the last two decades, thanks to the progress in cracked concretes permeability studies, scientists have approached it considering its independence from the other self-sealing reactions.

Hearn [10], stated that continuing hydration and the other healing mechanisms occur under different boundary conditions. In fact, continuing hydration is also observed in systems where there is not any presence of CO_2, where the carbonation cannot occur.
The phenomenon is more evident during the early ages of specimens: Hearn and Morley [9] observed that 26 years old concretes did not show unhydrated portions of cement, because the hydration was already consumed by then.
Furthermore, their experiments showed that the most important effect occurs in the first 100 hours of exposition to water. This could be explained considering the interaction among the different self-sealing mechanisms: when the autogenous healing occurs, particles precipitate on the surfaces of cracks and form a thicker shell as time progresses, which prevents the further hydration of particles.

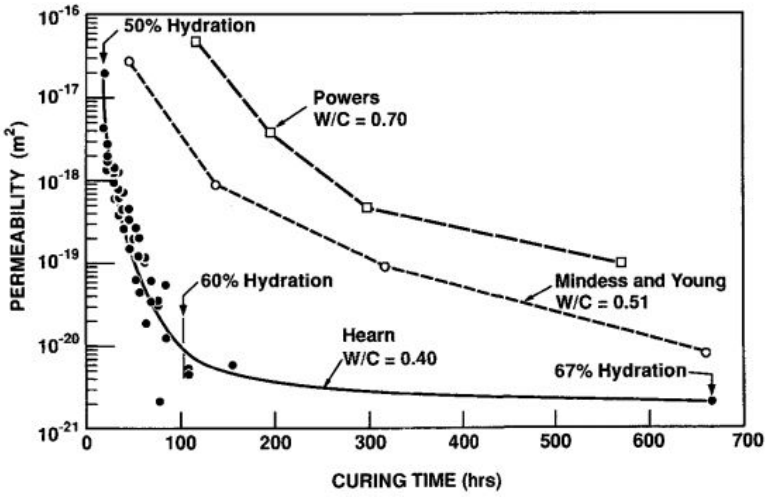

Figure 8: ***permeability versus extent of hydration by Hearn and Morley***

Ter Haide [12] reported that also Neville attributed importance to the continuing hydration only for concretes in their early ages

Another parameter that influences hydration is the water to cement ratio: a lower ratio advantages the reaction due to the presence of more particles of unhydrated cement that react upon the flowing of water inside the crack, as it can be observed in **Figure 8.**

2.5.3. Sedimentation of particles

The cracks can be clogged by particles carried by the liquid or by cement particles lost by the surface, that ultimately can get stuck in the most narrow parts of the concrete fractures.

Hearn [10] wrote that physical clogging has been one of the most common explication for self-sealing. Mc Millan and Lyse in 1930 would considered it to be the main cause of healing in cracked concrete.

Hearn and Morley [9] report that Glanville demonstrated that sedimentation of particles was not responsible for self-sealing. He conducted flow-reversal tests in order to detect the increase of permeability that occurred after several flow cycles. Comparing the results of concretes with the responses of sandstone specimens, Glanville observed that while the permeability of sandstone increased with every reversal, concrete exhibited a small increase only after the first reversal (**Figure 9**).
Glanville attributed the increase of flow in sandstone after every reversal to the opening of new passages, rather than to particle movement. On the other hand, concrete showed only a slight increase after reversing the flow, which means that physical clogging cannot be responsible of permanent self-healing of cracks.

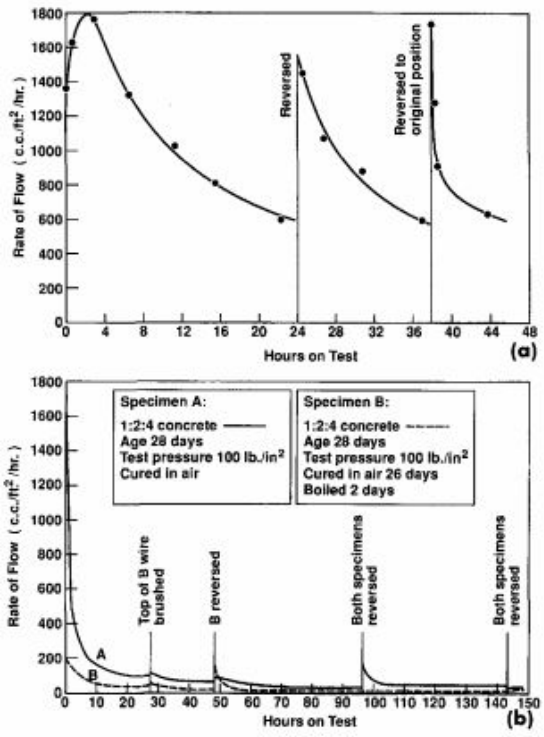

Figure 9: ***Glanville's permeanility curves from Hearn and Morley showing the effect of flow reversal on sandstone and concrete: a) effect of reversal direction of flow in a sandstone specime: permeability increases after each reversaln; b) effect of reversal flow direction in a concrete specimen: there is only a slight increase of permeability after the reversal; physical clogging is not responsible of permanent healing***

2.5.4. Swelling of the cement matrix

The movement of water into or out of a cement matrix causes respectively swelling or shrinkage. The expansion of matrix results in the closing of cracks as the flanks present on the either side move closer. On the other hand, shrinkage makes the flanks to move further away from each other and hence, the crack width increases.

The significance of swelling/shrinkage phenomena was well demonstrated by Hearn [10] with propan-2-o1/water replacement tests. The results showed that when CSH was not saturated by water its layer collapsed and the permeability appeared to be in one order of magnitude bigger than the that calculated for saturated specimens. She also stated that self-sealing effect or SSE encompasses the autogenous healing and continued hydration. She also designated the swelling of CSH as a "false SSE", since it influences the permeability depending on the saturation conditions, without permanent effects.

2.5.5. Factors influencing self-healing

Several factors participate in favouring the self-healing reactions. It is not easy to describe their singular influence on the phenomena of self-healing, because of their mutual interaction.

In the following paragraphs the most important parameters affecting the reactions are explained.

2.5.6. Mix constituents

The main constituents of concrete are water, cement, fine aggregates, which when hardened, are represented as mortar, and coarse aggregates. The characteristics and the quantity of these components determine the mechanical characteristics of concrete.

From a microscopic point of view, the cement paste is not homogeneous, but results in a pore structure determined by the level of hydration and the presence of additions such as fly ash or silica fume. These latter indeed reduce the size of pores, making the paste more compact and determining its behaviour when cracks occur.

Moreover, the quantity of additions and cement particles determine the reactivity of the material.
The lower the water to cement ratio, the lower will be the dimension of pores and, as a consequence, the width of cracks to repair. Also, an increase in cement will result in an increase of available particles for further hydration after cracking, due to the higher quantity of unreacted particles which will be brought in contact with air and water by the occurence of cracks.
Fly ash and silica fumes induce other hydration reactions that contribute to the formation of sealing products.

2.5.7. Presence of water and water type

Water is essential for all the aforementioned mechanisms: if there is no presence of water in the crack, the autogenous healing mechanisms do not occur.

In Ferrara [7] it is reported that Lauer and Slate stated that when the relative humidity is less than 95%, the extent of healing is much lower than in water-saturated conditions and the growth of the filling crystals is irregular.

Furthermore some authors tried to give an explication of this phenomenon: in a humid but not water-saturated environment, carbon dioxide is present only on the surface of water films and carbonation becomes slow. Equally, hydration is strongly retarded. Thus, in order to promote the autogenous healing, the surfaces must be in contact with water.
The type of water in terms of ion concentrations also affects the self-healing.

Edvardsen [11] investigated the effect of the hardness of water on the sealing of cracks. Her experiments revealed that the concentration of CO_3^{2-} and HCO_3^- ions didn't limit the calcites precipitations, as not all the ions were consumed by the reaction. This evidence might occur because the quantity of Ca^{2+} ions present in the exposed regions of the crack is less than the quantity of carbonate ions present in hard water in contact with the crack.

Fagerlund and Hassanzadeh [18] performed tests on pre-cracked specimens, exposed respectively to tap water, brackish water and sea water, under different modes of water exposure: permanent immersion, cyclic immersion and one-side capillary suction.

They found out that permanent immersion in sea water was the most effective healing method, followed by brackish and tap water respectively.

The topic of the effect of sea water on self-healing was furthermore investigated by Li [19] and a few others researchers [20][21] in the field of ECC and SAPs-modified concretes. Their results will be presented in the next paragraphs.

2.5.8. Water pressure

When the water flows too fast, through the crack, self healing is slower.

Edvardsen [11] conducted some experiments in order to verify the water flow in different width cracks, under different pressure conditions.
She found that after 7 weeks exposure, concrete specimens with a crack width of 0,2 mm under the pressure given by a water column of 6,25 m could completely heal. Differently, the same specimens under the pressure given by a column of 12 m showed only 25% of the cracks healed.

Ramm and Biscoping [22], who tested specimens under conditions of pressure of 2,5m and 12m, found that constant flow rate through the test specimens was achieved faster in the specimens under the pressure of 2,5 m than 12 m. They supposed that the phenomenon occurs because of a higher expansion in the area of the cracks flanks takes place in the specimens under 12m pressure.

In apparent contradiction to the above mentioned results, Fagerlund and Hassanzadeh [18] reported from Lauer and Slate's work that the cracks exposed to pressure healed more effectively in a given time than stress free crack.

The contrast among the results could be due to the influence of several factors, such as the different thickness of the specimens and the length of the crack. These parameters indeed affect the coefficient of flow through concrete.

2.5.9. Water pH

Not many studies have been conducted about the influence of water pH on the self-healing phenomena, because the aggressivity of water used is usually considered only in the studies of steel reinforcements corrosion.

Some results are available again in Ramm and Biscoping [22], who in their work not only tested specimens under different conditions of pressure and crack width, but also under different water pH degrees.
The results showed that higher degree of acidity of water implied a great increase of the flow-through quantity of water (**Figure 10**).

The authors do not explain how pH might influence healing. It could be hypothesize that some reaction takes place and prevents the unreacted particles from hydrating, or reduces the deposition of calcium carbonate at the crack's flanks.

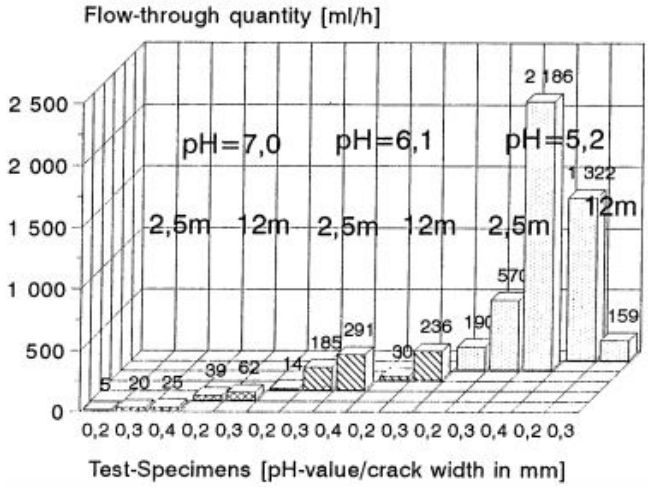

Figure 10: example of flow-through quantities after a 2 years test period by Ramm and Biscoping

2.5.10. Water temperature

The investigation on the influence of temperature on self healing was initiated by the design and construction of solar water storages, where the water temperature could reach 95 °C.

However, the correlation between water temperature and self healing has received only little attention.
Reinhardt and Jooss [23] made tests on specimens with different crack widths, keeping three different temperature levels: 20, 50 and 80 °C.
The permeability tests showed that on increasing the temperature, self-healing became faster (**Figure 11**). This property was more evident when the width of the crack was larger.

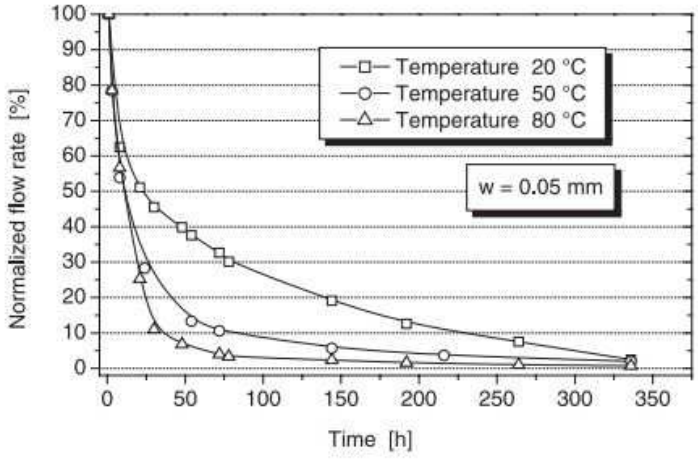

Figure 11: decrease of the normalized flow rate because of the self-healing of the crack for HPC at various temperatures and a pressure gradient of 1 MPa/m and a crack width of 0.05 m, by Rehinardt and Jooss

2.5.11. Crack width

The width of the crack is one of the most important parameters: it determines the volume to be filled by reactions products and the quantity of water that will flow through the fracture.

One can't establish the value of maximum width for the completion of autogenous healing process before hand, for too many factors simultaneously can affect this value. At first it depends on the causes of cracking (bending moment, tension, shrinkage, etc.), and on the exposure conditions during the curing period.

Generally the volume of hydration products of cement is not sufficient to close large cracks. Li and Yang [24] had reported in their studies on ECC (ch.2) that 50 µm is the maximum crack width to achieve the full recovery of mechanical and transport properties in concrete.
Between 50 and 200 µm in general only a partial recovery can be achieved.

Edvardsen [11] confirmed these numbers in her experiments on permeability of healed concretes, in terms of water flow through the specimen (**Figure 12**).

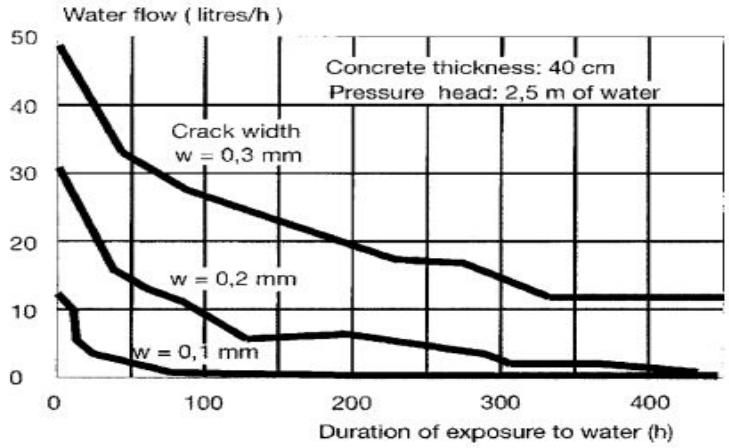

Figure 12: relationship between water flow and time for different crack widths by Edvardsen

2.5.12. Stability of the crack

The crack should be prevented from growth and motion, to allow the healing products to fill the space between the cracks wakes.

When the crack is dynamic, the healed cracks ruin again. Anyway, an autogenous healing also occur in active cracks. This healing is comparable to the one of dormant cracks only at the minimum crack width , as shown again in Edvardsen's [11] research work (**Figure 13**).

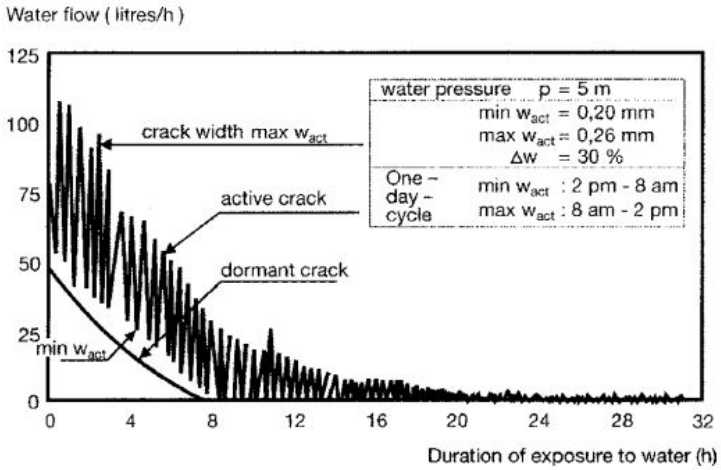

Figure 13: relationship between flow and time for active cracks by Edvardsen

2.6. Mechanical properties of healed cracks

Most of the studies about autogenous healing capacity of concrete were focused on the permeability characteristics of healed specimens. Only a few researches concentrated on the recovery of mechanical properties.

Jacobsen and Sellevold [13] investigated the recovery of compressive strength after the introduction of cracks made with rapid freeze/thaw tests.
Once the conditioning was done, the specimens were stored in water at 20 °C. After three months, the authors compared the mechanical properties of specimens after deterioration and after healing. They evaluated their frequency response as well.
The experiments showed that the specimens regained most of the resonance frequency. However, only a 4-5% of the mechanical capacity recovery was observed on an initial loss of 22-29%.

As Abdel Jawad [14] had already observed, resonance frequency does not, therefore, correlate with the recovery of strength of self healed specimens.

After Jacobsen, Ter Haide [12] provided some results on the behaviour of cracked concrete at the early ages.
In his study, he cracked up to different widths cement specimens that were cured for 20, 24, 48 and 72 hours respectively. The effect of an applied compressive stress during healing was investigated. After 2, 4 , 8 and 12 weeks, the samples were loaded up to failure, to evaluate the effect of time on self-healing.
The results revealed that compression was of great influence, since it allowed the specimens to heal to reach the strength of non cracked concrete. On the other hand, the specimens which were not under compression showed a total recovery of the stiffness with only a partial recovery of strength.

Granger et al. [15], in their study on ultra high performance cementitious materials, compared the effect of the storage in air and water for cracked specimens, measuring the healing capacities for different ages.
They observed that specimens aged in air had the same mechanical behaviour as that of samples reloaded just after cracking, while specimens stored in water showed an increase in stiffness and reloading peak that evolved with the time of aging.
Concerning the flexural strength, the evolution of the peak load depending on aging time never reached the initial value. This could be explained by the fact that crystals formed in the crack bridge it, but they cannot form the complex microstructure which provide the strength of the virgin material.

However, the aforementioned conclusions can hardly be generalized to the whole broad category of concretes and cement based materials, because of the great influence that the specific composition of each mix can have on healing phenomena.

2.7. Concrete incorporating admixtures

In the last few years, researchers have been conducting studies on the promotion of self healing with the addition of agents that favour the deposition of crystals inside the crack.
According to the definitions of JCI and RILEM, these materials provide an *autonomic or engineered healing*.

Different methods and additives can concur to optimize the self healing reactions. One way is to add fly ash or blast furnace slag, which, by reducing material porosity, allow to remain a portion of cement unhydrated even at later ages. In this case, autogenous healing of concrete is attributed to continuing hydration.

On the other hand, researchers had studied the self healing capacities of mixes including expansive materials, crystallizing agents and geo-materials.
In this latter case, chemical agents such as carbonates can activate the expansive agents and lead to the precipitation of calcium carbonate crystals and the formation of hydration products: CSH, CASH (gehlenite hydrate $2CaO*Al_2O_3*SiO_2$), $Ca(OH)_2$, AFt (minerals in which are present t=three groups of anhydrite, such as the ettringite), AFm (minerals in which is present one anhydrite group).
Although the addition of geo-materials and expansive agents can show healing, it always has to be accompanied by a superplasticizer, since they absorb a large quantity of water. Furthermore, the mix must be done carefully, for the wrong quantity of chemical agents can cause undesired expansions to result in the consequent formation of cracks. Moreover, the compatibility between the different materials is not always verified.

2.7.1. Concrete incorporating fly ash

Sahmaran *et al*. [25] tested the self healing capacity of specimens in which 35% or 55% of cement mass was respectively substituted by fly ash. The samples were pre-loaded up to 70% and 90% of compressive strength to generate micro cracks and then stored in water.
These experiments focused not only on the permeability properties but also on the mechanical ones. To analyze permeability properties, the authors performed sorptivity and rapid chloride permeability (RCP) tests; for mechanical properties, compressive strength and UPV tests were conducted.
The results in terms of mechanical capacity showed that the higher was the percentage of fly ash in the specimens, the lower was the initial compressive strength. On the contrary, the specimens with more fly ash were able to recover more strength than the others, especially after a long period (after 30 days).
Conversely, the UPV test, gave disaccording results, independently of the percentage of fly ash. For both the tests before and after the curing period, the values for the 55% fly ash specimens were comparable to those of plain cement specimens, while the 35% fly ash specimens showed higher values.
Finally the permeability tests exhibited a decrease in water flow, depending on the quantity of fly ash. This trend was more evident when the curing period was longer, probably because of the slower hydration of fly ash.

A possible explication of the previous results was given by Termkhajornkit *et al*. [26], who studied the physical effect of self healing on the pore structure of concrete by performing various compressive and RCP tests along a period of one year on specimens presenting cracks due to autogeneous shrinkage. The evidence was that the specimens with more slag and fly ash (50%) had the best healing capacities, though they needed more time to develop the hydration products and improve their strength.

A later study conducted by Zhou *et al*. [27], confirmed that after a thirty day curing period under different conditions, the specimens which showed the higher recovery of strength were the samples containing 20% to 30% of fly ash (**Figure 14**).

Jaroenratanapirom and Sahamitmongkol [28] conducted a research on the self healing of mortar with different mineral additives, subjected to water immersion. They compared the effect of fly ash, silica fume and crystallizing agents added individually to mortars. Their results showed that the crystallizing admixtures perform the best self healing for small crack widths and at the early ages, while for larger cracks fly ash and silica fume were the best agents.

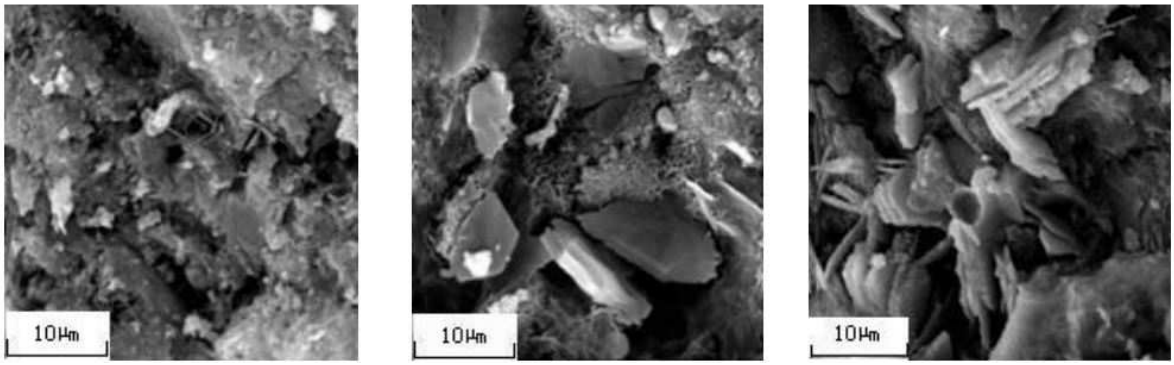

Figure 14: SEM cross-section picture for concrete after self-healing: (a) normal cement concrete; (b) concrete specimen with 30% slag; (c) concrete specimen with 40% fly ash by Zhou et al.

2.7.2. Concrete incorporating chemical admixtures, expansive agents and geomaterials

In 2007, Hosoda, Kishi *et al*. [29] compared the behaviour of concretes containing expansive agents, a crystallizing agent and a polycarboxylate-based superplasticizer. In particular, the expansive agents were constituted by calcium sulfo-aluminate mixes, which could expand thanks to the absorption of the water flowing through the cracks.
The specimens were cracked by means of a uni-axial tensile test and then stored in water with uni-axial tensile force kept constant.
The results showed how the separate use of crystallizing agent and expansive agent improved only a little the self healing of cracks. The crystallizing agent in particular was useful only at the early ages and for small crack widths.
The use of both the expansive and crystallizing agents instead guaranteed a good improvement of the sealing capacities: in the first 14 days the expansive agent swelled and after this period the crystallizing agent created bridges which connected and occluded the crack sides.

Ferrara *et al*. [7] found that crystallizing agent was able to help self-healing, with deposition of crystals that could completely seal cracks with a width of 200 µm in water.
The specimens, when reloaded later, featured a strength recovery, depending on the width of crack, thermal conditioning, duration of exposure and presence of additive. It was shown that not only the specimens improved their flexural load bearing capacity, but also, existed recovery in the stiffness.

Similar experiments were conducted by Sisomphon and Copuroglu [30] on mortars with a low water to binder ratio. They showed that the combined use of expansive and crystallizing agents could repair larger cracks (0,4 mm) under a confinement that simulated the condition of a real structure and the immersion in

water. In the analysis of the filling material the presence of ettringite crystals and depositions of calcium carbonate was found.

In another study, Kishi and Ahn [31] tested the addition of carbonates to different mixes. Their aim was to verify the effectiveness of these compounds in presence of expansive and superplasticizer agents, under water conditioning after cracking.
This research showed that all the carbonates led to the deposition of crystals on the cracks surfaces (**Figure 15**). However, crystal bridges were formed only in presence of C4A3S (hauyne). The best results were obtained only with the collaboration between the expansive and chemical agents.
Furthermore, the researchers investigated the chemical nature of crack fillers, which, in all the cases, were composed of CSH, CASH, $Ca(OH)_2$, AFt, AFm and calcium carbonate deposits, depending on the chemical agent employed.
In their last work [32] these scientists enhanced their previous studies by substituting not only expansive agents in the mix, but also different geo-materials in percentages up to 10%, whose function was to increase the precipitation of calcium carbonate crystals: geomaterial A was mainly composed by SiO_2 and Al_2O_3 with in addition montmorillonite, feldspar and quartz; geo-material B had a similar composition, with little chemical differences. Again, water conditioning was performed after cracking.
This experiment was more complicated, for various chemical components often showed their incompatibility. However, in the end it was confirmed that the right geo-materials in the right quantity could improve the chemical reactions and increase the speed of self healing.

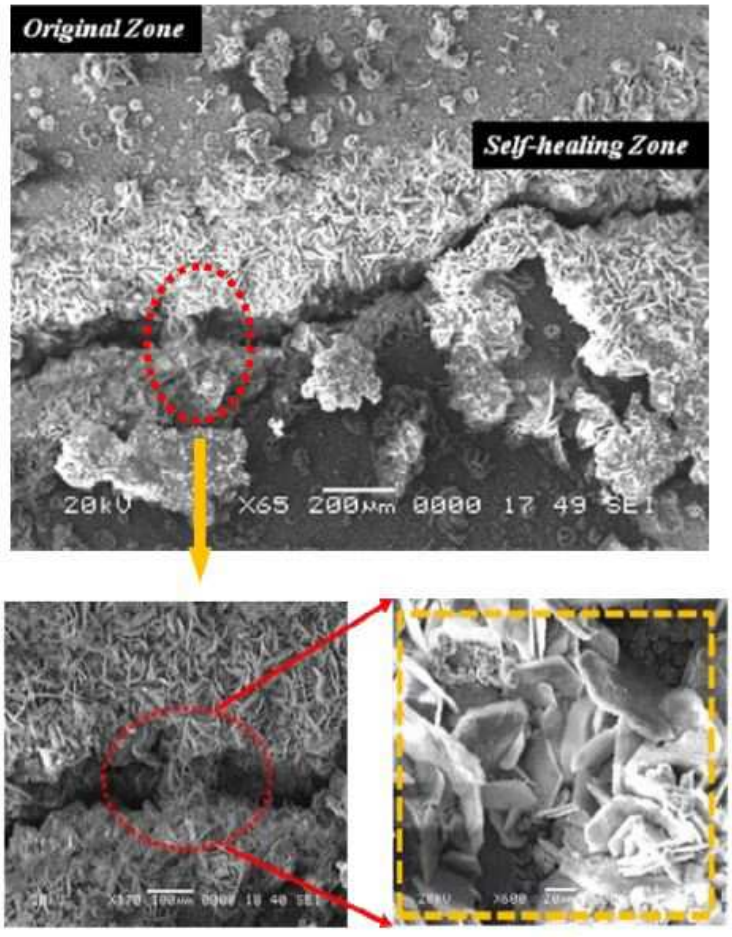

Figure 15: self-healed re-hydration products in crack by hydrogarnet phases C-A-H and calcite phases by kishi and Ahn

2.7.3. Pros and cons

The incorporation of various admixtures in concrete is the best way to enhance its capacity of autogeneous self-healing. Though, there are some pros and cons, which can be identified from the results of the above mentioned experimental investigation.

Pozzolanic materials are employed in concrete since long times and works with reactions of hydration which are well known; the preparation of the mixes does not require particular care due to some incompatibility and the repairing action is comparable to the autogeneous healing.
On the other hand, the use of high quantities of pozzolanic material affects the strength of concrete. Pozzolanic hydration is in fact slower than cement hydration and the development of the ultimate strength requires more time, such as the self repairing action.
Due to these reasons, an optimum quantity of pozzolanic material needs to be calculated in order to balance the exigencies in terms of strength development and healing capacities.

Chemical admixtures can be added to produce concretes where a strong self-repairing action is performed in short times. The most important characteristic from the point of view of self-healing is that these materials can repair cracks up to 400 μm in periods shorter than 30 days.
Their effectiveness depends on their combination: the use of expansive agents, carbonates or geomaterials which stimulate the deposition of crystals and crystallizing agents together is the best way to achieve good repairing results. The separate use of these admixtures can otherwise perform only limited effects.
Consequently, the calculation of the mix is not immediate and requires many trials, since some incompatibility might occur: the interaction between geomaterials and superplasticizer or among different carbonates can affect the deposition of crystals or cause a drop in the strength of concrete. This requires particular care to use such a mix in a structural application, where the mixing process may feature some inaccuracy.

2.8. Bioconcrete

One way to stimulate the production of calcium carbonate to fill cracks is the addition of mineral-producing bacteria to concrete.

Bacteria had already been employed in ecological engineering for the removal of chemical agents from waste water [33] and for bioremediation of contaminated soils [34].

As Mihashi [17] reports from Jonkers, in concrete environment there are several conditions to be satisfied to make the employment of bacteria possible: their lifetime should be at least as long as the lifetime of the structure; they must be enough resistant to survive the mixing process and the alkaline environment of concrete. Furthermore, bacteria shouldn't deteriorate properties like mechanical strength.
"Extremophilic bacteria" are likely to respect all the above mentioned conditions. The name "extremophilic" was given to bacteria species that can live in extreme environments; they can be found in deserts, rocks and also in ultra-alkaline environments that are comparable to that of internal concrete.
Furthermore, extremophilic bacteria are in general characterized by the capacity to form endospores, which can metabolize calcium carbonate. The endospores have resistance against high chemical and mechanical stresses and their lifespan varies between 50 and 200 years.

According to RILEM and JCI definitions, concrete containing bacteria can be defined as *engineered self-healing* material.

Siddique and Chahal [35] reported that calcium carbonate precipitation due to bacteria (**Figure 16**) is a result of both passive and active nucleation.
The first occurs due to the change in metabolic process of bacteria caused by the fluid surrounding the cells. The latter occurs when the bacteria cells are employed as nucleation sites: the cells, as matter of fact, are negatively charged and can attract Ca^{2+} ions, which subsequently attract CO_3^- ions, leading to the deposition of calcium carbonate, $CaCO_3$.

Schlangen [16] remarks that deposition of calcium carbonate is a chemical process governed mainly by four parameters: concentration of calcium, concentration of inorganic carbon, pH level and availability of nucleation sites.

In literature, different calcium carbonate-producing bacteria were investigated with different aims. Essentially two are the methods employed for repairing cracks in concrete by means of bacteria: the urea-based system and the calcium lactate-based system.

2.8.1. Degradation of urea

Ureolytic bacteria can precipitate $CaCO_3$ in their micro-environment by the conversion of urea into ammonium and carbonate.
Bacterial degradation of urea decreases the pH locally, thereby, favouring the formation of carbonates with calcium in calcium rich environments, thus, filling the cracks.
Bacteria precipitate $CaCO_3$ by means of the following chemical reactions of secretion of the enzyme urease which catalyses the conversion of urea into ammonium and carbonate:

$$\mathbf{CO(NH_2)_2 + H_2O \rightarrow NH_2COOH + NH_3}$$

$$\mathbf{NH_2COOH + H_2O \rightarrow NH_3 + H_2CO_3}$$

$H_2CO_3 \leftrightarrow HCO^- + H^+$

$2NH_3 + 2H_2O \leftrightarrow 2NH_4^+ + 2OH^-$

$HCO^- + H^+ + 2NH_4^+ + 2OH^- \leftrightarrow CO_3^{-2} + 2NH_4 + + 2H_2O$

The last two reactions increase the pH and shift the bicarbonate equilibrium to form carbonate ions.
Since the cell wall of bacteria is negatively charged, it attracts the Ca^{2+} ions to deposit on their surface, leading to reaction with CO_3^{2-} to form $CaCO_3$.

$Ca^{2+} + Cell \rightarrow Cell\text{-}Ca^{2+}$

$Cell\text{-}Ca^{2+} + CO_3^{-2} \rightarrow Cell\text{-}CaCO_3 \downarrow$

Hence, the bacteria surface serves as the nucleation site.

Gollapudi *et al.* [36] in 1994 foresaw the employment of a bacterium called *Bacillus Pasteurii* to test the possibility of plugging flow columns filled with sand. They found out that the microbial activity could enhance the production of $CaCO_3$, when bacteria were packaged with an ureolytic solution in the specimen. In their conclusions, they remarked that the optimal pH to favour the deposition of mineral was 8.5; furthermore, the experiments showed that contaminants, such as benzene, nitrate and carbon tetrachloride, slowed the growth of bacteria.

Ramachandran *et al.* [37] provided concrete remediation by using *Bacillus Pasteurii* and *Pseudomonas Aeruginosa.* They tested two types of Portland cement mortar specimens; specimens belonging to the first type were mixed with micro-organisms and the others, were notched and filled with microbial solutions. The tests confirmed that micro-organisms, when added in a low quantity, could increase the compressive strength in concrete cubes and remediate cracks by producing calcite.

Although in environments which presented pH higher than 12, no production of calcite was found out. To protect bacteria and enhance the production of calcium carbonate, scientists tried to immobilize them into different vectors. As per Van Tittelboom *et al*. [38] report, Polyurethane (PU) has been widely employed due to its rich biochemical inertness and mechanical properties.
Bang *et al.* [39] used PU foam to immobilize bacteria called *Bacillus Pasteurii* and studied the effect of embedding cells in the polymer. Results showed that the production of calcium carbonate in the immobilized cells was similar to the case of free cells. Also, there were no significant changes in the values of elasticity modulus and tensile strength. Furthermore, they tested the effectiveness of this system in repairing of concrete cracks by applying bacteria on the cracked surfaces of concrete cubes and found an increase in compressive strength.
Van Tittelboom *et al*. [38] in 2009 applied silica gel carrying *Bacillus Sphaericus* bacteria in concrete samples. They found that bacteria protected in silica gel filled the cracks completely while pure bacteria could not. According to their conclusions, silica gel itself acted as filling material for the cracks before the $CaCO_3$ precipitation started. Specimens were cured in an urea-calcium solution to provide food to bacteria.
In 2010 Wang *et al*. [40] started from this latter work to develop a system which could work from inside the specimens: they studied the employment of both polyurethane and silica gel as capsules to embed and protect bacteria during the mixing process. Their results remarked the better performances of polyurethane concerning the regain of strength and the diminution of water permeability. However, more will be written about bacteria encapsulation in the next paragraphs.

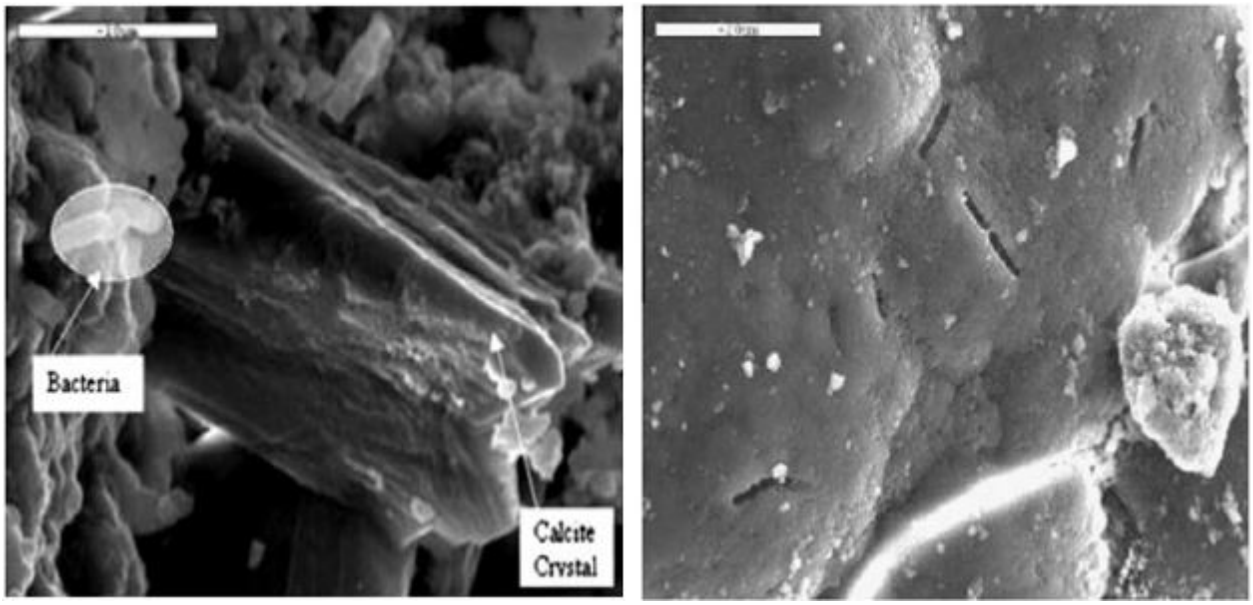

Figure 16: developing of calcite crystals at higher magnification by Siddique and Chahal. Rod-shaped objects, consistent with the dimensions of Bacillus Pasteurii are spread around the crystals.

2.8.2. Calcium lactate-based bacteria

As per Schlangen [41] reports, in order to guarantee the precipitation of calcium carbonate, bacteria cells need an organic substrate to convert metabolically into inorganic carbon, which can react with free calcium to precipitate calcium carbonate. Though cement matrix is rich of calcium ions due to dissolved portlandite, organic carbon is usually not present in the matrix. Many researchers tested the direct application of bacteria and their nutrients at the crack surfaces of bio concrete. In a real structure, the detection of cracks is a long and expensive work which would cost more than normal maintenance.

In 2010 Jonkers [42] tested the direct integration of bacteria in concrete which could automatically act as internal self-healing agent. He proposed the employment of a two component healing agent constituted by bacteria from genus *Bacillus* (*Pseudofirmus* and *Chonii)* and calcium lactate directly added to the mix. The experiments showed that bacteria acted like a catalyst, transforming the lactate into calcium carbonate (**Figure 17**), as per the following reaction:

$$CaC_6H_{10}O_6 + 6O_2 \rightarrow CaCO_3 + 5\,CO_2 + 5H_2O$$

The quantity of calcium carbonate precipitate increased when the produced CO_2 reacted with the molecules of portlandite, as per the following carbonation reaction.

$$5\,CO_2 + Ca(OH)_2 \rightarrow 5CaCO_3 + 5H_2O$$

Jonkers observed a large production of 20-80 µm sized particles in the first week, which precipitated on cracks surfaces. However, in 28 days long curing period, the study showed a decrease in particles production. This phenomenon was due to the loss of spores following the restriction to pores in the matrix: the pore diameter got reduced from 0.1-1 µm to 0.01-0.1 µm with age, as a result of which 0.8-1 µm diameter spores could not be accommodated.

This process not only presents the advantage of being a human-independent self-healing method but also considers the health of concrete, contrary to urease-based system. In the latter, production of ammonium considerably increases the risk of reinforcement corrosion and degradation of concrete which gets further oxidized by bacteria to form nitric acid [43].

Wiktor and Jonkers [43] immobilized a two-component healing agent in porous clays particles, which constituted calcium lactate and *Bacillus Alkalinitrilicus*. In this investigation, the authors tried to increase the service life of the spores, which in the above mentioned study had revealed a functional life of only 1-7 days, due to the effect of high alkalinity that generally decreased the viability and mineral-producing capacity of spores. Their research showed an increase of bacteria's life up to 100 days. Furthermore bacteria were able to enhance the self-healing capacity by closing 0.46 mm width cracks, while in normal concrete samples only 0.18 mm width cracks healed during the same curing conditions.

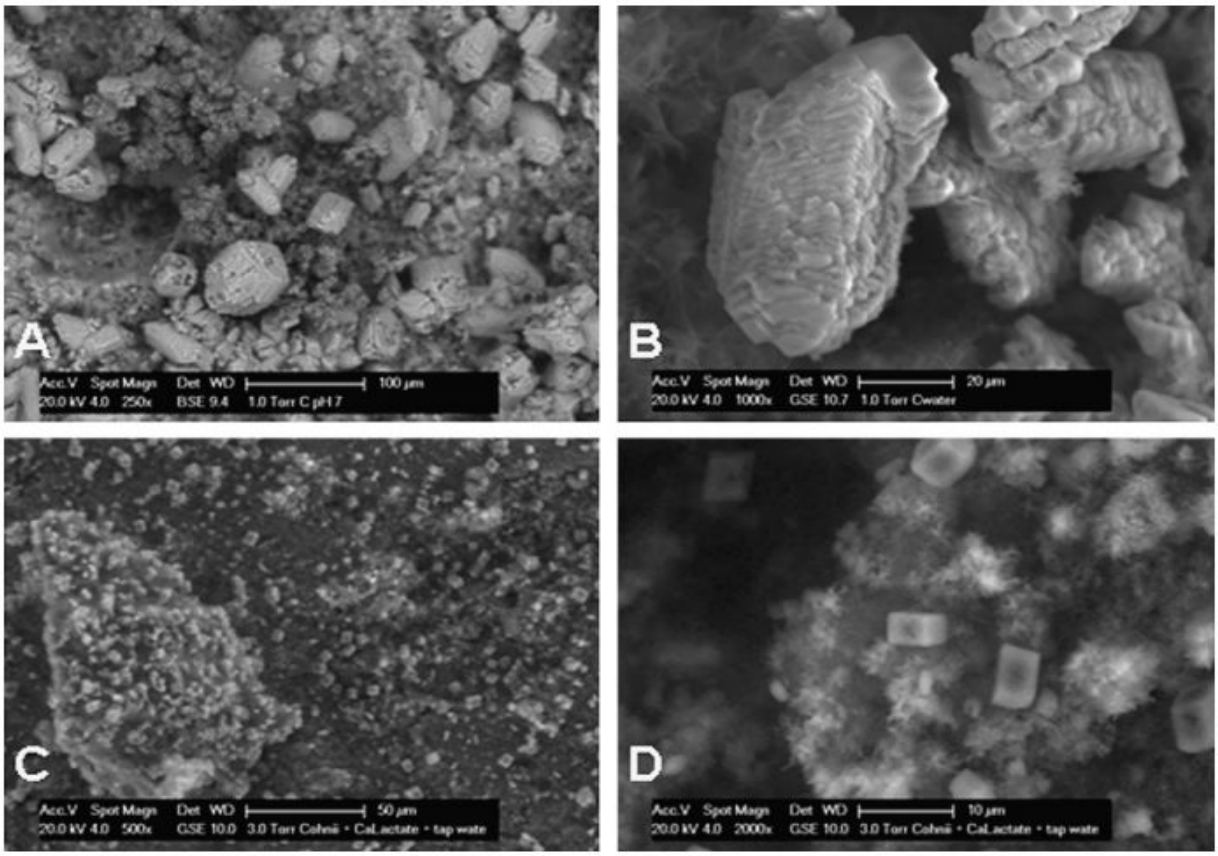

Figure 17: cement stone specimens with incorporating healing agent by Jonkers (B. Cohnii spores plus calcium lactate), cracked after 7 (panels A: 250x and B: 1000x) and 28 days curing (panels C: 500x and D: 2000x). the large mineral precipitatesvisible on the surface of the younger specimens seem to be due to the conversion of calcium lactate by bacteria. The small precipitates on older specimens surface resemble those produced by abiotic specimens

2.8.3. Effect of bacteria cells and walls on concrete strength

Many researchers drew conclusion that inclusion of different bacteria does have variable effects on the compressive strength of concrete. Furthermore, different kinds of nutrients revealed themselves to have a negative effect on specimens mechanical behaviour.

Pei *et al.* [44] tested the effect of bacteria cell walls on the mechanical properties of cement mortars and tried to quantify the resulting precipitation of calcium carbonate. They prepared specimens where cell walls, dead cells and live cells of *Bacillus Subtilis* were respectively added and studied their effect on strength in comparison with control mixes. They found out that cell walls of *bacillus Subtilis* significantly increased the compressive strength and decreased the porosity, whereas live and dead cells mixed with a urea-$CaCl_2$ medium did not contribute noticeable effects. In addition, they repeated the experiment with cell walls, dead and live cells of *Micrococcus Luteus* and *Escherichia Coli*. These results also showed a similar trend with an increment in compressive strength of concrete and calcium carbonate precipitation due to their activity. In contrast, similar to former case, dead and live cells did not improve the compressive capacity of the specimens.

Ghosh *et al.* [45] investigated the use of micro-organisms to improve the strength of cement mortar, by adding bacteria from genus *Shewanella* and *Escherichia Coli* to cement-sand mortars. They obtained an improvement of 25% in compressive strength after 28 days with the first bacterium when a cell concentration of 10^5 cells/ml of solution was used, while the latter wasn't able to improve mortar capacity. So far, they concluded that the increase of compressive strength is not a common property of bioconcrete.

The study by Jonkers [42] mentioned in earlier section showed that the addiction of a high number of bacterial spores leaded to a 10% decrease in the compressive strength of concrete measured at 3, 7 and 28 days. He even reported that many organic compounds, when added to the mix, showed some reduction in concrete compressive strength, which could be lowered to 50% of control specimens' strength by adding calcium acetate or could be totally lost by using peptone. Only calcium lactate revealed to be totally compatible.

Ramachandran *et al.* [37] tested mortar cubes in which *Bacillus Pasteurii* and *Bacillus Aeruginosa* were suspended with saline or phosphate buffer and compared the results with control specimens. Saline medium revealed a significant decrease in the compressive strength of concrete, probably due to the presence of chloride ions. Cubes prepared in phosphate solution showed otherwise a consistently higher strength. However, even in this latter case, a decrease of strength was noticed for the higher cell concentration in solution. Concerning the presence of biomasses, the study focused on adding dead or alive or combination of both cells of *Bacillus Pasteurii* in equal proportions . The results highlighted that an increase of compressive strength in cubes that contained all the form of biomasses. In particular, the 7-days-compressive test increased with the increase of cell concentration, regardless of their form. At 28 days, the compressive strength was enhanced by adding either live or dead cells of both the bacteria together, whereas the admixtures composed only by *Bacillus Pasteurii* showed the opposite trend.

2.8.4. Pros and cons

Incorporation of bacteria in concrete makes it possible to repair wide cracks up to 460 μm after 100 days of water immersion, by utilizing only the capacity of bacteria to produce calcium carbonate.

Bacteria can also yield other benefits: depending on the type of micro-organism embedded, concrete strength can increase and its pore structure become more fine.

Though, the use of bacteria presents many difficulties. At first, bacteria must survive to the mixing process; one way to improve the strength of cells is to embed bacteria in synthetic capsules, but also this method can be not convenient due to the incompatibility that could occur between capsules and bacteria or due to the changing that capsules perform on the micro-structure of concrete.

If bacteria survive to the mixing process, a low pH level must be guaranteed to have a significant production of calcium carbonate. Moreover, bacteria need food to produce calcium carbonate and consequently also their nutrients must be added during the mix.

When the production of calcium carbonate occurs, some bacteria (urea-based) produce substances, such as ammonium, toxic for the human's health even if assumed in little quantities. Ammonium is toxic also for concrete's health, since it leads to the formation of nitric acid which can corrode the rebars.
However, these last problems can be solved by employing lactate-based bacteria, which do not produce urea or other toxic substances during their reactions.

Anyway, the idea to have bacteria, though inactive, in their own walls, might scare people and limited the use of this technology, which at the moment is anyway not ready to be employed on a real structure.

2.9. Fiber reinforced concretes

Fiber reinforced concrete (FRC) basically is a concrete containing fibers, which can be made of different materials.

The development of fiber reinforced concrete (FRC) started in the early sixties with the aim of reducing the brittleness of concrete. For twenty years different types of fibers were tested, such as glass, carbon, synthetic and natural. The effect of length of fibres and aspect ratio on workability was also investigated [46].
Later, in the early eighties, scientists began to focus on the ductility and toughness of FRC. Ductility is the measure of material's capacity to deform without cracking. With FRC the toughness of material, ergo the capacity to absorb energy before breaking, was improved, but ductility wasn't.
High performance fiber reinforced cementicious composites (HPFRCC) were the result of these researches. Different degrees of ductility were achieved and generally these materials presented a hardening response, totally different from the tension-softening showed by normal FRC.
The primary and most important distinction between normal concretes, FRC and HPFRCC can be observed in their behaviour under tensile stresses. Cement is a brittle material while FRC is quasi-brittle. It means that during tension-softening the deformation is localized onto a single fracture plane, where the crack opens. But, HPFRCC shows a strain-hardening deformation with the opening of multiple sub-parallel micro cracks and elastic stretching of the materials between them.
Engineered cementitious composites or ECC are a particular category of HPFRCC, originally developed at the university of Michigan, which has a moderate tensile strength (4-6 MPa) and a very high ductility (3-5 %). They are low fiber content materials (less than 2% by vol.) which can perform a synergistic interaction between fibers, matrix and interface to maximize the tensile ductility by the development of multiple micro cracks.

The cracks, even at ultimate load, don't see an increase of their width, which remains in the range from 50 to 80 µm. This width of crack is a characteristic of the material and it is independent by the presence or absence of reinforcing bar and reinforcement ratio [47].

According to JCI and RILEM definition, FRC might be included in the category of engineered self-healing materials: fibers are included in the mix from the beginning and have the function to limit the width of cracks when they occur. Hence, the volume to fill is lower and the mechanism of autogeneous healing is more effective .

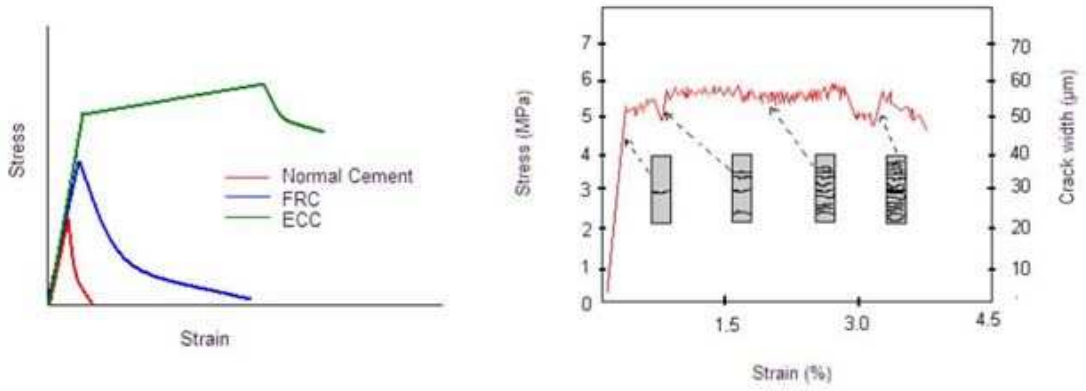

Figure 18: at the left: type of failure in cementicious materials; at the right: typical behaviour of ECC. Picture by Antonopoulos

2.9.1. Self-healing capacity of FRC

The attention of researchers in the field of self healing cementicious composites has been focused on ECCs, thanks to their intrinsic capacity of crack control and their ductility.
However, a few researches also focused on the capacity of FRC to self-repair.

Hannant and Keer [48] studied the autogeneous healing of thin polypropylene-fiber reinforced mortar sheets, by investigating the recovery of tensile strength and stiffness of cracked specimens after a long period.
After having induced multiple cracks (more than 20) in their polypropylene-reinforced specimens, Hannant and Keer stocked half of them in the open air and the remaining inside a laboratory, to prevent them from exposure to weather changes.
The specimens were retested after a period of 7 months to 2 years in direct tension. The results indicated that healing occurred and its effects were achieved almost completely after 7 months of weathering; the tensile strength of the healed cracks after two years in natural weathering conditions was about the 50% of the tensile strength of the uncracked samples of same age: healed cracks indeed started to re-crack at 6 MPa, while the cracking stress of virgin specimens was about 12 MPa. On the other hand, these specimens showed almost complete recovery of stiffness.
In contrast, no autogenous healing was observed in samples stocked indoor, nor was noticed a recovery of stiffness.

Gray [49] analyzed the self healing at the interface between matrix and fibers in fiber reinforced mortars. He carried out single fiber pull out tests on specimens tested at 7 and 28 days before healing which were then cured and tested again at 28 and 90 days respectively.
His results concluded that the apparent bond strength increased by a factor of 3 for specimens healed between 7 and 28 days and by a factor of 1.7 for samples healed between 28 and 90 days.
In this study, recovery of compressive strength was also analyzed. Grey remarked that the results weren't as important as in the previous case: some healing was noticed between 7 and 28 days, but the samples never recovered their strength completely. Furthermore, almost no healing was seen between 28 and 90 days.

Homma *et al*. [50] Investigated self-healing of FRCC with different reinforcements. Samples containing polyethylene fibers (PE), steel cords (SC) and hybrid fibers composites containing both PE and SC were casted. Tensile strength and permeability tests were performed to investigate self-healing after a curing period of 28 days in water after pre-cracking.
Different fibers and different volumes of fiber highlighted different behaviours in the specimens: the short PE fibers led to a quasi-brittle cracking and after the first crack occurred, there was an evident decrease of tensile stress.
Hybrid fibers improved the ductile behaviour of the specimens. The long steel fibers in fact created the strongest bonds, while the PE fibers were able to prevent the matrix from spalling after the steel cords were pulled out. Although the ductility improved, the rupture came after the diffusion of multiple cracks followed by a unique big crack.
Finally specimens reinforced with steel cords presented a lower strength and a little less ductility than the hybrid samples, with multiple cracks in a small range observed in certain cases.
Microscope observation was performed at 3, 7 and 28 days of curing. After 3 days, it was already possible to remark the formation of crystals in PE and PE plus SC samples due to the attachment both at the crack surface and at the PE fibers. But the specimens with steel cord didn't show attachment of crystals.

The authors concluded that this difference was due to the higher percentage in volume of fibers contained in PE samples, which constituted a network that supported the formation and increase of crystals between the faces of cracks.

Mihashi [17] reported that Koda *et al*. carried out an experiment on FRC similar to the above mentioned study by Homma [50]. They employed PE and PVA fibers at 1.5% by volume and investigated the self-healing of cracks caused by pre-loading. Their results concluded that the capacity to heal cracks thinner than 100 µm was about the same for both the fibers, but for larger openings, the chemical polarity of PVA fibers increased the capacity of the samples to self-heal.

Again Mihashi [17] wrote that Sanjuan *et al.* noticed in their study that FRC containing only 0,5% by volume of polypropylene and a water to cement ratio of 0.5 showed the capacity to self-repair in a corrosive environment.

2.9.2. Self-healing capacity of ECC and HPFRCC

Yang et. Al [24] investigated the self healing capacity of pre damaged ECC samples subjected to different wet/dry cycles. The experimental program was organized in two cyclic wetting and dry regimes to cure the specimens for 6 months: the first cycle consisted of 24 hours of conditioning in water at 20 °C followed by 24 hours of drying in a laboratory room at 21 °C, to simulate outdoor cycles such as the change from rainy days to unclouded days. The second regime consisted of immersion in water for 24 hours, followed by 22 hours of drying at 55 °C in an oven and 2 hours of cooling at 21 °C in a laboratory room, to simulate environmental cycles such the alternation among rainy days and uncloudy days with high peak temperature. Resonance frequency measurements, permeability and uniaxial tensile strength tests were carried out.
Yang stated that the crack widths in cement-based materials should be controlled to below 150 µm and preferably to below 50 µm to observe a recovery of the mechanical performances.
ECC materials have the capacity to undergo high tensile strains under load, while maintaining a width of crack under 60 µm up to failure.
The widths of these cracks are much smaller than the cracks which are usually observed in normal concretes with steel reinforcements. This characteristic of ECC makes the material ideal to develop durability and self healing of cracks, whereof width affects the process.
The results concluded that after at least 4 or 5 cycles, the full benefit of self healing could be achieved: resonance frequency was totally recovered and the stiffness was actually enhanced. Furthermore, Yang remarked that the temperature played its role in self-healing: the specimens subjected to the second cycle with the highest temperatures showed worse performances in terms of resonance frequency and even stiffness. These results are in contrast to those of Reinhart and Joss [16].

Ferrara et al. [51] tested the self-healing capacity of 500x100x30 mm beams, with fibers oriented both parallel and perpendicular to the bending tensile stresses. Beams where precracked after 2, 6 and 11 months aging and then exposed under different environmental conditions, in order to detect the effect of different humidities, temperatures or cycles on self-healing.
After one month treatments they found out that about all the mixes, under different exposures were able to recover at least 50% of the load bearing capacity lost upon cracking, but for the mixes exposed to dry air (50% relative humidity), which showed the worst healing behaviour.

Moreover, they stated that immersion time into water was more important when the crack width increased; in particular for COD = 2mm specimens must stay immersed at least 2 months to measure significant effects.

Tziviloglou [52] studied the self-healing capacity of PVA reinforced-ECC materials with low content of different micro-fibers and micro-particles.
Five different mixes were prepared: the first contained 2% PVA fibers by volume, three mixes employed PVA at 2% along with steel fibers at 0.5%, rockwool fibers at 0.5% and 4 grams of SAP polymers and the last one saw a reduction of the PVA fibers from 2 to 1% by volume and the addition of steel fibers at 2%.
The samples, 120x30x10 mm prisms, were fabricated and then tested after 7 and 28 days with four-point bending tests. For both the groups, some specimens were tested up to failure and others just preloaded up to 2mm (measured with a coupleof LVDTs) and then stocked for 28 days. Both water and air curing conditions were applied continuously for 28 days.
The results showed that the specimens were able to self-heal only after storing in water. The five mixes influenced the crack width and the healing behaviour of the material differently, where SAP polymers showed remarkable results by enhancing the reduction of the width of crack by 4 to 5 times in comparison to the control specimens.
Furthermore, Tziviloglou found out that the flexural strength of all the healed specimens increased more than that of virgin specimens cured in the same conditions, especially in the samples cracked at a later age, which showed the best recovery capacity. However, the regain of stiffness never reached the original values, although a recovery was observed.

Antonopoulos [53] worked on a complementary investigation in which high content of micro-fibers and SAP polymers in an ECC matrix were considered (**Figure 19**).
Her materials consisted of five mixes: the first contained 2% PVA fibers by volume, three mixes employed PVA at 2% along with steel fibers at 1, rockwool fibers at 1% and 8 grams of SAP polymers and the last one saw a reduction of the PVA fibers from 2 to 1% by volume and the addition of steel fibers at 2%.
She stated that a higher proportion of additives could negatively influence the recovery of mechanical capacity: the mixture by Tziviloglou [52] containing SAPs in a lower quantity attained 31% higher value in strength recovery and 18% in stiffness. Similarly, the mix containing PVA at 2% and the 0.5% of steel fibers improved the recovery of strength by 10% and the recovery of deformation by 16% higher value than the corresponding mix with 1% of steel fibers.

The capacity of ECC to control the width of crack makes these materials ideal even to prevent the penetration of aggressive agents, such as chloride ions.

Sahmaran et al. [47] conducted experiments on ECC beam specimens preloaded to different deformation levels and then exposed to chloride ponding. Cracked and uncracked ECC and steel reinforced mortar specimens were tested and their performances in terms of chloride penetration profile, depth and their diffusion coefficient were calculated as a function of the deformation level and were compared. Moreover, immersion tests were conducted on ECC and mortar cylinders to determine the chloride penetration depth as a function of immersion time. They found out that ECC chloride penetration depth was lower than the depth in mortar specimens at all the ages. This is probably due to the capacity of ECC to maintain the width of crack below to 50 μm, while in mortar samples the failure comes with the formation of one big crack that constitutes a weak point in terms of permeability as well.

Li [19] analysed the self healing of ECC under aggressive conditions, testing the specimens in a 3% NaCl solution, to simulate the sea-water conditions.
Li found that in this environment the specimens could self repair, but he remarked that their crack widths increased from 45 µm of air cured specimens to 100 µm and that they lost about 10% of their first cracking strength and ultimate tensile strength.
Chemical analysis showed that the chloride ions interacted with the interface between matrix and fibers and with the matrix, by the promotion of the leaching of calcium hydroxide, which increased the porosity in the mix.

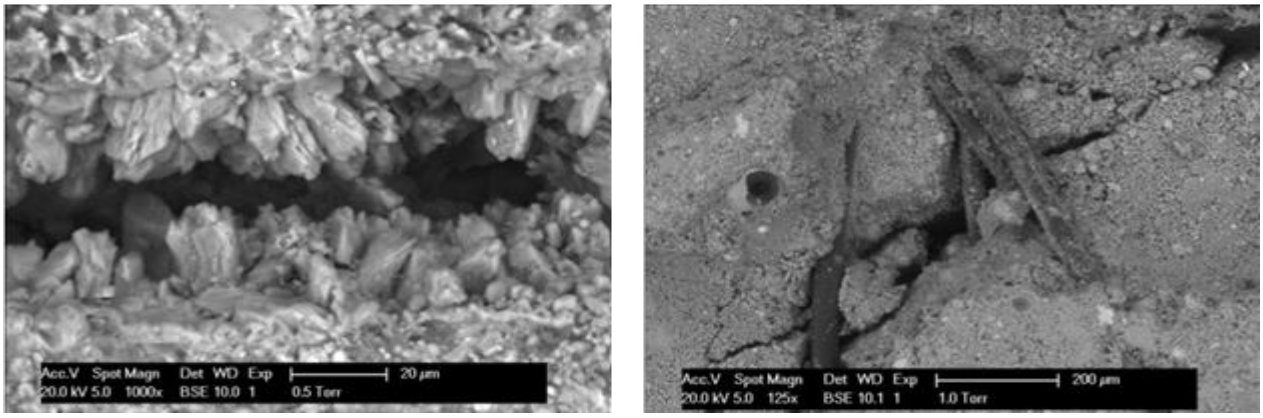

Figure 19: at the left: partial crack healing in an ECC with PVA fibers by Antonopoulos. The scale bar has a height of 20 µm; at the right: bridging effect of PVA fibers by Antonopoulos

2.9.3. Natural fibers to enhance the performances and healing capacities of concrete

The idea of employing natural fibers to improve the self-healing properties of concrete is relatively new.

In 2009 De Rooij et al. [54] published a paper on their research at the DTU, in which they studied the physical and mechanical properties of different types of natural fibers in order to prepare future works on self-healing of concrete.
Basically, De Rooij recognized the possibility of using fibers extracted from different plants or leafs, (such as larch, pine, lianas, sisal and similar) as vectors for carrying some healing agent in concrete.
These fibers indeed, are present in a large variety of sizes, ranging in length from 30 to 150000 µm and diameters from 5 to 800 µm. Moreover, they're environmentally friendly and available in wide quantities all over the world.
The characteristics previously mentioned, combined with the pore structure of the fibers, that can store in their holes and cell walls up to 0.5mm³ of healing agent per millimiter fiber length, would be ideal to act as a vial system as the glass hollow pipe systems on which it will be discussed in the next paragraphs.
Natural fibers have another fundamental characteristic that makes them suitable to be employed in concrete: their tensile strength and capacity to bond with the cement paste. Ranging from 130 to 900 MPa, the strength of natural fibers is comparable to the strength of polymeric fibers, such as PP (770-780 MPa), or steel fibers (1200 MPa).
Starting from the experience of ECC, it is possible to state that natural fibers can be used in substitution of PVA fibers in the cement matrix. Their length can be kept in a range from 8 to 12 mm, with an aspect ratio of 100 to 200. In respect to the PVA fibers of ECC, natural fibers should present a further characteristic: their strength should be lower than the strength of the bond that they form with the matrix. Otherwise, the

matrix would break before the fibers and the healing agent would not flow out, preventing the matrix from the required reparation.

The use of natural fibers in concrete has been widely studied later, in the contest of the international cooperation project *EnCoRe*, in which participated six universities all over the world. The project has the aim to investigate the physical, chemical and mechanical behaviour of concretes made out of recycled and natural components, to improve the sustainability of concrete production in building industry and its environmental compatibility.

Ferreira et al. [55][56] investigated the effect of natural reinforcements on self-healing of concrete.
In their project, after giving a characterization of the materials, they compared the effects of different natural fibers on improving the healing performances of a HPFRCC.
In the detail, they fabricated specimens whose matrix was reinforced with respectively sisal fibers, steel fibers plus eucalyptus microfibers, steel fibers plus sisal fibers, sisal fibers plus nano pulp, steel fibers plus a combo of sisal and eucalyptus fibers and only steel fibers as control mix. No coarse aggregates were employed, but the mortar contained only cement, slag and sand.
In order to quantify the healing, direct tension tests on prismatic specimens 300 mm long, with a section of 30x60 mm, were performed. These tests consisted of two stages: at first a pre-cracking phase was carried out and then, after scheduling the required conditioning period, the samples were loaded until failure.
Four points bending tests were performed as well. The specimens in this case had a length of 500 mm and a cross section of 100x15mm.
In both tests, different conditioning were tried after the pre-cracking phase. The specimens were subjected to immersion in water, open air, dry conditions with 50% of relative humidity, moist conditions with 90% of relative humidity and wet/dry cycles for periods of one, three and six months before reloading.

The preliminary results of the tensile test permitted to appreciate only a limited recovery, in terms of tensile stress after one month of water immersion and the precipitation of calcium hydroxide in the zones surrounding the reinforcing sisal fibers.
The same precipitation has partially occluded the cracks formed, due to the first bending tests, after one month of immersion in water.

Many works and studies still have to be conducted on the topic of natural fibers. Notwithstanding, the results achieved until now seem to be promising.

2.9.4. Pros and cons

Fiber reinforcement of concrete is a way for optimizing the process of material's autogeneous healing by controlling one of the parameters that regulate this property. The reduction of the width of crack due to the bonds between fibers and concrete matrix has the effect of reducing the volume of cracks to be filled during the reparation. Thus, less reactive material is needed to fill the fractures whose dimension can be contained.

By means of adding fibers, autogeneous healing is promoted also in normal concrete with higher water to cement ratio, since less reactive particles are needed to repair little cracks. Also, fibers create bridges between the sides of cracks and give a support to the forming crystals; this latter phenomenon increases its importance when high volumes of fibers are employed, for it contributes to distribute crystals along the entire surface of the crack's faces.

When reparation occurs, the filling material can locally establish a bond with the fibers' extremities stronger than the original bond between fibers and cement paste. Consequently, in HFRPCC it is possible that repaired cracks are stronger than the cement paste and new cracks open if the sample is reloaded.

Fibers are currently used in concrete industry and are totally compatible with the admixtures currently employed. This versatility is a characteristic that makes this technology simple and effective and opens the way to a combined experimentation along with the above mentioned methods to enhance self-healing in concrete. Especially, a combination of fibers and chemical agents, such as crystallizing agents or carbonates could be foreseen. Also, it might be possible to try the effect of fibers and expansive agents together, to investigate a possible effect of auto tension (induced by the expansive agent on the fibers) on self-healing.

The main cons linked to the employment of fibers can be the initial investment required to built an entire fiber reinforced concrete structure and the negative effect of fibers on workability, which could make difficult the operation of pumping and the vibration of concrete.
However, fibers in concrete are nowadays a reality which is knowing an important growth and promises lots of future developments.

2.10. Concretes employing polymers

Since 1990, the worldwide interest in polymer-concrete has become stronger, thanks to the research and development of high performance and multifunctional construction materials [57].
Concrete-polymer composites are made by replacing a part of the cement hydrate binder of conventional mortar or concrete with polymer. They can be classified into three categories:

- Polymer modified mortar (PMM) or concrete (PMC), which is a category of concrete-polymer composites made by partially replacing the cement hydrate binders of conventional cement mortar or concrete with polymers or polymeric admixtures.
- Polymer concrete (PC), which is formed by polymerizing a mixture of a monomer and aggregate, without other binding materials;
- Polymer-impregnated concrete (PIC), which is produced by impregnating or infiltrating a hardened portland cement concrete with a monomer and subsequent polymerizing the monomer in situ.

In the following paragraphs, the self-healing capacity of polymer-modified concretes will be considered.

According to JCI and RILEM definition, polymer-modified concrete can be included in the category of engineered self-healing materials.

2.10.1. Concretes with the addition of polymers in emulsion

Polymer modified concretes are mostly produced with polymers in dispersion or emulsion added to ordinary cement concrete during mixing. They are attractive materials because their production is really similar to the one of normal concrete.
Many different polymers have been employed in the last forty years for modifying concrete. Among them styrene-butadiene rubber latex (SBR), ethylene-vinyl acetate (EVA), polyacrylic-ester emulsion (PAE) and epoxy resin (EP) are widely used.

Tian *et al.* [58] referred to Ohama's step model for polymer modified concrete, to describe the effect of the addition of latex to normal concretes. According to it, the polymer particles would be, at the moment of mixing, uniformly dispersed in the cement paste. This particles would start to flocculate and deposit at the surface of cement particles since the hydration starts, creating a continuous close-packet. As the hydration goes on and the water is absorbed, this close-package would transform in a thin film which form a monolithic network around the cement particles.

Research on self-healing properties of polymer modified concretes is a relatively new topic. Not many types of PMC have been studied yet nor has been the interaction and behaviour of this polymeric film with the self-healing reactions.

Abd Elmoaty [59] studied the autogenous healing behaviour of concrete containing SBR latex and ACR (acrylic) with a solid content of about 52%. Different mixes were tested to investigate the different parameters which can enhance this property: the project focused mainly on the effect of the dosage of SBR, but even the effect of cement content, the type and the age of deterioration were considered.
100 mm cubes were employed in this research: after a 28 days long curing period they were tested up to failure and then cured again in water. UPV tests were conducted to determine the level of self-healing immediately after testing and then after 20, 40 and 60 days of conditioning.

The results showed an evident increase of UPV in the first 20 days; it means that the healing process took place in this period. Differently, in the period between 20 to 60 days, the rate of healing process decreased evidently. The authors concluded with stating that 20 days of curing must be enough to convert most of unhydrated particles to hydrated particles.
Among the mixes, the polymer modified concrete with the highest percentage of SBR showed the best increase in self-healing during the period between 20 and 60 days. Probably, it was due to the membrane of polymer formed around the unhydrated particles, which prevented them from the hydration, thereby retarding this process.
Cement content and water to cement ratio proved themselves to be important parameters to enhance self-healing. The lowest ratios showed the best healing, thanks to the higher availability of unhydrated cement to convert.
Moreover, the increase of the age of damage decreased the self-healing capacity.

Lukowski and Adamczewski [60] conducted experiments on concretes modified with epoxy resins (EP) without hardener.
Their method was based on the assumption that in a composite material, components can have separate structural and repairing functions. Following this idea, epoxy resin was directly mixed with concrete and constituted the 20% of the binder. At this quantity, the degree of cross-linking of epoxy resin (used without hardener) was about of 50%. The excess of resin remained unhardened into the pores of the hardened paste and at the occurrence of cracks could flow out and repair the voids (**Figure 20**).

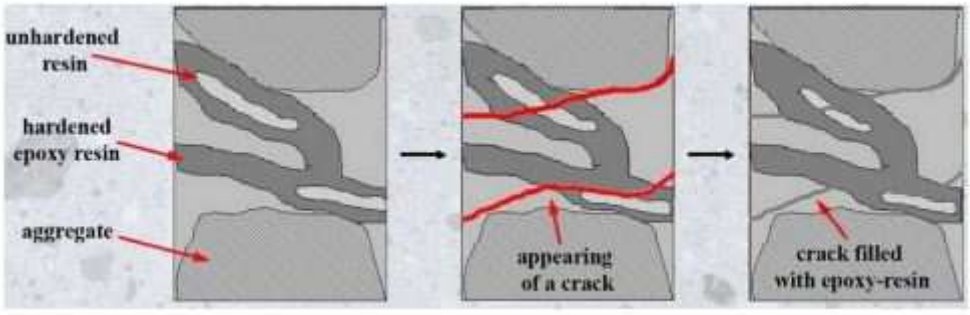

Figure 20: self-repairing by modification of concrete using an epoxy resin without hardener

Reparation after cracking would happen due to the accessibility of calcium hydroxide in the cement paste. Calcium hydroxide acts as a catalyst in the formation of cross-links in order to harden the resin when it comes in contact (**Figure 21**).

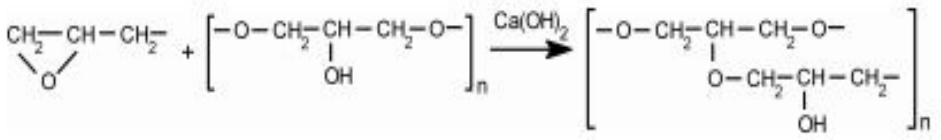

Figure 21: cross-linking of epoxy resin in presence of calcium hydroxide by Lukowski and Adamczewski

Flexural strength tests were carried out to evaluate the capacity of the samples and the degree of self-repairing after the preload. Moreover, compressive strength tests were also performed to characterize the material, which showed an ample decrease in permeability, compressive and flexural strengths whereas the tensile strength increased slightly.

Observation of the microstructure showed that the introduction of polymers in the form of conventional liquid resins, which have quite a high density, caused dispersion of particles, each independent of the others, both in the paste and at the interface with aggregates. On the other hand, the employment of an epoxy resin in emulsion led to the formation of a continuous film which coated the cement particles. This later revealed to be the best way to enhance the self-healing in the samples (**Figure 22**).

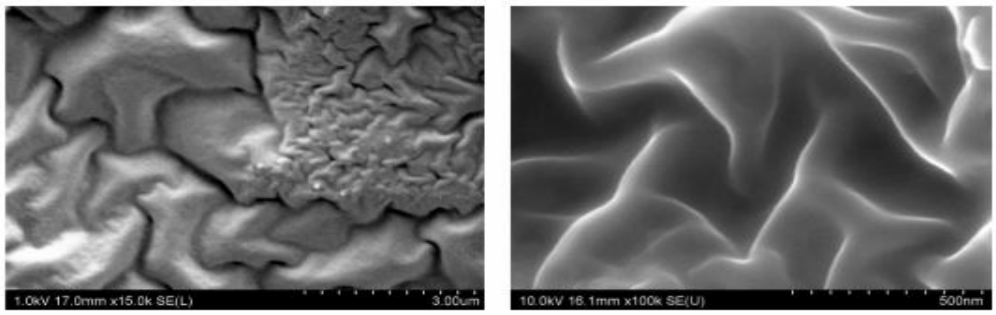

Figure 22: polymer film in epoxy cement composite by Lukowski and Adamczewski

Yuan [61] tested specimens containing ethylene vinyl acetate (EVA). Once a crack occurred, optical fibers embedded in concrete detected it and shape memory alloys (SMA) heated the material by the means of electrifying. With increase of temperature EVA, normally hard at room temperature, softened, melted and penetrated into crack, filling and sealing it.

2.10.2. Sap-modified concrete

Another family of polymers which have been widely studied are superabsorbent polymers (SAP). SAPs are cross-linked polymers that absorb, swell and retain large quantity of liquid without dissolving and depending on the pH degree of liquid, its salinity and the presence of various types of ions. For example, the free swelling of SAPs can reach values of 5000g/g in deionised water, where as it can decrease to 10 g/g and less in concrete pore solution.

Chemically, SAPs are described as copolymeric networks based on partially neutralised acrylic or acrylamide.

In concrete technology, these polymers have been employed for enhancing strength, internal curing, workability and prevent the adverse effects of shrinkage.

SAPs are added directly to the mix during casting. At this first stage, swelling is limited by the high pH of the solution (12.5-13). Furthermore, the swelling can also be limited by the calcium ions, which can form bidentate complexes with acrylates. Hydration of cement let the SAPs release water, thereby, leaving pores in concrete paste, the sizes of which range from ten to hundreds microns. These pores can be seen as defects in the paste, which will be intercepted by the occurring cracks. Again in contact with the environment humidity, SAPs are free to swell again (**Figure 23**).

Usually ground water and rain have a ionic concentration much lower than the pore solution. So, the swelling ratio is sensibly higher. In this way, SAPs can physically block the infiltration of water by obstructing the cracks. The progressive release of the water absorbed can favour the self healing process [20].

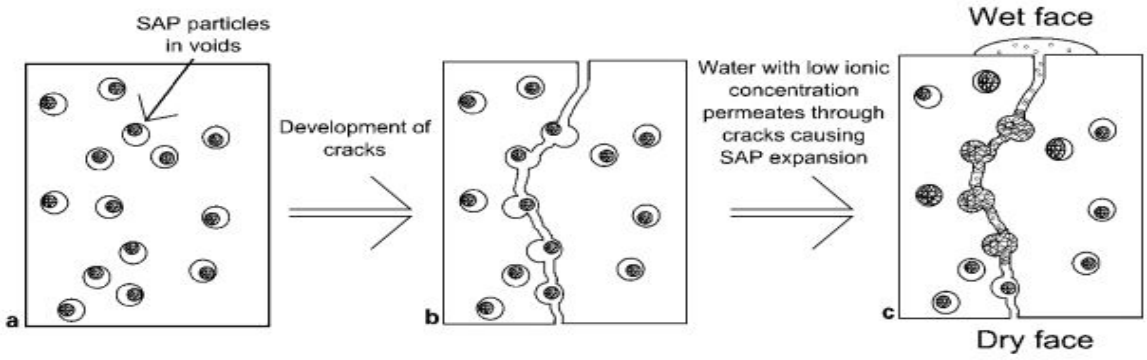

Figure 23: schematic showing potential mechanisms of self-sealing cracks using SAP by Lee

Lee [20] measured the flow rates of various solutions through a model crack containing SAPs in percentages which varied up to 1%. Specimens containing OPC and SAPs at 1% were casted and a microscope observation was conducted.

The results confirmed that the swelling of polymers in a pore solution was slight, while the reswell after the penetration of deionised or tap water in the crack resulted in a large increase of the swelling ratio. Microscopic observation concluded that the paste of concrete containing SAPs is full of pores due to the presence of polymer and at the interface between SAPs and the paste often results in large portlandite deposits and microcracks.

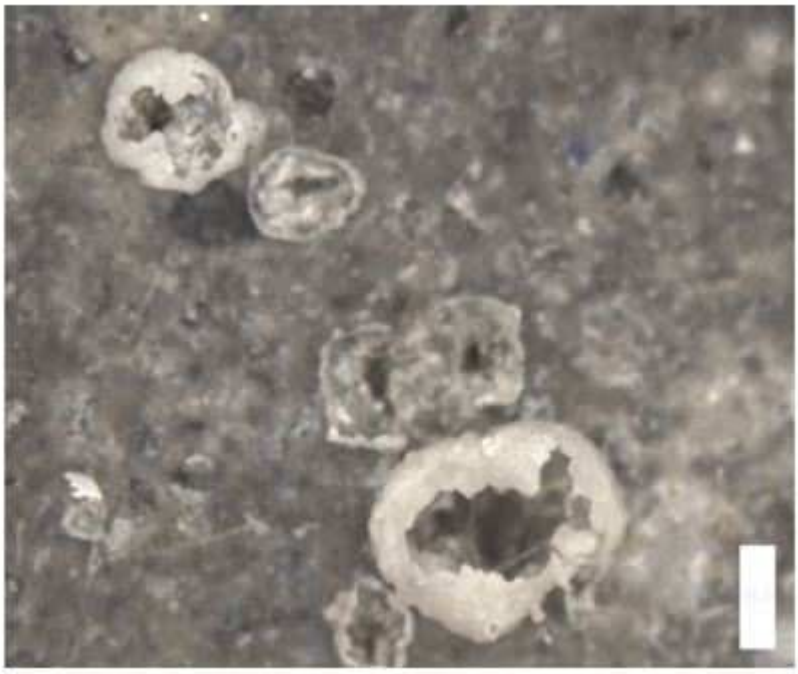

Figure 24: formation of $CaCO_3$ domes on the sample surface after shrinking of SAPs by Snoeck. The height of the scale bar is 500 µm

Kim and Shlangen [62] investigated the self-healing in ECC stimulated by SAPs under flexural cyclic loads.

Exposure cycles (wet/dry), open air and water represented the curing condition of the samples after cracking. The specimens subjected to wet/dry showed an improvement in their mechanical behaviour during the first two cycles; after that, no improvement of mechanical characteristics was observed. Kim and Schlangen concluded that this behaviour is due to the reaction of unhydrated cement, that is consumed after the first two cycles.

Snoeck et al. [21] studied mortar mixtures with fiber reinforcements and varying amount of SAPs. Four-point bending tests were performed to investigate the mechanical capacities and the regain of strength in the mix and water permeability tests were conducted to measure the sealing capacity of these materials.
Various curing conditions were applied. It was found out that when not completely submerged in water, only admixtures containing SAPs showed self-healing due to moisture uptaking. Humidity condition of more than 90% could be compared with wet/dry cycles, due to high capacity of SAPs to retain water. For this reason, Snoeck concluded, SAPs can be useful in environment with almost no rain, as they absorb water from the air and provide it for stimulating the deposition of $CaCO_3$ (**Figure 24**).
Also, the results concluded that a very high percentage of SAPs in the mix (more than 1%) led to a decrease in peak strength and first-cracking strength, due to the voids formed in the paste.

Snoeck's results were confirmed by the complementary works on self-healing of ECC containing SAPs performed by Tzivilouglu [52] and Antonopoulos [53]. They found out that the increase from 1% to 2% by mass of the polymer led to a great decrease in strength and stiffness recovery.

2.10.3. Pros and cons

Polymer modified concrete represents a relatively new field, which can be considered likely, for the possibility they offer of manipulating and enhancing the characteristics of concrete. Such as the mechanical characteristics of concrete, the healing properties of many possible mixes still have to be studied. Only a little experimental investigation concerning healing was carried out on the most common modified concretes: attention was indeed paid to latex, epoxy resin and recently to SAP-modified concrete; though, much more researches have to be conducted to completely understand the nature of the modifications and their effects on the self-healing capacity of the material.

Regarding latex modified concrete, it seems that the most part of its self-healing capacity is exploited during the first 20 days of conditioning, due to the progressive formation of a film around the cement particles, which slows the hydration of unhydrated cement that, after cracking, is in contact with water or moist.
Similarly, the modification of epoxy resin revealed the formation of a film around the particles and seemed to fill the cracks, by naturally reacting with calcium hydroxide present in the paste.
However, it still has to be clarified whether the recovery after precracking is due to self-healing or only to cement hydration, this latter retarded by the filtering action exerted by the polymeric film.
Moreover, the worsening of some mechanical performance of concrete, represents a limit for the possible employments of the material. The actual use of latex-modified concrete as material for bridge and road desks could be confirmed and an effective self-healing capacity would contribute to its interest for these applications. At the actual state of the art, also a concrete modified with epoxy resin could cover a secondary function in structural applications.

The most interesting polymeric modification from the point of view of self-healing is the one realized by the addition of SAPs to concrete. When SAPs' content is confined to little percentages by volume (no more than 1%), concrete's mechanical characteristics are only slightly influenced. Furthermore, SAPs act as internal reservoirs which capture water when cracks occur and expose them to the external environment. For their nature, they can absorb water also from the air moisture and for this reason their application is interesting in dry environment, where normally autogeneous self-healing could not occur due to the absence of water in high concentrations.

On the other hand, a limitation in the employment of SAPs is determined by the decrease in their swelling capacity when the absorbed water is rich of dissolved elements. Also, the quantity of water they can absorb is limited because of the necessity of keeping the quantity of polymer low. Consequently, their influence on self-healing will be limited.
Anyway, among the above described systems, SAP modification seem to be the only one suitable for a normal structural application.

2.11. Concrete with capsules

Microencapsulation can be described as the process of enclosing different sized particles of solids, liquids or gasses in an inert shell, which isolates and protects them from undesirable reactions with the external environment.

According to the above described definitions of JCI and RILEM, concretes containing capsules owe to the category of *smart or intelligent materials*. As reported by Mihashi [17] and represented in **Figure 25** in fact, capsules are able to sense the crack (sensing function) and automatically release the healing agent (processing function), which fills the crack (actuating function).

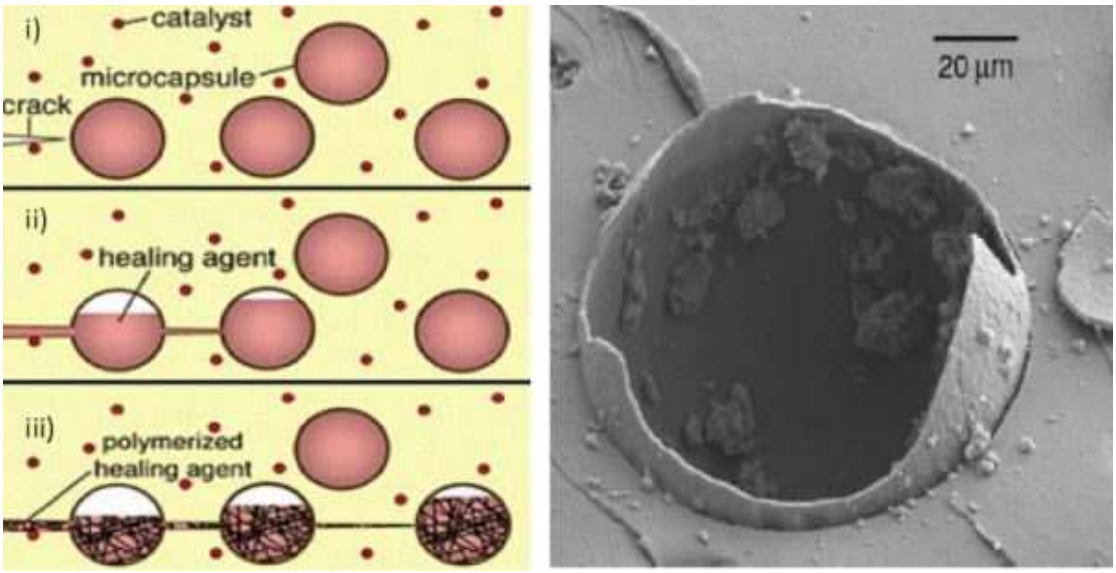

Figure 25: (a) basic method of the microcapsule approach: (i) cracks form in the matrix; (ii) the cracks rupture the microcapsules, releasing the healing agent through capillary action; (iii) the healing agent contract the catalyst, triggering polymerization thus ensuring the closure of the nearby cracks and (b) ESEM image showing a ruptured microcapsule. Image by Van Tittelboom and D Belie

However, micro-capsules are usually incorporated into concrete in advance, during the mix phase. Because of it, it is possible to operate a further classification, which allocates these systems in the category of *autonomic healing systems*, where is performed a *passive self-repairing*.

In these way, the outright microencapsulation can be distinguished by other encapsulating systems, such as the vascular ones. Vascular systems properly consist in *engineered healing systems,* where generally a more or less developed network of hollow tubes containing the healing agent is embedded in the cement matrix. In some kind of these devices, is usually present a couple of proper sensor and actuator which activate the controlled release of the sealing agent in case of cracking. We speak in these case of *activated-repairing systems.*

The following paragraphs will present and describe the different types of capsules employed in literature in both automatic and activated-repairing systems, focusing on the employed materials, the pros and the cons of each method.

2.11.1. Autonomic healing in encapsulated materials

White [63] is the father of the encapsulation systems. In 2001 he investigated this approach inthe polymeric composite, embedding microcapsules containing an healing agent into a polymeric matrix in which was present a catalyst.

The idea is to embed into the cement matrix a healing agent with an engineered structure, typically spherical or cylindrical. When capsules are broken by the occurring cracks, the healing agent is supposed to flow out and react in the region of the damage. Some agents react in contact with air, moisture or heating; others can react with the cement matrix; others finally can be activated only in presence of catalysts directly mixed with the cement paste (mineral admixtures) or embedded in capsules.

Capsules can be spherical or cylindrical, with external diameters in the range of 4.15 to 4000 μm for the spheres and 40 to 7000 μm for the cylinders. These last can have varying from 15 to 250 mm. The shape is due to the fabrication process, which generally consists for the spheres in an *in-situ* polymerization of an oil-in-water emulsion.

Capsule shells can be fabricated with different materials, that must be chosen carefully to avoid the arising of malfunctions in the mechanism. As Van Tittleboom [64] reports, the points to consider are:

- Survival to the mixing process;
- Influence of mechanical properties and workability;
- Compatibility with the healing agent and the cement matrix;
- Probability and release efficiency of the capsule and healable crack volume

2.11.2. Survival to the mixing process

Capsules have to resist during the mixing process, when they can be in contact with the aggregates present in the mixer. Additionally, the release of the healing agent can occur only if the bond between the capsules and the cement matrix is stronger than the ultimate strength of the capsules; in this last case in fact, the crack wouldn't be able to pass through the capsule, but would interest the interface between the shell and the paste, preventing the release of the healing agent.

Because of these reasons, generally brittle materials are employed and capsules thickness is optimized. Schlangen [16] reports for example that Thao *et al.* tested hollow glass and perspex tubes as encapsulating vehicles for epoxy resin. The higher ductility and strength of perspex delayed the rupture, so glass was finally chosen (**Figure 26**).

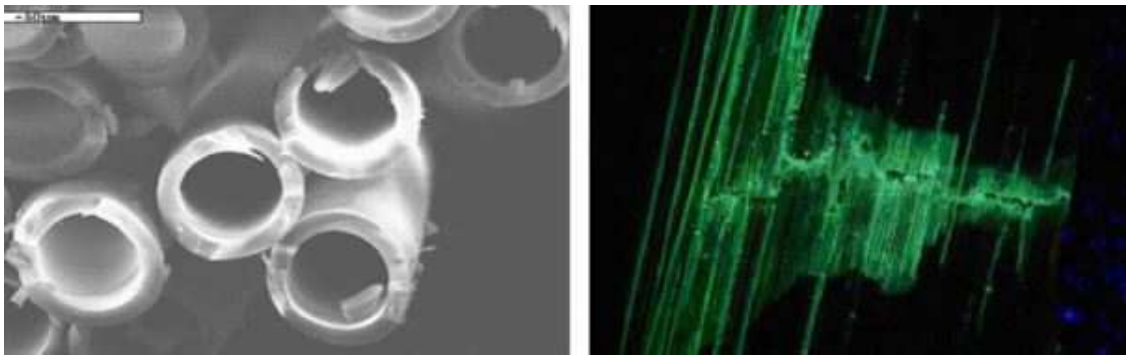

Figure 26: (a) hollow glass fibers and (b) damage visual enhancement in composite laminate by the bleeding action of a fluorescent dye from hollow glass fibers. Image by Van Tittelboom and De Belie

Sometimes capsules can combine a proper shell with a layer designed to protect the container during the mix. Van Tittleboom [64] wrote that Dry proposed a system in which cylindrical capsules were protected during the mix by a water soluble glue.

Van Tittleboom [64] also reported that Xia studied in his MSc thesis the encapsulation of SAP polymers protected by a cement plus paraffin layer.

Again Schlangen [16] described Pang *et al.*'s experiments, in which capsules were coiled with a spiral steel wire, followed by a thin mortal layer, to prevent them from premature damage.

2.11.3. Influence on mechanical properties and workability

Capsules might affect the mechanical performance of concrete. Huang and Ye [65] tested specimens in which a sodium silicate solution was stored in sponge capsules of 5 mm diameter. They remarked that flexural strength was reduced by 27%, while the maximum deflection by about 50%.

Pelletier *et al.* [66], similarly to the above mentioned authors, tested a sodium silicate solution stored in polyurethane capsules, whose diameters varied from 40 to 800 μm. Comparing the results of compression and flexural strength of control and healing samples, they found out that the final strengths did not change, rather sometimes were increased.

Van Tittleboom [64]reported that Feng *et al.* Used UF (urea-formaldehyde) spherical microcapsules with a diameter of 120 μm, without noticing any decrease in compression strength.

It can be stated that if the diameter of the capsules is contained in the macro-pore dimensions the mechanical properties are not affected. For larger diameters or cylindrical fibers, a decrease of strength can be expected, due to the introduction of weak points in the concrete matrix. The same can be supposed for the workability: hollow fibers might have the effect of decreasing the workability as like as fibers in FRC, while spherical capsules should not affect it significantly.

2.11.4. Compatibility with the healing agent and the cement matrix

Capsules must guarantee a compatibility both with the strong alkali cement matrix and the healing agent. Generally, inert materials, such as glass [67][68][69] or ceramics [64] have been employed.

As reported by Schlangen [16], Thao *et al.*'s experiments on perspex hollow fibers showed a chemical interaction between perspex and the epoxy resin contained in the tubes, which led to visible cracks on the capsule surface.

However other polymers have been employed as encapsulating materials, as PP (polypropylene), PU (polyurethane), UF (urea-formaldehyde), EVA (ethylene vinyl acetate) and gelatin [64][66], giving good results.

Also nano clays [43][70] and silica [71] were sometimes employed. Van Tittleboom [64] quoted Kaltzakorta and Erkizia, who justified the employment of the latter material as a way to built microcapsules more compatible with the cement matrix, which may create a stronger interface between the shell and the paste.

2.11.5. Probability and release efficiency of the capsules and healable crack volume

The probability that the occurring crack would hit the embedded capsules is determined by several factors, which concern capsule size and distribution and crack size and length.

Actually, it can be said that the probability of hitting capsules increases when the diameter of the spheres or the length of the hollow fibers increases. In terms of shape, cylinders will most likely break for two reasons: at first their characteristic length and its distribution in the specimen increases the probability of the crack crossing through; furthermore, this brittle hollow fibers easily break without being pulled out, while sometimes the spheres bond is stronger than the shell-matrix bond and crack does not interest the capsule.

As Van Tittleboom [64] reported, capsules might create weak points in the cement matrix and the probability of rupture for cracks through them increases. For example, it may occur when the capsule dimensions are bigger than the macro-pores, or when defects are present.

Some statistical models have been proposed to predict the probability of a crack hitting spherical capsules. Zemskov *et al.* [72] developed two methods to calculate the optimum number of capsules and size to be applied in a self-healing material. One of the models simplifies the specimens as a layer structure with spheres randomly embedded, while the other considers a casual embedding of spheres in a homogeneous structure. In both of them probability is an explicit function of particle size, crack size and healing agent content ratio.

Huang and Ye [73] proposed an analysis based on Montecarlo method, under the hypothesis of spherical shells which always can break in contact with crack. Their study started from the variation of probability for a determined fraction of broken capsules with a 5 mm diameter, to the investigation of the optimum size of the capsules in relation with their volume percentage. To give an idea of the numbers, for 5 mm diameter spheres, they find out that the probability to break with a crack more than 6% of the capsules in the specimen is almost zero, while the value 1 corresponds to the probability to break 0,5% of the embedded capsules.

A high probability of crack hitting capsules is not the only parameter that influences self-healing. It's in fact important that the release of the agent would be easy. Such a problem does not occur in case of spherical capsules, while can be a critic point of cylindrical capsules, depending on their diameter, their length and the material they are made of.

When the healing agent is contained in an hollow fiber, after the occurrence of the crack, it has to overcome the capillary force in the tube to flow out (**Figure 27**). Sometimes the crack width is larger than the diameter of the tube and exercises a lower capillary action, so the agent can partially remain in the broken capsule.

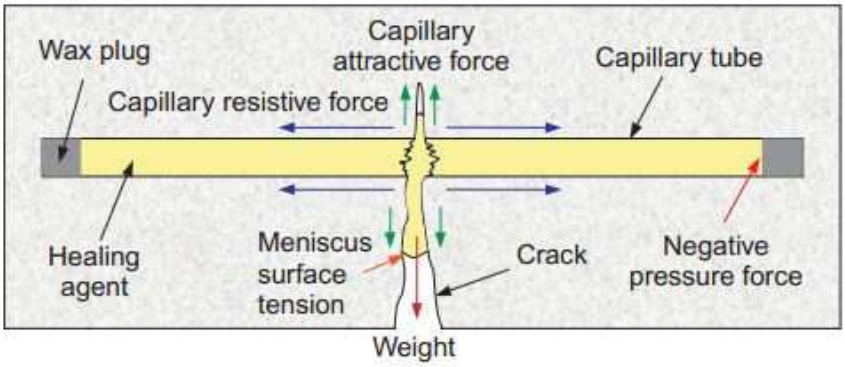

Figure 27: schematic illustration of the forces acting on an internally encapsulated healing agent

This evidence was exposed for example by Joseph *et al.* [68] that tested mortars containing long hollow glass fibers filled with cyanoacrylate. They stated that the local released volume of healing agent was minimal if compared to the volume contained in the tubes and they observed that this evidence did not occur in the experiments of ECC conducted by Li [67], where tubes presented multiple cracks.

To avoid the retaining of healing agent, the crack widths should be contained in the diameter of the tubes, in order to assure capillarity forces higher than the ones exerted by the tubes. Otherwise as Van Tittleboom [64] suggested, it would be possible to employ encapsulating materials that are repellent to the encapsulating healing agents.

The last important parameter which determines the efficiency of healing is the quantity of healing agent, since in encapsulated traditional systems it cannot be replaced. Van Tittleboom [64] attested that Fang *et al.* remarked the shortage of healing agent when employed spherical capsules filled with epoxy resin.

Mookhoek [74] developed a simulating model based on a representative volume space, where the capsules, featuring a spherical or elongated shape, are randomly positioned, in order to calculate the amount of healing agent released at a particular crack plan from a particular shaped capsule.
He obtained that, given the volume and the quantity of capsules by volume, the calculated release of healing agent per unit area is always less than the one calculated in case of cylindrical capsules (**Figure 28**). Furthermore he discovered that varying the length to diameter ratio for a fixed volume of a cylindrical capsule corresponded to an additional volume released. It implicates that fixing the quantity by volume of cracks, the performance can be optimize chosen the optimum length to diameter ratio.

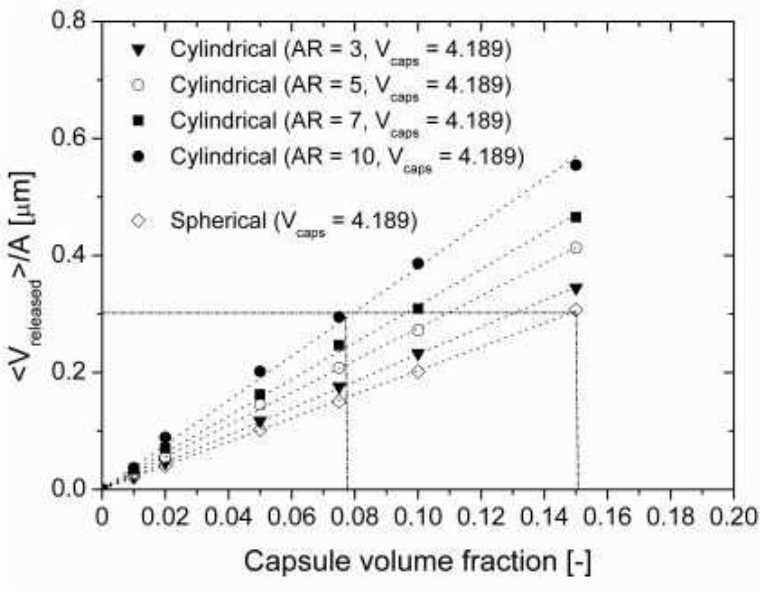

Figure 28: calculated average released volume as function of the capsules concentration for different values of aspect ratio

2.11.6. Classification of encapsulated materials

Encapsulated healing agents can be classified on the base of the mechanisms they employ to trigger the healing actions. One first distinction is done between agents designed to heal the cracks and agents designed to seal the cracks with a polymeric composite.

In literature different methods have been employed to heal the cracks. The easiest way to pursue this aim is to stimulate the mechanisms of autogeneous healing, such as carbonation and further hydration, encapsulating water.

Janssen [75] tested paraffin spherical capsules with a 90 µm diameter, which presented a central core filled with water. Even if these capsules were homogeneous, evidences showed that they lost 60% by water in six days. Since the microscopic analysis did not highlight any defect which could constitute a direct link from the internal core to the external environment, Janssen attributed the inconvenient to a diffusion mechanism of water through the paraffin shell.
Another way to store water inside the cement matrix is to employ superabsorbent polymers (SAP). Two methods can be followed: it's possible to embed SAPs directly in the mix without any encapsulation. Otherwise SAPs can be encapsulated before being added to the mix. Van Tittleboom [64] reports that Xia followed this latter way to test the self-healing of engineered cementitious composites, embedding SAPs in cement plus paraffin spherical shells.

Capsules have also been employed as carrying agents for bacteria in concrete to avoid their death during the mix process.

Wiktor and Jonkers [43] employed a two-chemical-healing agents in which spores of a bacterium homologue to *bacillus alkalinitrilicus* were embedded with calcium lactate in nano clays.
Wang *et al.* [76] employed diatomaceous earth (**Figure 29**) to protect ureolytic bacteria from the high-pH environment of concrete. They noticed that diatomaceous earth could immobilize bacteria and guarantee a protected micro-environment, which increased the ureolytic activity of bacteria by 12 to 17 times, comparing with unimmobilized bacteria.

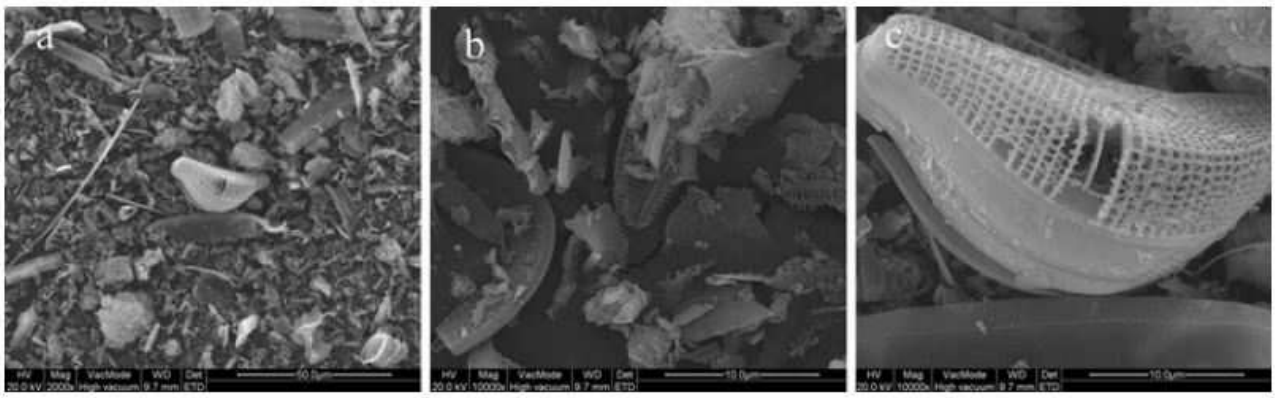

Figure 29: morphology of the diatomaceous earth powders

Wang *et al.* [40] again studied the use of polyurethane and silica gel cylindrical capsules as bacteria protection. They find out that silica gel immobilized bacteria exhibited a higher ureolytical activity than the polyurethane embedded bacteria, with deposition of 25% by mass for the firsts and 11% by mass for the latter.

Self-healing can be triggered employing chemical agents that stimulate the production of CSH. Different scientists employed for examples sodium silicate solutions that react with the calcium hydroxide present in the cement matrix to form amorphous products as CSH that fill the cracks.

Huang and Ye [73] tested the self-healing capabilities of engineered cementitious composites in which 5 mm diameter capsules were used to carry the healing agent. Thanks to the ESEM observation, they concluded that filling products consisted of CSH formed in the reactions of calcium cations present in the paste with the sodium silicate solution. However, they stated that calcium ions were not sufficient to replace all the sodium cations in the solution, thus sodium silicate crystals could be seen after the evaporation of the water.
Pelletier *et al.* [66] stored the same sodium silicate solution in polyurethane spherical microcapsules and obtained a partial healing of the cracks by the formation of CSH.
Sisomphon and Coporoglu [70] tested the employent of an encapsulated sodium monophluorophosphate (Na_2FPO_3) solution to create a self-healing system in blast furnace slag mortars.
They found out that the solution reacted with calcium hydroxide, increasing the amorphous phase and improving the porous structure and the properties at the interface between aggregates and cement matrix. Fluorapatite $Ca5(PO4)_3F$, carbonate fluorapatite $Ca5(PO4,CO_3)_3F$ and numerous amorphous humps were recognized with ESEMs investigations.

In order to fill the cracks resins and polymers can also be employed.

Yang *et al.* [71] tested cementitious composites containing silica gel capsules with oil core. They proposed a two-components system in which the healing agent consisted in methylmethacrylate (MMA) and the catalist consisted in triethylborane (TEB). When crack occurred, MMA and TEB went in touch and polymerized, sealing the empty space.
Li *et al.* [67] tested hollow glass cylindrical fibers carrying cyanoacrylate as a self-healing system for ECC, obtaining a regain in stiffness after the healing action.
Similar results were obtained by Sun *et al.* [69], who also investigated self repairing of ECC containing encapsulated CA (cyanoacrylate).

Joseph *et al.* [68] employed again the same system, that was unsuccessful due to the negative pressure exerted by the tubes on the healing agent, whose exit was prevented.
As reported by Van Tittleboom [64], many scientists employed epoxy resins encapsulated in glass fibers as sealant, also resulting in a total strength regain. However, as Joseph [68] stated, epoxy resins are employed as two-components systems, that cure the specimens in absence of oxygen. Therefore their encapsulation is unsuitable, since the presence of a minimal quantity of air in the capsule can cure the epoxy inside the shell, preventing the outflow of the healing-agent when cracks occur.
Van Tittleboom [64] reports that also polyurethane has been employed as sealing agent, remarking that only a partial recovery of strength was seen.

2.11.7. Vascular systems: engineered healing systems

Vascular systems consist of a more or less developed network of hollow tubes that connect the internal part of the structure with external environment, where *reservoires,* in which the healing agent is stored, can be placed.

Actually, these devices have been designed to solve the problem of the lack of healing agent . In fact, it's possible to maintain a constant level of healing agent and provide new material in case of latter cracking. The probability of crack passing through is almost a certain event, since these devices constitute weak lines inside concrete structures, which attract cracks.
Also, the problem of the compatibility with the cement matrix and the healing agent is automatically solved, because the cylinders are mostly made of glass, which is inert.

The dimensions of the tubes, such as the length and the diameter (at least 0.4 mm) suggest that a decrease of mechanical properties can be expected.

Furthermore, vascular systems cannot be normally added to the mixes, but need to be implemented with care. Hence, they cannot be employed in normal concrete structures, but are confined in laboratories.

Vascular systems can be classified into singular and multiple channel systems (**Figure 30**).

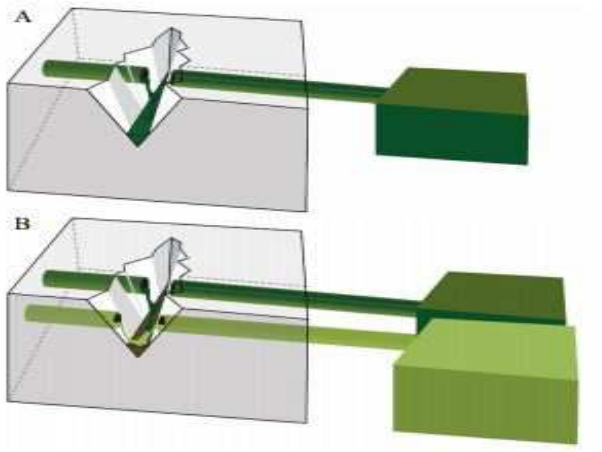

Figure 30: vascular based self-healing approache, reported by Van Tittelboom. Leakage of the healing agent from the tank via the vascular into the crack due to gravitational and capillary forces and eventual (hydrostatic) pressure. One channel (A) and multiple channel vascular systems (B).

Among the singular channel based systems, a further classification can be done based on the method of supplying the healing agent, type of agent and material of the tube.

Joseph *et al.* [68] and Sun *et al.* [69] embedded long glass tubes in concrete specimens. One extremity of these tubes was sealed by a wax plug, while the other was curved towards the upper side of the beams, to guarantee a pressure in the healing agent, cyanoacrylate. When the crack occurs, further healing agent can be manually provided via the open end of the tube.
Van Tittleboom [64] reports that Dry *et al.* tested miniature concrete frames in which hollow glass tubes were embedded. The tubes were kept in contact with the external environment and filled with healing-agent. Furthermore, Schlangen [16] wrote that Dry *et al.* tested the efficiency of filling tubes before and after the occurring of crack. He stated that it was better to provide en external reservoir with healing agent which is released once the cracks appear.

Again Van Tittleboom [64], wrote that Mihashi tested a system similar to the above mentioned one, in which human intervention wasn't necessary, since the healing agent was stored in a tank, directly connected to the tubes and placed at a higher level, to guarantee the flow of the healing agent. Stereochromies with alkali silica as healing agent and epoxy resin were tested as different solutions.

Sangadji and Schlangen [3] simulated the "spongious bone" structure to create a porous network in their concrete specimens. The porous cores were covered with PVA films and put in the middle of a bigger mould. Self compacting concrete cylinders were casted around them. During the tests, when cracks occurred manual injection of healing agent was possible to fill up or seal voids.
Furthermore they [77] implemented the system above with optic fibers as sensors of the damage state of the specimen and pumps as actuators for the supply of the healing agent and its diffusion from the pore core through the cracked specimen (**Figure 31**).

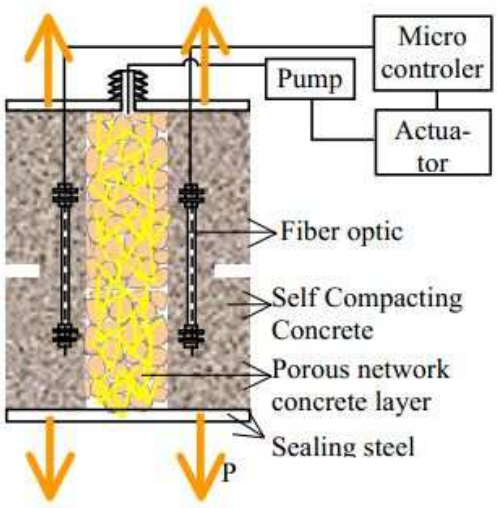

Figure 31: general concept proposed by Sangadji and Schlangen, which make use of porous network concrete

The idea of creating a store of healing agent directly inside the specimens was adopted by Pareek and Oohira, as Van Tittleboom [64] reported. These researchers provided holes inside the concrete, which were filled with epoxy by a syringe connected to an open end of the specimen.

Van Tittleboom [64] again described the multiple channel vascular systems of Mihashi *et al.* and Dry and Mc Millan. The first consisted of two glass pipes embedded in the cement specimen. These tubes were

connected to separated reservoirs, respectively filled with epoxy resin and a catalyst. When crack occurred, the agents got into contact and polymerized, hence, sealing the voids.
Otherwise Dry and McMillan employed a three part MMA to achieve the healing and instead of using glass tubes, they created holes throughout the length of the specimens by means of a steel rounded rod that was pulled out 24 hours after the casting.

2.11.8. Vascular systems: engineered activated-repairing systems

Among the vascular systems, some devices belong to a particular category that can be defined as *engineered activated-repairing systems.* According to JCI and RILEM, these devices represent an artificial and intentional method for filling and sealing of the crack and are designed in advance to respond to sensors, such as optic fibers or other intelligent materials, and some actuator, such as heating disposal or pumps.

In the previous paragraph, Sangadji and Schlangen [77] devices was already discussed.

Mihashi and Nishiwaki [17] reported their experiments on engineered activated-repairing systems. In 2006, Nishiwaki designed a devices which combined the functions of detection and actuation [78][79]. The sensor was a conductive composite, which included pipes made of heat-plasticity films that served the function of heating specific locations through electrification (**Figure 32**).

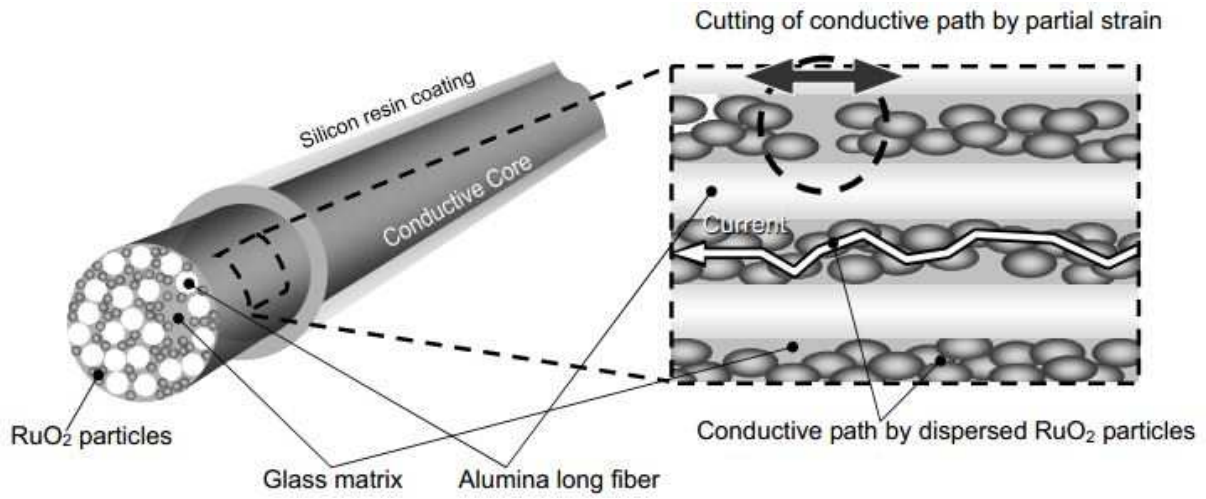

Figure 32: schematic diagram of self-diagnosis composite structure by Mihashi and Nishiwaki

The sensor monitors the strain in the specimen through a conductive path of dispersed particles. When a crack occurs, part of the electrical conduction path is cut off and the electrical resistance locally increases.
Mihashi and Nishiwaki [17] employed this system, by connecting the couple sensor-actuator to a healing device consisting of copper plates. Once the crack was detected, the increase in electrical resistance promoted the heat transfer through the copper plates and melted the healing supplier pipes; the healing agent- epoxy resin- flowed out and sealed the crack (**Figure 33**).

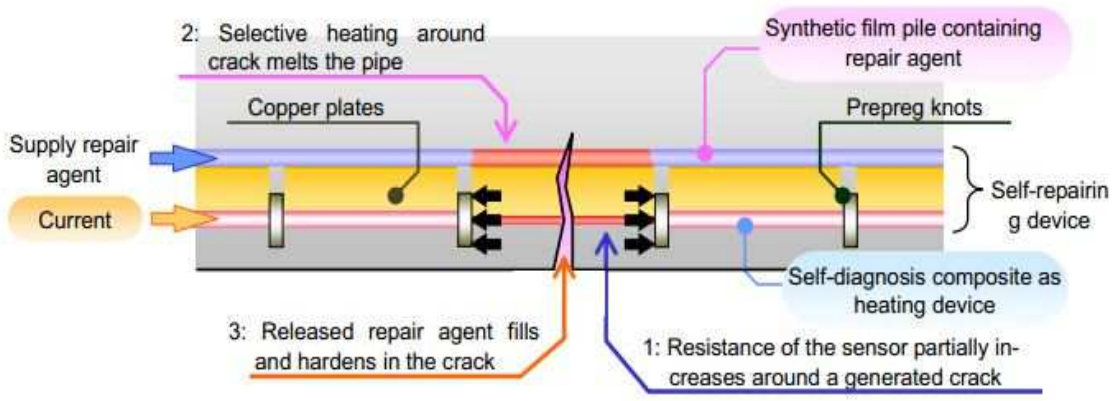

Figure 33: schematic illustration of activated repairing system by Nishiwaki and Mihashi

2.11.9. Pros and cons

Some traditionally employed healing agents for concrete, are added to repair the structure after the occurrence of cracks, due to the impossibility of a direct mix at the moment of casting. The reasons are different: the healing agent could react before the requested time because of the interaction with the components of the mix; also, it could flow through the internal pore structure or being destroyed due to the crashes with the coarse aggregates while mixing.

Encapsulation is the way to prevent the loss or reaction of the healing agent before time and to guarantee its internal storage in the structure.
The industry of nano-technologies is nowadays able to produces microscopic capsules made of glass or different polymeric or natural materials. Consequently, capsules can be compatible with all kinds of healing agents and the cement paste. Moreover, the employment of capsules makes possible the use of different healing agents together; this opens the possibility of adding materials which reacts together to repair concrete, such as epoxy resin with a hardener and increases the possible choice of agents to introduce in concrete in advance.
Different shapes of capsule can be produced, such as different dimensions can be chosen. Concrete strength is affected only when the dimension of the capsule is larger than the average dimension of the macro pores in the element. Designers can chose to embed macro capsules to create weak points in the elements and give a path to cracks; on the other hand they can embed a higher number of nano capsules and create a homogeneous material.

Unfortunately, when big cracks are expected, as it happens in normal concrete structures, nano capsules do not contain enough healing agent to fill the fractures. An effective result can be achieved only by employing macro-capsules, affecting the concrete strength.
Another problem due to capsules' size is that sometimes the flow out of the healing agent at the occurrence of the crack is prevented because of the capillary force exerted by the same capsule. It happens when capsule's diameter is smaller than the width of crack and only for cylinders.
As discussed in the previous paragraphs, shape does not influence only the flowing of the healing agent, but the probability of the occurring crack to hit the capsule. Small spherical capsules might create a bond between the shell and the cement paste weaker than the capsule's strength, favouring the pull out without breaking of the capsule. On the contrary, cylindrical capsules, usually made of glass, break easily.
However, only the 0.5% of the capsules embedded in an element has the certain probability to break.

The performed experiments seem to suggest that only big capsules guarantee an adequate quantity of healing agent for the repairing action if the width of the crack is large (wider than 150 μm). Unless an ECC or HPFRC is employed, allowing a reduction of the needed quantity of healing material, a normal concrete would have its strength affected by the addition of large amounts of capsules.
To guarantee a high quantity of healing agent and the possibility to refurbish, vascular systems were also tested, but these solutions are too complicated to be integrated in buildings or normal structures, which moreover would be weakened as experimented above.

At the state of the art, encapsulation does not seem really suitable for concrete structures, due to the actual difficulty in adapting capsules' parameters (such as dimension, shape, probability to be hit and quantity of carried healing agent) to the exigencies of strength of concrete. Also, cost to benefit should be investigated.

2.12. Conclusions

The present chapter started from the presentation of self-healing phenomena in concrete-based structures as a necessity due to economical and environmental factors.

In the first section, carbonation of concrete and chloride attacks have been described as the main causes of deterioration of reinforced concrete. Self-healing of materials has been illustrated as an answer to the problem of material deterioration, in order to increase the life-cycle of structures, by improving their durability.

The second section illustrated the background of research on self-healing of cement-based materials. A review of the past studies and research works has been written and the various methods have been organized in categories, highlighting the pros and cons of each one.

3. Experimental Program

3.1. Introduction

The present chapter presents the organization of the experimental investigation and is divided into four sections.

The first is a summary of the work and focuses on the different materials employed and the tests that have been performed.
After that, the properties of each addition have been described, in order to introduce the third section, which explains the process of fabrication of the specimens and presents the properties directly measured on the employed concretes.

Finally, the performed tests and their procedures are described.

3.2. Summary of the experimentation

The experimental program was divided into two parts. The first was conducted at Indian Institute of Technology of Madras and investigated the effect of different additions on the self-healing capacities of concrete.
The experiments were performed on beams of four different mixes with a conventional geometry of 150x150x700mm. The reference mix consisted of plain concrete. The second consisted of plain concrete reinforced with 20 kg/m³ steel fibers; the third of FRC containing a commonly employed crystallizing agent (Penetron admix) and the last was a latex-modified concrete, containing steel fibers.
The beams were moulded in traditional steel moulds, then demoulded after one day and stored in a mist-room for 28 days. 3 mm wide and 28 mm deep notches were cut on the 25th day of curing and then the specimens were again stored before testing.
Also nine 150 mm sides cubes were casted along with the beams in plastic moulds, then stored in the mist-room for the 28 days before testing.

The second part of this work, conducted at Politecnico di Milano, consisted of the investigation of the effect of a through-crack compressive stress on self-healing. The two FRC mixes with and without crystallizing agent replicated the FRC mixes previously casted in India and a compressive stress equivalent to one third of the residual stress at precracking was applied through an appositely designed setup.
Beams casted in Milan had a dimension of 150x150x600 mm. Fabrication of the specimens was carried out like in Madras, but notches were cut on the 19th day of curing, then samples were put again in the mist room until the day of tests.
Also in this second part of the investigation 9 cubes per mix were casted.

Compressive tests on cubes were performed in order to characterize the compressive strength of the employed materials and to determine whether the additions could influence the material compressive strength. In India these tests were conducted only after 28 days of curing, while in Italy cubes were tested after 7, 14 and 28 days of curing, in order to compare the obtained results with the curve proposed by EC2 to forecast the strength development.
Three point bending tests were performed both to characterize the flexural strength of the sample along with their capacity of bearing a residual load and to study their self-healing performance.
Tests were performed in order to pre-crack the beams after 28 days of curing in the mist-room.
In India an investigation of the effect of crack width was done, consequently beams were divided into two groups containing 7 to 8 specimens per type. The samples from the first group were cracked up to 4000 µm, while the specimens belonging to the second group were cracked up to 600 µm.
In Italy specimens were precracked only up to 600 µm.
Samples were then subjected to wet/dry cycles, by alternating one week storage in the mist-room and in the open air (external climate conditions in Madras and Milan are reported in the appendix). In Milan a compressive stress was applied.
After 30, 90 and 270 days the tests were finally repeated.

In the first part of the experimental investigation, UPV tests were performed before subjecting specimens to the bending tests at 0, 30 and 90 days, to measure their frequency both in the cracked and uncraked zone. Along with UPV tests, low permeability tests were performed. The aim was to try to investigate if cracks were progressively filling due to any self-healing reaction. Sealing of cracks would have resulted in a decrease of the wave speed through the sample and an increase of the time needed to the water to flow through the crack.

However, these latter tests failed, due to their incompatibility with beams geometry and in the second part of the work they were definitely abandoned.
In **Figure 34 - 35** a synopsis of the whole experimental programme is provided.

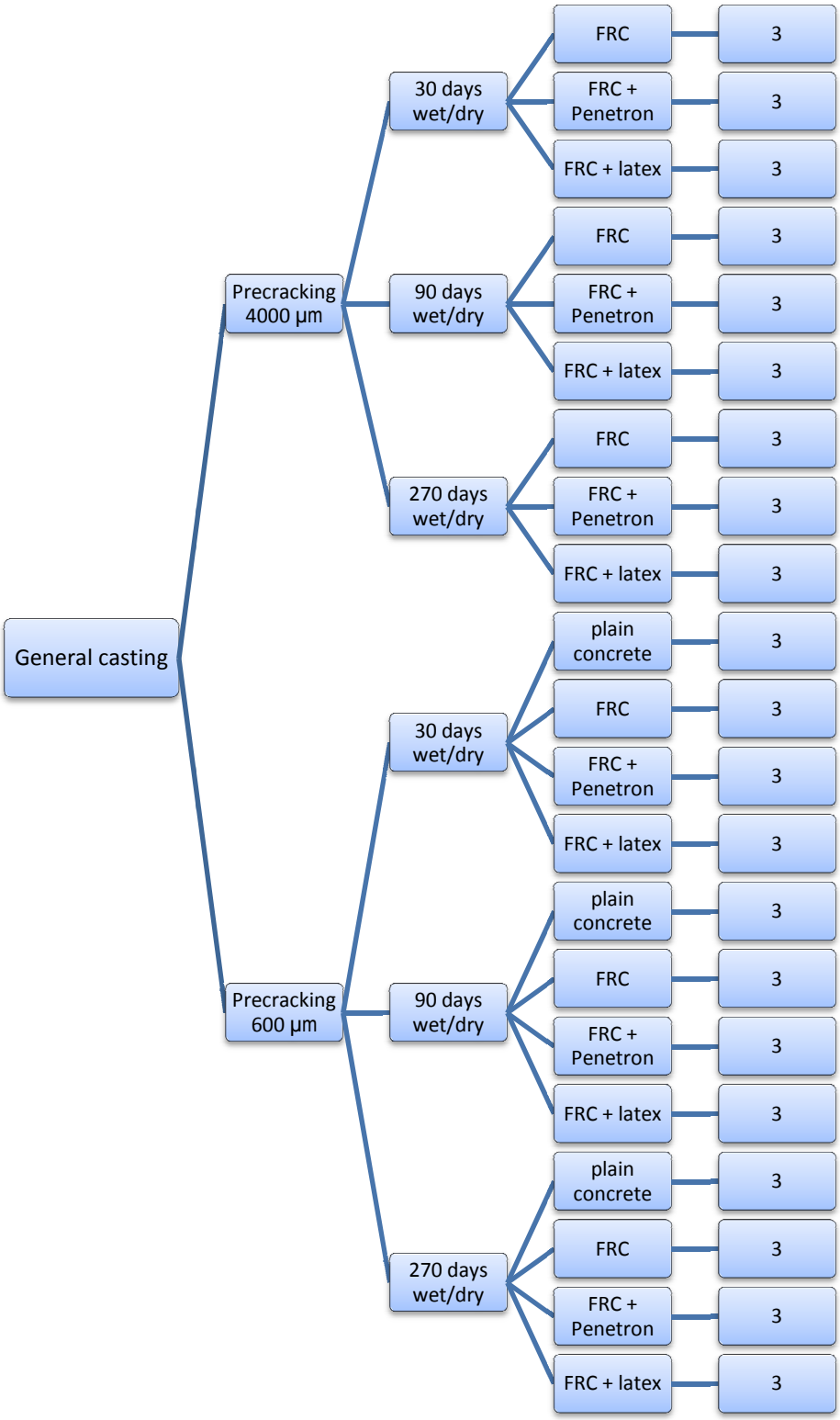

Figure 34: resume of the specimens casted in India. For each of them three point bending, UPV and low permeability tests were performed. Three samples per batch were tested after different conditioning periods

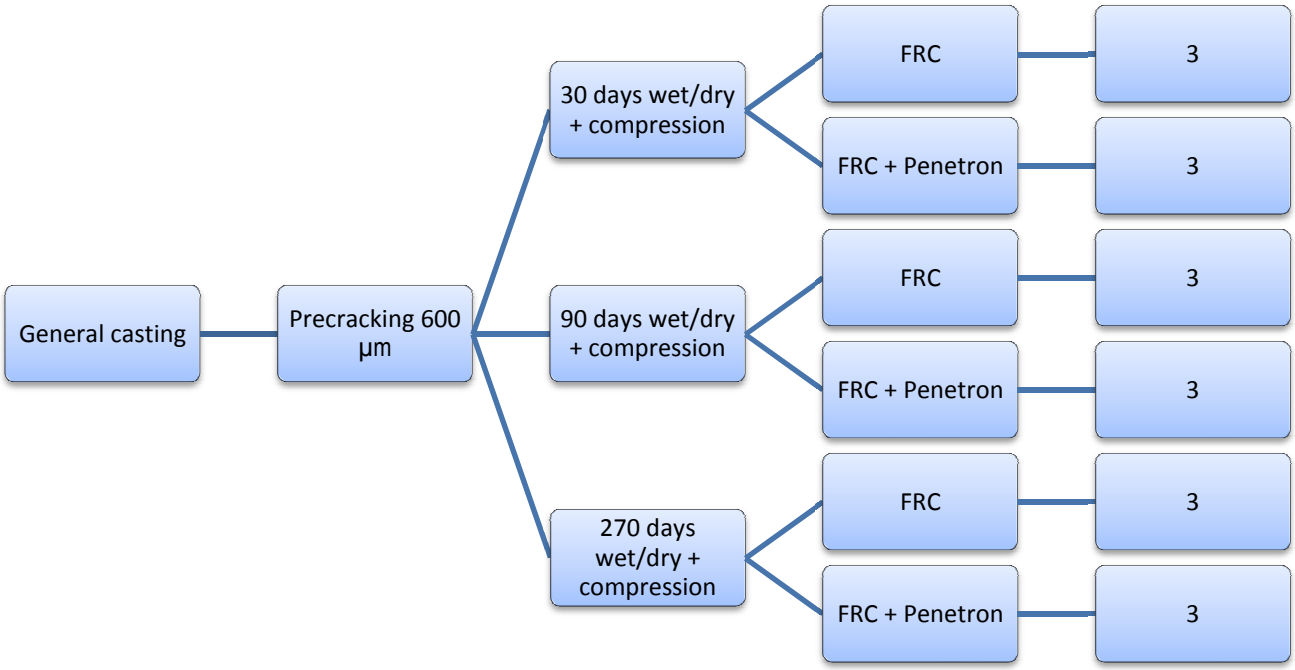

Figure 35: resume of the specimens casted in Italy. For each of them three point bending tests were performed. Three samples per batch were tested after different conditioning periods

3.2.1. Application of compressive stress

The second part of the present work, investigated the effect of a through-crack compressive stress on the self-healing capacity of concrete.

A compressive stress of 3.125 MPa was applied to the samples. This latter was calculated as half of the maximum residual stress measured on the samples at a crack opening of 600 µm.

The setup designed in order to apply the compressive stress (**Figure 36**) consists of a couple of steel plates 2 cm thick, reinforced with a couple of cross stiffeners of 1 cm thickness. Plates and crosses are coupled and connected by four threaded rods. Compression is applied by bolts: four are employed to fix the rods at the couple cross-plate positioned at the bottom of the specimen; four are used to tighten the setup from the top and apply the force needed to provide the requested stress by dynamometric key.

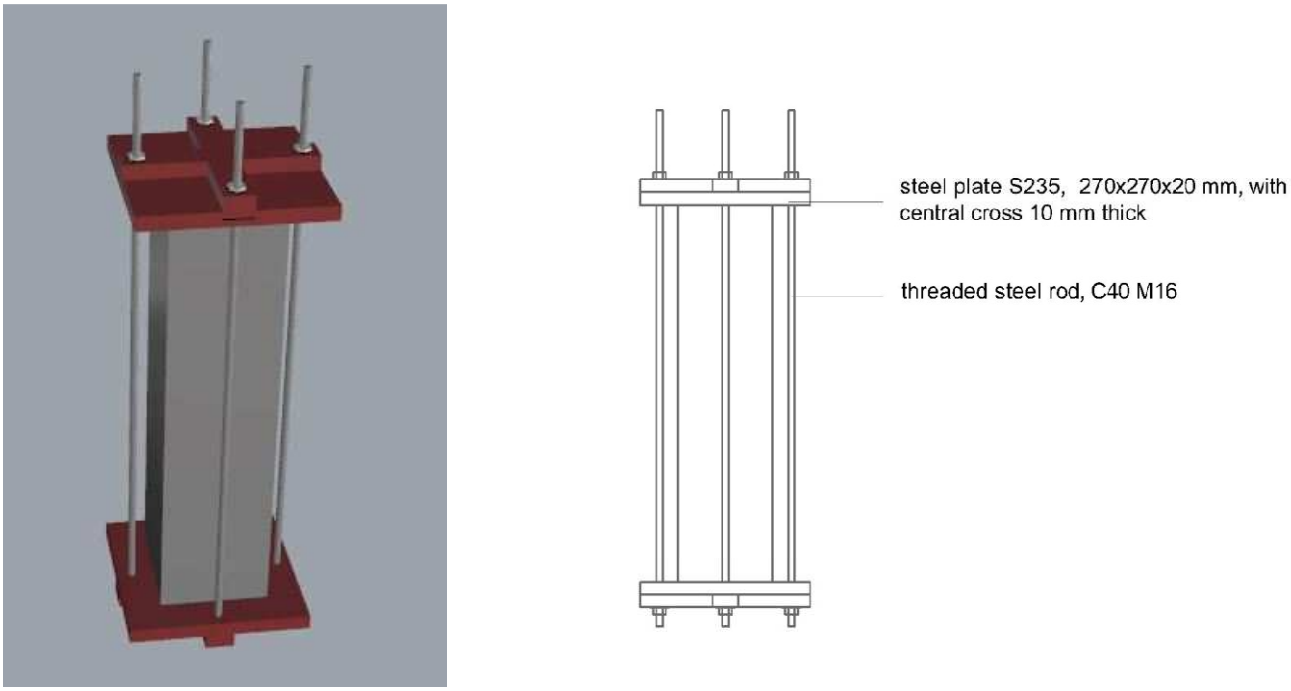

Figure 36: setup designed for the application of compression

Care was taken in order to design a very stiff system and avoid any undesired deflection of the plates. The design procedure is explained in its details in the appendix.

3.3. Characteristics of the employed materials

3.3.1. Constituents of concrete

The concrete matrices in this work consisted of Portland cement, aggregates, water, superplasticizer and self-healing engineering additions.

Plain concrete matrix designed for a conventional strength of 35 MPa was taken as reference to design all the other mixes. Three mixes employing steel fibers, steel fibers plus a commonly employed crystalline admixture and steel fibers plus SBR latex were casted.

Table 1 summarizes the constituents of each of the mix designs. Modifications to basic plain concrete matrix were not made due to the incorporation of the additions. But, superplasticizer content was slightly modified for FRC samples due to the presence of fibers (from 0.205 to 0.255% by weight of cement). Specimens containing Penetron had also a partial substitution of cement by the crystallizing agent (0.8%).
FRC casted in Italy were subjected to a further increase in superplasticizer content, due to difficulties occurred during the mixing phase.
Water to cement ratio was maintained at 0.5 for all the mixes; this value was calculated from the quantity of water added to the mix, after incorporating the effect of water absorption by aggregates and the increase in water content due to addition of chemical admixtures and SBR latex. This latter was present only in the fourth indian mix in a percentage of 7.5% by weight of cement.

MIX	FIBERS	PENETRON	LATEX 7.5%	w/c	SUPERPLASTICIZER %
Plain concrete (India)	-	-	-	0.5	0.205
FRC (India)	X	-	-	0.5	0.255
FRC+Penetron (India)	X	X	-	0.5	0.255
FRC+latex (India)	X	-	X	0.5	0.255
FRC (Italy)	X	-	-	0.5	1
FRC+Penetron (Italy)	X	X	-	0.5	1

Table 1: summary of the employed mixes

The cement employed in the first session of experimentation was ordinary Portland cement OPC 53 grades provided by suppliers in Chennai area; in the second phase ULTRACEM 52,5 R provided by Italcementi was used.

One type of sand and two types of coarse aggregates were mixed.
The sand was siliceous (specific gravity = 2.311, coefficient of absorption = 0.2%), with grain size in the range of 0-4 mm.
The coarse aggregates were respectively crushed granite limestone from Chennai area, of two grain size ranges, 5-10 mm and 10-20mm (specific gravity = 2.814, coefficient of absorption = 0.11%) and crushed granite limestone from the area of Milano (Truccazzano) characterized by dimension in the ranges 5-8 mm and 8-16 mm.

A polycarboxylate-based hyperplasticizer, GLENIUM SKY 8233 (density = 1.18 kg/l, 30% solid content), was employed as water reducer, in order to provide the required slump and workability.

Table 2 shows the mix design for the basic matrix of plain concrete.

DESCRIPTION	CEMENT	SAND	COARSE AGGREGATE (10mm)	COARSE AGGREGATE (20mm)	WATER
M35 CONCRETE	360.0	814.0	348.0	740.0	184.4

Table 2: components of the basic concrete matrix

3.3.2. Characteristics and effect of steel fibers

The type of fibers and their volume fraction influence the properties of concrete: by increasing the fiber content, the modulus of rupture, fracture toughness and the impact resistance of concrete increase.
A fiber-reinforced specimen, unlike plain concrete, does not break after the propagation of the first crack, but the composite can carry increasing loads due to the pull-out resistence of the fibers, which is generally greater than the load at first cracking. Once crack occurs, the matrix cannot carry any load in the cracked zone and the fibers act as bridges which take the entire load and transfer it to the uncracked portion of concrete through bond stresses. If the load exceeds the bond strength, the fibres get pulled out else, the cracks propagate through the matrix. Furthermore, if the bond is stronger than the fiber tensile strength, the rupture can occur due to the breaking of the fibers.
The bond between fibers and matrix must be optimized to have the best performances of the material. If this bond is too strong, many fibers might break before dissipating energy by being pulled-out. On the other hand, if the bond is weak, the fibers can slip out at low loads and their contribution to the increase in toughness would be reduced.
Size of the fibers largely influences the behaviour of the composite. Short fibers increase the toughness of the paste without significantly influencing its workability, but their bridging capacity is limited to microcracks. Long fibers create stronger bonds with the matrix and can bridge wider cracks, but their employment decreases the workability. For this reason, the amount of fibers in concrete is in general limited to 2% by volume, with a maximum aspect ratio of 100 [80]

In this work, BAEKAERT's steel fibers DRAMIX 3D RC 80/60 have been employed with a dosage of 20kg/m^3. These collated fibers are available in the market for flooring, tunnel applications and pavements employing slabs. Their characteristics are reported in the following Tab.3.

FIBER	TENSILE STRENGTH (MPa)	YOUNG'S MODULUS (MPa)	LENGTH (mm)	DIAMETER (mm)	ASPECT RATIO
DRAMIX 3D RC 80/60	1225	210000	60	0.75	80

Table 3: characteristics of the steel fibers

3.3.3. Characteristics and effect of Penetron

The pore nature of concrete, combined with the occurrence of cracks, can result in the penetration of water through the structure, due to the presence of pressure gradient or the capillary absorption. Water activates chemical reactions, such as the dissolution of calcium hydroxide or the corrosion of steel reinforcement caused by the presence of aggressive ions , that degrade the material.

In the past few years, concretes containing "supplementary cementitious granoulometry" have been developed. The *supplementary cementitious materials* are fillers characterized by a finesse higher than

cement. These materials, such as fly ash, blast furnaces, slags and silica fume, densify the concrete matrix and reduce the pore diameter, resulting in decrease of permeability.

Besides the *supplementary cementitious materials*, specific waterproofing additions have attested their effectiveness in the last few years. The latter, consist of *hydrophobic materials* and *crystallizing agents.* Hydrophobic materials act by deposing a water-repellent layer on the pores surface. Crystallizing agents are hydrophilic powders that can directly be added to the dry mix by substituting a small portion of cement. They react with water and humidity and lead to a decrease in permeability due to the densification of the matrix [81].

Penetron belongs to the category of crystallizing agents. Its function is to catalyze hydration of unreacted concrete components, resulting in a crystalline lattice that lowers permeability.

In this work, Penetron Admix was used at suggested mass percentage of 0.8% by cement mass to cast MIX3.

3.3.4. Characteristics and effect of SBR-latex

Latex, which is a colloidal suspension of polymer in water (emulsion), is used as admixture in latex-modified concrete (LMC).
In the past, polyvinyl acetate or polyvinylidene chloride-based latexes have been used, but now they are seldom employed, due to the low wet strength in the first case and the risk of steel corrosion in the second. Nowadays, latexes employ styrenebutadiene and polyacrylate copolymers.
Generally a latex contains at least 50% by weight of spherical polymeric particles, whose diameters vary from 0.01 to 1 μm. These solid particles are suspended in water by surface-active agents, which tend to incorporate a large amount of air in the mix.
The reduced solid content is the reason for which as low as possible extra mixing water is used in mixes containing latex. Moreover, the spherical particles and the entrained air strongly enhance the workability.
The hardening of latex takes place by loss of water or drying. Some internal loss is identified during the hydration process, but this is not sufficient to develop adequate strength. For this reason, dry curing is mandatory for LMC. After the drying process, the polymer forms a continuous film around the cement particles, the aggregates and the pores.
LMC is better than normal concrete as far as tensile and flexural strength are concerned. However, the improvement of this characteristics is not sufficient to justify the employment of expensive latex. One important property of this concrete is its ability to create bonds with old concrete and to resist the entry of water and aggressive solutions. It seems that the polymeric film plays its role in this: it impedes the fluid to flow through the pores. This characteristic has made LMC to be widely employed in overlays where durability and resistance to environmental conditions is required, such as rehabilitation of deteriorated floors, pavements and bridge decks [1].

In this work, CERALATEX SBR (density = 1.02 kg/l, solid content = 36,03%) has been employed.

3.4. Fabrication of the specimens

All the beams, were prepared in steel moulds.
The concrete was produced in forced action mixers of 250 litre capacity with a rotating drum, an eccentric set of blades and a high speed agitator.
The material constituents were stored to avoid significant affect of climatic conditions and their variation. Chemical admixtures were used within their shelf-lives.

All the concrete specimens were produced following this sequence: at first sand, coarse aggregates and cement were dry mixed for a couple of minutes. In case of mixes containing the crystallizing agent, Penetron was directly added to the cement before the dry mixing. Then, water was added and the mixing was continued for further 2 minutes. Finally, in the case of FRC mixes, the fibers and the superplasticizer were added and mixing was continued for another couple of minutes.
Since the forecasted 0.255% by cement weight of superplacistazer resulted insufficient, the quantity was increased up to 1% for the FRC mixes casted in Italy.
Fibers were not added directly to the mix to avoid the risk of deformation and for the same reason the mixing time was long enough to separate the collated fibers and guarantee their homogeneous distribution within the mixture.
In case of latex-modified FRC, the polymer in emulsion was added to the water before mixing.

A vibrating table was used to consolidate cubes and beams in the experimental phase conducted in India. Moguel [82] reported that table vibration is specified in most of the standard and recommendations (ACI committee 544, 1988a; AENOR UNE 83-504, 1990; ASTM C 1018,1992; AFNOR P 18-409, 1993; JCI-SF2, 1984). The moulds were put on the table, filled and vibrated for 15-20 seconds which is within the range of 15-60 seconds recommended by AFNOR P 18-409,1993.
In the second session of the experimentation, table was employed to consolidate cubes, but prisms was consolidated with a hand vibrator.

The top surfaces of the specimens were manually finished and specimens were demoulded after 1 day and placed in a mist-room (20°C, 98% R.H.) until testing.

In India, specimens were notched with a marble cutter machine SKIL 9816 on 25th day of curing. In Italy a fixed blade for concrete was used to cut notches on 19th day of curing. The cut was produced to be 28mm deep and 3 mm wide in both the cases.
After notching the samples were again put in the mist-room.

3.4.1. Standard properties of the concrete

The mixes were designed to have a slump variable in the range of 80 to 120 mm (measured with the 30 cm Abrams cone). Since the fibers reduce the workability of concrete, superplasticizer was added to recover the loss of slump. In case of latex-modified FRC the loss was balanced by the improvement given by the polymer. For the latter, a slump higher than the expected was accepted, after considering the retard in hardening, according to Ohama's model for LMC.

The unit weight and temperature of fresh concrete varied in a range from 2336 to 2531 kg/m³ and 27.59 to 29 °C respectively.

Concerning FRC mixes casted in Italy, temperature of concete, temperature of the room and weight were not measured.

Results of measurements are tabulated in the following **Table 4**.

MIX	AVERAGE SLUMP [mm]	AVERAGE TEMPERATURE [°C]	AVERAGE ROOM TEMPERATURE [°C]	DENSITY [Kg/m³]
Plain concrete (India)	95.71	27.59	25.00	2511
FRC (India)	91.67	28.19	24.60	2531
FRC+Penetron (India)	98.75	28.27	24.57	2531
FRC+latex (India)	120	29.00	25.00	2336
FRC (Italy)	50	-	-	-
FRC+Penetron (Italy)	80	-	-	-

Table 4: standard properties of the employed mixes

3.5. Performed tests

3.5.1. Compressive test

Compressive tests were performed on cubes for each mix, in order to study the mechanical characteristics of the materials. Nine cubes per mix were loaded up to failure and the characteristic strength was determined.

In the first part of the work, cubes were tested after 28 days of storage in a mist room, where the relative humidity was kept constant at about 100%. Latex-modified samples were tested after 32 days due to the unavailability of the testing machine.
In the Italian part, cubes were tested respectively after 7, 14 and 28 days of storage in a mist room and results were compare with the strength growing curve of material proposed by EC2.

3.5.2. Three point bending test

The three point bending test had a double aim: the first was to determine the bending-tensile strength of the beams; the second was to study the self-healing property of the samples: specimens from each batch were initially precracked up to the required width of crack, then the test was repeated after one, three and nine months, in order to investigate if any recovery in terms of strength or stiffness had occurred.

In India a center-point loading (CPL) set up was arranged in accordance with the European Standard EN 14651. This standard provides the guidelines for determination of the flexural tensile strength through an evaluation in terms of residual flexural tensile strength. Residual strength is determined from the load-crack mouth opening displacing curve (or load-deflection curve) which is obtained by applying a central load on a notched beam sample.
The specimen span was 500 mm. The beam deflection was measured at mid-span through displacement sensors (LVDT) mounted on a rigid aluminium rod that was fixed to the beam at mid height, with pins placed above its support. One end of this rod was free to rotate in the plane of loading, while the other was free to move longitudinally. Another aluminium rod was attached perpendicularly to which an adjustable acrylic plate was attached to hold the transducers (**Figure 37**).
This configuration was used on both sides of the sample, in order to measure the deflection with a couple of LVDTs. The LVDTs were put in contact with the beam through 0.5mm thick aluminium plates to have smooth contact with the surface.
The mouth-opening at the notch was measured through a clip gauge, held by 3 mm thick steel knives, collated at the either sides of the notch, at the centre of the specimen.

In Italy this setup was not arranged, and measurements were taken with the only employment of a clip gauge. Indeed, measurements taken from LVDTs were definitely ignored also in the first part of the experimental programme.

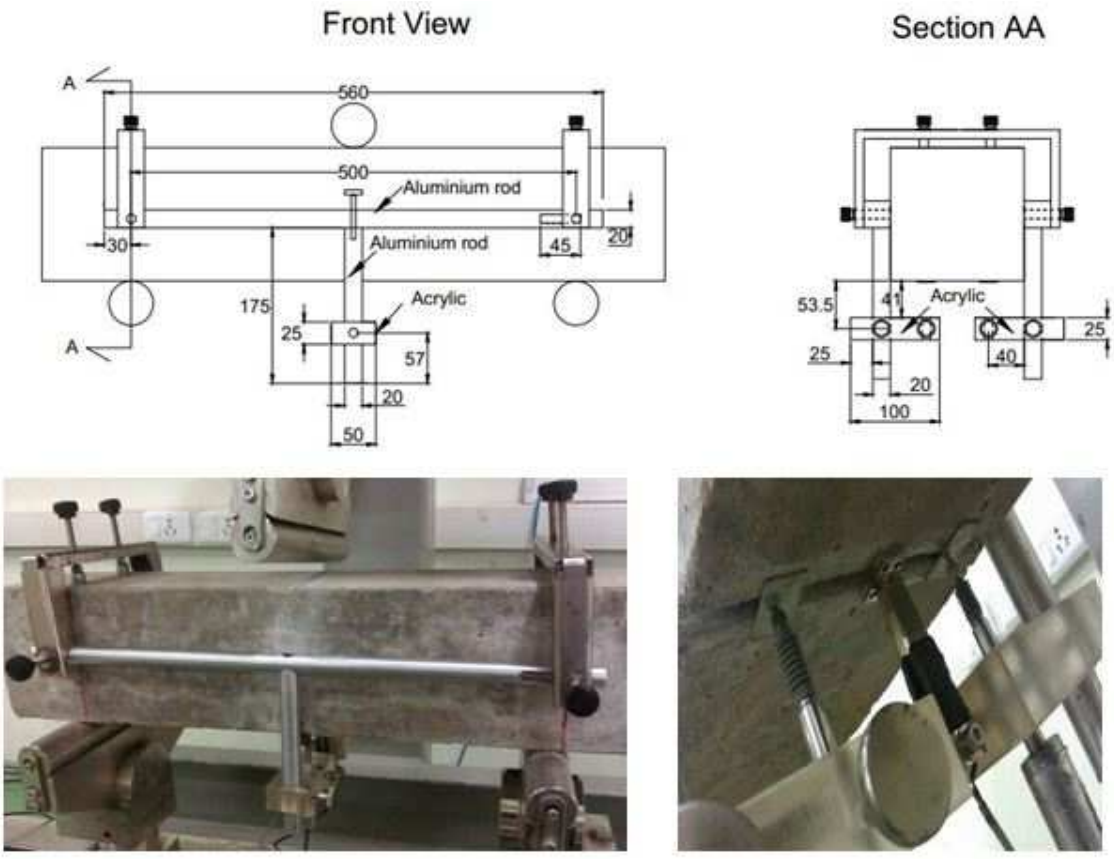

Figure 37: three-point bending test set up

Three point bending test procedure

The three point bending tests were carried out on the beams 28 days after their storage in a mist room where the relative humidity was kept constant at 98%. The beams had been notched after 25 days (in India) and 19 days (in Italy) of curing and then stored again in the mistroom until the day of the test.

In the first part of the work, tests were performed in a 1 MN closed-loop servo-controlled testing system and load controlled up to 40% of the expected peak load. Then, the control variable was switched to displacement. Under load control, the test was perfomed at a rate of 100 N/s, while under displacement control the initial speeds were 0.2 µm/s and 0.7 µm/s for MIX1 and the other mixes respectively.
The rate under displacement control was progressively increased after reaching the peak load, with a maximum of 1.4 µm/s for plain concrete and 2.8 µm/s for the specimens containing fibers.
This switching of the control variables was performed after some trial to optimize the error correction in the close loop of the system.
Under load control, a decrease in stiffness lowers the level of tuning, leading to more inert response and the application of a much higher load than intended.
On the other hand, under displacement control a decrease in stiffness may lead to higher than optimum gains causing instability [83].
The correction of this trend was conducted through the direct action on the proportional coefficient K_p, which was lowered during the test in order to provide a more sluggish response while increasing the mouth opening of the crack.

Concerning tests conducted in Italy, a self-controlled machine was employed.

After positioning the sample under the machine, a load of about 100 N was manually applied, by leaning the central knife on the top surface of the specimen.
After that, the test was started with a speed of 3.33×10^{-5} mm/s. This speed was maintained until the crack reached an opening of 100 µm and then increased up to 5×10^{-5} mm/s, until the crack reached the target opening of 600 µm.

Tests were performed again after 30, 90 and 270 days. K_p coefficient was varied depending on the expected stiffness of the specimen.

3.5.3. UPV tests

Directly velocity measurements were taken at 5 locations in each of the FRC specimens casted in India, both in the cracked and uncracked zones, in order to investigate if any filling material had sealed the crack. In the cracked zone, the direct length of measurement was 150 mm and corresponded to the tickness of the sample. On the other hand, measurements were taken in the direction of the main axis of the specimens to intercept the crack.

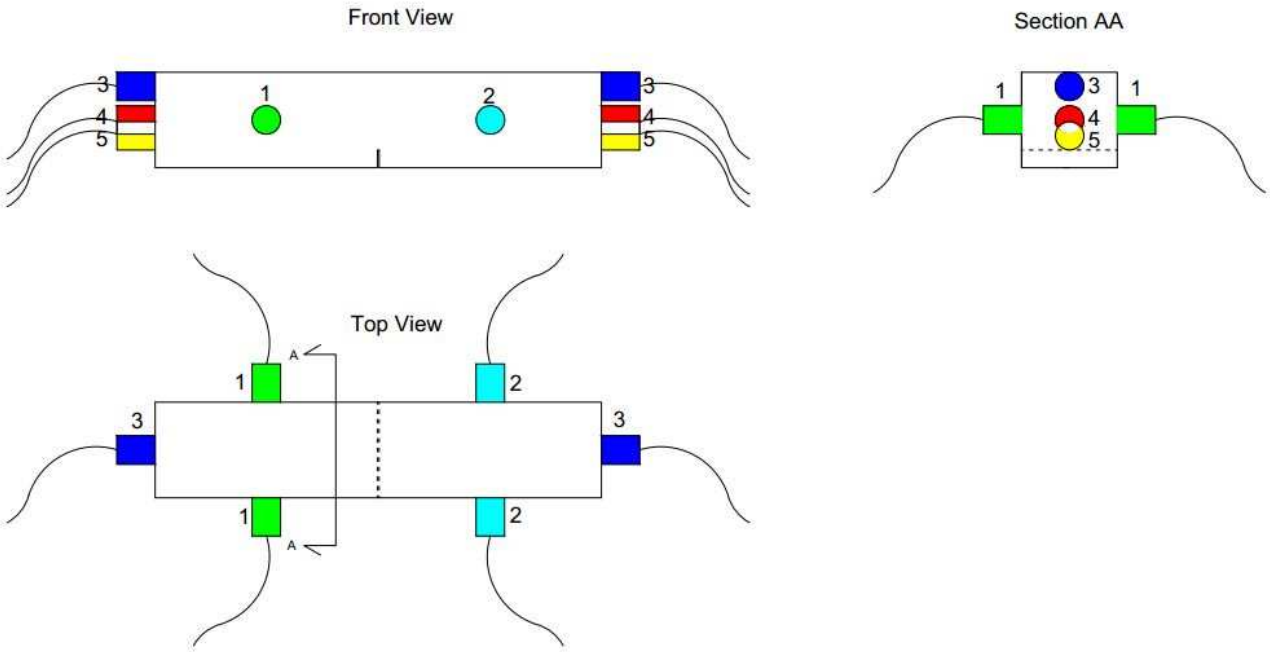

Figure 38: different locations considered in performing the UPV tests

The UPV system consisted of a pair of transducers, a pulse-receiver unit and a data acquisition system. The transducers had a narrowband of 54 kHz and a diameter of 38.8 mm. One transmitted the pulse and the other received the signal.
The conditioned receiver signal was acquired by an analog to digital (A/D) data acquisition board.

Crack sealing is supposed to increase along with time and recovery in strength of the samples.
The wave propagation is relented when the signal emitted by the transducer passes from the plain material to the void generated by the crack. What is expected is that the time needed to cross the sample is maximum after precracking and then decreases when the sealing reactions occur.
What was expected was a significant variation in the crossing-time, with an increase from point 3 (top of the crack) and 5 (bottom of the crack, in correspondence with the notch). Also, a decrease in crossing-time was expected with an increase in the time of conditioning.

Tough, results did not present any order and an interpretation was not possible: referring to **Figure 38**, for measurements taken from positions 3,4 and 5 a decrease in crossing time was expected from 0 to 30 days, but some of the specimens presented the opposite trend.

The increase of crossing time could be due to many reasons: UPV tests is totally reliable only with microscopically homogeneous materials, while concrete presents a not homogeneous matrix, where

different densities can distort the wave direction; the amplitude characteristic of the wave employed to investigate concrete requires, in order to have back comparable results, to position the emitter at points located at least 8 cm from each other, while in these test a distance of 4 cm about was guaranteed; since the direction of the wave is influenced by the density of material, it is possible that the wave passed through the top part of the specimens, bypassing the crack, whatever was the position of the transducer.

A second session of UPV was performed after 90 days of conditioning according to **Figure 39**, trying to solve the above mentioned problem. However, other results to which these alternative measurements could be compared were not available and this test will be a suggestion for the future.

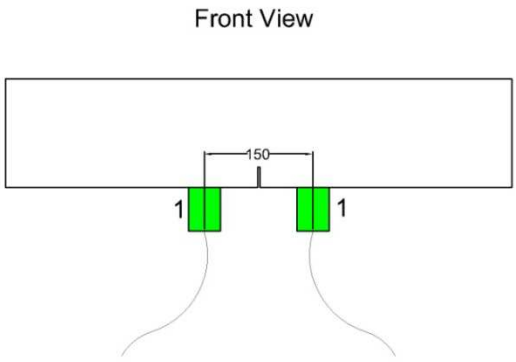

Figure 39: new location considered in performing the UPV test

3.5.4. Permeability test

Along with UPV tests, a permeability test was performed in order to measure the level of crack sealing of the specimens precracked at 600µm after 30 days.
Samples presenting a width of crack of 4000 µm were not considered in these test, because of the impossibility of measuring with a sufficient precision the speed of leakage of the water through the crack.

The setup of this permeability test was taken from Schlangen [16] and employed a funnel with a long pipette, which was fixed and sealed to the specimen by impermeable tape and silicon gel. The test was carried out by applying a column of water on the cracked zone and measuring the time required for the leakage through the fracture. This test adapted and employed a standard test for water permeability through coating materials for the textured finishing of building (JIS A 6909).

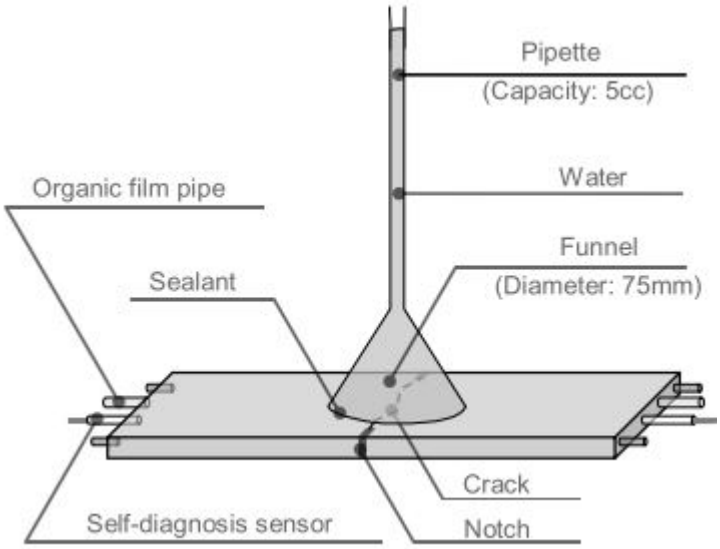

Figure 40: water leakage test setup by Schlangen

In the present experiment, a 80 mm diameter funnel was employed (**Figure 41**) and the pipette was filled with 5cc of water. Then, the time required to the water to flow through the crack was calculated by means of a chronometer.

Figure 41: water leakage setup realized

Low permeability test resulted really tough to be conducted: Schlangen's setup presented in fact some issues that made complicated the achievement of meaningful results. First of all, it was difficult to fix the funnel at the specimen and to make the system impermeable; during the test, the employed silicon was sometimes removed due to the pressure developed at the base of the funnel and some leakage of water occurred.
Moreover, the test had to be conducted on saturated specimens, in order to guarantee that the flowing water would not be absorbed by the sample, but silicon needed time in a dry environment to harden.
Moreover, the notch could not be totally sealed and water flowed through it instead of flowing through the proper crack.

In conclusion, this geometry of beams with a section of 150x150 mm^2 has to be considered not compatible with this kind of test.

3.6. Conclusions

The present chapter presented the details of the experimental programme, with reference to the employed materials, the performed tests and their procedures.

Initially, a summary of the project was given; then, the characteristics of steel fibers, Penetron, SBR-latex and GLENIUM hyperplasticizer have been described. The properties of the concrete produced have been discussed as well.
The last section focused on the performed mechanical, UPV and permeability tests, their procedure and their reference to the standards.

The next chapter will expose the results obtained from the tests. A comparison among the behaviour of the different specimens will be performed and self-healing will be quantified.

4. Discussion of Results

4.1. Introduction

The present chapter reports the results obtained from the tests described in chapter 3. It is divided into two main sections: the first concerns the material characterization and reports the average results of the tests; it includes the results of compressive and three point bending tests. The second is an analysis on the self-healing properties of the employed materials, which is based on their behaviour obtained by the three point bending tests before and after conditioning.

4.2. Material characterization

4.2.1. Compressive test results

In the following **Tables 5-6-7-8-9-10** are reported the average values obtained for each group of specimens and the characteristic strength obtained. Nine cubes per Indian mix were tested after 28 days, while batches of three cubes from the Italian mixes (fibers and fibers plus Penetron) were tested after 7, 14 and 28 days.

PLAIN CONCRETE	WEIGHT [kg]	LOAD [N]	STRESS Rc [Mpa]
AVERAGE	8.45	1221.87	54.39
DEV ST	0.07	45.03	1.93
CHARACTERISTIC STRENGTH			51.20

Table 5: compressive strength of plain concrete after 28 days

FRC (INDIA)	WEIGHT [kg]	LOAD [N]	STRESS Rc [Mpa]
AVERAGE	8.50	1251.48	55.63
DEV ST	0.06	113.03	5.02
CHARACTERISTIC STRENGTH			47.34

Table 6: compressive strength of FRC (India) samples after 28 days

FRC+Pen (INDIA)	WEIGHT [kg]	LOAD [N]	STRESS Rc [Mpa]
AVERAGE	8.54	1267.42	56.44
DEV ST	0.08	55.14	2.30
CHARACTERISTIC STRENGTH			52.65

Table 7: compressive strength of FRC + Penetron samples after 28 days

FRC+Latex	WEIGHT [kg]	LOAD [N]	STRESS Rc [Mpa]
AVERAGE	7.82	703.91	31.28
DEV ST	0.04	30.25	1.34
CHARACTERISTIC STRENGTH			29.07

Table 8: compressive strength of FRC + Latex samples after 28 days

FRC (ITALY)	WEIGHT [kg]	LOAD [N]	STRESS Rc [Mpa]
AVERAGE 7 days	8.10	1142.80	50.68
DEV ST 7days	0.09	43.15	2.47
CHARACTERISTIC STRENGTH 7 days			46.60
AVERAGE 14 days	8.07	1117.53	49.25
DEV ST 14 days	0.10	82.80	3.47
CHARACTERISTIC STRENGTH 14 days			43.52
AVERAGE 28 days	8.05	1326.25	58.36
DEV ST 28 days	0.07	35.07	1.49
CHARACTERISTIC STRENGTH 7 days			55.91

Table 9: compressive strength of FRC (Italy) samples at 7, 14 and 28 days

FRC+Pen (ITALY)	WEIGHT [kg]	LOAD [N]	STRESS Rc [Mpa]
AVERAGE 7 days	7.92	1052.90	47.12
DEV ST 7days	0.09	43.15	2.10
CHARACTERISTIC STRENGTH 7 days			43.66
AVERAGE 14 days	8.35	1168.65	51.77
DEV ST 14 days	0.07	24.25	0.14
CHARACTERISTIC STRENGTH 14 days			51.54
AVERAGE 28 days	8.05	1320.50	58.11
DEV ST 28 days	0.01	37.48	1.92
CHARACTERISTIC STRENGTH 7 days			54.94

Table 10: compressive strength of FRC + Penetron (Italy) samples at 7, 14 and 28 days

The results highlight that fibers do not play any essential role in the determination of the compressive strength of concrete. Indian FRC specimens in fact are only slightly stronger than plain concrete specimens.

Indian FRC specimens containing Penetron showed the best performances. Though, their strength is absolutely comparable to the strength of plain concrete and plain FRC specimens. So, it can be stated that also the crystallizing agent has no role in the determination of the compressive strength at 28 days.

Finally, Latex modified FRC specimens showed the worst compressive behaviour, with a failure stress of about the half of the strength of plain concrete, Indian FRC with and without the addition of Penetron. This is due to the presence of SBR Latex that, in accordance with the model for emulsion-modified concrete, delays the hydration of the specimens.

Concerning the Italian FRC with and without Penetron, their compressive strength is absolutely comparable with the one of Indian concretes.
The same considerations can be done: crystallizing agent does not play any role in determining the compressive strength. Moreover, the results of both the mixes are aligned with the ideal development of strength forecasted by the application of the hardening law of concrete, in accordance with EC2 (**Figure 42**) through the formulas:

$$f_{ctm}(t) = \beta_{cc}(t) f_{cm}$$

$$\beta_{cc}(t) = \exp\left\{ s\left[1 - \left(\frac{28}{t}\right)^{1/2}\right]\right\}$$

Where:

- $f_{ctm}(t)$ is the strength of concrete at *t* days;
- f_{cm} is the average strength of concrete at 28 days;
- β_{cc} is a coefficient depending on the age of concrete;
- *t* is the age of concrete in days;
- *s* is a coefficient of concrete depending on the speed of the strength development and on the type of cement, here *s* = 0.2

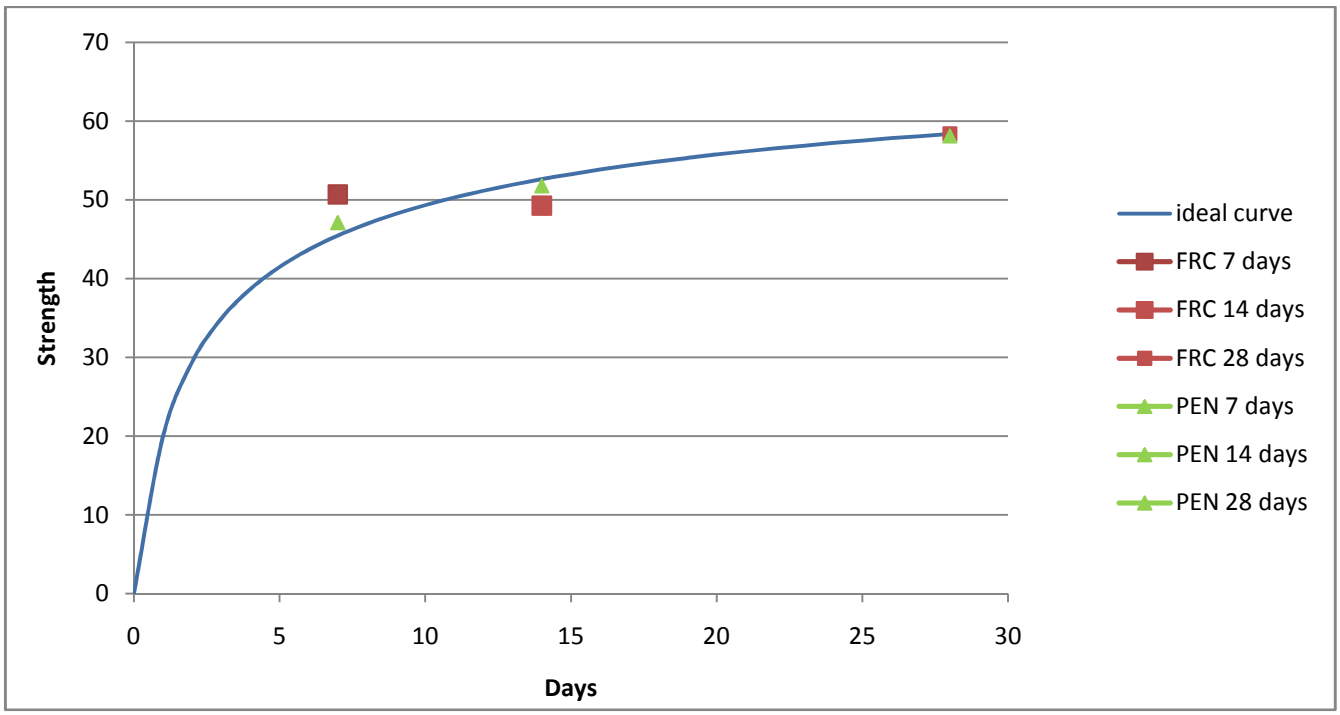

Figure 42: representation of the obtained results in comparison with the EC2 growing-strength curve of concrete

4.2.2. Bending test results

The flexural strength for plain concrete specimens has been calculated from the results obtained by the three point bending test, through the following formula:

$$\sigma = \frac{M}{W}$$

M is the bending moment acting at mid-span
W is the section modulus

The methodology of calculation of the stress is explained in the appendix (paragraph A.6).

On the other hand, the flexural strength for fiber reinforced specimens has been calculated from the results obtained by the three point bending test, following the prescription of the standard EN14651.
This strength is so expressed through the limit of proportionality LOP. This latter is the stress at the tip of the notch, which is assumed to act in the uncracked mid-span section of the beam subjected to the three point bending test.
The LOP is calculated for a CMOD of 50 μm, through the following formula:

$$f_{ct,L}^{f} = \frac{3lF_L}{2bh_{sp}^2}$$

$f_{ct,L}^{f}$ *is the LOP, in Newton per square millimiters*
L *is the span length, in mm*
b *is the width of the specimen, in mm*
h_{sp}^2 *is the distance between the tip of the notch and the top of the specimen, in mm*

Moreover, the fiber reinforced specimens have been classified by expressing the residual flexural tensile strength, which is the residual fictitious stress that is assumed to act in the uncracked mid-span section of the beam subjected to the three point bending test, with a linear stress distribution, for a chosen CMOD.
In this case CMOD 600 μm and CMOD 4000 μm are considered. The residual flexural strength is calculated as following:

$$f_{r,j} = \frac{3lF_j}{2bh_{sp}^2}$$

$f_{r,j}$ *is the residual flexural strength, in Newton per square millimiters*
F_j *is the residual loadcorresponding with CMOD = CMOD$_j$ or δ= δ$_j$ (j=1,2,3,4) in Newton*
b *is the width of the specimen, in mm*
h_{sp}^2 *is the distance between the tip of the notch and the top of the specimen, in mm*

The flexural strength of plain concrete has been calculated following the same standard and considering beams with a section 150 mm wide and 120 mm deep and a span length of 500 mm.
The following **Tables 11-12-13-14-15** report the values obtained by the three point bending tests and characterize the employed concretes represented in **Figure 43** for respectively CMOD 600 μm and CMOD 4000 μm.

Plain concrete	F_L [kN]	W [mm^3]	Flexural strength [Mpa]
AVERAGE	16.22	360000	5.63
DEV ST	0.797		0.28
CH STRENGTH	14.90		5.17

Table 11: flexural characterization of plain concrete samples casted in India

FRC (India)	F_L (50) [kN]	LOP [Mpa]	L (600) [N]	$f_{,R}$ (0.6) [Mpa]	L (4000) [N]	$f_{,R}$ (4) [Mpa]
AVERAGE	19.25	7.09	12.32	4.28	11.89	4.13
DEV ST	1.38	0.34	2.19	0.76	1.26	0.44
CH STRENGTH		6.52		3.03	9.81	3.41

Table 12: flexural characterization of FRC samples casted in India for CMOD = 600 µm and CMOD = 4000 µm

FRC+Pen (India)	F_L (50) [kN]	LOP [Mpa]	L (600) [N]	$f_{,R}$ (0.6) [Mpa]	L (4000) [N]	$f_{,R}$ (4) [Mpa]
AVERAGE	19.00	6.6	12.37	4.3	11.01	3.82
DEV ST	1.57	0.55	3.14	1.09	2.96	1.03
CH STRENGTH		5.7		2.5		2.13

Table 13: flexural characterization of FRC samples containing Penetron for CMOD = 600 µm and CMOD = 4000 µm

FRC+Latex (India)	F_L (50) [kN]	LOP [Mpa]	L (600) [N]	$f_{,R}$ (0.6) [Mpa]	L (4000) [N]	$f_{,R}$ (4) [Mpa]
AVERAGE	13.95	4.77	6.91	2.4	6.05	2.1
DEV ST	1.44	0.50	2.29	0.8	2.1	0.73
CH STRENGTH		3.94		1.09	0.9	0.9

Table 14: flexural characterization of latex-modified FRC samples for CMOD = 600 µm and CMOD = 4000 µm

FRC (Italy)	F_L (50) [kN]	LOP [Mpa]	L (600) [N]	$f_{,R}$ (0.6) [Mpa]	L (4000) [N]	$f_{,R}$ (4) [Mpa]
AVERAGE	13.097	4.55	12.7	4.41	6.37	2.21
DEV ST	-	-	-	-	-	-
CH STRENGTH	-	-	-	-	-	-

Table 15: flexural characterization of FRC samples casted in Italy for CMOD = 600 µm and CMOD = 4000 µm

4.3. Bending behaviour and self-healing properties of the specimens

The three-point bending test results are hereby plotted in terms of Load-CMOD curves.

4.3.1. precracking phase

FRC specimens behaviour is compared with the behaviour of plain concrete samples, which were precracked up to only 600 µm. Beyond this value, plain concrete specimens showed in fact a brittle rupture.

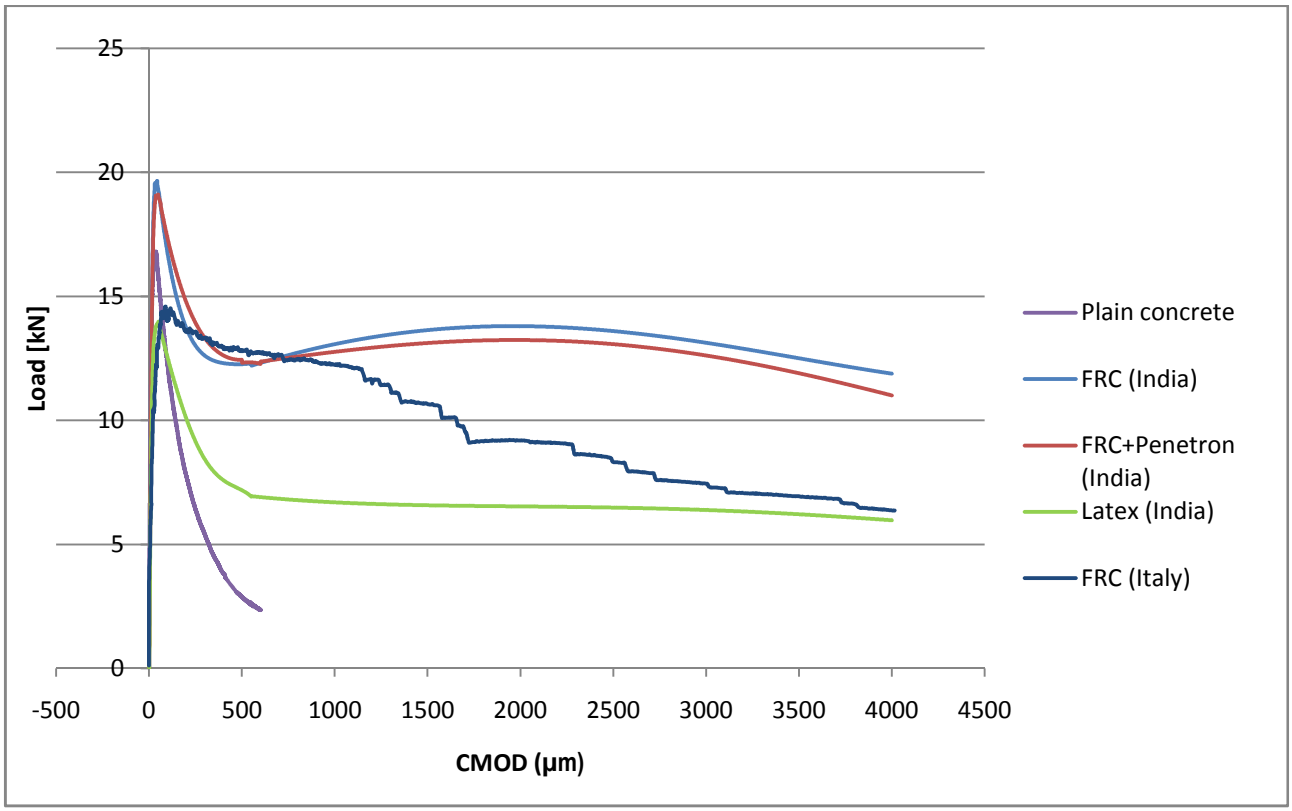

Figure 43: average flexural behaviour of the samples of each tested batch of specimens, subjected to three point bending test 28 days after casting. After the first softening branch, a hardening is performed by Indian FRC samples both with and without crystallizing agent.

Under little deformations the load-CMOD graph shows a straight, elastic part. This linear behaviour is maintained until the peak load is reached, for CMOD in a range of 30 to 60µm for all the mixes.

Substantially, plain concrete samples show, after the peak, a softening branch which extends till the deformation reaches the value of 600 µm; this value of deformation corresponds a residual load of about 10-15% of peak load. Below this value, specimens showed a brittle rupture.
If FRC samples with and without additions are considered, there is not any important difference between their behaviour: the peak load deformations are similar, such as the peak loads (respectively, average peak loads of 19.44 and 19.88 KN for average peak load deformations of 46.81 µm and 38.37 µm).
After reaching the peak load, both the mixes show an increase of displacement while the force decreases. This behaviour is called *softening*. During the softening, the deformation is localised into the crack and so, the deformation is equal to the crack opening. This branch leads to a point of minimum that can be localised in the neighbourhood of CMOD 500 µm; in some specific case this latter corresponded to a deformation of more than 1000 µm, and the graph described a sort of plateau.

The following branch consists of a slight *hardening*, where, to the increase of displacement, corresponds an increase of the force. This behaviour is due to the redistribution of the forces in the fibers and the bonds that they establish with the cement paste. A second peak load, which is localised around CMOD 2200 µm, is reached at the end of the hardening branch.
Finally a new softening can be observed.

Specimens containing SBR Latex, reach an average peak load (13.92 KN)sensibly lower than the peak loads of FRC samples without polymer. However, the stiffness is comparable; indeed, the peak loads corresponded to an average deformation of 48 µm, comparable to the peak load deformation of the other FRC samples. This lower level of load could be due to the lower level of hydration of the specimens.
Moreover, Latex-modified samples showed a different behaviour after reaching the peak load: as it can be inferred from the graph, the softening branch is continuous until the end of the test. However, in a few cases a slight hardening was seen.

The average behaviour of Italian FRC specimens with and without addition is represented in the graph by only one plain FRC specimen that was precracked up to 4000 µm. The other tests were arrested at 600 µm, due to the unavailability of samples.
However, this behaviour can also be assumed as reference for specimens containing crystallizing agent, since the corresponding Indian mixes had previously showed that Penetron does not influence significantly the mechanical characteristics of concrete during the precracking phase.
As in the case of concretes casted in India, the peak loads reached by these two mixes after the linear branch are similar (average of 14.438 kN at CMOD 58 µm for FRC samples without addition, and 13.55 kN for specimens with addition at CMOD 62 µm).
After reaching the peak load, the curve shows a softening, which takes place up to failure, for CMOD 4000 µm.

4.3.2. CMOD 600 µm - reloading after 30 days

After 30 days of conditioning, Indian FRC samples precracked up to 600 µm presented the induced cracks partially filled of a white material (presumably calcium carbonate, **Figure 44**).

Figure 44: level of crack sealing after 30 days of conditioning for specimens precracked up to 600 µm

Specimens were definitely reloaded up to failure.
The load-CMOD curves plotted in **Figure 45-46-47-48-49** describe the behaviour of the samples. Plain concrete curve is not represented, since, during reloading, samples had a very brittle behaviour and broke after the application of a really low load.

For all the batches the initial behaviour assumed during the tests was linear for loads up to 30% of residual load of precracking. Then, the stiffness decreased gradually, until the slope of the curve dropped, when load increased up to values close to the residual load of precracking. This value of load was reached only in proximity of CMOD 1500 µm.
After the peak-load, the load-CMOD curves followed the same trend, highlighted by the samples during the phase of precracking.

FRC casted in Italy, subjected to compression during wet/dry cycles, showed during reloading a shortest initial linear branch, which ranged up to loads lower than 15% of residual load of precracking before that stiffness decreased. However Italian FRC samples containing the crystallizing agent overtook significantly the residual load of precracking at CMOD 1500 µm, before showing the same softening behaviour previously registered by the monotone curves in the precracking phase.

In summary it can be stated that:

- *Generally specimens, after 30 days of conditioning, tend to assume the behaviour highlighted during precracking*
- *Self-healing has a significant mechanical effect only when compression is applied during conditioning and crystallizing agent is added to the mix*

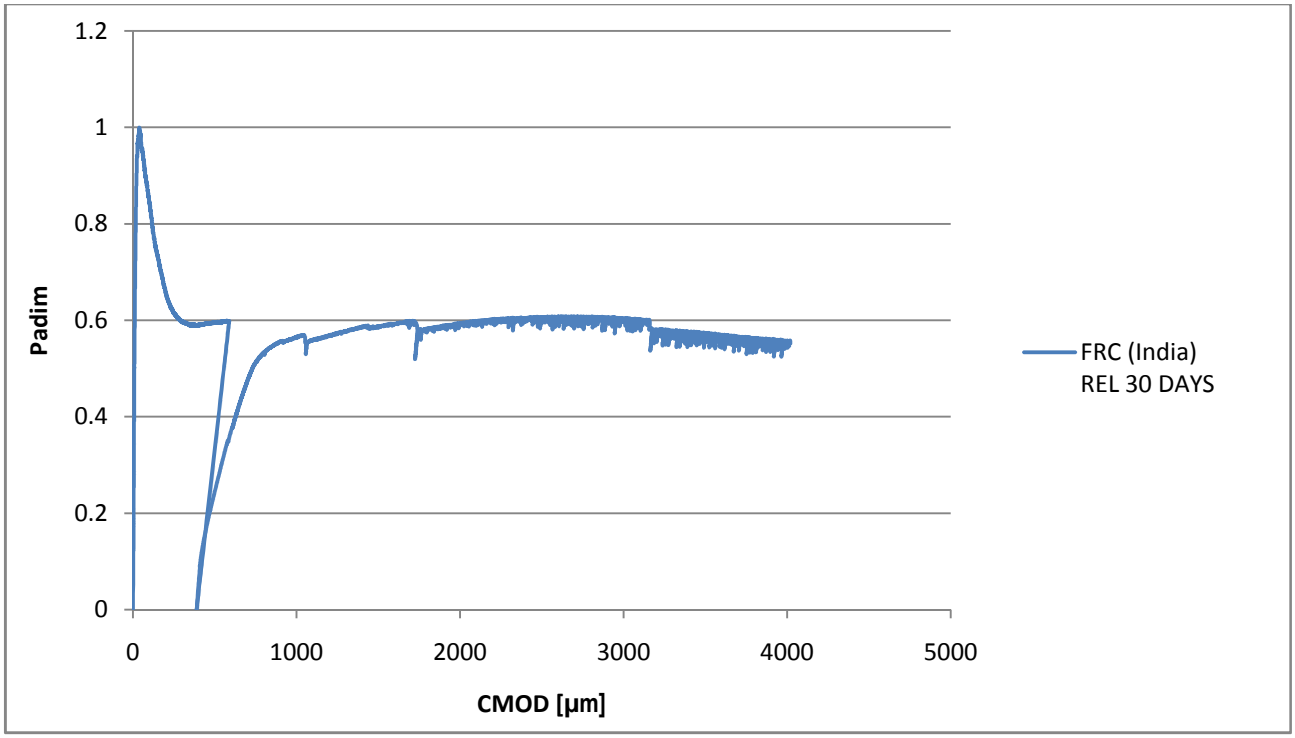

Figure 45: average behaviour during precracking up to 600 µm of virgin FRC specimens casted in India and reloading after 30 days. The residual load of precracking is recovered only at CMOD 1500 µm

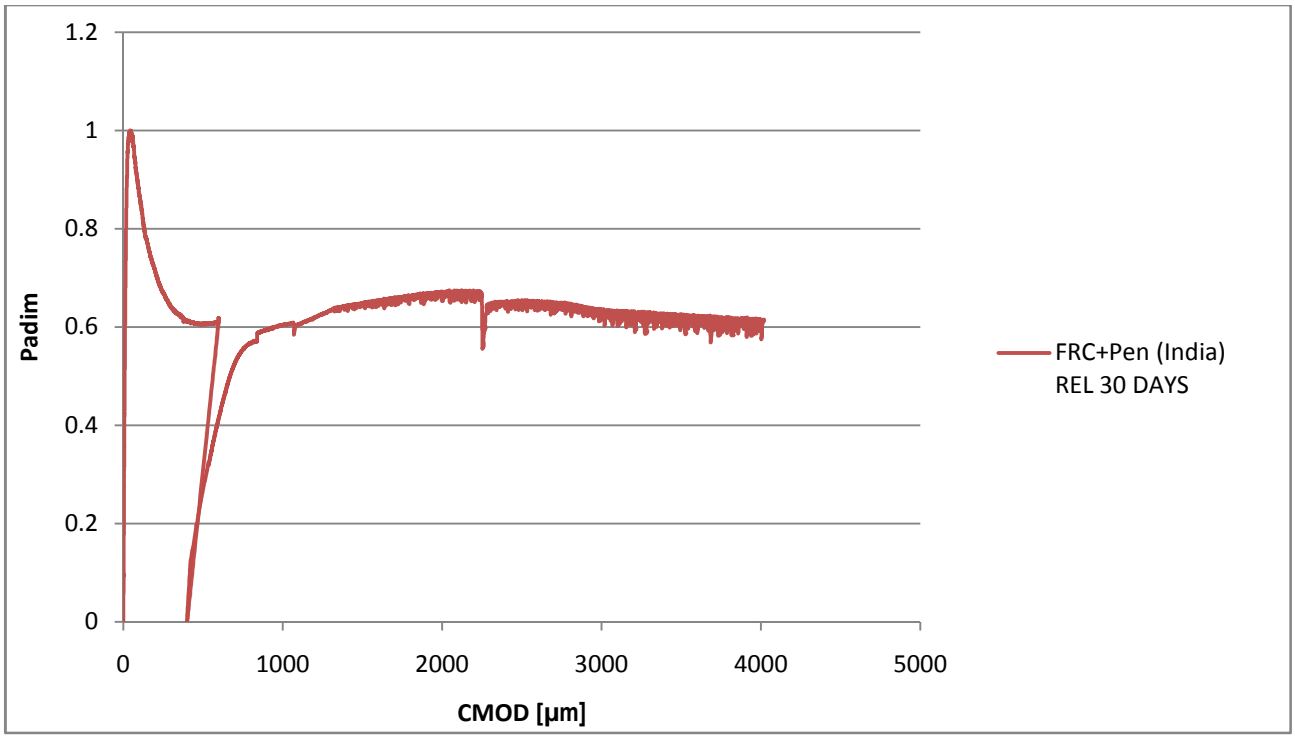

Figure 46: average behaviour during precracking up to 600 µm of virgin Indian FRC specimens containing Penetron and reloading after 30 days. The residual load of precracking is recovered only at CMOD 1500 µm, but load bearing capacity increases up to 2000-2500 µm

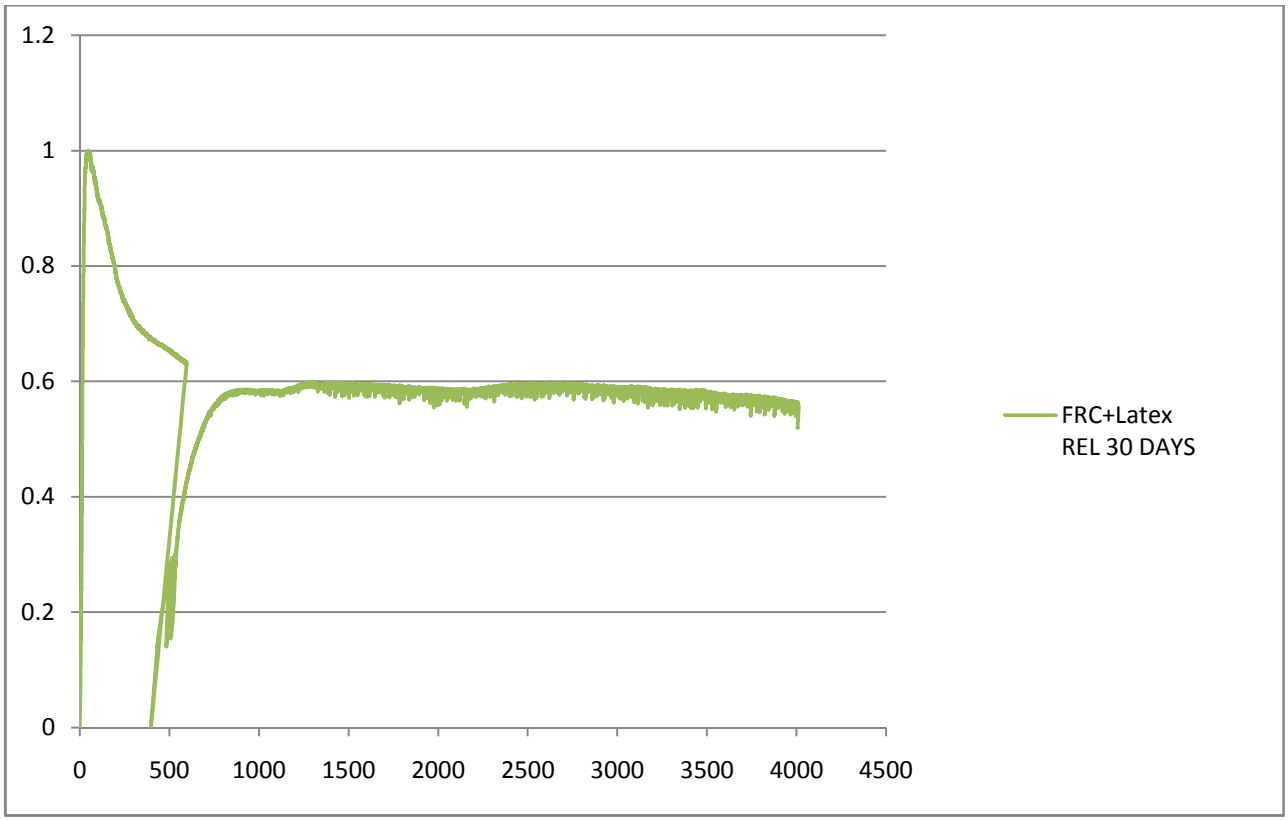

Figure 47: average behaviour during precracking up to 600 µm of virgin latex-modified FRC specimens and reloading after 30 days. Any hardening behaviour is highlighted

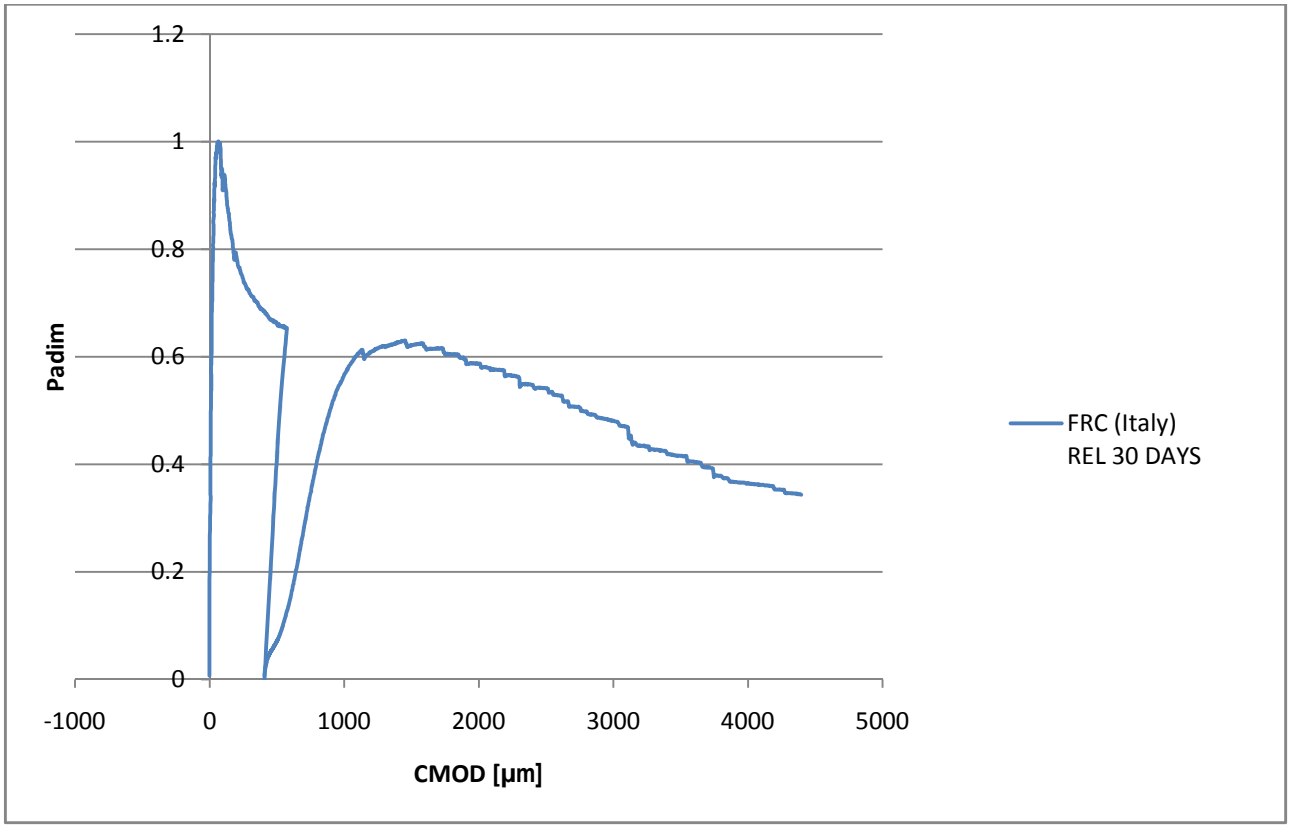

Figure 48: average behaviour during precracking up to 600 µm of virgin FRC specimens casted in Italy and reloading after 30 days. The reloading curve seems a natural prosecution of the precracking curve

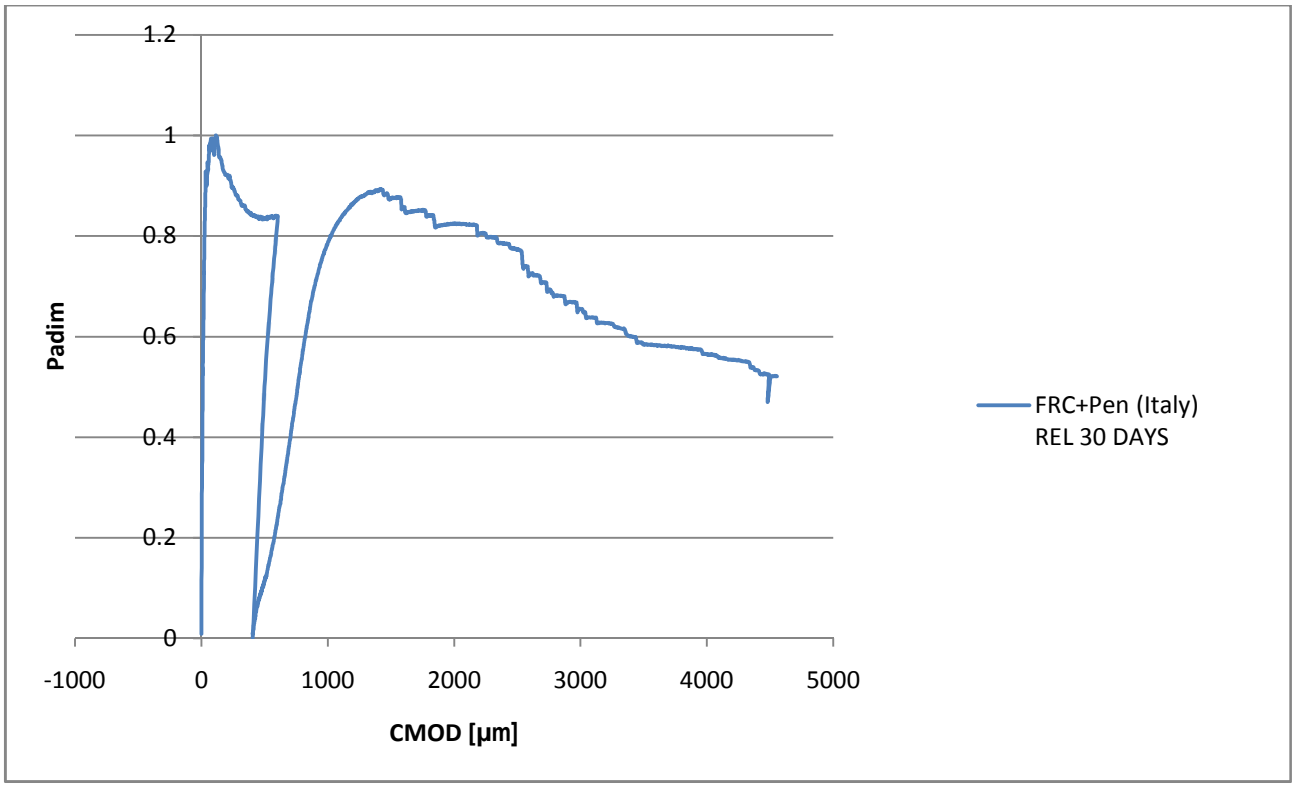

Figure 49: behaviour during precracking up to 600 µm of virgin Italian FRC specimens containing Penetron and reloading after 30 days. The peak load of reloading overtakes significantly the residual load of precracking, in contrast with the average softening behaviour performed by the samples

4.3.3. CMOD 600 µm - reloading after 90 days

After 90 days of conditioning, all the samples presented their cracks almost completely filled by the white material described in the previous paragraph (**Figure 50**). It was particularly difficult to see the crack without an accurate observation.

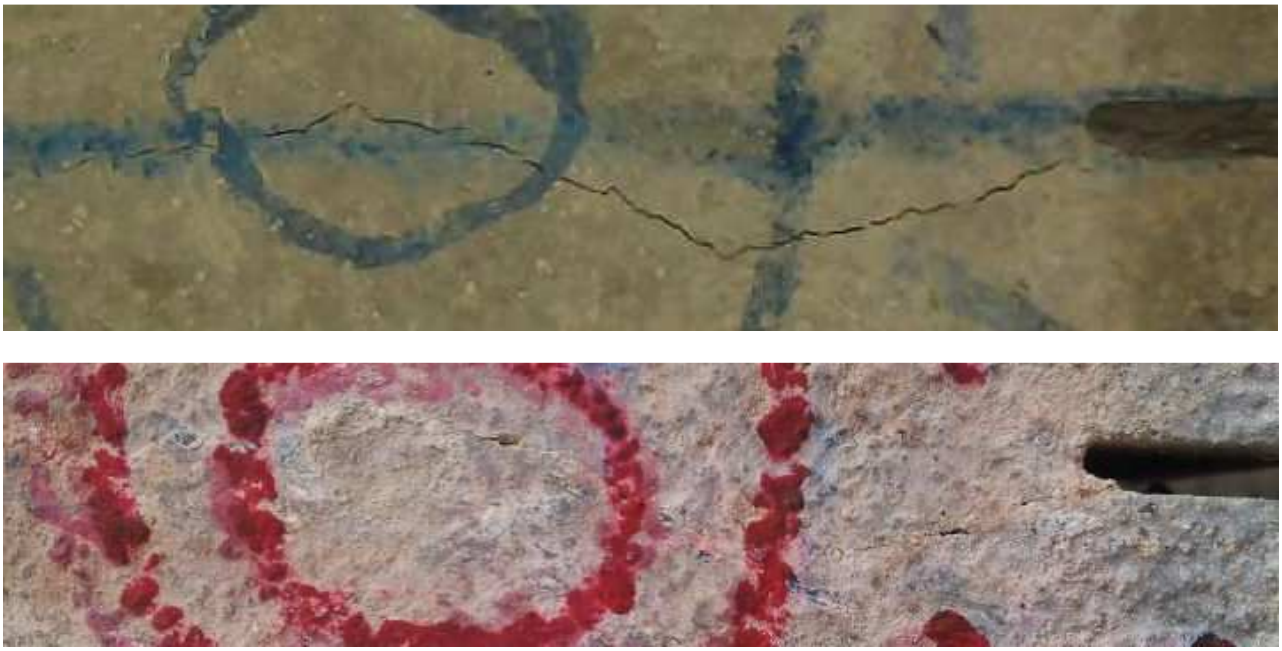

Figure 50: level of crack sealing after 90 days of conditioning for specimens precracked up to 600 µm

The load-CMOD curves of samples tested after 90 days of conditioning (**figure 51-52-53-54**) highlight a behaviour similar to the one described for samples tested after 30 days of conditioning.

It is interesting the fact that it was possible to test also plain concrete specimens, while previously they had shown a completely brittle behaviour. Even if the respective load-CMOD curve does not highlight any recovery in terms of load, some crystallization must have occurred, making samples strong enough to be re-loaded.

Concerning FRC specimens, their behaviour was firstly linear, with an initial branch which seemed more extended than previously, ranging up to loads of 30 (plain FRC and latex) to 60 % (FRC+Pen) of residual load of precracking.
For higher loads, stiffness decreased gradually, following a slight hardening that leaded to the peak load of reloading. Finally, the behaviour changed into softening up to failure.

The residual load of precracking was in average overtaken by the reloaded samples, while after a conditioning of 30 days specimens could be barely loaded up to this value.

By comparing the graphs of specimens tested at 90 and 30 days respectively, it can be observed that:

- *Crystallization due to self-healing reactions increases along with time of conditioning, resulting in a more complete crack sealing*
- *The initial stiffness during reloading is maintained for higher values of applied load, resulting in a more extended linear branch*
- *Samples overtake faster the residual load of precracking*

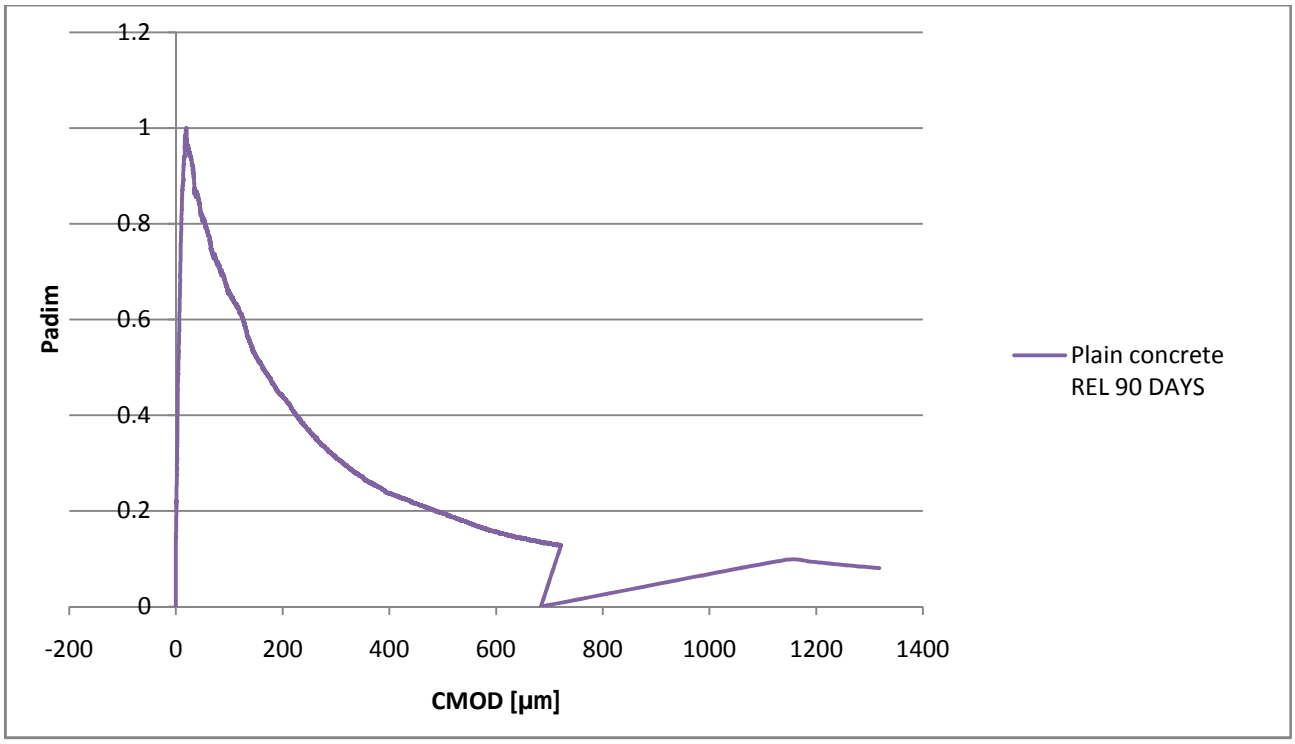

Figure 51: average behaviour of plain concrete samples subjected to three point bending test after 90 days. Any particular recovery happened, but samples were strong enough to be tested

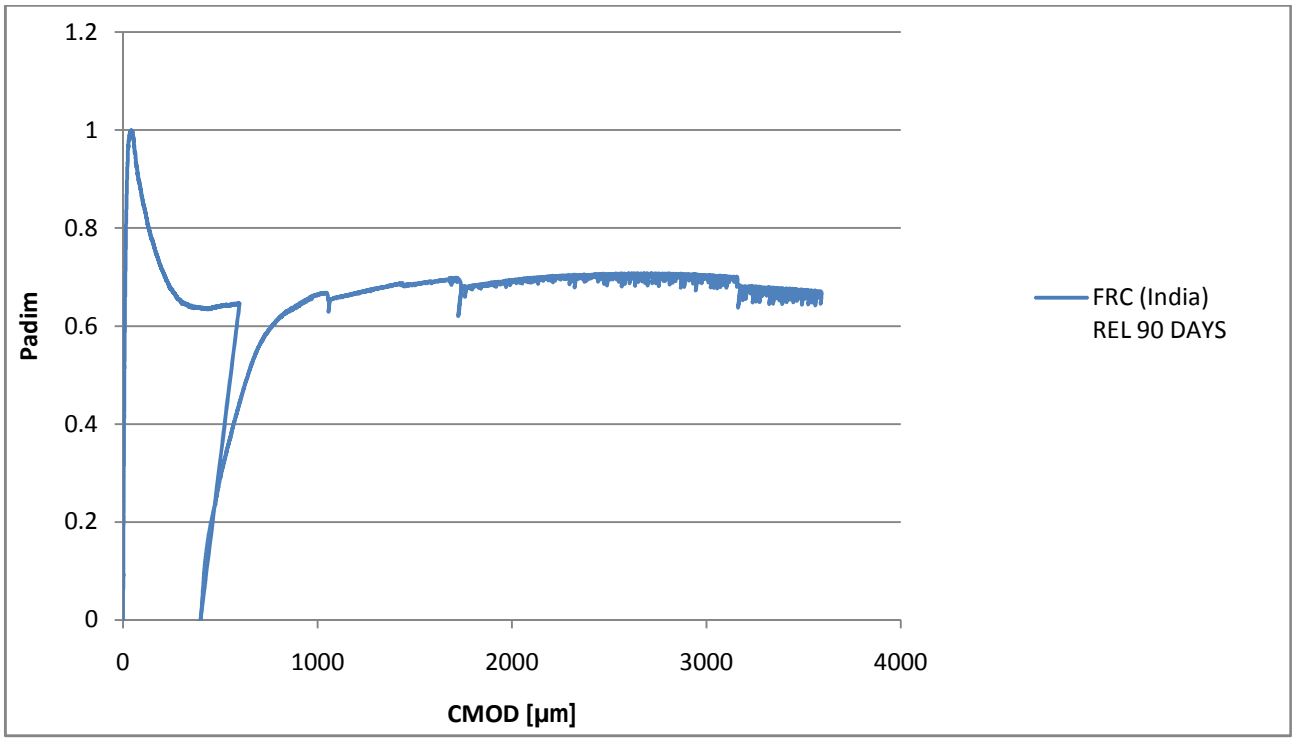

Figure 52: average behaviour during precracking up to 600 µm of virgin FRC specimens casted in India and reloading after 90 days. The graph highlights a slight increase in stiffness and strength in comparison with the tests at 30 days

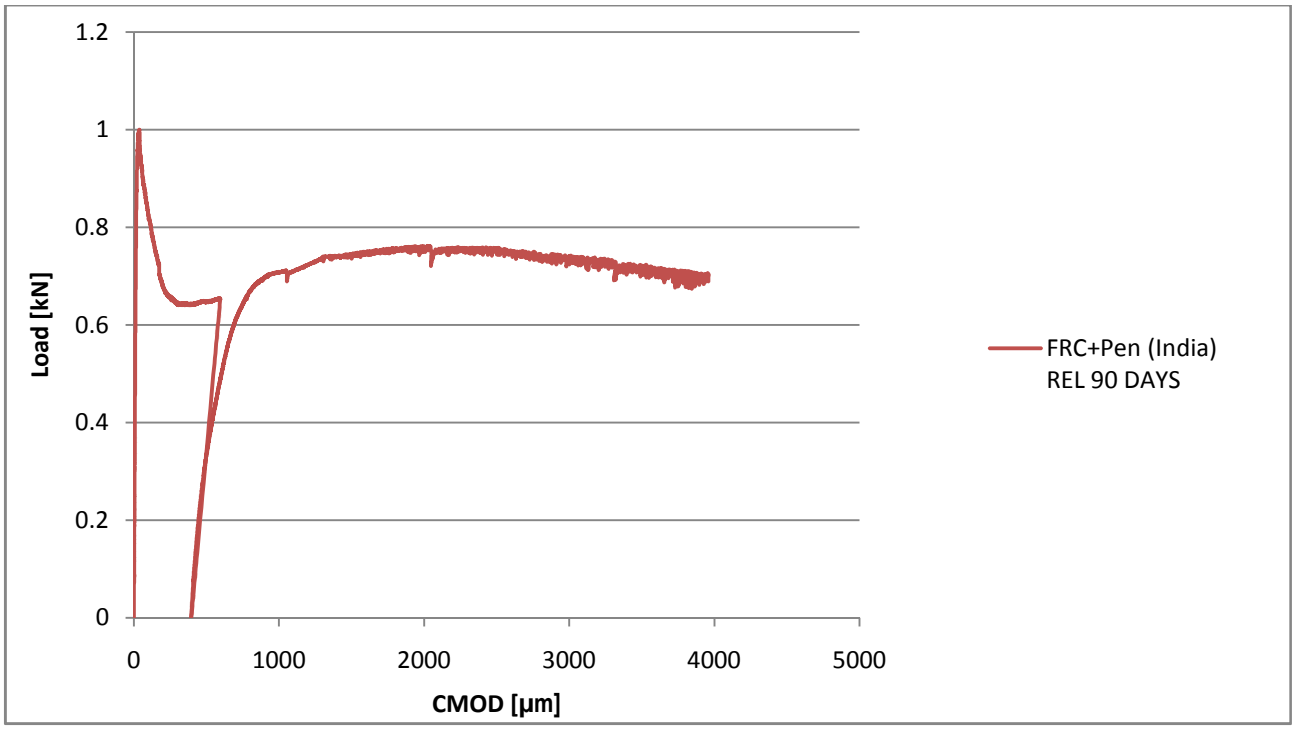

Figure 53: average behaviour during precracking up to 600 µm of virgin FRC Indian specimens containing Penetron and reloading after 90 days. The graph highlights a slight increase in stiffness and strength in comparison with the tests at 30 days

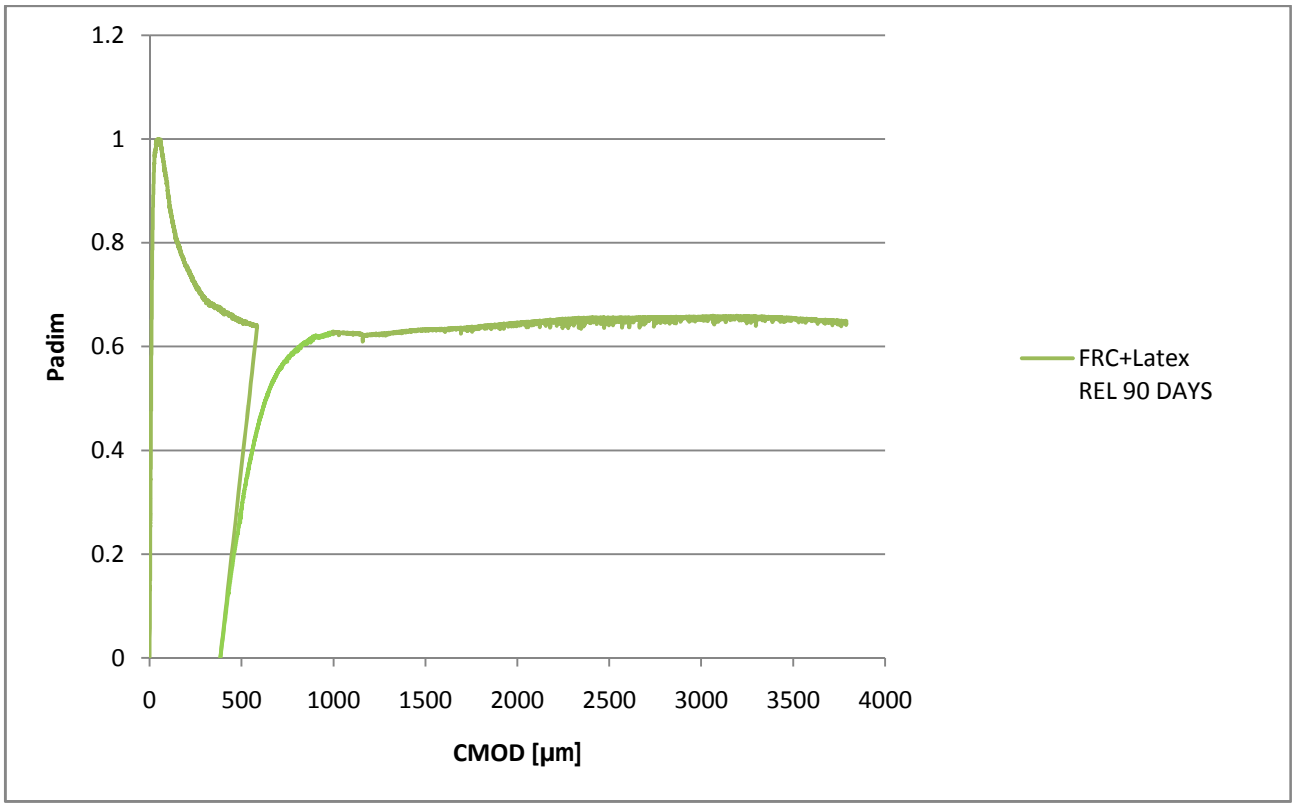

Figure 54: average behaviour during precracking up to 600 µm of virgin latex-modified FRC specimens and reloading after 90 day . The graph highlights an increase in initial stiffness in comparison with the tests at 30 days. A slight hardening is showed

4.3.4. CMOD 600 µm - reloading after 270 days

After 270 days of conditioning, FRC samples casted in India showed a behaviour (**Figure 55-56-57**) characterized by an initial linear branch which covered the unloading curves up to a load of 75% of residual load of precracking (55% for specimens without addition). After the first linear branch, the stiffness decreased and FRC samples with and without addition reached the peak load of reloading around CMOD 1500 µm. Beyond, a slight softening behaviour has showed and became much more accentuated for CMOD higher than 3000 µm.

This softening behaviour of FRC specimens with and without crystallizing agent could be associate to the softening behaviour highlighted by samples precracked up to 4000 µm and tested after 90 days of conditioning that will be illustrated in the following paragraphs.
Conditioning with wet/dry cycles compromised the strength of the fibers by inducing oxidation. This latter phenomenon was much faster and more evident for wide crack sizes, since the access of water and moist into the crack could not be prevented.
For lower dimensions of cracks (in this case 600 µm) oxidation might happen anyway along with longer times, decreasing the load bearing capacity of samples, based on the integrity of fibers.
However, it can be assumed that further hydration and development of crystals due to crystallizing agent could balance the corrosive phenomena, partially protecting fibers and developing bridges between the crack faces, which contributed to increase the global tensile strength of the samples.

Finally, latex-modified concrete appeared less stiff than in the previous tests: the initial linear branch extended up to 30% of residual load of precracking and the consequent loss in stiffness was more accentuated.
However, in the case of latex-modified concrete, stiffness decreased softly and without sudden ruptures of fiber, resulting in a gradual, slight hardening up to failure and suggesting that latex gave to the concrete paste some elasticity that the other concretes employed did not have.

It can be concluded that:

- *Crystallization can fill completely the cracks after long expositions to conditioning*
- *The effect of self-healing is a further increase in linearity during reloading, due to the capacity of samples to maintain their residual stiffness*
- *Samples highlight an increased strength on average*

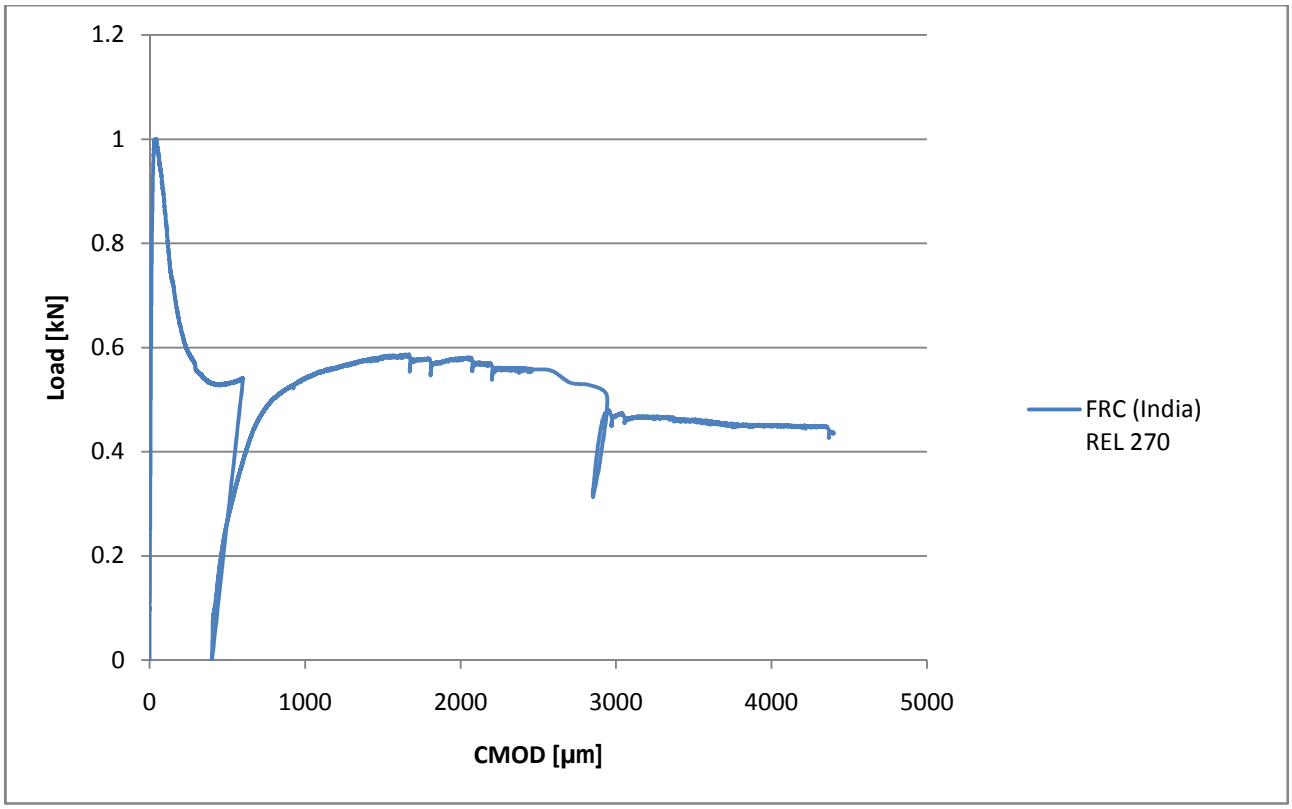

Figure 55: average behaviour during precracking up to 600 µm of virgin FRC specimens casted in India and FRCreloading after 270 days.

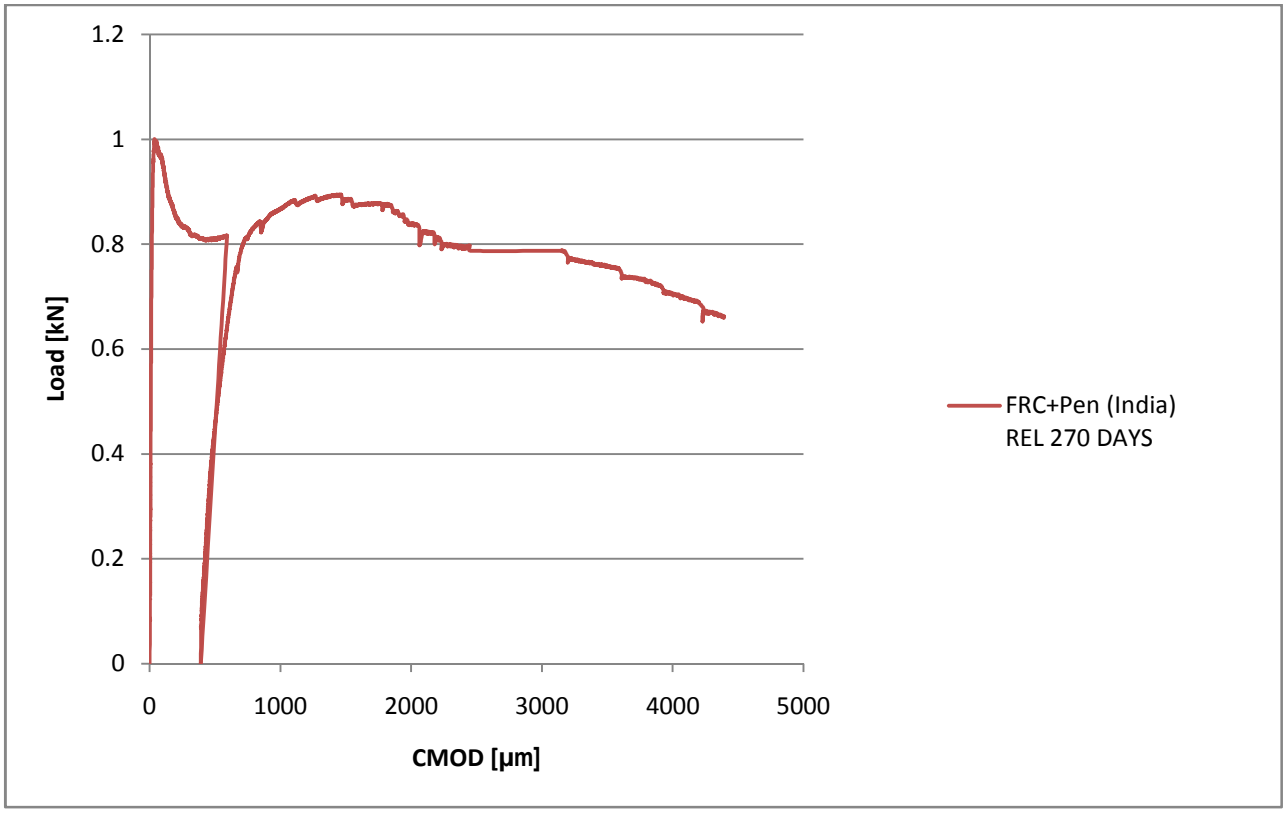

Figure 56: average behaviour during precracking up to 600 µm of virgin FRC specimens casted in India with Penetron and reloading after 270 days

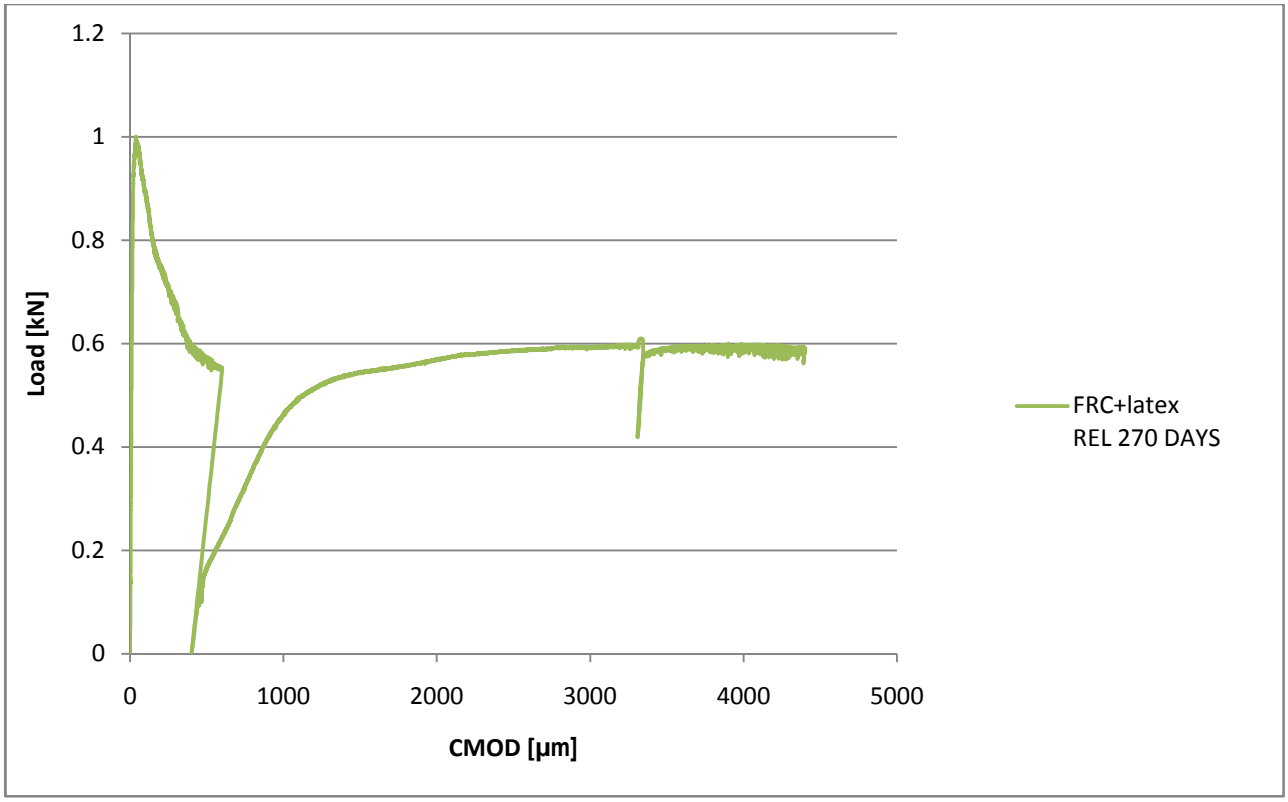

Figure 57: average behaviour during precracking up to 600 µm of virgin latex-modified FRC specimens and reloading after 270 days

4.3.5. CMOD 4000 µm: reloading after 30 days

Samples precracked up to 4000 µm presented some crack sealing only when crystallizing agent was put in the mix (**Figure 58**). In particular, after conditioning, cracks resulted filled at the tip.

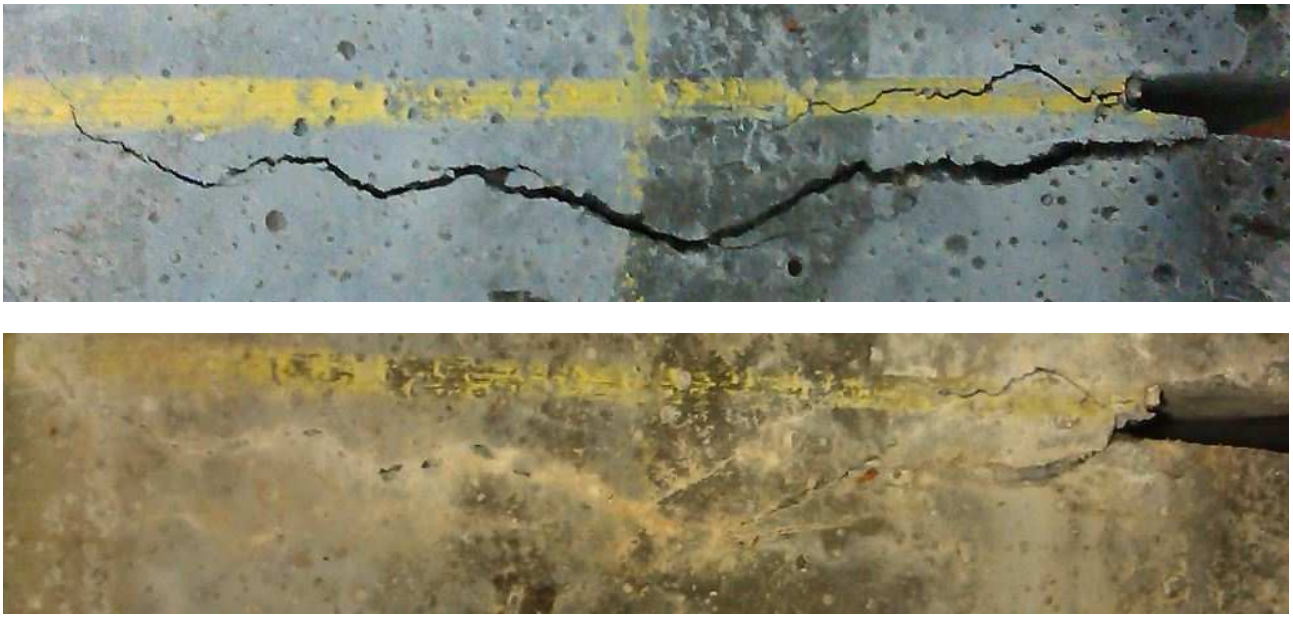

Figure 58: level of crack sealing after 30 days of conditioning for specimens precracked up to 4000 µm

The initial behaviour during reloading of these specimens (**Figure 59-60**) was linear only up to really low loads (about 10% of residual load of precracking), then the stiffness decreased, until the specimens reached the peak load for further openings of 1000µm.
Differently, latex-modified specimens presented a stiffness initially really low, which increased along with the crack opening, until the peak load was reached and a slight softening took place (**Figure 61**).

In this session of test, the reloading curves could be seen as a prosecution of the softening branch of precracking phase.

Consequently:

- *Samples recover and maintain the trend they had during precracking*
- *Self-healing does not have any significant effect, but results in a partial filling of cracks, especially for samples containing crystallizing agent*
- *The effect of self-healing is balanced by the effect of corrosion on fibers, consequently, any important mechanical recovery is highlighted*

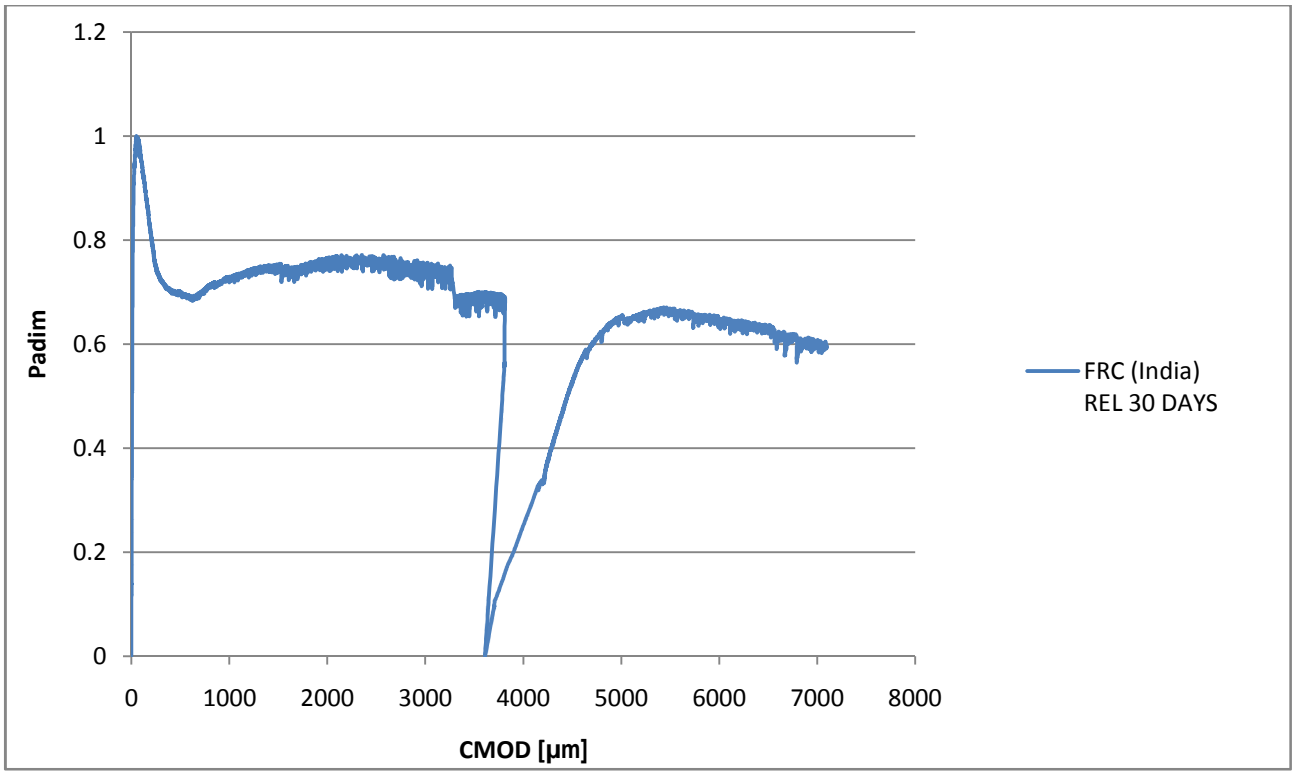

Figure 59: average behaviour during precracking up to 4000 µm of virgin FRC specimens casted in India and reloading after 30 days.

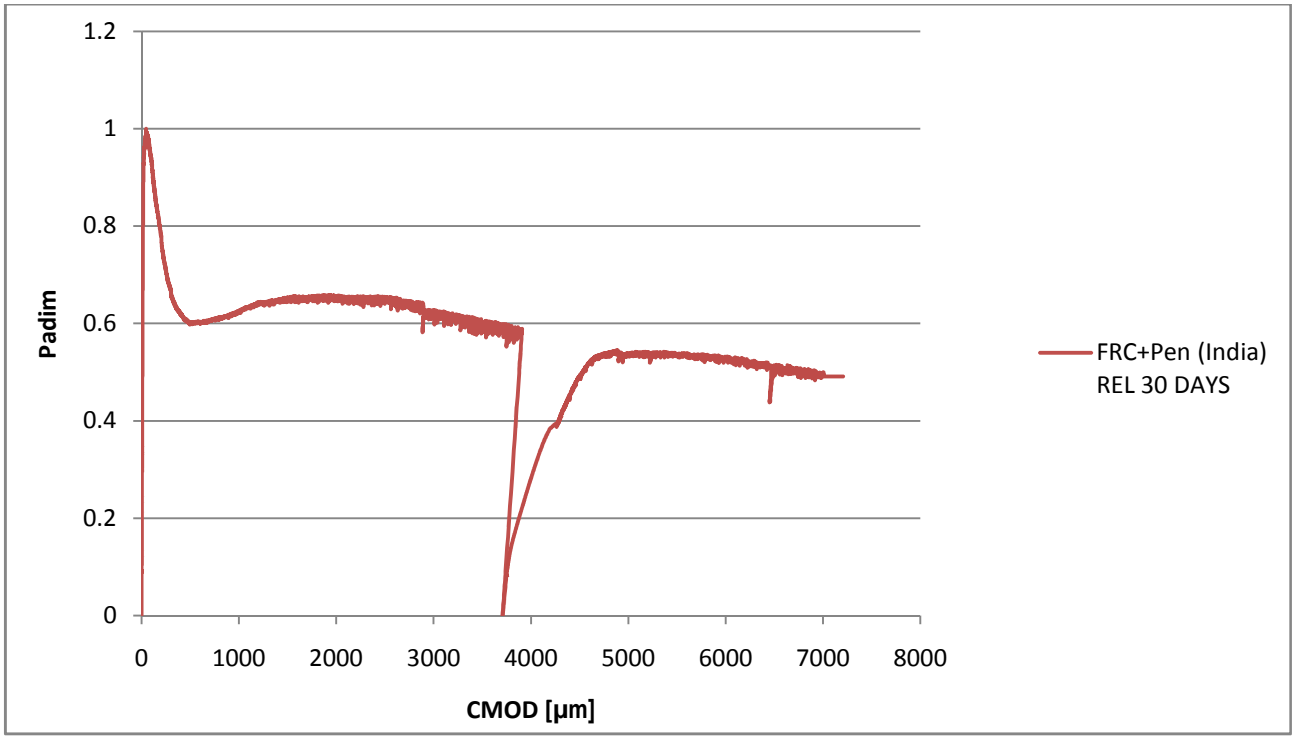

Figure 60: average behaviour during precracking up to 4000 µm of virgin FRC specimens casted in India with crystallizing agent and reloading after 30 days.

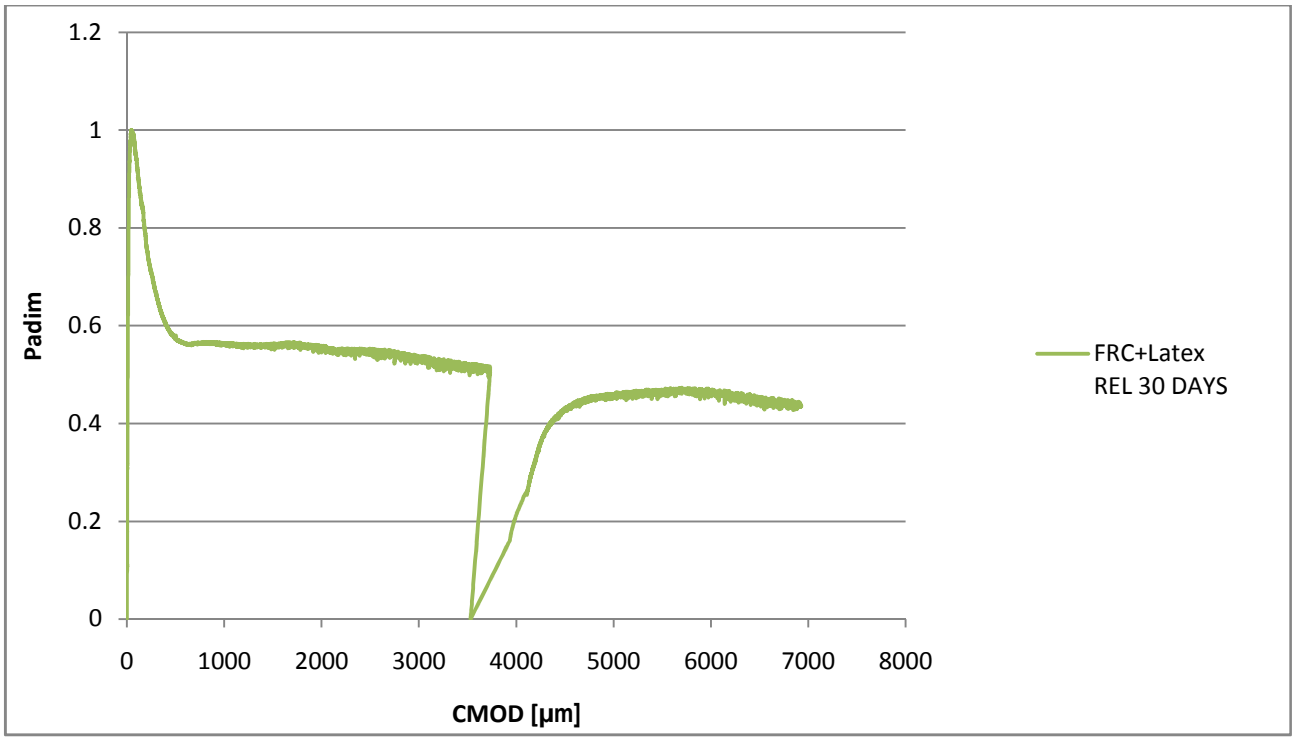

Figure 61: average behaviour during precracking up to 4000 µm of virgin latex-modified FRC specimens casted in India and reloading after 30 days.

4.3.6. CMOD 4000 µm: reloading after 90 days

After 90 days of conditioning, samples containing crystallizing agent presented almost the total filling of the upper part of the crack (**Figure 62**) , while samples casted without the addition of crystallizing agent still resulted almost unsealed.

***Figure 62: level of crack* sealing after 90 days of conditioning for specimens precracked up to 4000 µm**

The load-CMOD curves of FRC specimens (**Figure 63**) highlights a drop of load bearing capacity. If previously the reloading curves appeared as a natural prosecution of the precracking curves, for this batch of samples, some loss became evident during testing.
This effect was mitigated for samples containing crystallizing agent (**Figure 64**) and for latex-modified beams (**Figure 65**).
Both the FRC with and without addition showed a first linear branch which reached loads of 20% of residual load of precracking, supporting the hypothesis made for samples precracked up to 600 µm, that stiffness recovery occurs along with conditioning time.
Crystallization that occurs during conditioning, has the effect of increasing the global stiffness of samples.

After this first linear branch, stiffness decreased and, before reaching the residual load of precracking, a sudden rupture of the fibers leaded to an immediate decrease in carried load, followed by a slight softening.
Fiber ruptures was accompanied during the tests by a characteristic sound which announced that steel was breaking.
This phenomenon was probably due to the corrosion of the steel, that occurred because of the humid/dry cycles and concerned mainly FRC specimens without addition of latex or crystallizing agent.
Samples containing crystallizing agent were actually more controllable during the tests and the loss of strength was less pronounced.
It might be hypothesized that sealing effect of crystallizing agent might have protected fibers from steel corrosion and contributed to establish strongest bonds between fibers and cement paste.

Latex-modified FRC beams, finally, did not highlight any weakness due to fibers oxidation. Probably due to the delayed hydration of samples. Because of the formation of the polymeric film around the cement particles, fibers were also in this case prevented by corrosion.
However, any particular recovery was highlighted also for this batch of specimens.

In conclusion:

- *Along with exposition time to conditioning, specimens without additions highlight a loss of strength due to fibers oxidation*
- *Self-healing effect results in a partial filling of cracks, especially in samples containing the crystallizing agent*
- *Crystallization due to self-healing results in the prevention of fibers from corrosion*

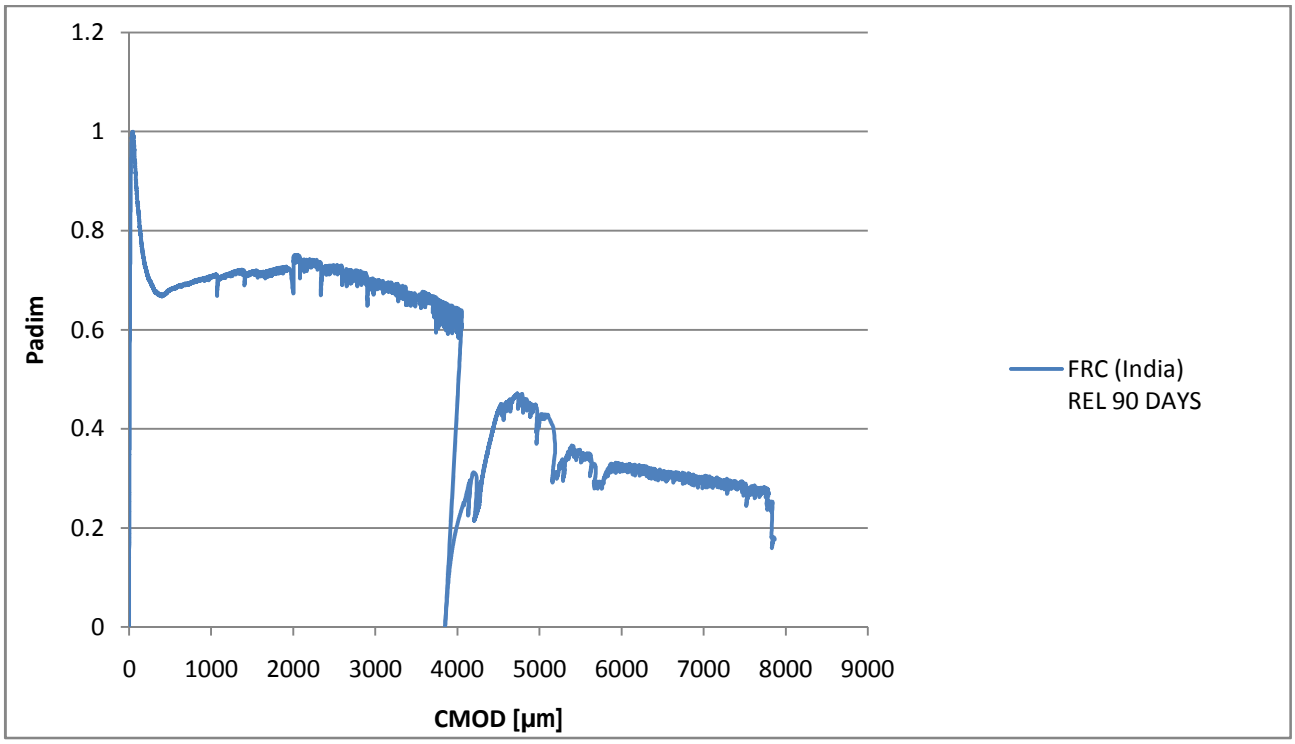

Figure 63: average behaviour during precracking up to 4000 µm of virgin FRC specimens casted in India and reloading after 90 days.

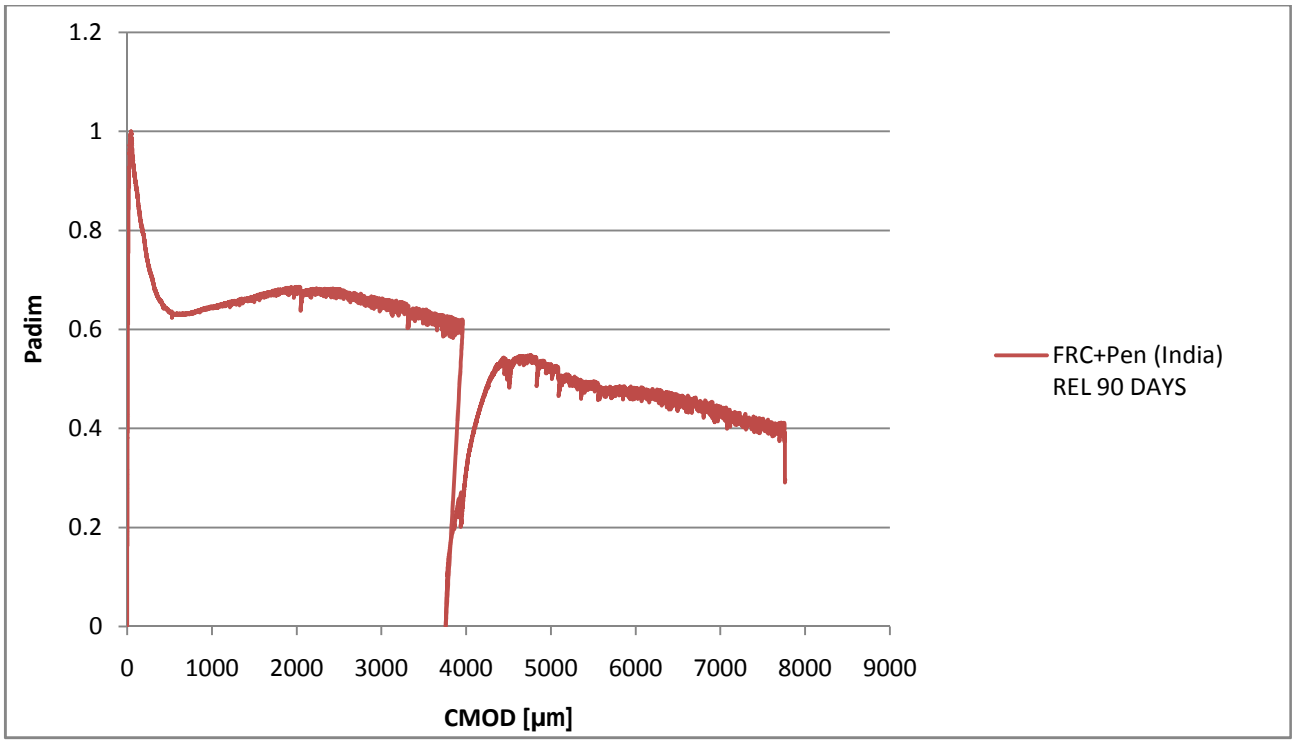

Figure 64: average behaviour during precracking up to 4000 µm of virgin FRC specimens casted in India with crystallizing agent and reloading after 90 days.

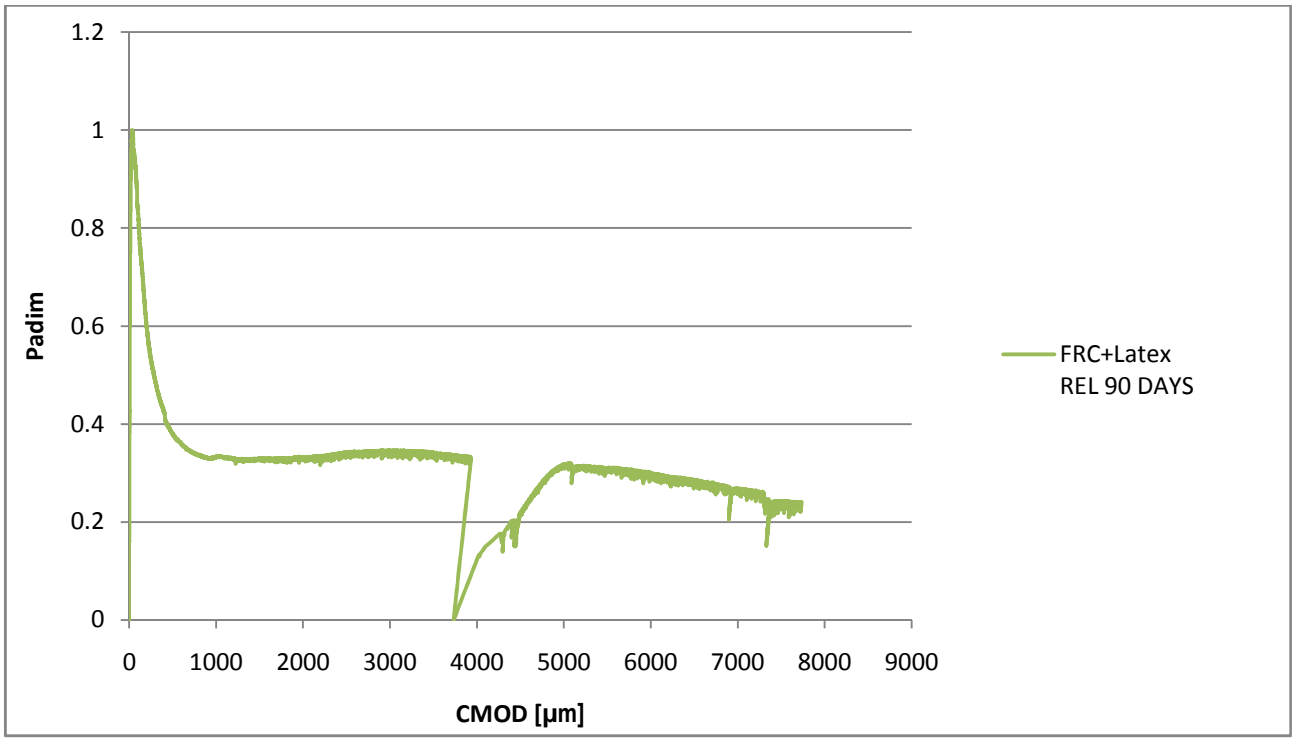

Figure 65: average behaviour during precracking up to 4000 µm of virgin latex-modified FRC specimens casted in India and reloading after 90 days.

4.3.7. CMOD 4000 µm: reloading after 270 days

After 270 days of conditioning, specimens showed a completely brittle behaviour (**Figure 66**).

If the previous cycle of tests after 90 days had highlighted a drop of load bearing capacity limited to FRC specimens without crystallizing agent, in this session of tests all the three mixes featured to load presented a complete loss of strength. Most of the samples failed during the preloading phase, while others failed under loads of 1.5 to 2 kN, which corresponds at 10 to 20% of residual load of precracking. Moreover, fibers appeared completely oxidized.
This latter observation would confirm what hypothesized in the paragraph above:

- *A prolonged conditioning with wet/dry cycles is detrimental due to the oxidation of fibers, due to wet/dry cycles, causes a drop of strength*
- *When prolonged conditioning and wide crack opening are combineds, self-healing effect is overwhelmed by the effect of corrosion and samples completely lose their load bearing capacity*

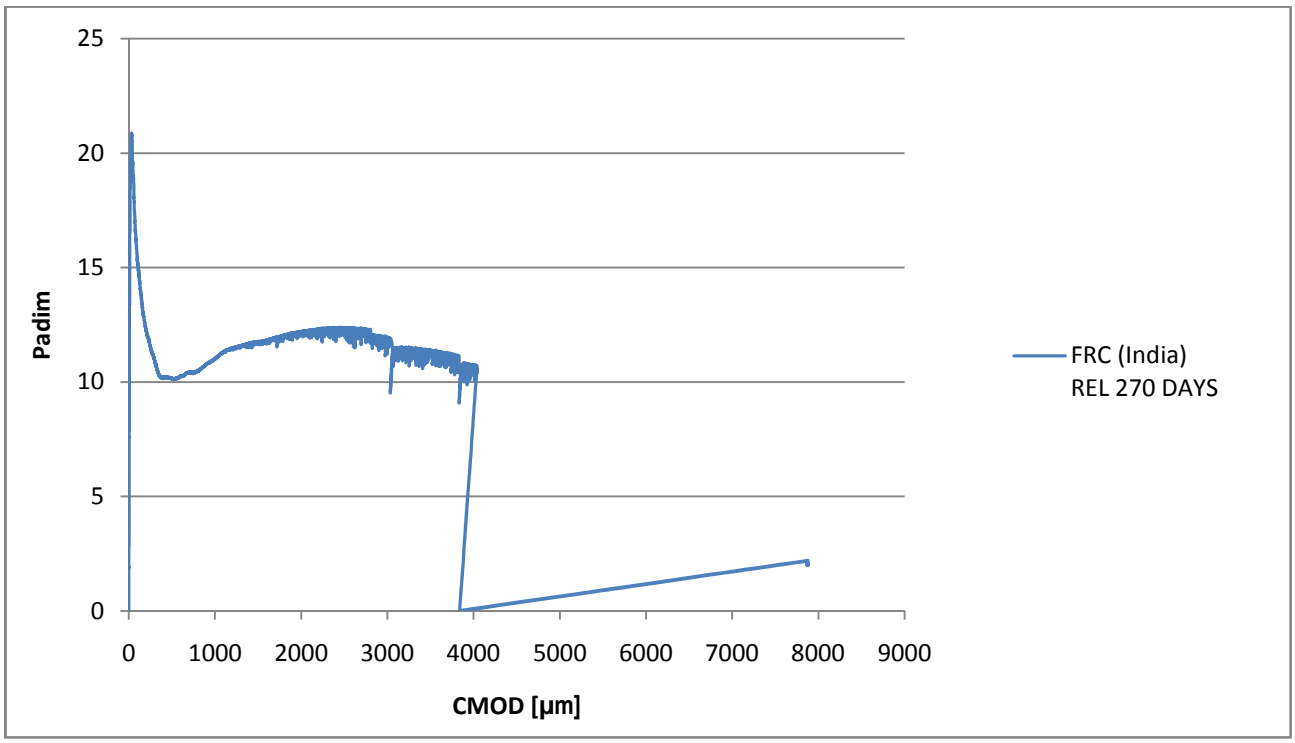

Figure 66: average behaviour during precracking up to 4000 µm of virgin FRC specimens casted in India and reloading after 270 days.

4.3.8. Choosing a measure for self-healing

In order to provide a quantitative evaluation of the self-healing capacity, in this work will be considered the difference between the peak load, obtained after reloading and the residual load of precracking (**Figure 67**).

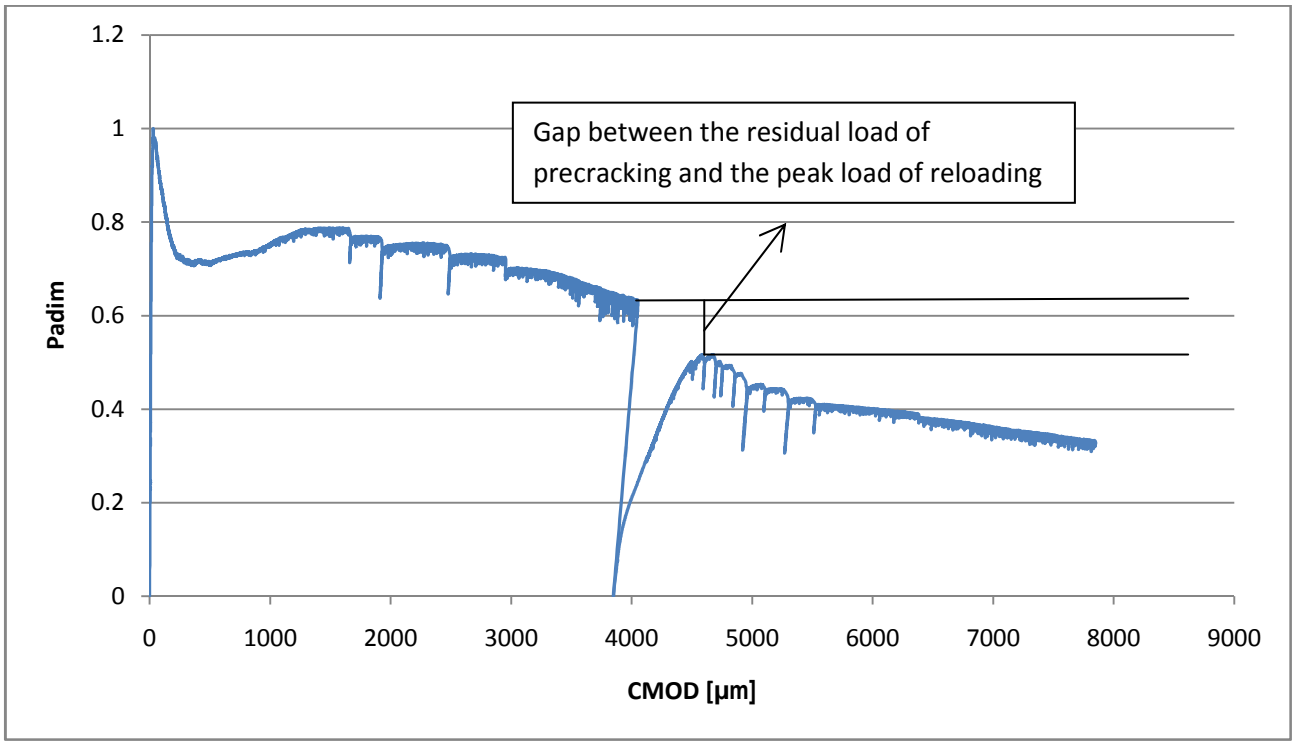

Figure 67: Precracking and reloading after 30 days of an Indian FRC sample. By comparing the precracking and reloading curves, the self-healing can be evaluated. If any healing takes place, the peak load of reloading is higher than the residual load of precracking.

If the specimen presents any significant healing, in fact, it can be expected that the peak load obtained by the second test overtakes the residual load obtained in the precracking phase. Moreover, the performed recovery cannot be affected by any particular hardening or softening phenomenon, which would have happened between CMOD 500 and 2500 µm.
The recovery in terms of load that the specimens precracked at 4000 µm eventually perform will be definitely calculated as following:

$$recovery\ \% = \frac{(PL(r) - RL(p))}{RL(p)} \times 100$$

- PL(r) = peak load of reloading
- RL(p) = residual load of precracking

For the specimens precracked with a CMOD of 600 µm, further considerations are needed.
The load-CMOD curves previously illustrated, showed the presence of a hardening branch from deformations of about 500 to 1500-2500 µm for FRC specimens casted in India and, in opposition, FRC samples casted in Italy highlighted a strong softening behaviour.

The computation of self-healing, in this case, must consequently keep into account the increase or decrease of load due to the hardening or softening of the material.

Additionally, specimens of different type reached the peak load of reloading under different deformation and in dependence with the time of conditioning.

Consequently in this research, the peak load at reloading of the tested specimens has been compared with the average monotone curve, shifted as explained in the following **Figure 68**, in order to keep into account any possible effect of hardening.
In order to fix a reference CMOD for the self-healing quantification, measurements were taken at CMOD 1500 µm. The latter is the value of deformation at which samples from each batch, along with time, tended to localize the peak load of reloading, exhausting their recovery capacity.
Furthermore, fixing a defined value of crack opening at which quantifying self-healing, was essential in order to establish a comparison among the results achieved by the different materials.

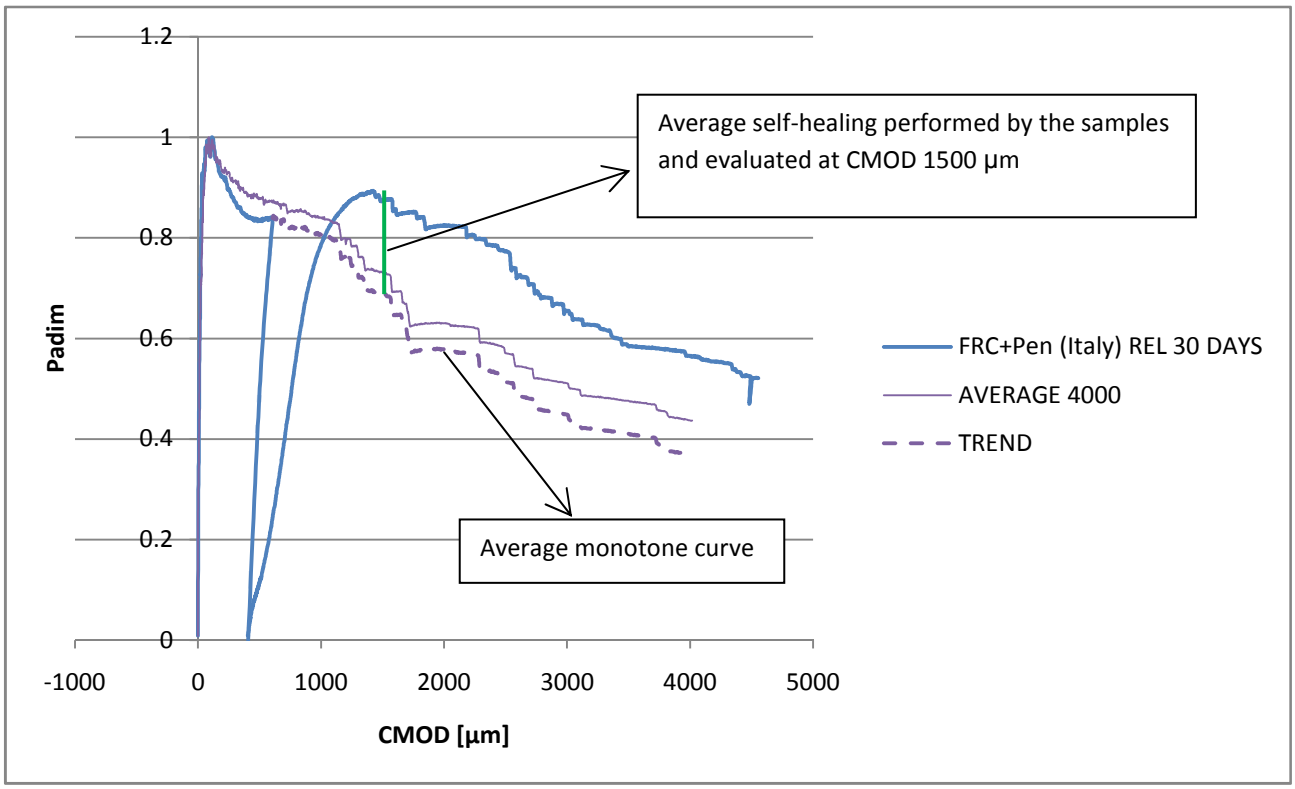

Figure 68: self-healing is evaluated as difference between the load corresponding to CMOD 1500 µm during reloading and the residual load of precracking. To this latter is added the contribution of softening (or hardening), calculated on the average curve of precracking. Global self-healing is expressed by the green line

The recovery in terms of load that the specimens precracked up to 600 µm eventually perform will be calculated as following.

$$recovery\ \% = \frac{\left(PL(r) - TL(p)\right)}{RL(p)} \times 100$$

- TL(p) = "trend load"; it represents the effect of hardening or softening. It is the load that the curve precracked up to 600 µm would have reached by continuing the tests and its prevision is based on the analysis of the average monotone curve of precracking at 4000 µm of each batch of samples
- PL(r) = peak load of reloading
- RL(p) = residual load of precracking

4.3.9. Evaluation of self-healing: CMOD 600 µm

FRC specimens casted in India: reloading after 30 days

The following **Tables 16-17-18** report the results performed in the tests. In particular the trend load TL, which keeps into account the average hardening or softening behaviour of the samples precracked up to 4000 µm is compared with the peak load of reloading. Recovery is quantified as percentage of the residual load of precracking.

SAMPLE	RL(p) [kN]	PL(r) [kN]	TL(p) [kN]	PL(r)-TL(p)	Rec%
FRC6	9.858	10.71	11.18	-0.47	**-4.97**
FRC13	16.362	15.79	17.68	-1.89	**-11.55**
FRC17	10.398	9.67	11.718	-2.05	**-19.72**
AV					**-12.08**

Table 16: characteristic values obtained for plain FRC specimens casted in India and reloaded after 30 days

SAMPLE	RL(p) [kN]	PL(r) [kN]	TL(p) [kN]	PL(r)-TL(p)	Rec%
PEN4	12.942	11.1	13.69	-2.59	**-20.01**
PEN7	11.633	14.9	12.38	2.52	**21.66**
PEN15	11.394	12.0	12.14	-0.144	**-1.26**
AV					**0.48**

Table 17: characteristic values obtained for FRC specimens with the addition of Penetron casted in India and reloaded after 30 days

SAMPLE	RL(p) [kN]	L(1500) [kN]	TL(p) [kN]	PL(r)-TL(p)	Rec%
LAT13	6.3	6.559	5.97	0.589	**9.35**
LAT14	12.322	10.95	11.99	-1.55	**-12.58**
AV					**-1.62**

Table 18: characteristic values obtained for latex-modified specimens reloaded after 30 days

Samples precracked up to 600 µm, presented after thirty days an average loss of strength, with the exception of one sample containing crystallizing agent, which showed a slight regain, as summarized by **Figure 69**.

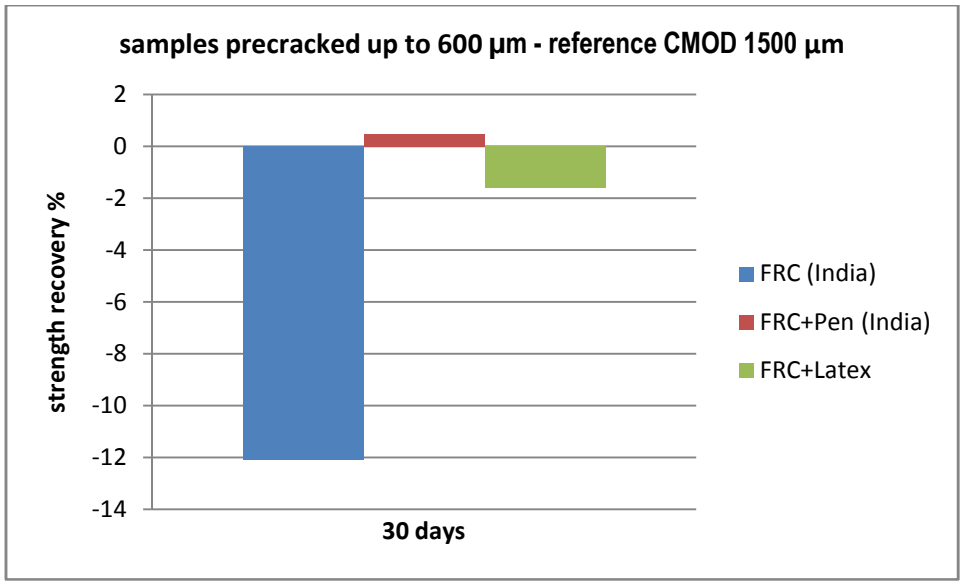

Figure 69: percentage strength recovery of FRC samples precracked at CMOD 600 µm and reloaded after 30 days of conditioning

FRC samples without Penetron did not show any complete recovery after conditioning. Even without considering any effect of hardening, the difference between the load of reloading at CMOD 1500 µm and the residual load of precracking was in average negative.
After considering the possible effect of hardening through the previsional term TL, the absence of strength recovery performed by FRC samples without crystallizing agent was highlighted: the loss was 12.08%.
On the other hand FRC specimens containing crystallizing admixture did show better results, though scattered, recovering the 0.48%. It can be hypothesized that crystallizing agent acted somehow on the matrix, protecting fibers and increasing the average strength and compactness on the paste
Finally, latex-modified specimens showed an average decrease of strength of 1.62% .

In conclusion, it can be stated that, after short conditioning times, specimens casted with crystallizing agent are merely able to balance the negative effect of wet/dry cycles on fibers, while other samples highlights a more pronounced loss of strength.

In the following graphs (**Figure 70-71-72**), the average behaviour during precracking and reloading after 30 days of the Indian FRC samples is represented in comparison with the shifted monotone curve employed to simulate the effect of hardening or softening.

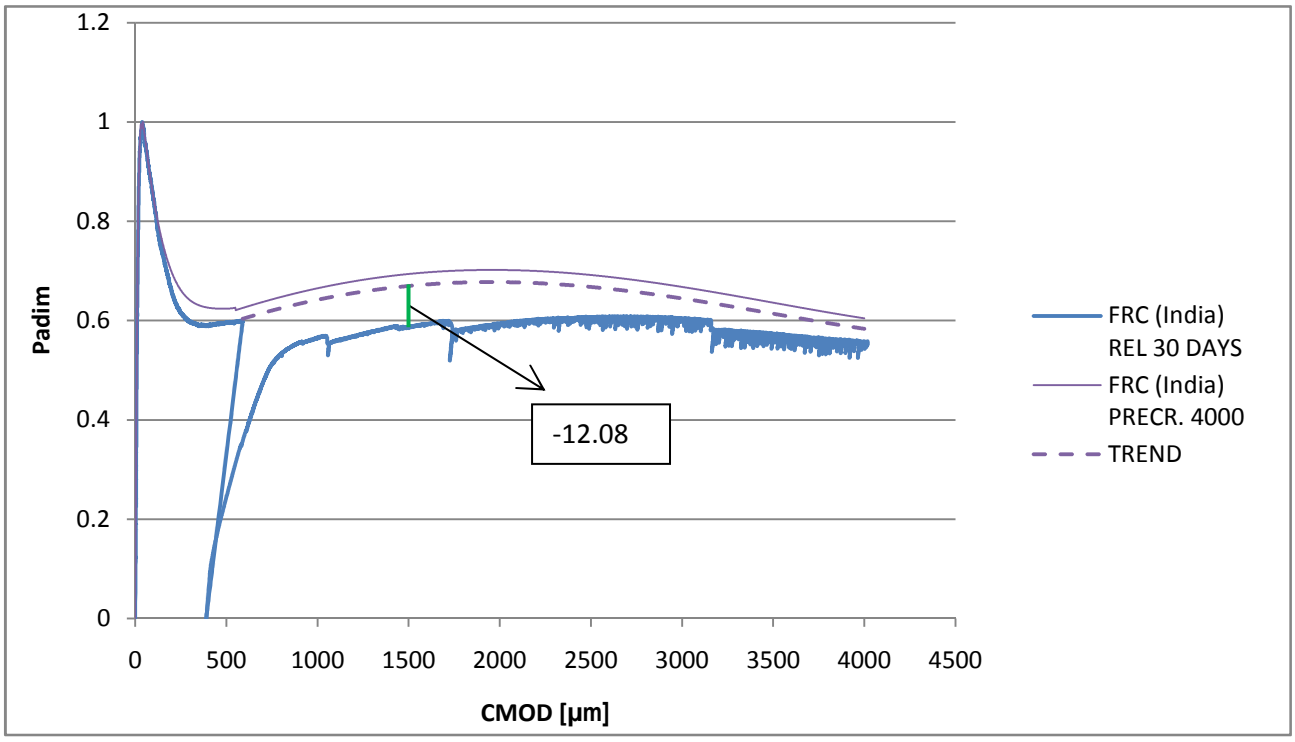

Figure 70: evaluation of the self-healing after 30 days of conditioning on FRC samples casted in India without the addition of crystallizing agent.

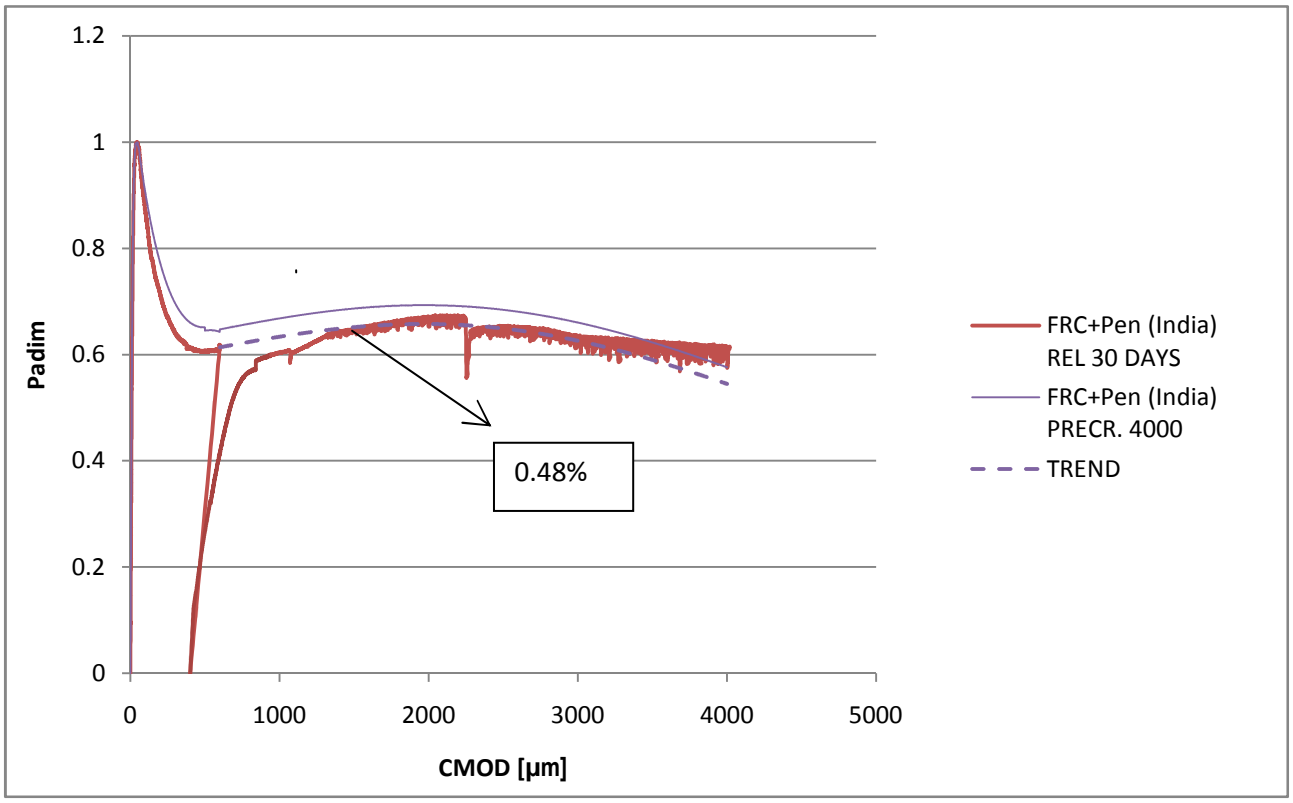

Figure 71: evaluation of the self-healing after 30 days of conditioning on FRC samples casted in India with the addition of crystallizing agent.

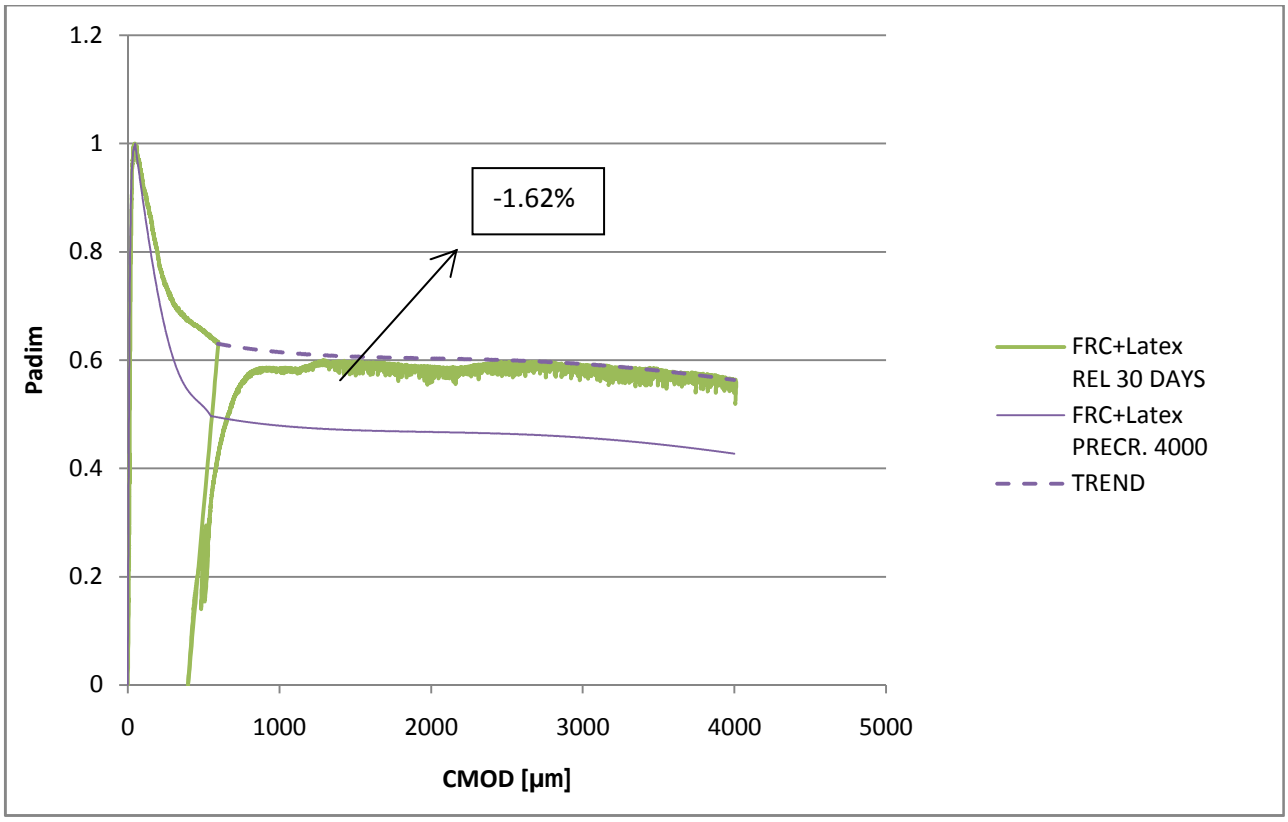

Figure 72: evaluation of the self-healing after 30 days of conditioning on latex-modified FRC samples casted in India

FRC specimens casted in Italy: reloading after 30 days

The following **Tables 19-20** reports the results of the tests for FRC samples casted in Italy, to which a through-crack compressive stress was applied during conditioning.

SAMPLE	RL(p) [kN]	PL(r) [kN]	TL(p) [kN]	PL(r)-TL(p)	Rec%
S1	10.94	10.50	8.90	1.6	**14.63**
S2	10.50	10.48	8.46	2.02	**19.25**
S4	9.18	9.10	7.14	1.96	**21.35**
AV					**18.41**

Table 19: characteristic values obtained for FRC specimens without crystallizing agent reloaded after 30 days

SAMPLE	RL(p) [kN]	PL(r) [kN]	TL(p) [kN]	PL(r)-TL(p)	Rec%
C1	8.35	9.21	6.31	2.9	**34.73**
C6	14.19	15.17	12.15	3.02	**21.28**
AV					**28.01**

Table 20: characteristic values obtained for FRC specimens containing the crystallizing agent reloaded after 30 days

Even without taking into account the softening behaviour of these batch of samples, specimens without Penetron presented the entire recovery of the residual load of precracking, while samples with the addition of the crystallizing agent overtook abundantly the corresponding value.

Considering softening, the average recovery achieved can be quantified at 18.4% (plain FRC samples) and 28.01% (FRC samples containing the crystallizing admixture) of residual load of precracking.

The following graphs (**Figure 74-75**) highlight the effect of compression on self-healing. Due to compression, FRC samples with or without addition were able to increase their self-healing performances up to 30% more than samples without compression applied (**Figure 73**).

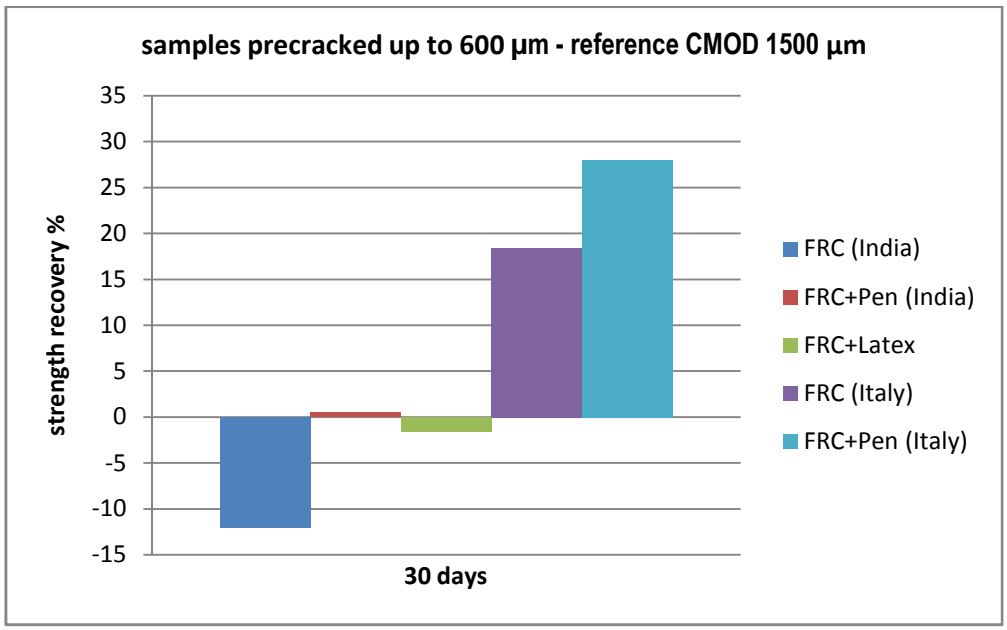

Figure 73: percentage strength recovery of FRC samples casted in Italy and precracked at CMOD 600 µm and reloaded after 30 days of conditioning, in comparison with the corresponding Indian results

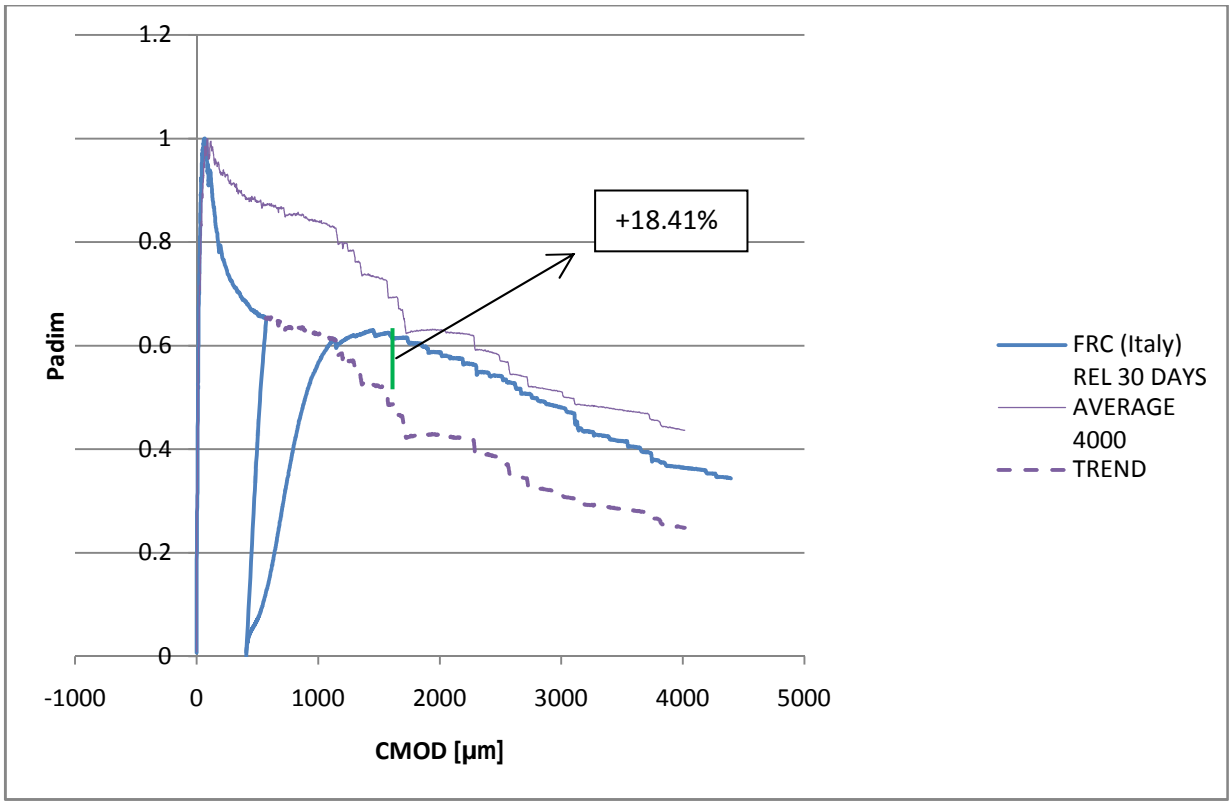

Figure 74: evaluation of the self-healing after 30 days of conditioning on FRC samples casted in Italy without the addition of crystallizing agent.

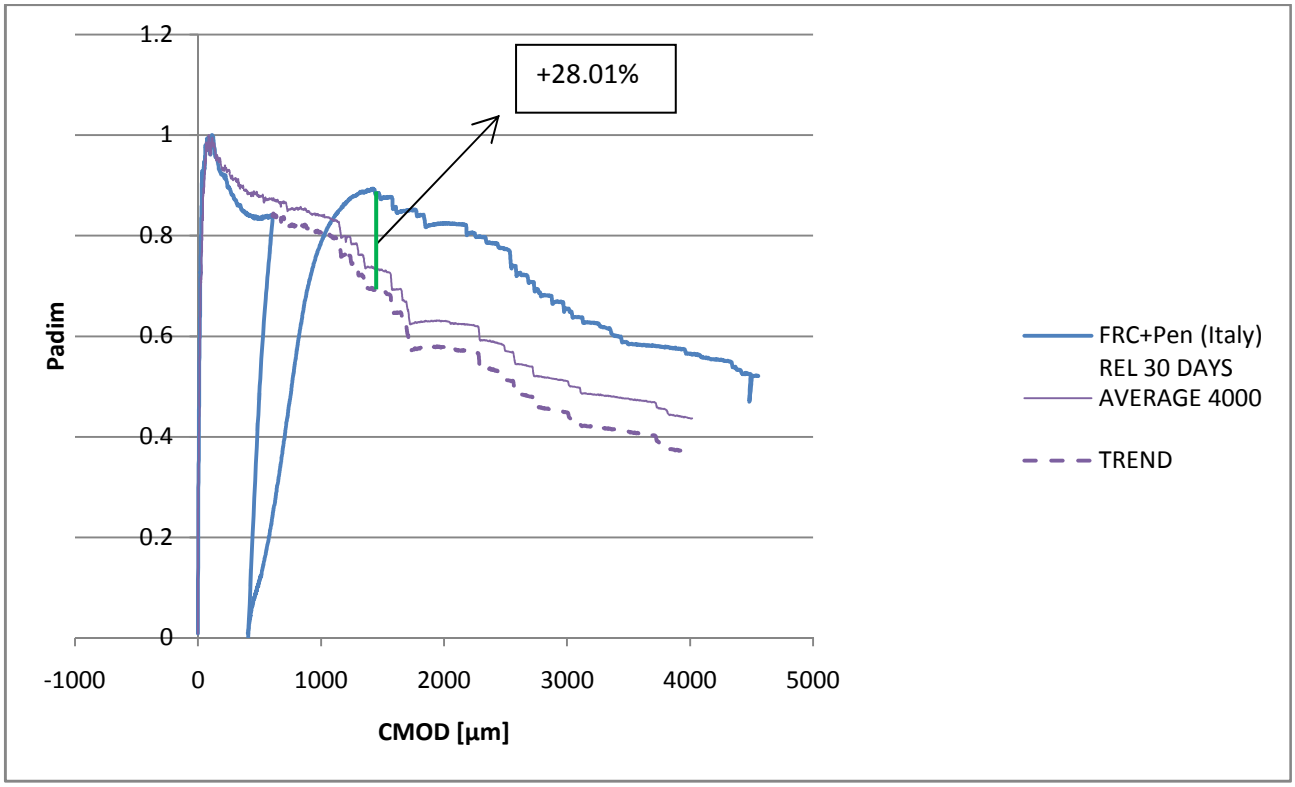

Figure 75: evaluation of the self-healing after 30 days of conditioning on FRC samples casted in Italy with the addition of crystallizing agent.

FRC specimens: reloading after 90 days

The following **Tables 21-22-23** report the results of the tests after 90 days of specimens conditioning for FRC samples respectively without and with crystallizing agent and containing latex.

SAMPLE	RL(p) [kN]	PL(r) [kN]	TL(p) [kN]	PL(r)-TL(p)	Rec%
FRC5	10.806	11.973	12.126	-0.153	**-1.42**
FRC13	17.113	18.6	17.68	0.92	**5.38**
FRC14	12.394	12.73	13.714	-0.98	**-7.94**
AV					**-3.98**

Table 21: characteristic values obtained for FRC specimens casted in India reloaded after 90 days

SAMPLE	RL(p) [kN]	PL(r) [kN]	TL(p) [kN]	PL(r)-TL(p)	Rec%
PEN6	14.446	15.35	15.196	0.154	**1.07**
PEN3	13.697	16.58	14.45	2.133	**15.57**
AV					**7.79**

Table 22: characteristic values obtained for FRC specimens casted in India reloaded after 90 days

SAMPLE	RL(p) [kN]	PL(r) [kN]	TL(p) [kN]	PL(r)-TL(p)	Rec%
LAT9	10.951	11.973	10.62	1.353	**12.36**
LAT10	8.299	7.51	7.97	-0.46	**-5.54**
LAT17	9.75	9.58	9.42	0.16	**1.64**
AV					**2.82**

Table 23: characteristic values obtained for latex-modified FRC specimens reloaded after 90 days

All the batches, along with time, increased their performances in comparison with samples tested after 30 days of conditioning.

If plain FRC specimens globally balanced the loss of load showed at 30 days, the other batches increased their performances of some percentage point (**Figure 76**).

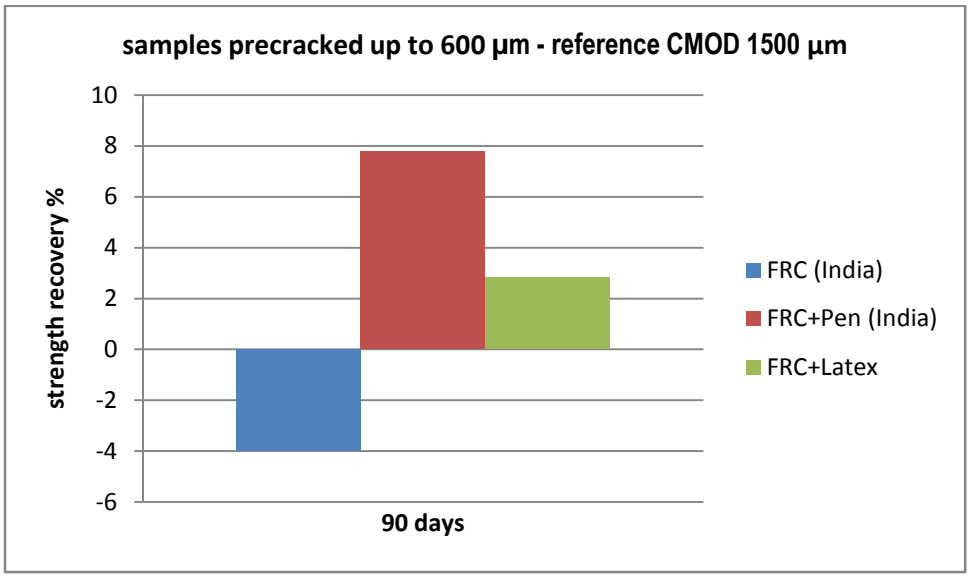

Figure 76: percentage strength recovery of FRC samples precracked at CMOD 600 µm after 90 days of conditioning

Concerning FRC specimens without additions, an almost complete recovery of the residual load of precracking occurred, and the loss of load showed at 30 days (-12.08%) was reduced (-3.58%).
Samples containing Penetron showed again the best self-healing capacity and recovered 7.79%.
Also specimens modified with latex showed a recovery of strength, which was 2.82%.

In these two latter cases, the effect of additions must have results in an increase of the crystallization (Penetron) and in the further hydration of cement particles, retarded by the formation of a polymeric film in samples containing latex.
Figure 77-78-79 represent the precracking and reloading of the batches after 90 days of conditioning, in comparison with the monotone curve.

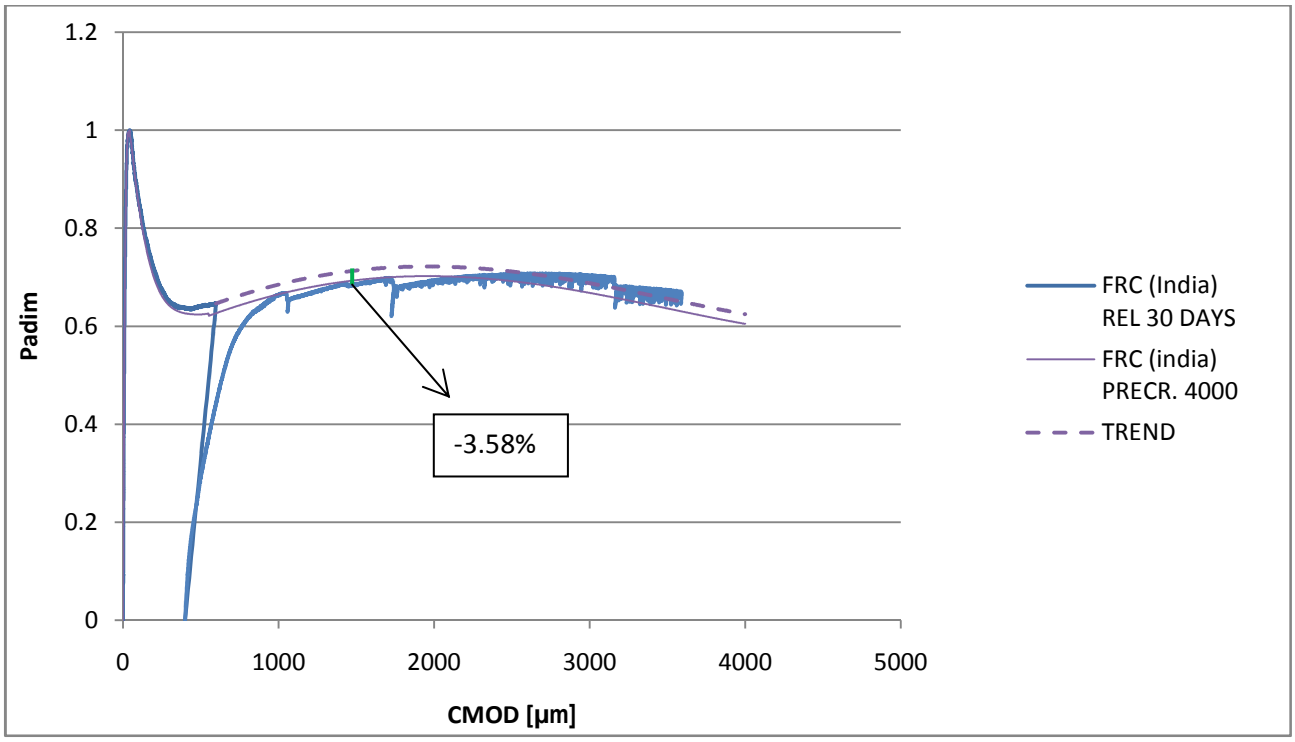

Figure 77: evaluation of the self-healing after 90 days of conditioning on FRC samples casted in India without the addition of crystallizing agent.

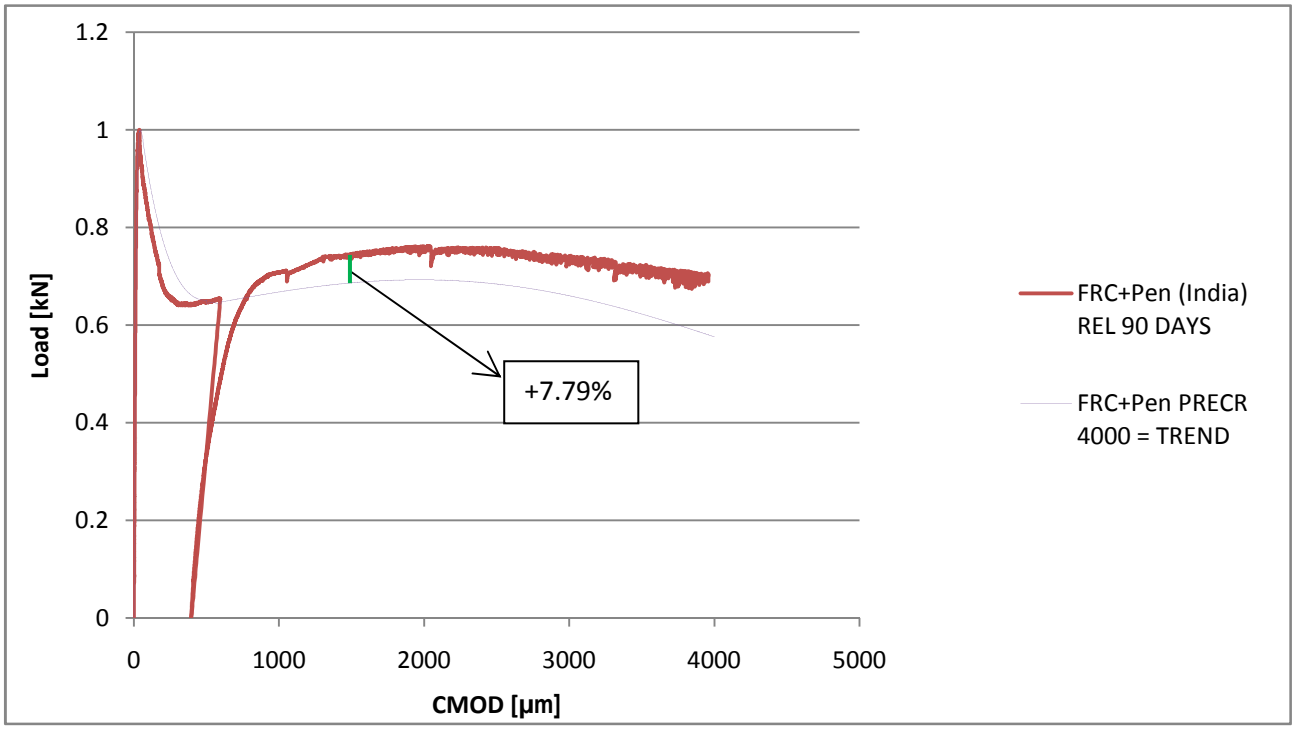

Figure 78 evaluation of the self-healing after 90 days of conditioning on FRC samples casted in India with the addition of crystallizing agent.

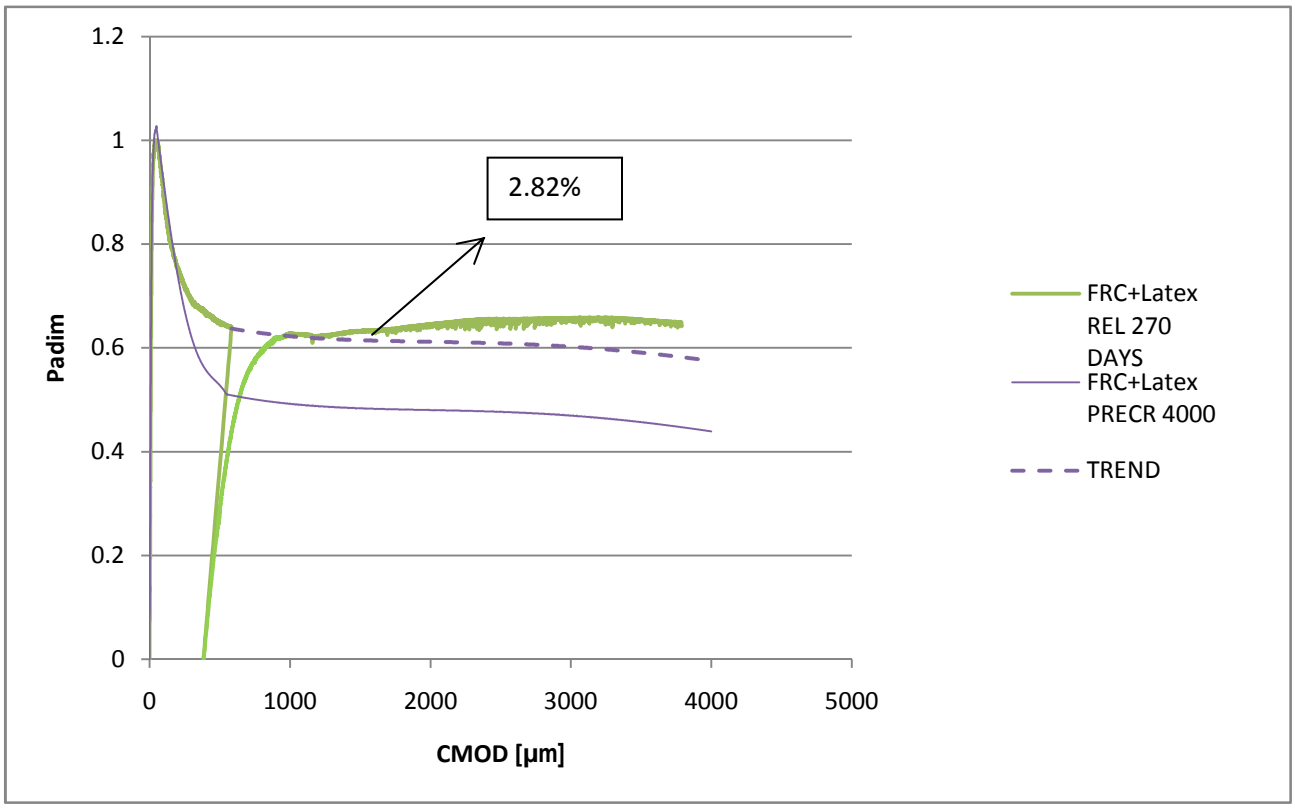

Figure 79 evaluation of the self-healing after 90 days of conditioning on latex-modified FRC samples casted in India

FRC specimens: reloading after 270 days

Specimens precracked up to 600 µm presented after 270 days of conditioning an important recovery of strength. In the following **Tables 24-25-26**, the registered results are summarized.

SAMPLE	RL(p) [kN]	PL(r) [kN]	TL(p) [kN]	PL(r)-TL(p)	Rec%
FRC15	9.38	10.85	10.7	0.15	**1.6**
FRC16	13.294	14.30	14.61	-0.31	**-2.33**
AV					**-0.37**

Table 24: characteristic values obtained for FRC specimens casted in India and reloaded after 270 days

SAMPLE	RL(p) [kN]	PL(r) [kN]	TL(p) [kN]	PL(r)-TL(p)	Rec%
PEN2	18.964	21.22	19.71	1.506	**7.94**
PEN5	16.045	16.756	16.795	-0.039	**-0.24**
PEN 8	16.362	19.90	17.11	2.788	**17.04**
AV					**8.24**

Table 25 characteristic values obtained for FRC specimens casted in India with the addition of crystalizing agent and reloaded after 270 days

SAMPLE	RL(p) [kN]	PL(r) [kN]	TL(p) [kN]	PL(r)-TL(p)	Rec%
LAT18	8.07	7.98	7.74	0.24	**2.97**
AV					**2.97**

Table 26: characteristic values obtained for latex-modified FRC specimens reloaded after 270 days

In average, after 270 days of conditioning, all the batches presented a recovery of strength, except plain FRC samples, which performed only a slight recovery in comparison with the previous tests, but a loss in absolute terms (**Figure 80**).

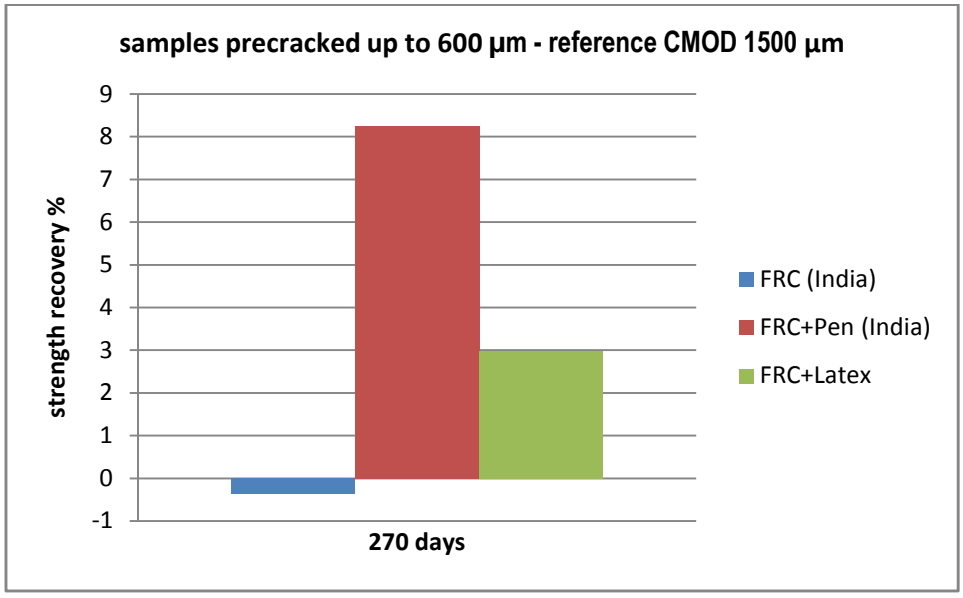

Figure 80: percentage strength recovery of FRC samples precracked at CMOD 600 µm after 270 days of conditioning

Plain FRC samples casted in India showed an average loss of 0.37%, though better than the loss of 3.9% performed at 90 days.
FRC samples containing crystallizing agent achieved the recovery of 8.24%, not far from the 7.79% performed at 90 days.
Similarly, the only latex-modified specimen tested registered a recovery of 2.97%, while at 90 days the same samples had performed a recovery of 2.82%.

Essentially, after 270 days, specimens with the addition of crystallizing agent and latex did not highlight an increase in load bearing capacity, but recovery was limited to their capacity of maintaining the initial stiffness. FRC showed performances 3% better of the ones the samples had at 90 days.
This behaviour suggest that the triggering action on self-healing of the additions could be maximum on the short-medium period and that oxidation of fibers balance the effect of crystallization when conditioning is prolonged.

Figure 81-82-83 represents the average behaviour of the tested batches, in comparison with the monotone curve.

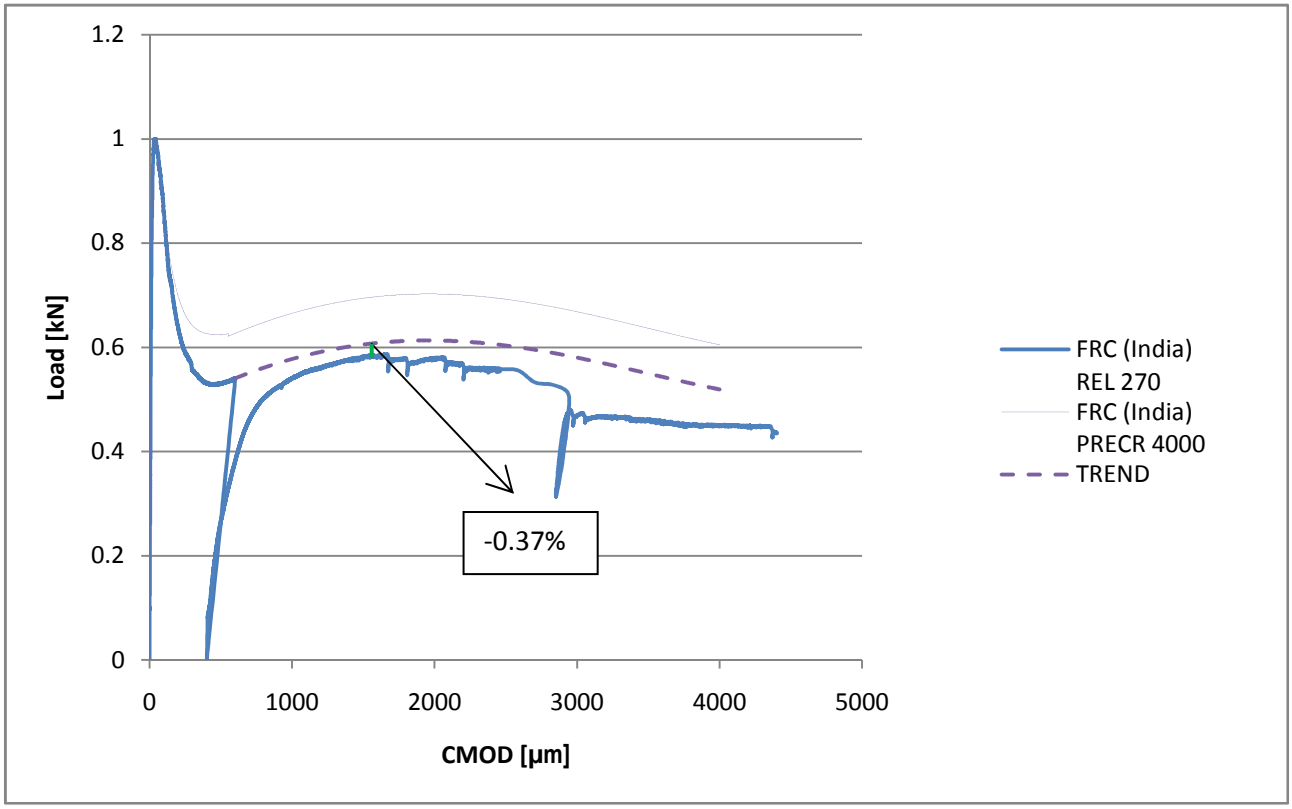

Figure 81 ***evaluation of the self-healing after 270 days of conditioning on FRC samples casted in India without the addition of crystallizing agent.***

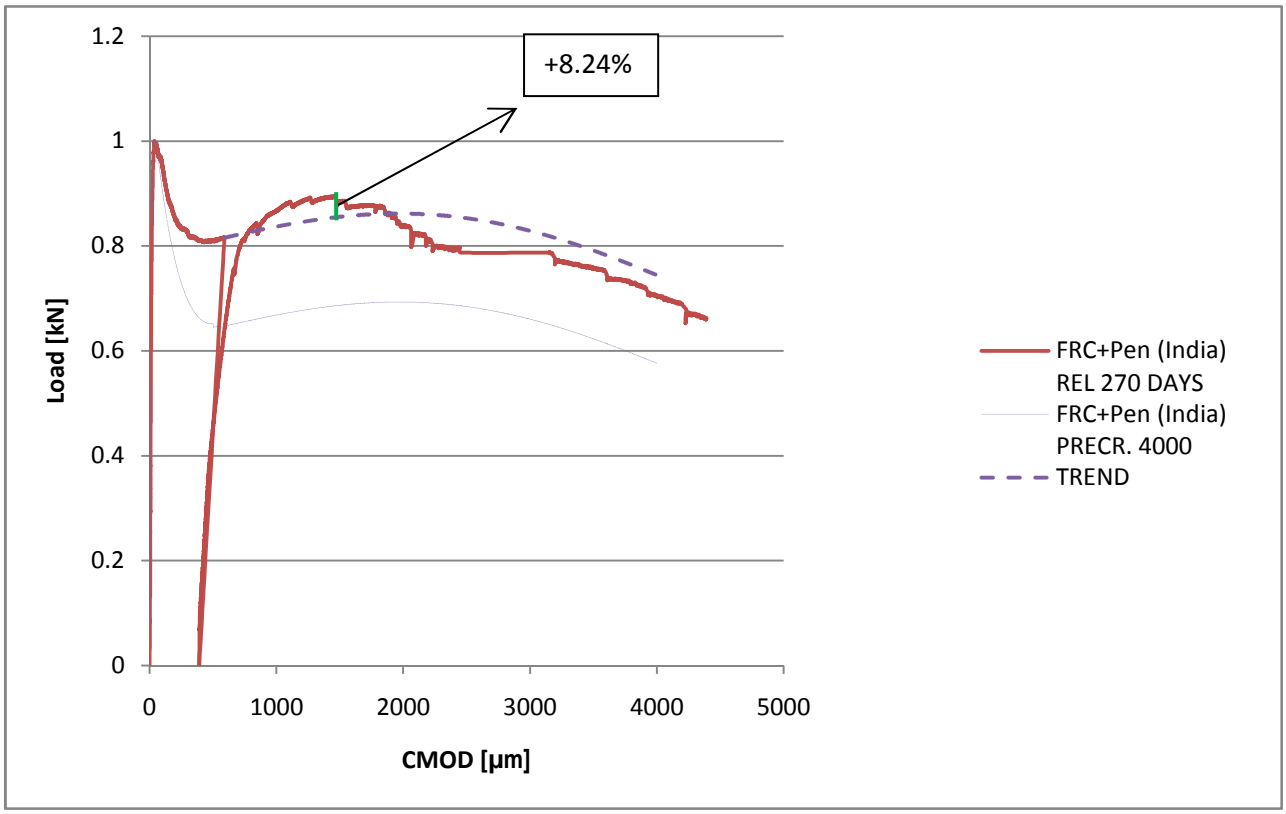

Figure 82: evaluation of the self-healing after 270 days of conditioning on FRC samples casted in India with the addition of crystallizing agent.

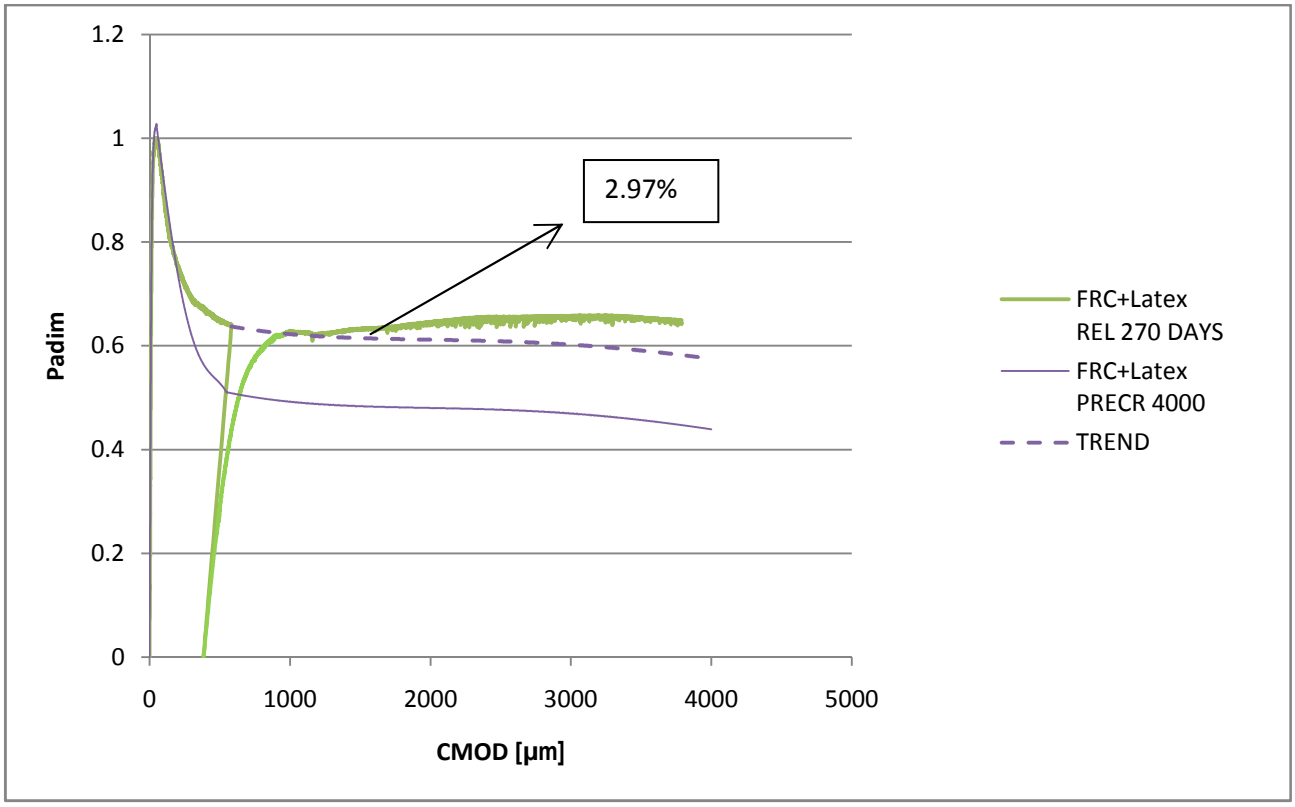

Figure 83: evaluation of the self-healing after 270 days of conditioning on latex-modified FRC samples casted in India

4.3.10. Evaluation of self healing: CMOD 4000 µm

In this section, the effects of the additions on promoting the self-healing of the material for CMOD 4000 µm will be considered.

FRC specimens: reloading after 30 days

In the following **Tables 27-28-29**, the values of peak load of precracking, residual load of precracking, peak load during reloading and the difference between the two latter are reported for all the tested specimens.

SPECIMEN	PL (p) [kN]	RL(p) [kN]	PL(r) [kN]	PL(r)-RL(p) [kN]	Recovery%
FRC2	19.653	11.238	11.404	0.166	**1.47**
FRC3	20.347	14.43	14.446	0.016	**0.11**
FRC16	16.583	10.984	9.772	-1.212	**-11**
AV	18.861	12.217	11.874	-0.343	**-3.14**

***Table 27: values* of peak load and residual load of precracking, peak load of reloading and quantification of recovery for FRC specimens casted in India and reloaded after 30 days**

SPECIMEN	PL (p) [kN]	RL(p) [kN]	PL(r) [kN]	PL(r)-RL(p) [kN]	Recovery%
PEN 1	21.548	13.534	13.31	-0.224	**-1.66**
PEN 10	18.463	9.084	8.435	-0.649	**-7.1**
AV	20.006	11.309	10.873	-0.437	**-4.38**

***Table 28: values of peak load and residual load of precracking, peak load of reloading and quantification of recovery for FRC* samples casted in India with the addition of crystallizing agent and reloaded after 30 days**

SPECIMEN	PL (p) [kN]	RL(p) [kN]	PL(r) [kN]	PL(r)-RL(p) [kN]	Recovery%
LAT2	14.349	7.46	7.16	-0.3	**-4.02**
LAT3	15.091	3.819	3.779	-0.04	**-1.04**
LAT7	13.605	9.248	9.327	0.079	**0.85**
AV	14.348	6.842	6.755	-0.087	**-1.40**

***Table 29: values of peak load and residual load of precracking, peak load of reloading and quantification of recovery for latex-* modified FRC specimens reloaded after 30 days**

if the recovery of load is considered, all the specimens precracked up to 4000 µm did not show any healing after the first thirty days of conditioning. The samples, in fact, did not show a complete recovery of the residual load of precracking test (**Figure 84**).

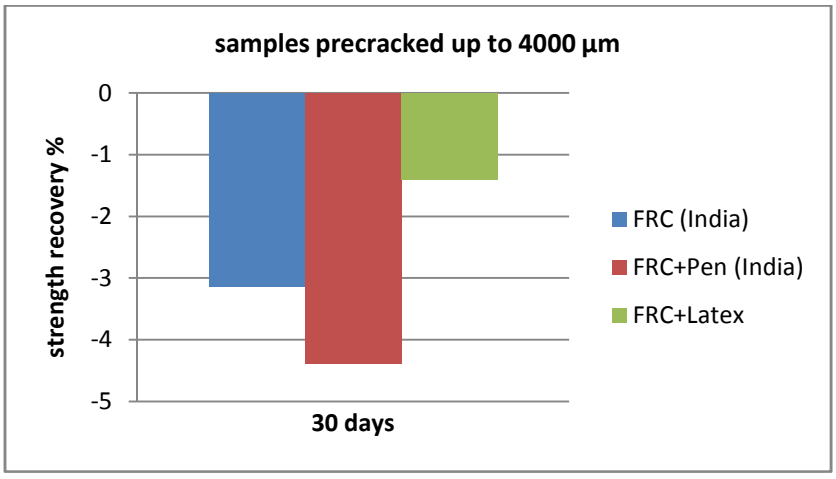

Figure 84 percentage strength recovery of FRC samples precracked at CMOD 4000 µm after 30 days of conditioning

All the mixes present similar results, with an average loss of strength that varies from 3.14% for Indian FRC samples, to 4.38% for specimens containing the addition of Penetron.
Latex-modified beams performed better with a lower loss of 1.4%.

Figure 85-86-87 represents the samples behaviour.

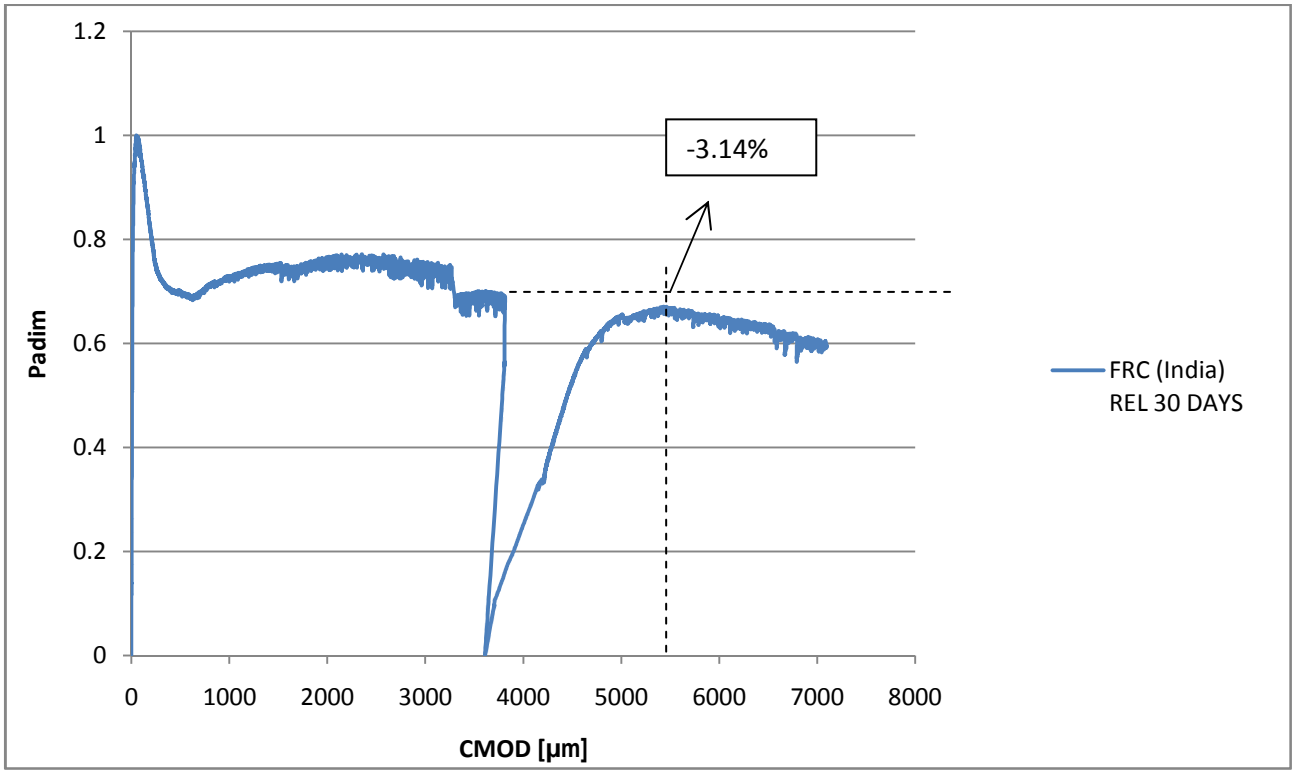

Figure 85: evaluation of the self-healing after 30 days of conditioning on FRC samples casted in India without the addition of crystallizing agent

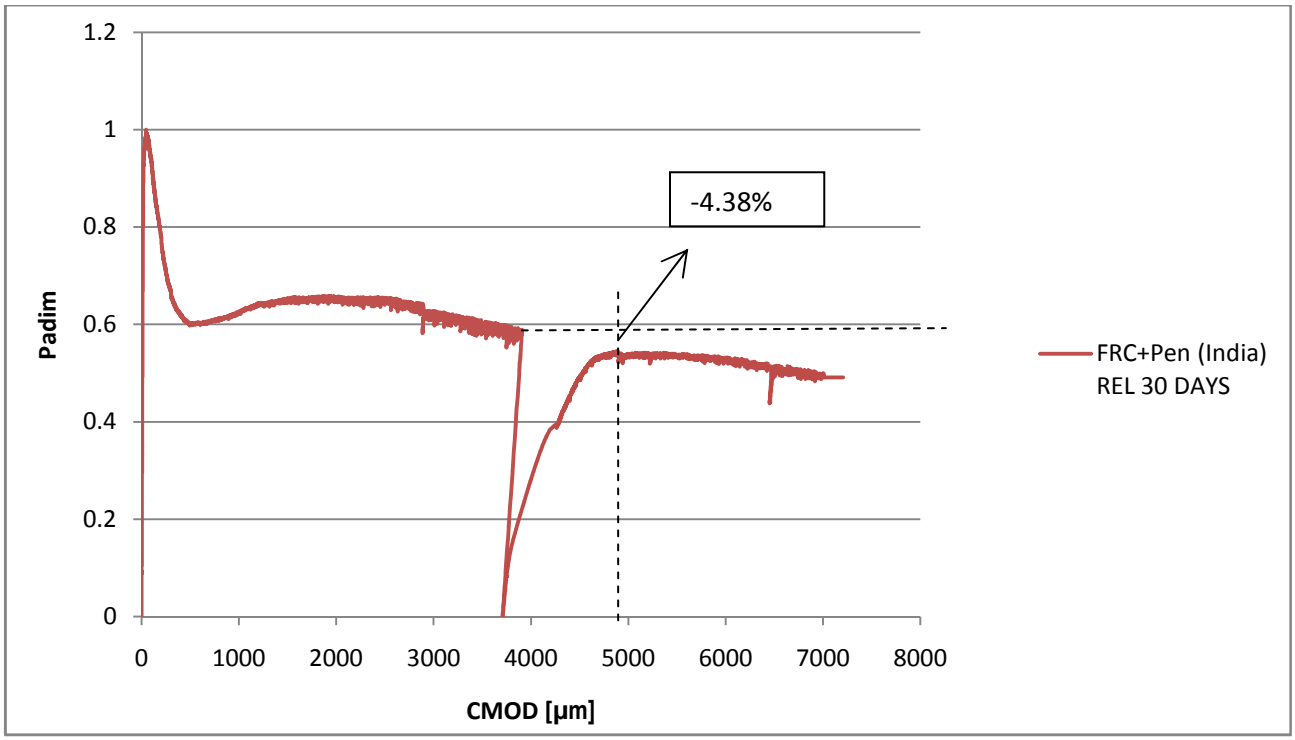

Figure 86: evaluation of the self-healing after 30 days of conditioning on FRC samples casted in India with the addition of crystallizing agent

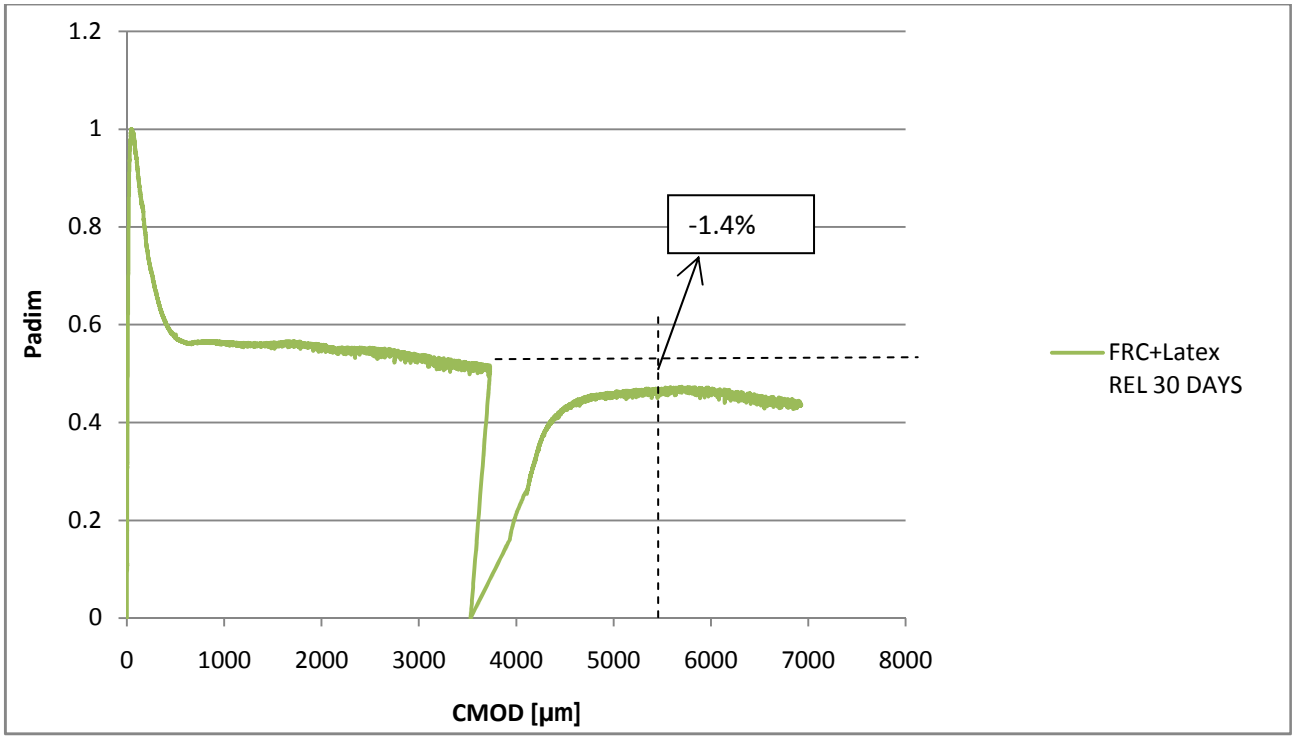

Figure 87: ***evaluation of the self-healing after 30 days of conditioning on latex-modified FRC samples casted in India***

FRC specimens: reloading after 90 days

Tables 30-31-32 summarize the results registered by specimens tested at 90 days.

SPECIMEN	PL (p) [kN]	RL(p) [kN]	PL(r) [kN]	PL(r)-RL(p) [kN]	Recovery%
FRC8	20.528	12.451	10.604	-1.847	**-14.83**
FRC12	21.371	13.973	9.858	-4.115	**-29.45**
FRC7	20.533	12.378	9.169	-3.209	**-25.93**
AV	20.811	12.934	9.877	-3.057	**-23.40**

Table 30: values of peak load and residual load of precracking, peak load of reloading and quantification of recovery for FRC specimens casted in India and reloaded after 90 days

SPECIMEN	PL (p) [kN]	RL(p) [kN]	PL(r) [kN]	PL(r)-RL(p) [kN]	Recovery%
PEN 9	19.722	13.519	12.827	-0.692	**-5.12**
PEN 12	17.535	11.158	10.044	-1.114	**-9.98**
PEN 14	19.008	7.772	7.834	+0.062	**0.80**
AV	18.755	10.816	10.235	-0.581	**-4.77**

Table 31: values of peak load and residual load of precracking, peak load of reloading and quantification of recovery for FRC specimens casted in India with the addition of Penetron and reloaded after 90 days

SPECIMEN	PL (p) [kN]	RL(p) [kN]	PL(r) [kN]	PL(r)-RL(p) [kN]	Recovery%
LAT4	12.652	4.355	4.457	-0.102	**-2.34**
LAT6	16.172	4.87	4.842	0.028	**0.57**
AV	14.412	4.6125	4.6495	-0.037	**-0.89**

Table 32: values of peak load and residual load of precracking, peak load of reloading and quantification of recovery for latex-modified FRC specimens reloaded after 90 days

It would have been expected that increasing conditioning time the specimens would had recovered either in stiffness and in peak load more than after 30 days.

Though, in terms of peak load during reloading, it was observed a pronounced decrease for FRC specimens casted without crystallizing agent (**Figure 88**).

On the other hand, FRC samples casted with Penetron and latex-modified FRC samples at 90 days did not show a changing in comparison with the behaviour at 30 days.

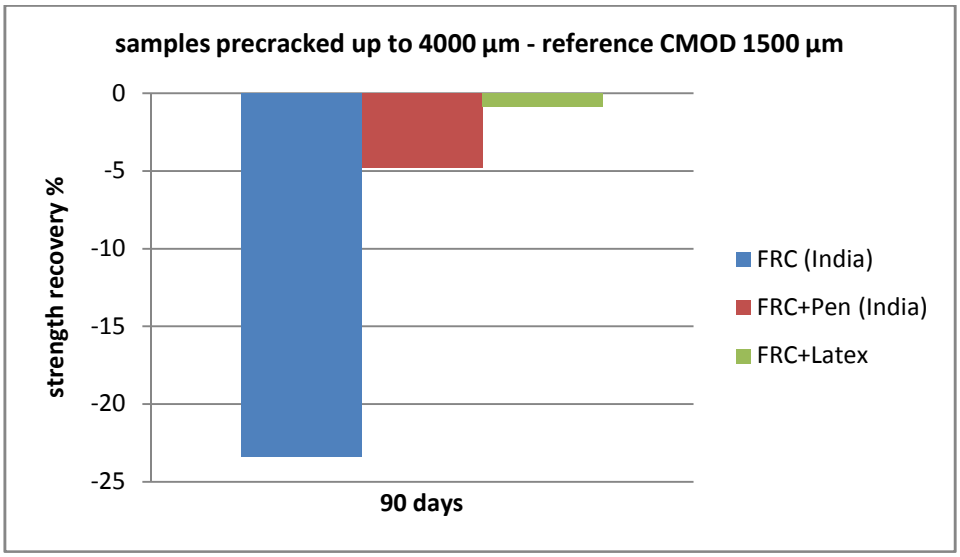

Figure 88: percentage strength recovery of FRC samples precracked at CMOD 4000 µm after 90 days of conditioning

FRC samples without Penetron did not recover the residual load of precracking, but the peak load of reloading was 23.4% lower.
It has to be highlighted that, during testing, it was evident the premature rupture of the fibers, which was accompanied by a peculiar sound and made the test difficult to be conducted. This rupture was due to the oxidation of the fibers, that took place because of the wet and dry cycles that in 90 days acted deeply on steel.
The logic conclusion is that the flexural strength, which mainly depends on the strength of fibers and on their bond with the paste, is in this case governed by the decreased strength of the rusted steel, which is lower than the bond with the paste.
Also samples containing the crystallizing agent featured a decrease in strength at 90 days. Only one specimen recovered completely the residual load of precracking, but in average this batch lost 4.77%.
The better performances of samples with crystallizing agent can be due to the action of crystallizing agent: samples resulted filled of a white substance in the upper part of the crack, while this phenomenon was really limited on specimens without addition.
Finally, latex-modified samples did not show important differences from the test at 30 days, though some premature rupture of the fiber occurred in this case.

Both the specimens tested recovered completely the residual load of precracking. Consequently, it has to be concluded that this capacity of maintaining the residual strength could be due to the advancing of the hydration of the paste: this process should be almost complete after three months of conditioning, creating bridges between the crack sides and protecting fibers from corrosion.

Load-CMOD curves are plotted in **Figures 89-90-91.**

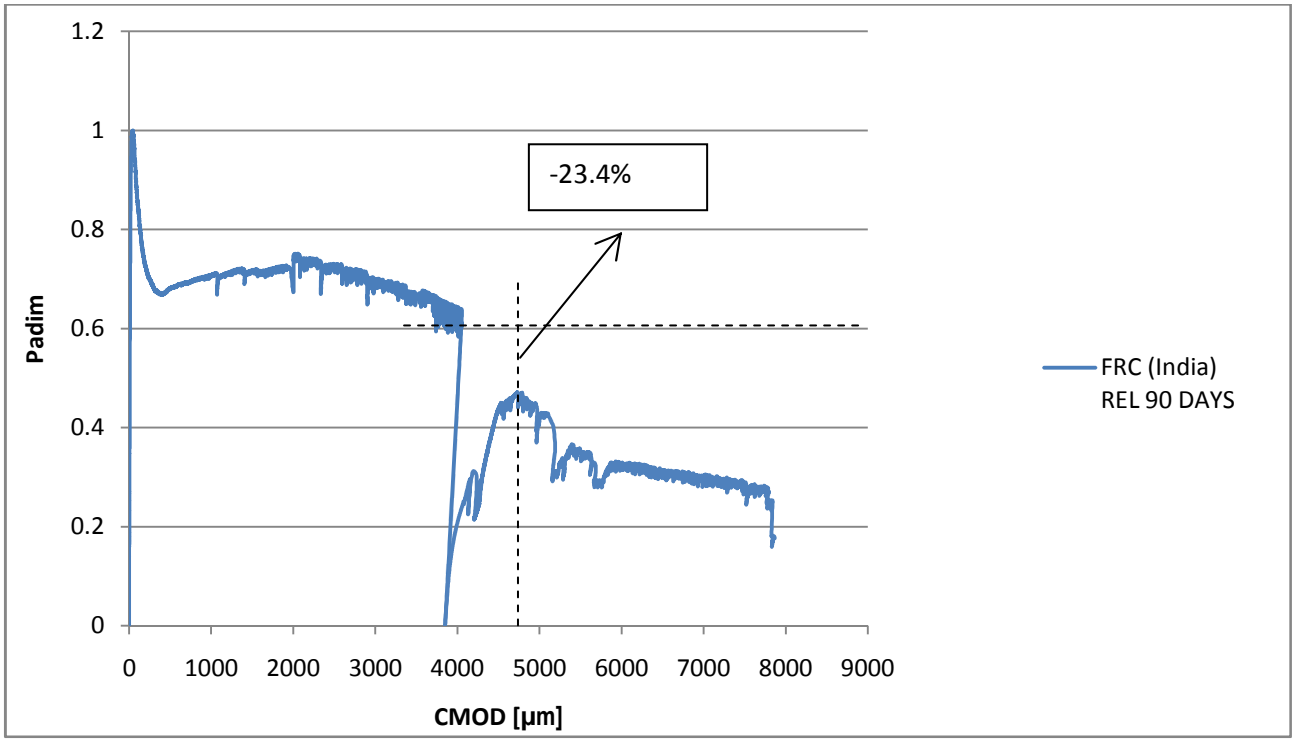

Figure 89: evaluation of the self-healing after 90 days of conditioning on FRC samples casted in India without the addition of crystallizing agent

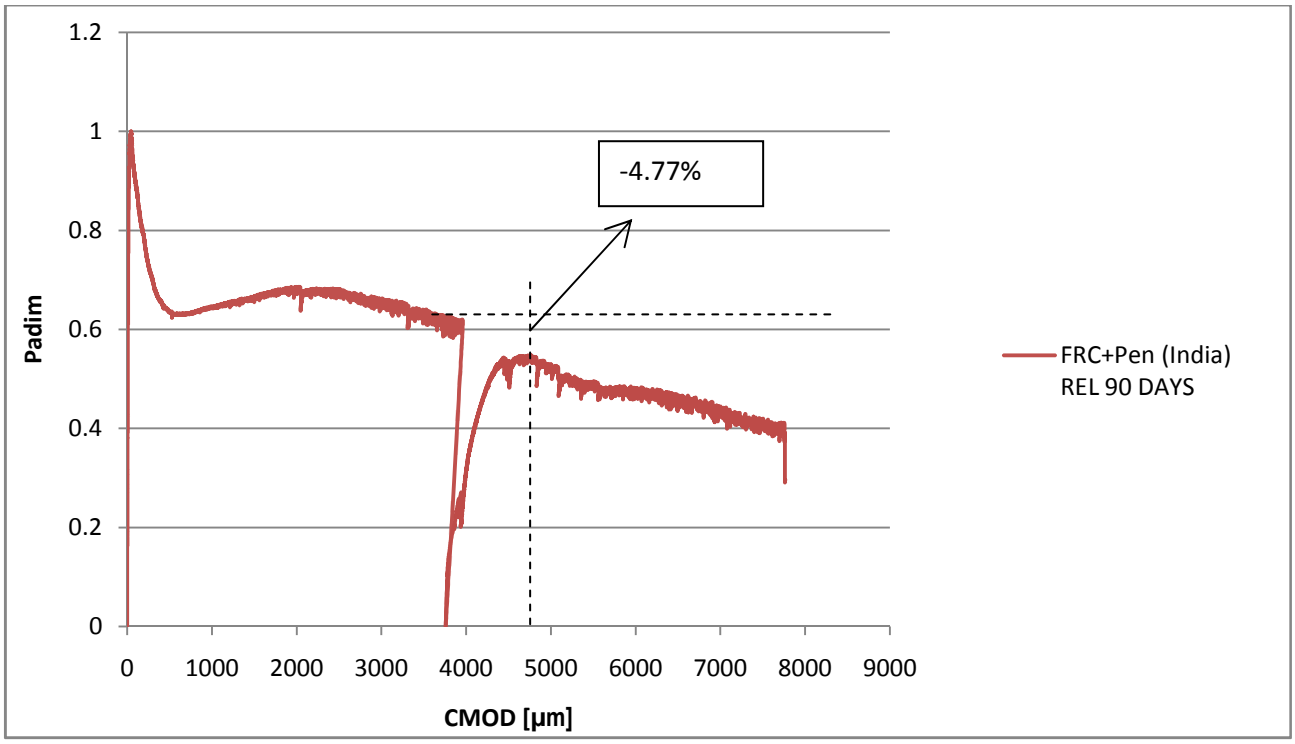

Figure 90: evaluation of the self-healing after 90 days of conditioning on FRC samples casted in India with the addition of crystallizing agent

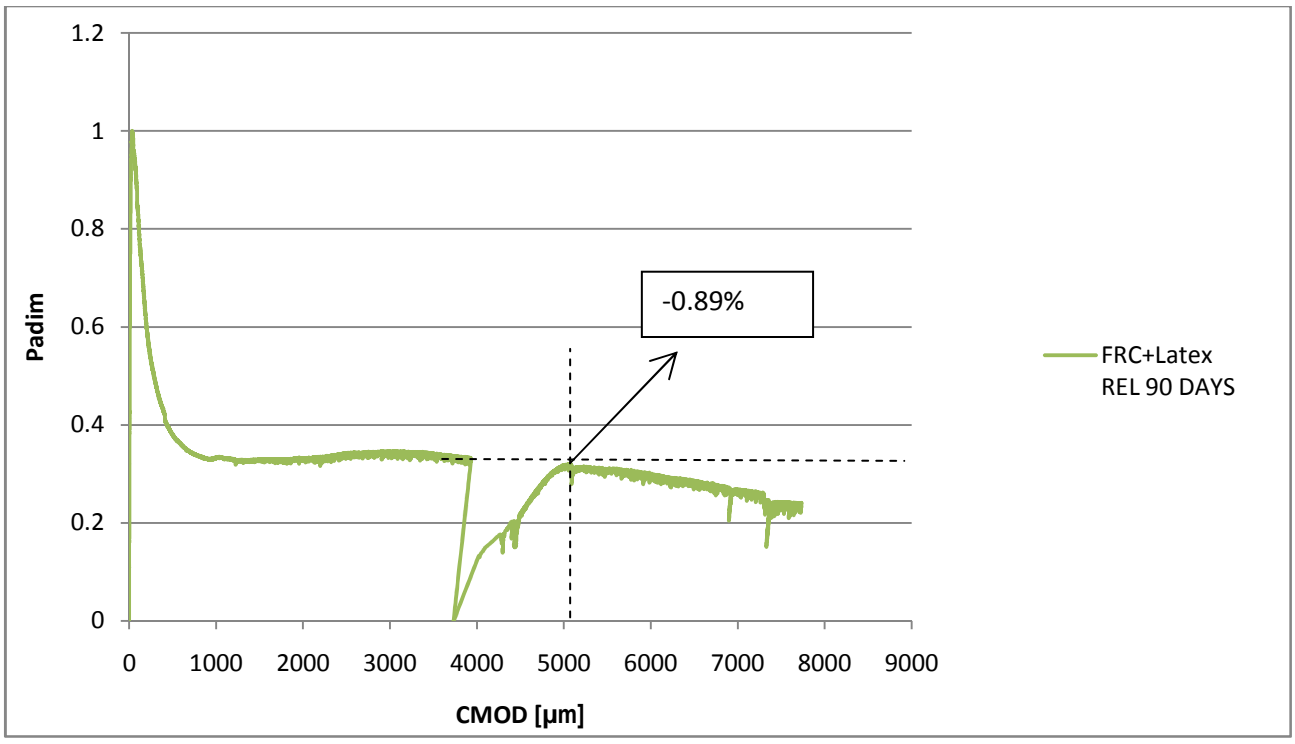

Figure 91: evaluation of the self-healing after 90 days of conditioning on latex-modified FRC samples casted in India

FRC specimens: reloading after 270 days

After 270 days of conditioning, specimens showed a complete drop of strength, which, as previously discussed, could have been caused by the oxidation of fibers. In order to quantify healing, it can be assumed that a loss of 100% occurred, since in most case samples failed during the preloading phase.

4.4. Conclusions

The aim of this research was to compare the self-healing behaviour of mixes with the same concrete matrix and different additions, to verify whether these latter have the capacity to enhance the healing reactions. It is clear from the results that the self-healing of cracks does occur, especially when the crystallizing agent and the fibers are combined in the same mix. Self-healing yields considerable effects when the width of crack is maintained below 600 µm: in this case the reparation can also result into a recovery of load bearing capacity along with time and cracks result sealed.

In this work, recovery was evaluated as regain of strength after some conditioning, in relation with the residual load of precracking.
The effect of hardening or softening were also kept into account for samples precracked up to 600 µm.
For this category of specimens, self-healing was calculated at CMOD 1500 µm, while for specimens precracked up to 4000 µm self-healing was quantified on the base of the peak load of reloading.

The following **Figure 92** represents the percentage recovery of strength of the specimens tested after 30, 90 and 270 days of conditioning, divided per batch of specimens tested.

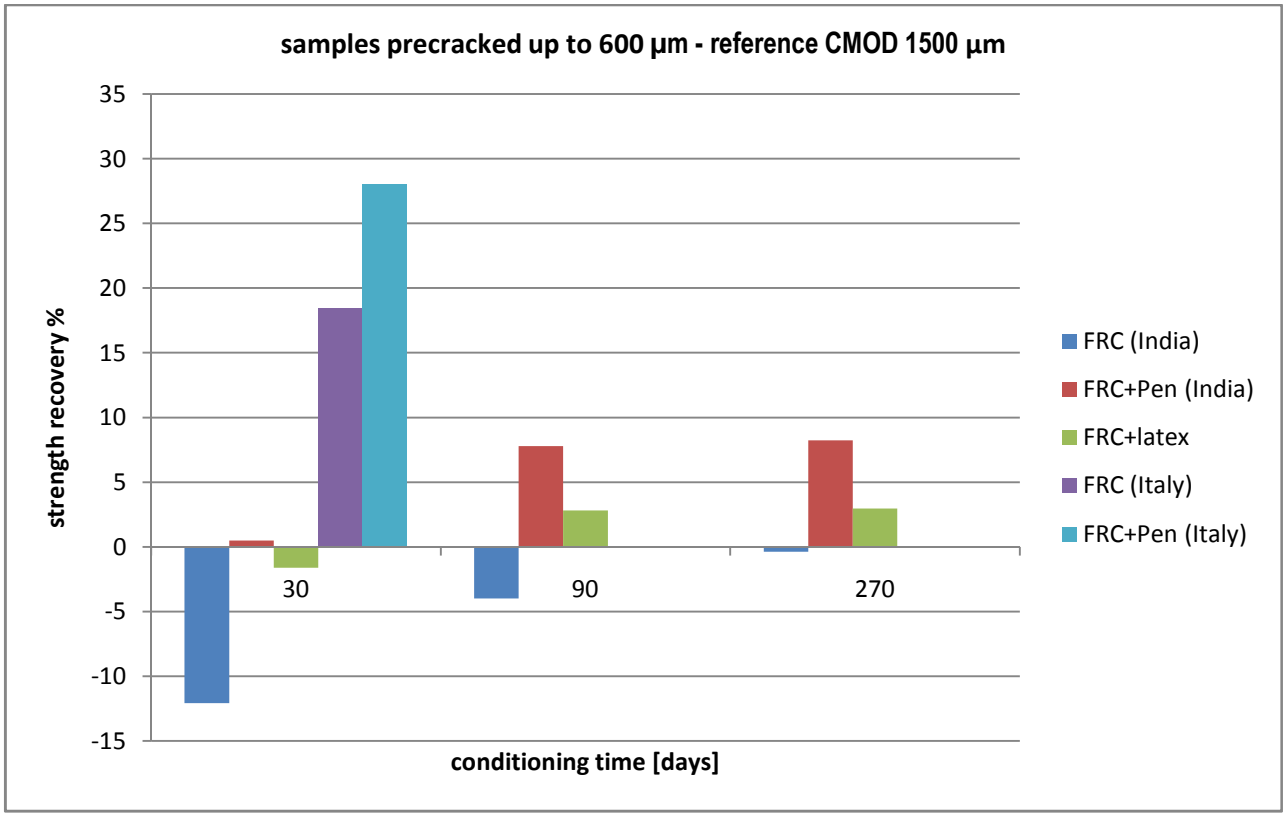

Figure 92: percentage recovery of the different batches along with time, calculated on the reference CMOD 1500 µm (precracking 600 µm)

FRC samples casted in India highlight an increase in recovery of load along with time. In particular specimens without crystallizing admixture passes from an initial loss of 12% registered after 30 days of conditioning, reduced to 0.37% after 270 days of conditioning. When crystallizing agent is added to the mix, specimens show the best performances: after 30 days of conditioning, samples do not show any loss in strength, while after 90 days the recovery amounts to 7.8% of residual load of precracking. This value remains stable even after 270 days (8%), suggesting that, if there is any further effect of crystallizing agent,

it might be balanced by the oxidation of fiber. This latter observation could also explain the slight softening behaviour that specimens tested after 270 days of conditioning presented.
It can be concluded that the presence of this addition enhance self-healing of 20% in periods longer than 90 days.
Also latex-modified samples highlighted the same trend, though the increase of self-healing performances was limited in a range from -2% to 3%.

Another conclusion that results suggest is the importance of an applied through-crack compressive stress. FRC mixes casted in Italy, to which compression was applied during conditioning, registered absolutely the best recovery in only one month, with a respective regain of 18% and 28% of residual load of precracking.
If these mixes are compared to the respective Indian mixes, it can be stated that compression increases self-healing of about 30% on the short period (30 days).

Figure 93 represents the performances of samples precracked up to 4000 µm.

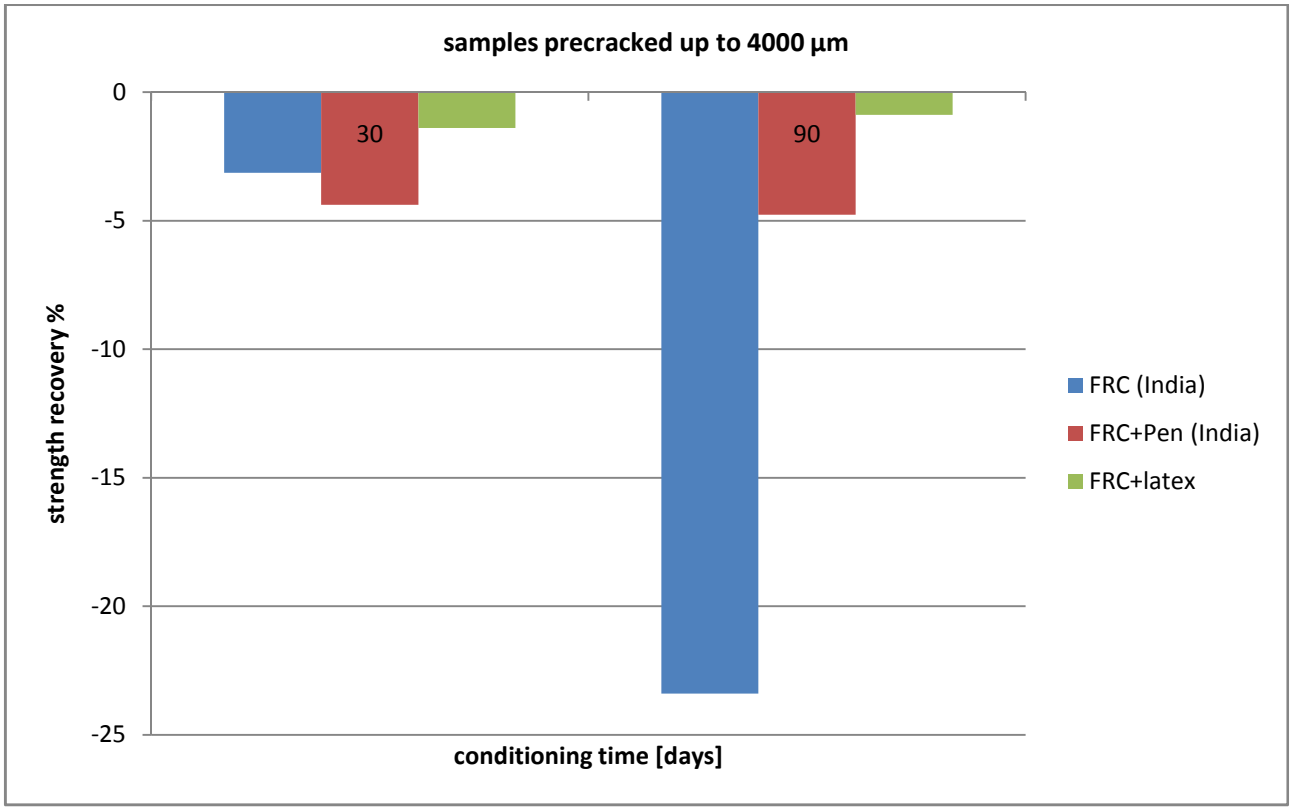

Figure 93: percentage recovery of the various mixes along with time, calculated on the reference CMOD 1500 µm (precracking 4000 µm)

For the higher widths tested, mechanical self-healing does not occur, but when latex or crystallizing agent are added to concrete, durability results increased and the specimens exhibit on the short period a slower decay, due to a partial filling of the cracks.
Tough, when treatments last for long (270 days), also mixes containing latex or crystallizing agent cannot prevent fibers from corrosion and strength drops.

FRC samples casted in India without any addition show a rapid decay of performances and after 90 days lose more than 20% of its load bearing capacity. On the other hand mixes containing Penetron or latex have the capacity of maintaining for a longer period their residual strength.

However, after 270 days all the specimens present a complete drop of strength, due to the oxidation of the fibers.

4.4.1. Discussion of some critical points

Scatter of the results

The results of this experimental research showed a quite high scatter for each batch of specimens tested. Many factors occurred, from the fabrication of the specimens to their tests, to determine this scatter.

- *Geometry of the crack*

The heterogeneity of concrete and the distribution of the coarse aggregates determine the geometries of the crack. Cracks, use to develop following the path requiring a lower loss of energy; this path connects the week zones of the samples, which usually coincides with the interfaces between the paste and the aggregates. The exact position of the aggregates in the samples is casually determined; as well it is the development path of cracks.
In this experimentation, notches were cut in order to minimize the effects due to crack geometry. However, even if crack is induced by the notch, its path can vary from sample to sample and it is function of the exact position of the fibers and the coarse aggregates located nearby the notch.

- *Imperfections due to the fabrication of notches*

Fabrication of notches is a manual process, which requires the manual employment of a blade for cutting concrete. So fabricated notches cannot be perfectly straight; moreover, blade can comport a state of stress around the notch, with the consequent formation of micro-cracks and weakening of the zone.

- *Distribution of the fibers*

Steel fibers are directly added to concrete at the moment of mixing. Their distribution is macroscopically quite homogeneous, but two considerations are needed: at first, the orientation of fibers is not casual, but is observed an alignment in the direction of the samples during the phase of vibration. Second, their distribution inside the single specimen can vary from sample to sample, due to the little dimension of the beams casted.
Different orientations and distributions of fibers in the zone of crack, lead to a variation of the mechanical capacities of the specimens.

- *Strength of the specimens*

Strength of the specimens is quite scattered due to the points above. In particular, the residual capacity of carrying loads under a defined deformation, which is the measure used to characterize these specimens, is highly influenced by the distribution and orientation of fibers in the samples.

5. Conclusions

In this work, the self-healing properties of steel fiber reinforced concretes for pavements and industrial floors with different additions have been investigated. The general aim was to find out whether concrete presenting a medium-high water to cement ratio could perform any significant healing, from the point of view of mechanical self-repairing.
Furthermore, this work had the intention of studying the effects of each addition, different widths of crack and different conditioning times in enhancing self-healing.
This research was finally completed with the investigation of the effect of a through-crack compressive stress application during conditioning.

Three point bending tests were performed on four different concrete mixes, which, keeping fixed the concrete matrix, presented respectively the addition of steel fibers, steel fibers and a crystallizing agent (Penetron admixture), steel fibers and SBR latex.
The effects of two different widths of crack on the self-healing capacities were studied, by dividing each group of specimens in two batches that were respectively notched and precracked at CMOD values of 600 and 4000 μm.
The effect of time was considered, by conditioning some precracked samples from each batch for one, three and nine months with wet/dry cycles.
The application of a through-crack compressive stress was investigated on steel fiber reinforced concrete precracked up to 600 μm, with and without the addition of a crystallizing agent. To these concretes, which replied the mixes already employed, a controlled compressive stress was applied with a suitably designed device.

In the first phase of tests, trying to quantify the progression of the crack sealing, UPV tests and a water-permeability test designed to the purpose were carried out before breaking the samples.

The results achieved allow to state that also concrete presenting a medium-high water to cement ratio can perform self-healing, depending on various factors.

In terms of sealing of the crack, visual results confirmed this capacity, but the initial aim of quantifying the decrease of permeability in healed concrete failed, due to the thickness of the specimens and the dimension of the crack: a leakage of water through the notch positioned on the side of the samples was evident. Instead, the liquid should had flowed from the top of the specimens (where, at the tip of the crack the pressure was applied) to the bottom.
Also UPV tests gave results which could not be interpreted; this happened probably because of the geometry of the samples (whose dimensions were not compatible with the transducers and the length of the emitted wave) and for the nature of the test itself, that could have been influenced by not quantifiable factors, such as the distribution of the fibers and the penetration and path of the cracks.

The mechanical tests on the other hand, revealed interesting results regarding the recovery ability of load bearing capacity of samples, summarized in the following points:

- *The width of crack has a direct influence on the mechanical self-healing capacity of concrete. By increasing the width of crack, the capacity of self-repairing decreases.*

Specimens precracked at 600 µm presented a regain in the capacity of carrying loads depending on type and time of conditioning and additions.
On the other hand, specimens precracked up to 4000 µm did not highlight any recovery of load bearing capacity, but a loss of mechanical performances which ended in a complete drop of strength after 270 days of conditioning.

- *By increasing the time of conditioning after cracking, crystallization on the crack faces increases. Though, an increase in conditioning time may results in negative phenomena of corrosion*

With the increase of the time of conditioning, unhydrated cement particles made available by the occurrence of cracks can hydrate in contact with water and moist in a more complete way. Moreover, crystallizing agent powder and latex have time to react completely and enhance the self-healing reactions normally occurring.
However, An increase in time may lead to negative effects, such as the oxidation of fibers due to longer expositions to wet/dry cycles.

- *Self-healing has the effect of improving the durability of material*

Specimens precracked up to 4000 µm did not show any interesting mechanical recovery. Though, on the medium period, self-healing on specimens casted with the addition of latex and crystallizing agent resulted in a slower decay of load bearing capacity.
This phenomenon could be due to the enhancement of the crystallization promoted by the crystallizing admixture, which seals the crack faster and prevents them from the access of moist and water. On the other hand, prevention in specimens containing latex would be due to the effect of the polymeric coating, which protects fibers from the direct contact with water.
It is reasonable to assume that this effect is much more significant on samples presenting low widths of crack, because self-healing reactions can more easily seal the induced fractures, preventing fibers from corrosion.

- *The addition of crystalline admixture accelerates the reactions of self-healing and makes stronger the bridges that crystals form between the crack sides*. *Crystallizing agent increases both self-sealing and self-repairing properties.*

The crystallizing agent catalyzes the reactions of hydration in the cement paste. It is recognized its function of improving the permeability of cracked concrete, due to the reaction of powder and unhydrated cement in contact with the water which can flow into the crack.
Specimens containing the crystallizing agent presented a more effective sealing of the crack, even in case of precracking at 4000 µm, resulting in a complete filling at least at the tip.
Load bearing capacity during reloading was increased and accelerated by the addition of the crystallizing agent. Samples precracked up to 600 µm and containing Penetron powder achieved after three months important regains in strength and stiffness, that increased in further six months.

- *Compression enhances self-healing.*

FRC specimens to which has been applied a compressive stress during conditioning, highlighted after only one month a recovery of 18% in case of samples casted without crystallizing agent. The 28% of recovery, acheived when crystallizing admixture was added to the mix, resulted the best performances. It can be hypothesized that compression has the effect of hold together the crack sides, favouring the formation of bridges.

5.1. Recommendations for the future

This research gave some promising results about the possibility of promoting self-healing in concrete with low water to cement ratios and low amount of fibers, especially by adding some crystallizing agent.

As following, some suggestions are given in this section, to improve the present work and carry out further research on the topic.

5.1.1. Improvement of the present work

- Repetition of more identical tests because of the scatter in the results
- Investigation on the effect of the application of tensile stress during conditioning[1]
- Investigation on the effect of longer time of conditioning on steel fibers

5.1.2. Different concrete admixtures

- Influence of the water to cement ratio
- Influence of the quantity of crystallizing agent
- Influence of different types of fibers
- Influence of aggregates and particle size distribution of the aggregates

5.1.3. Other properties of healed cracks

- Creep behaviour of healed cracks[2]

[1] [2] A device for the application of tensile stresses and the study of creep behaviour of cracked specimens has been designed and reported in the appendix

Bibliography

[1] the S. D. C. SDC, “Vision 2020 A Vision for the Concrete Repair Protection and Strengthening Industry,” pp. 1–25, 2004.

[2] S. Dunn, “Self Healing Concrete – A Sustainable Future 2 . Self Healing of Cementitious Composites.”

[3] S. Sangadji and E. Schlangen, “Self Healing of Concrete Structures - Novel Approach Using Porous Network Concrete,” *J. Adv. Concr. Technol.*, vol. 10, no. 5, pp. 185–194, 2012.

[4] M. Li, R. Ranade, L. Kan, and V. C. Li, “ON IMPROVING THE INFRASTRUCTURE SERVICE LIFE USING ECC TO MITIGATE REBAR CORROSION,” in *2nd International Symp. on Service Life Design for Infrastructure*, 2010, no. 1.

[5] A. K. H. Kwan and H. H. C. Wong, “Durability of Reinforced Concrete Structures , Theory vs Practice,” *CEDD Bull. Board H.K. Gov. web site*, pp. 1–20.

[6] K. Van Breugel, “IS THERE A MARKET FOR SELF-HEALING CEMENT- BASED MATERIALS?,” in *First International Conference on Self Healing Materials*, 2007, no. April.

[7] L. Ferrara and V. Krelani, “A FRACTURE TESTING BASED APPROACH TO ASSESS THE SELF HEALING CAPACITY OF CEMENTITIOUS COMPOSITES,” in *VIII International Conference on Fracture Mechanics of Concrete and Concrete Structures*.

[8] A. D. Abrams, *TESTS OF BOND BETWEEN CONCRETE AND STEEL*. 1913.

[9] N. Hearn and C. T. Morley, “Self-sealing property of concrete Experimental evidence,” *Mater. Struct.*, vol. 30, no. September, pp. 404–411, 1997.

[10] N. Hearn, “Self-sealing , autogenous healing and continued hydration : What is the difference ?,” *Mater. Struct.*, vol. 31, no. October, pp. 563–567, 1998.

[11] C. Edvardsen, “Water Permeability and Autogenous Healing of Cracks in Concrete,” *ACI Mater. J.*, pp. 448–455, 1999.

[12] N. Ter Heide, “Crack healing in hydrating concrete,” Delft University of Technology, 2005.

[13] E. J. Jacobsen, S.; Sellevold, “SELF HEALING OF HIGH STRENGTH CONCRETE AFTER DETERIORATION BY FREEZE/THAW,” *Cem. Concr. Res.*, vol. 26, no. I, pp. 55–62, 1996.

[14] R. Abdel-Jawad, Y.; Haddad, “EFFECT OF EARLY OVERLOADING OF CONCRETE ON,” *Cem. Concr. Res.*, vol. 22, no. 2, pp. 927–936, 1992.

[15] S. Granger, a. Loukili, G. Pijaudier-Cabot, and G. Chanvillard, “Experimental characterization of the self-healing of cracks in an ultra high performance cementitious material: Mechanical tests and acoustic emission analysis,” *Cem. Concr. Res.*, vol. 37, no. 4, pp. 519–527, Apr. 2007.

[16] E. Schlangen, *Self-Healing Phenomena in Cement-Based Materials*. 2013.

[17] T. Mihashi, H.; Nishiwaki, “Development of Engineered Self-Healing and Self-Repairing Concrete-State-of-the-Art Report,” *J. Adv. Concr. Technol.*, vol. 10, pp. 170–184, 2011.

[18] M. Fagerlund, G.; Hassanzadeh, “SELF-HEALING OF CRACKS IN CONCRETE EXPOSED TO DIFFERENT TYPES OF WATER - Effect on chloride penetration,” Lund, 2011.

[19] M. Li, “MULTI-SCALE DESIGN FOR DURABLE REPAIR OF CONCRETE STRUCTURES,” 2009.

[20] H. Lee, “Potential of superabsorbent polymer for self-sealing cracks in concrete,” *Adv. Appl. Ceram.*, vol. 109, no. 5, 2010.

[21] D. Snoeck, K. Van Tittelboom, S. Steuperaert, P. Dubruel, and N. De Belie, “Self-healing cementitious materials by the combination of microfibres and superabsorbent polymers,” *J. Intell. Mater. Syst. Struct.*, vol. 25, no. 1, pp. 13–24, Mar. 2012.

[22] W. Ramm and M. Biscoping, “Autogenous healing and reinforcement corrosion of water-penetrated separation cracks in reinforced concrete,” *Nucl. Eng. Des.*, vol. 179, no. 2, pp. 191–200, Feb. 1998.

[23] H.-W. Reinhardt and M. Jooss, “Permeability and self-healing of cracked concrete as a function of temperature and crack width,” *Cem. Concr. Res.*, vol. 33, no. 7, pp. 981–985, Jul. 2003.

[24] Y. Yang, M. D. Lepech, E.-H. Yang, and V. C. Li, “Autogenous healing of engineered cementitious composites under wet–dry cycles,” *Cem. Concr. Res.*, vol. 39, no. 5, pp. 382–390, May 2009.

[25] M. Şahmaran, S. B. Keskin, G. Ozerkan, and I. O. Yaman, “Self-healing of mechanically-loaded self consolidating concretes with high volumes of fly ash,” *Cem. Concr. Compos.*, vol. 30, no. 10, pp. 872–879, Nov. 2008.

[26] P. Termkhajornkit, T. Nawa, Y. Yamashiro, and T. Saito, “Self-healing ability of fly ash–cement systems,” *Cem. Concr. Compos.*, vol. 31, no. 3, pp. 195–203, Mar. 2009.

[27] S. Z. Qian, J. Zhou, and E. Schlangen, “Influence of curing condition and precracking time on the self-healing behavior of Engineered Cementitious Composites,” *Cem. Concr. Compos.*, vol. 32, no. 9, pp. 686–693, Oct. 2010.

[28] D. Jaroenratanapirom, “Effects of Different Mineral Additives and Cracking Ages on Self-Healing Performance of Mortar,” in *Annual Concrete Conference 6, thailand Concrete Association*, 2010, pp. 551–556.

[29] Y. Hosoda, A.; Kishi, T.; Arita, H. and Takakuwa, “SELF HEALING OF CRACK AND WATER PERMEABILITY OF EXPANSIVE CONCRETE,” in *First International Conference on Self Healing Materials*, 2007, no. April.

[30] E. A. B. Sisomphon, K.; Copuroglu, O. and Koenders, “SURFACE CRACK SELF HEALING BEHAVIOUR OF MORTARS WITH EXPANSIVE ADDITIVES,” in *3rd International Conference on Self-Healing Materials*, 2011, no. June.

[31] T. Kishi, T. Ahn, A. Hosoda, S. Suzuki, and H. Takaoka, “SELF-HEALING BEHAVIOUR BY CEMENTITIOUS RECRYSTALLIZATION OF CRACKED CONCRETE,” in *First International Conference on Self Healing Materials*, 2007, no. April, pp. 1–10.

[32] T.-H. Ahn and T. Kishi, “Crack Self-healing Behavior of Cementitious Composites Incorporating Various Mineral Admixtures,” *J. Adv. Concr. Technol.*, vol. 8, no. 2, pp. 171–186, 2010.

[33] A. Gross, D. Kaplan, and K. Baker, “Removal of chemical and microbiological contaminants from domestic greywater using a recycled vertical flow bioreactor (RVFB),” *Ecol. Eng.*, vol. 31, no. 2, pp. 107–114, Oct. 2007.

[34] S. Chaturvedi, R. Chandra, and V. Rai, “Isolation and characterization of Phragmites australis (L.) rhizosphere bacteria from contaminated site for bioremediation of colored distillery effluent,” *Ecol. Eng.*, vol. 27, no. 3, pp. 202–207, Oct. 2006.

[35] R. Siddique and N. K. Chahal, “Effect of ureolytic bacteria on concrete properties,” *Constr. Build. Mater.*, vol. 25, no. 10, pp. 3791–3801, Oct. 2011.

[36] M. R. Gollapudi, U.K.; Knutson, C.L.; Bang, S.S. and Islam, “A NEW METHOD FOR CONTROLLING LEACHING THROUGH PERMEABLE CHANNELS,” *Chemosphere*, vol. 30, no. 4, pp. 695–705, 1995.

[37] S. S. Ramachandran, S.K.; Ramakrishnan, V. and Bang, “Remediation of Concrete Using Micro-Organisms,” *ACI Mater. J.*, p. 9, 2001.

[38] K. Van Tittelboom, N. De Belie, W. De Muynck, and W. Verstraete, “Use of bacteria to repair cracks in concrete,” *Cem. Concr. Res.*, vol. 40, no. 1, pp. 157–166, Jan. 2010.

[39] S. S. Bang, J. K. Galinat, and V. Ramakrishnan, “Calcite precipitation induced by polyurethane-immobilized Bacillus pasteurii.,” *Enzyme Microb. Technol.*, vol. 28, no. 4–5, pp. 404–409, Mar. 2001.

[40] J. Wang, K. Van Tittelboom, N. De Belie, and W. Verstraete, “Use of silica gel or polyurethane immobilized bacteria for self-healing concrete,” *Constr. Build. Mater.*, vol. 26, no. 1, pp. 532–540, Jan. 2012.

[41] E. Schlangen, H. Jonkers, S. Qian, and A. Garcia, “Recent advances on self healing of concrete,” in *FRAMCOS7*, 2010.

[42] H. M. Jonkers, A. Thijssen, G. Muyzer, O. Copuroglu, and E. Schlangen, “Application of bacteria as self-healing agent for the development of sustainable concrete,” *Ecol. Eng.*, vol. 36, no. 2, pp. 230–235, Feb. 2010.

[43] V. Wiktor and H. M. Jonkers, “Quantification of crack-healing in novel bacteria-based self-healing concrete,” *Cem. Concr. Compos.*, vol. 33, no. 7, pp. 763–770, Aug. 2011.

[44] R. Pei, J. Liu, S. Wang, and M. Yang, “Use of bacterial cell walls to improve the mechanical performance of concrete,” *Cem. Concr. Compos.*, vol. 39, pp. 122–130, May 2013.

[45] P. Ghosh, S. Mandal, B. D. Chattopadhyay, and S. Pal, “Use of microorganism to improve the strength of cement mortar,” *Cem. Concr. Res.*, vol. 35, no. 10, pp. 1980–1983, Oct. 2005.

[46] V. C. Li, “Engineered Cementitious Composites (ECC) – Material , Structural , and Durability Performance,” in *Concrete Construction Engineering Handbook*, C. Press, Ed. 2007.

[47] M. Sahmaran, M. Li, and V. C. Li, “Transport Properties of Engineered Cementitious Composites under Chloride Exposure,” *ACI Mater. J.*, no. 104, pp. 303–310, 2008.

[48] D. J. Hannant and J. G. Keer, “Autogenous healing of thin cement based sheets,” *Cem. Concr. Res.*, vol. 13, no. 3, pp. 357–365, May 1983.

[49] R. J. Gray and B. Shear, “AUTOGENEOUS HEALING OF FIBRE/MATRIX INTERFACIAL BOND IN FIBRE-REINFORCED MORTAR,” *Cem. Concr. Res.*, vol. 14, no. c, pp. 315–317, 1984.

[50] D. Homma, H. Mihashi, and T. Nishiwaki, “Self-Healing Capability of Fibre Reinforced Cementitious Composites,” *J. Adv. Concr. Technol.*, vol. 7, no. 2, pp. 217–228, 2009.

[51] M. Ferrara, Liberato; krelani, Visar; Gorlezza, Raffaele; Geminiani, “HIGH FIBER REINFORCED CEMENTITIOUS COMPOSITES: AUTOGENEOUSLY SELF HEALING MATERIALS,” 2013.

[52] E. Tziviloglou, “Self healing in ECC materials with low content of different micro-fibers and micro-particles,” Delft University of technology, 2009.

[53] S. Antonopoulou, “MSc-thesis Self-healing in ECC materials with high content of different micro-fibres and micro-particles,” Delft University of Technology, 2009.

[54] M. R. De Rooij, S. Qian, H. Liu, W. F. Gard, and J. W. G. Van De Kuilen, “Using natural wood fibers to self heal concrete,” *Concr. Repaiir, Rehabil. Retrofit. II*, pp. 229–234, 2009.

[55] L. Ferrara, S. R. Ferreira, V. Krelani, F. Silva, R. Dias, T. Filho, E. Engineering, U. Federal, C. Engineering, and P. U. Catolica, “EFFECT OF NATURAL FIBRES ON THE SELF-HEALING CAPACITY OF HIGH PERFORMANCE FIBRE REINFORCED CEMENTITIOUS,” no. 1, pp. 1–8.

[56] S. R. Ferreira, M. Della Torre, V. Krelani, L. Ferrara, F. de Andrade Silva, and R. D. T. Filho, “Effect of natural reinforcement on self-healing capacity of cement based composite Saulo Rocha Ferreira,” 2014.

[57] Y. Ohama, “Recent Progress in Concrete-Polymer Composites,” *Adv. Cem. Based Mater.*, pp. 31–40, 1997.

[58] Y. Tian, Z. Li, H. Ma, X. Jin, and N. Jin, “An investigation on the microstructure formation of polymer modified mortars in the presence of polyacrylate latex,” 2006.

[59] M. Abd Elmoaty, “Self-healing of polymer modified concrete,” *Alexandria Eng. J.*, vol. 50, no. 2, pp. 171–178, Jun. 2011.

[60] P. Łukowski and G. Adamczewski, “Self-repairing of polymer-cement concrete,” *Bull. Polish Acad. Sci. Tech. Sci.*, vol. 61, no. 1, pp. 195–200, Jan. 2013.

[61] X. Yuan, W. Sun, X. Zuo, and H. Li, “The crack self-healing properties of cement-based material with EVA heat-melt adhesive,” *J. Wuhan Univ. Technol. Sci. Ed.*, vol. 26, no. 4, pp. 774–779, Jul. 2011.

[62] J. S. Kim and E. Schlangen, “SELF-HEALING IN ECC STIMULATED BY SAP UNDER FLEXURAL CYCLIC LOAD,” in *3rd International Conference on Self-Healing Materials*, 2011, no. June.

[63] S. R. White, N. R. Sottos, P. H. Geubelle, J. S. Moore, M. R. Kessler, S. R. Sriram, E. N. Brown, and S. Viswanathan, “Autonomic healing of polymer composites.,” *Nature*, vol. 409, no. 6822, pp. 794–7, Feb. 2001.

[64] K. Van Tittelboom and N. De Belie, “Self-Healing in Cementitious Materials—A Review,” *Materials (Basel).*, vol. 6, pp. 2182–2217, May 2013.

[65] H. Huang and G. Ye, “Application of sodium silicate solution as self-healing agent in cementitious materials,” Delft, 2011.

[66] A. Pelletier, M.M.; Brown, R.; Shukla, A. and Bose, “Self-healing concrete with a microencapsulated healing agent,” Kingston.

[67] V. C. Li, Y. M. Lim, and Y.-W. Chan, “Feasibility study of a passive smart self-healing cementitious composite,” *Compos. Part B Eng.*, vol. 29, no. 6, pp. 819–827, Nov. 1998.

[68] C. Joseph, R. Lark, B. Isaacs, D. Gardner, and A. D. Jefferson, “Experimental investigation of adhesive-based self-healing of cementitious materials,” *Mag. Concr. Res.*, vol. 62, no. 11, pp. 831–843, Nov. 2010.

[69] L. Sun, W. Y. Yu, and Q. Ge, “Experimental Research on the Self-Healing Performance of Micro-Cracks in Concrete Bridge,” *Adv. Mater. Res.*, vol. 250–253, pp. 28–32, May 2011.

[70] K. Sisomphon, O. Copuroglu, and A. Fraaij, “Application of encapsulated lightweight aggregate impregnated with sodium monofluorophosphate as a self-healing agent in blast furnace slag mortar,” *HERON*, vol. 56, no. 1, pp. 13–32, 2011.

[71] Z. Yang, J. Hollar, X. He, and X. Shi, “A self-healing cementitious composite using oil core/silica gel shell microcapsules,” *Cem. Concr. Compos.*, vol. 33, no. 4, pp. 506–512, Apr. 2011.

[72] S. V. Zemskov, H. M. Jonkers, and F. J. Vermolen, “Two analytical models for the probability characteristics of a crack hitting encapsulated particles: Application to self-healing materials,” *Comput. Mater. Sci.*, vol. 50, no. 12, pp. 3323–3333, Jul. 2011.

[73] H. Huang and G. Ye, “THE EFFECTS OF CAPSULES ON SELF-HEALING EFFICIENCY IN CEMENTITIOUS MATERIALS,” in *second International Conference on Microstructural-related Durability of Cementicious Composites*, 2012, no. April, pp. 11–13.

[74] S. D. Mookhoek, “Novel routes to liquid-based self-healing polymer systems,” Technische Universiteit Delft, 2010.

[75] D. Janssen, “Water encapsulation to initiate self-healing in cementitious materials,” Delft University of Technology, 2010.

[76] J. Y. Wang, N. De Belie, and W. Verstraete, “Diatomaceous earth as a protective vehicle for bacteria applied for self-healing concrete.,” *J. Ind. Microbiol. Biotechnol.*, vol. 39, no. 4, pp. 567–77, Apr. 2012.

[77] S. Sangadji and E. Schlangen, “POROUS NETWORK CONCRETE: A NEW APPROACH TO MAKE CONCRETE STRUCTURES SELF-HEALING USING PREFABRICATED POROUS LAYER,” in *3rd International Conference on Self-Healing Materials*, 2011, no. June.

[78] T. Nishiwaki, H. Mihashi, B.-K. Jang, and K. Miura, “Development of Self-Healing System for Concrete with Selective Heating around Crack,” *J. Adv. Concr. Technol.*, vol. 4, no. 2, pp. 267–275, 2006.

[79] Q. City, T. Nishiwaki, H. Mihashi, H. Matsubara, K. Miura, and Y. Okuhara, “SMART CONCRETE SYSTEM WITH STRAIN MONITORING,” in *2nd International Symposium on Advances in Concrete through Science and Engineering*, 2006, no. September.

[80] P. J. M. Metha, P.K. and Monteiro, *CONCRETE - Microstructure, Properties, and materials*. 2006.

[81] L. Ferrara, “CRYSTALLINE ADMIXTURES IN CEMENTITIOUS COMPOSITES : FROM POROSITY REDUCERS TO CATALYSTS OF SELF HEALING,” pp. 1–10.

[82] H. S. Moguel, “thoughness characterization of steel fiber reinforced concrete - study of experimental methodologies and size effects,” Universitat Politècnica de Catalunya, 1999.

[83] R. Gettu, B. Mobasher, S. Carmona, and D. C. Jansen, “Testing of Concrete Under,” *elsevier*, 1996.

A. Appendix

A.1 Compressive test results

Plain concrete	WEIGHT [kg]	LOAD [N]	STRESS Rc [Mpa]
S1	8.41	1230.3	54.68
S2	8.42	1183.6	52.61
S3	8.41	1224.6	54.43
S4	8.49	1301.6	57.85
S5	8.52	1257.1	55.87
S6	8.51	1244.9	55.33
S7	8.53	1181.9	53.33
S8	8.41	1221.3	54.28
S9	8.32	1151.5	51.15
AVERAGE	**8.45**	**1221.87**	**54.39**
DEV ST	**0.07**	**45.03**	**1.93**
CHARACTERISTIC STRENGTH			**51.20**

Table A-1: compressive strength on plain concrete samples

FRC (India)	WEIGHT [kg]	LOAD [N]	STRESS Rc [Mpa]
S1	8.58	1332.2	59.21
S2	8.52	1330.8	59.15
S3	8.50	1392.1	61.87
S4	8.53	1090.3	48.46
S5	8.48	1072.3	47.66
S6	8.51	1271.1	56.49
S7	8.35	1173.0	52.16
S8	8.46	1292.5	57.45
S9	8.54	1309	58.18

AVERAGE	**8.50**	**1251.48**	**55.63**
DEV ST	**0.06**	**113.03**	**5.02**
CHARACTERISTIC STRENGTH			**47.34**

Table A-2: compressive strength on FRC samples casted in India

FRC+Pen (India)	WEIGHT [kg]	LOAD [N]	STRESS Rc [Mpa]
S1	8.52	1190.6	53.91
S2	8.51	1313.9	58.39
S3	8.48	1270.4	56.46
S4	8.45	1207.3	53.66
S5	8.62	1251.8	55.64
S6	8.42	1266.5	56.29
S7	8.63	1346.5	59.85
S8	8.62	1225.9	54.49
S9	8.62	1333.9	59.29
AVERAGE	**8.54**	**1267.42**	**56.44**
DEV ST	**0.08**	**55.14**	**2.30**
CHARACTERISTIC STRENGTH			**52.65**

Table A-3: compressive strength on FRC samples casted in India with Penetron

FRC+Latex	WEIGHT [kg]	LOAD [N]	STRESS Rc [Mpa]
S1	7.79	745.7	33.14
S2	7.84	686.3	30.5
S3	7.84	665.6	29.58
S4	7.77	685	30.44
S5	7.86	706	31.38
S6	7.79	702	31.2
S7	7.81	735.1	32.67
S8	7.79	669.7	29.77
S9	7.89	739.8	32.88
AVERAGE	**7.82**	**703.91**	**31.28**
DEV ST	**0.04**	**30.25**	**1.34**
CHARACTERISTIC STRENGTH			**29.07**

Table A-4: compressive strength on latex-modified FRC samples

FRC (ITALY)	WEIGHT [kg]	LOAD [N]	STRESS Rc [Mpa]
S1	8.008	1094.7	48.33113
S2	8.109	1155.6	51.36
S3	8.191	1178.1	52.36
AVERAGE 7 days	8.10	1142.80	50.68
DEV ST 7days	0.09	43.15	2.47
CHARACTERISTIC STRENGTH 7 days			46.60
S4	7.968	1193.7	53.05333
S5	8.087	1029.4	45.14912
S6	8.163	1129.5	49.53947
AVERAGE 14 days	8.07	1117.53	49.25
DEV ST 14 days	0.10	82.80	3.47
CHARACTERISTIC STRENGTH 14 days			43.52
S7	\	1352	59.29825
S8	8.008	1358	59.95585
S9	8.011	1284	57.06667
S10	8.123	1311	57.12418
AVERAGE 28 days	8.05	1326.25	58.36
DEV ST 28 days	0.07	35.07	1.49
CHARACTERISTIC STRENGTH 7 days			55.91

Table A-5: compressive strength at 7, 14 and 28 days of FRC samples casted in Italy

FRC+Pen (ITALY)	WEIGHT [kg]	LOAD [N]	STRESS Rc [Mpa]
C1	8.009	1036.6	46.07111
C2	7.826	1069.2	48.16216
AVERAGE 7 days	7.92	1052.90	47.12
DEV ST 7days	0.09	43.15	2.10
CHARACTERISTIC STRENGTH 7 days			43.66
C3	8.4	1151.5	51.86937
C4	8.302	1185.8	51.66885
AVERAGE 14 days	8.35	1168.65	51.77
DEV ST 14 days	0.07	24.25	0.14
CHARACTERISTIC STRENGTH 14 days			51.54
C5	8.051	1347	59.4702
C6	8.041	1294	56.75439
AVERAGE 28 days	8.05	1320.50	58.11
DEV ST 28 days	0.01	37.48	1.92
CHARACTERISTIC STRENGTH 7 days			54.94

Table A-6: compressive strength at 7, 14 and 28 days of FRC samples casted in Italy with Penetron

A.2 Design of the through-crack compressive setup

The setup designed in order to apply the compressive stress consists of a couple of steel plates 2 cm thick, reinforced with a couple of cross stiffeners of 1 cm thickness. Plates and crosses are coupled and connected by four threaded rods. Compression is applied by bolts: four are employed to fix the rods at the couple cross-plate positioned at the bottom of the specimen; four are used to tighten the setup from the top and apply the force needed to provide the requested stress by dynamometric key.

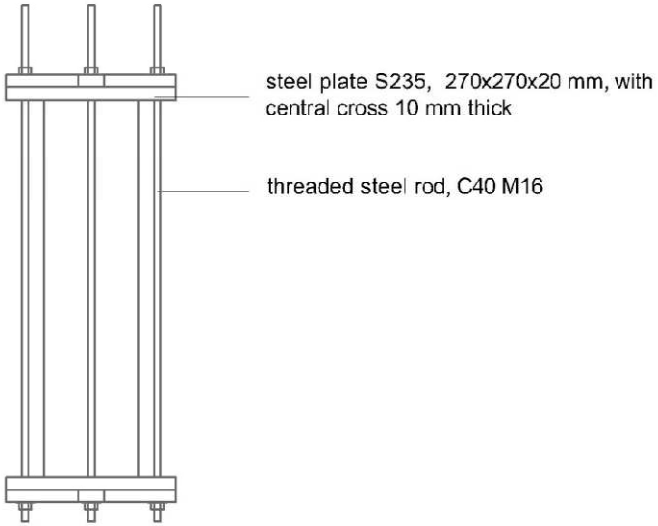

Figure A-1: compressive setup

Design of the threaded rods

The experimentation conducted in India on concrete samples precracked up to 600 μm had found the maximum tensile residual load to be:

$$F = 18\ kN = 18000N$$

On the other hand, the transversal section of the specimens, considered the presence of the notch, was:

$$A = b \times h_{net} = 150 \times 120 = 18000\ mm^2$$

It is possible to calculate the agent stress. To simplify the calculation, it is considered a linear distribution of the stress, though the sample is widely outside the field of an elastic behaviour.

In this conditions, the stress is given by:

$$\sigma = \frac{M}{W}$$

- M is the bending moment, equal to $\frac{F \times l}{4}$
- l is the span between the supports, equal to 500 mm
- W is the modulus of inertia, calculated as $\frac{b \times h_{net}^2}{6}$

It is obtained:

$$\sigma = \frac{18000 \times \frac{500}{4}}{150 \times \frac{120^2}{6}} = \frac{2250000}{360000} = 6.25MPa = 6.25\frac{N}{mm^2}$$

The aim is the application of a compressive stress $\sigma 1$ on the reduced section of the specimen (notch excluded), at least equal to the half of the maximum stress above calculated:

$$\sigma 1 = \frac{\sigma}{2} = 3.125\frac{N}{mm^2}$$

It means that the forces to be applied on the section is:

$$P = \sigma 1 \times A = 56250N$$

Due to the availability of the materials, threaded rods of steel C40 will be employed. Consequently:

$$f_{y,d} = 325\ \frac{N}{mm^2}$$

$$A_{s,r} = \frac{P}{f_{y,d}} = \frac{56250}{325} = 173.08\ mm^2$$

In order to guarantee a durability of the connections, roads with a diameter of 16 mm will be used. Considering the threading, it means that the effective area for each and for the four rods is respectively:

$$A_U = 157\ mm^2$$

$$A_{stot} = 4 \times A_U = 628\ mm^2$$

The maximum tension to which the rods can be subjected is:

$$F_{max,s} = f_{y,d} \times A_s = 325 \times 628 = 204100\ N > P$$

Calculation of the steel plate with sap2000

The compression stresses transmitted to the specimen through a steel plate of 270x270 mm. In order to have an effective transmission of the stress, this plate should not bend excessively, due to the forces that the bolt apply on its corners. Moreover it is necessary that the stress on the plate itself does not exceed the limit stress acceptable for a steel S235.

The plate has been designed with SAP2000. The presence of the holes has been omitted in order to simplify the calculation. Similarly, the stress applied by the washer to the plate has been modelled as the resulting force applied in the hole center.

The plate has been modelled as a *shell-thick* element with meshes of 5x5 mm. The specimen to which the plate apply the compression has been represented as a continuous support, which follow the perimeter of the cross section of the sample.

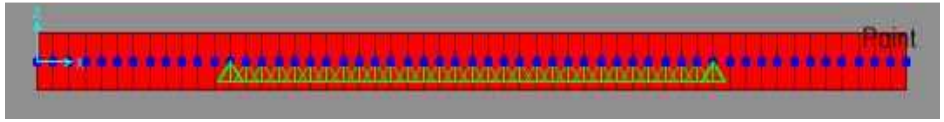

Figure A-2: plate modeling in sap2000

Each of the applied forces is calculated as:

$$P' = \frac{P}{4} = 14062.5N$$

The deflection in correspondence with the applied force is equal to:

$$v1 = 0.06176\ mm$$

At the plate center the deflection is instead:

$$v2 = 0.04398\ mm$$

Regarding the stress to which is subjected the steel plate in this configuration, it is always below the limit of steel S235 as the following figure reports.

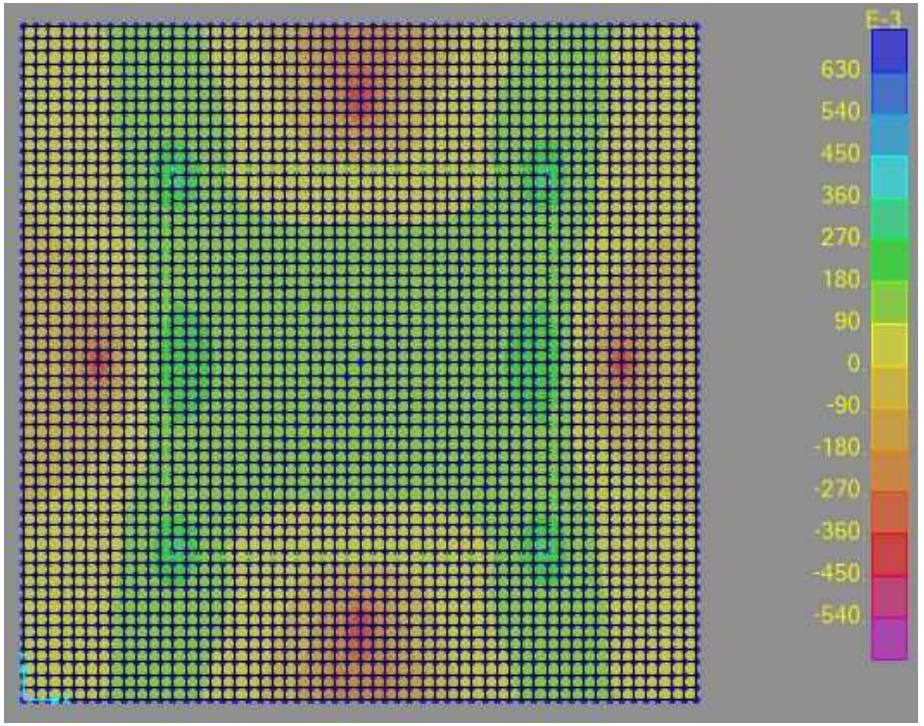

Figure A-3: stresses on the plate in sap2000

Reduction of the deflection

In order to guarantee a more homogeneous application of the stress on the transversal section of the specimens, the plate section is increased up to 20 mm.

Then the stiffness of the plateis increased by increasing the thickness of its central zones, by adding a steel cross of 1 cm thickness.

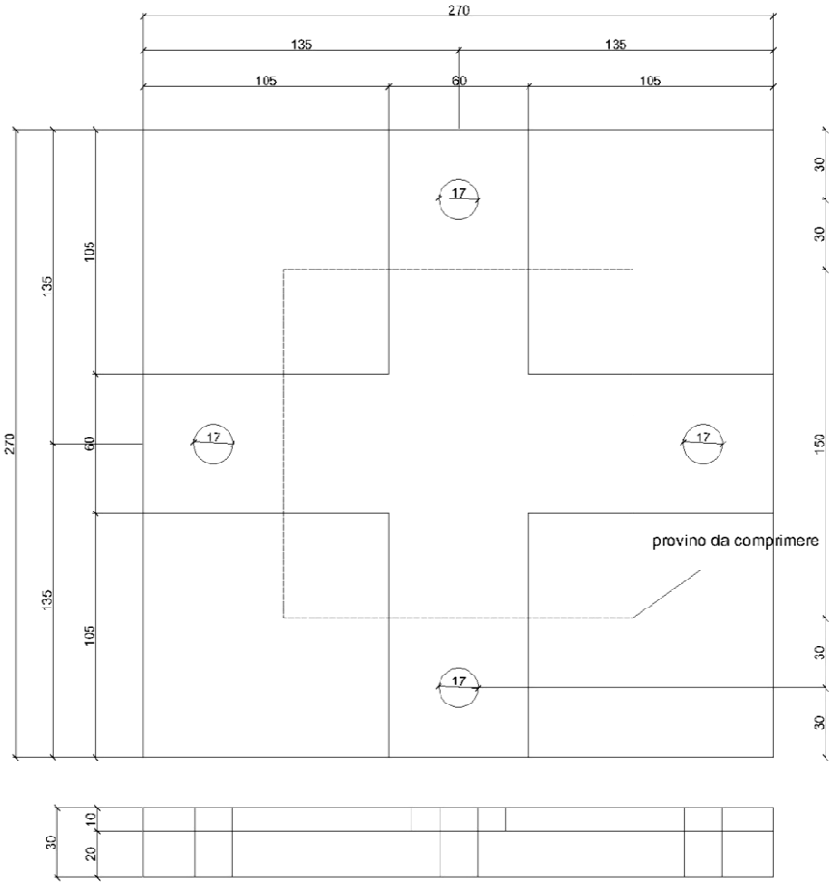

Figure A-4: geometry of the plate and the cross stiffener

In this case, the model is built with solid elements extruded from the base of the plate to an height of 2 cm for the same plate and 3 cm for the central zones. The geometry of the plate and the position of the holes is unvaried.

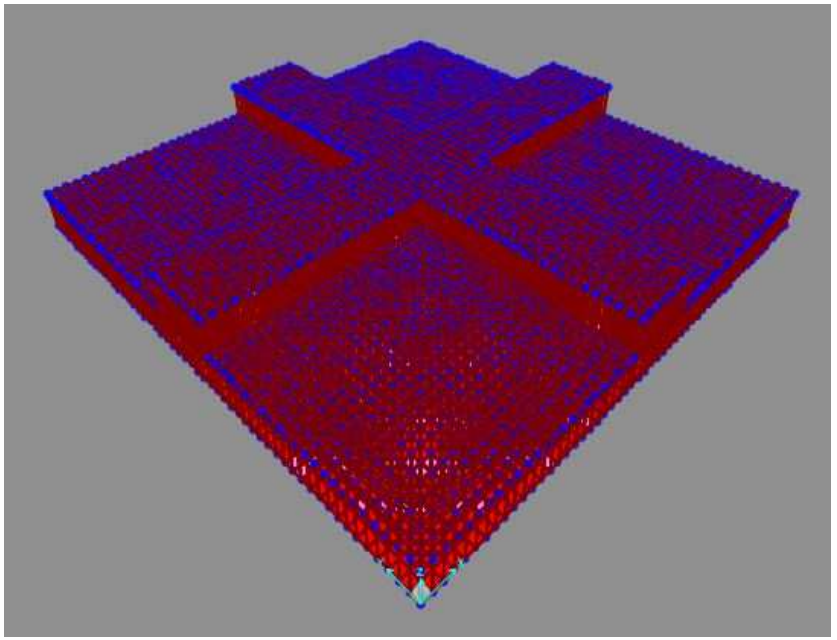

Figure A-5: simplified modeling of plate and cross in sap2000

In the points were the forces are applicated, the deflection is limited to:

$$v1 = 0.00356\ mm$$

At the center of the plate the deflection is in this configuration:

$$v2 = -0.00148\ mm$$

Finally, the stress is definitely lower than the material limit.

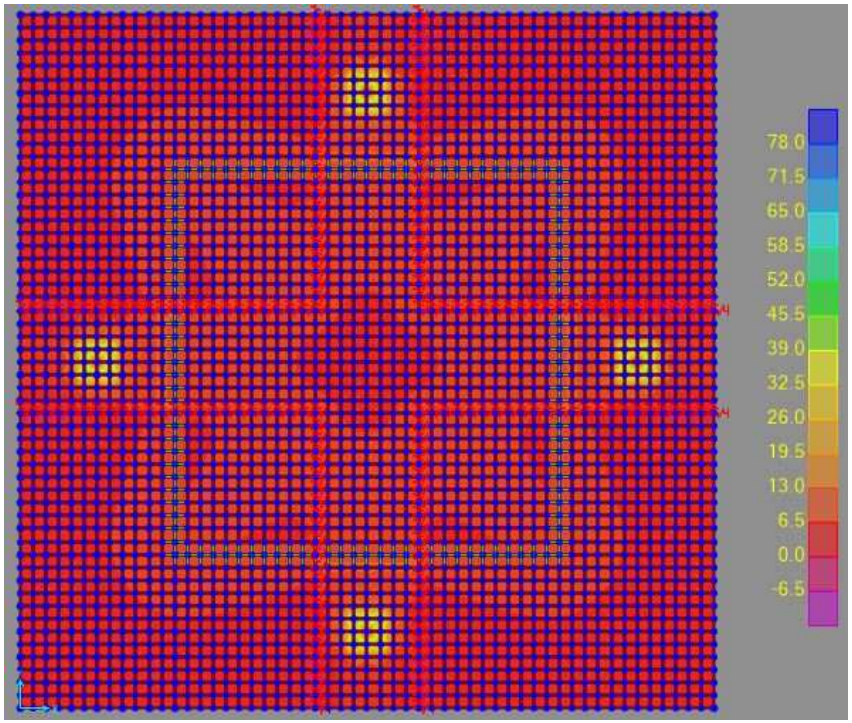

Figure A-6: stress on plate and cross in sap2000

Calculation of the couple of tightening

The couple of forces necessary to tighten the bolt is calculated by imposing an upper limit to the tensile stress applied from the bolt to the threaded rod. This limit corresponds to the 70% of the tensile stress necessary to yield the road:

$$N = 0.7 \times f_y \times A_{eff} = 0.7 \times 325 \times 157 = 35717.5\ N$$

Being the force to be applied widely lower than the calculated limit, the connection is verified to failure.

The value of the couple of tightening is calculated as:

$$T = k \times N \times d$$

- k is a coefficient depending on the treatment of the surface and its oiling (k=0.17 if oil is employed)
- N is the force to apply
- d is the diameter of the bolt.

Being the diameter of the rods of 16 mm:

$$T = 0.17 \times 14062.5 \times 16 = 38250\ Nmm = 38.25\ Nm$$

A.3 Design of the bending-tensile setup

This section considers the design of a setup which will be used to subject the specimens to a tensile stress. The setup employs a couple of the devices previously used to compress the samples and appositely modified.
The plates and crosses connected by the rods are used this time to apply, through semi-cylinders fixed on the plates, the required forces on a couple of samples horizontally oriented and separated by a central support.
The idea is to simulate the forces that the supports transfer to the samples during the three point bending test; however, there is a difference: the force is not applied at the mid span of the specimen, but at the extremities. Then, The central support employed to distance the couple of samples reacts passively and transfers the forces at the centre.

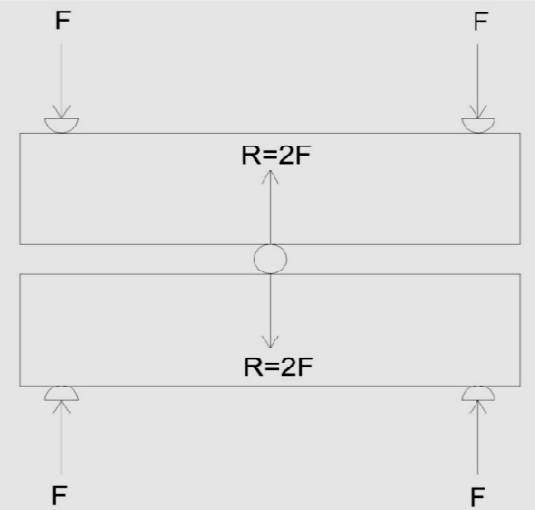

Figure A-7: distribution of the forces

In order to solve the problem of viscous creep, the central support is designed as a couple of semi-cylinders connected by a spring.

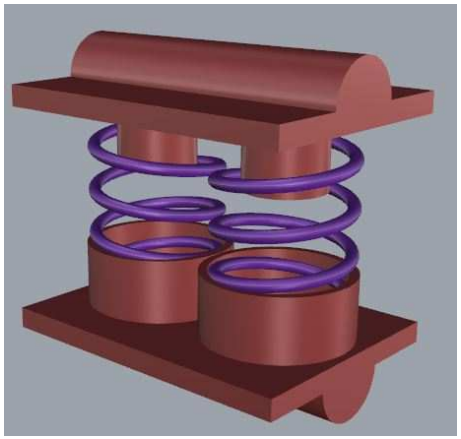

Figure A-8: central support

The application of the forces is controlled by dynamometric key and verified by measuring the shortening of the spring.

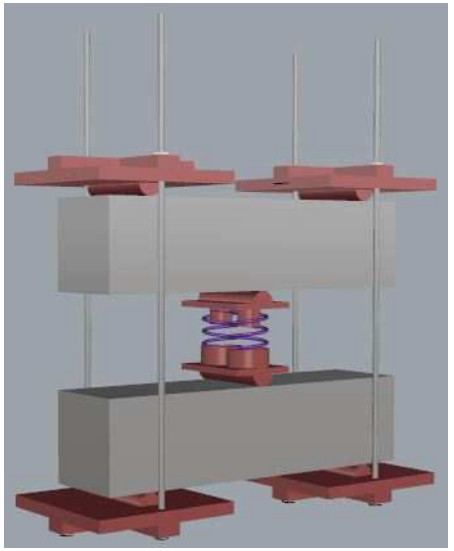

Figure A-9: bending-tensile setup

Design of the spring

The experimentation conducted in India on concrete samples precracked up to 600 μm had found the maximum tensile residual load to be:

$$F = 18\,kN = 18000N$$

Since the setup designed in this section has the same configuration of the three point bending test, it is possible to consider directly the forces to apply and omit the calculation of the stresses.

The setup will be design to apply a force of 18000N at the centre of the sample. Anyway, it will be more likely employed to apply a force of 5000N, equal to a half of the average residual load of the specimens tested in Italy.

The spring should present an elastic constant which consent to have a measurable deformation in the range of forces considered, in order to control with LVDTs or also less sophisticated instruments the shortening due to the forces and, further, to creep.

The characteristics of the springs can be found in the catalogues furnished from the producers. In particular, it must be considered the range of forces in which the spring can operate:

- f_{bl} is the maximum deformation to which the spring can be subjected.
- F_1 is the minimal pre-load that must be applied; this latter is equal to 13% of f_{bl} and corresponds to the deformation f_1.
- The load F_2 corresponds to the deformation f_2, which is equal to 80% of f_{bl} and conventionally represents the upper limit of load and deformation that the spring should bear during loading.

In our case the lower limit F_1 will be fixed to at least at 5000N, since it is the load we want to apply at the centre of the couple of samples.

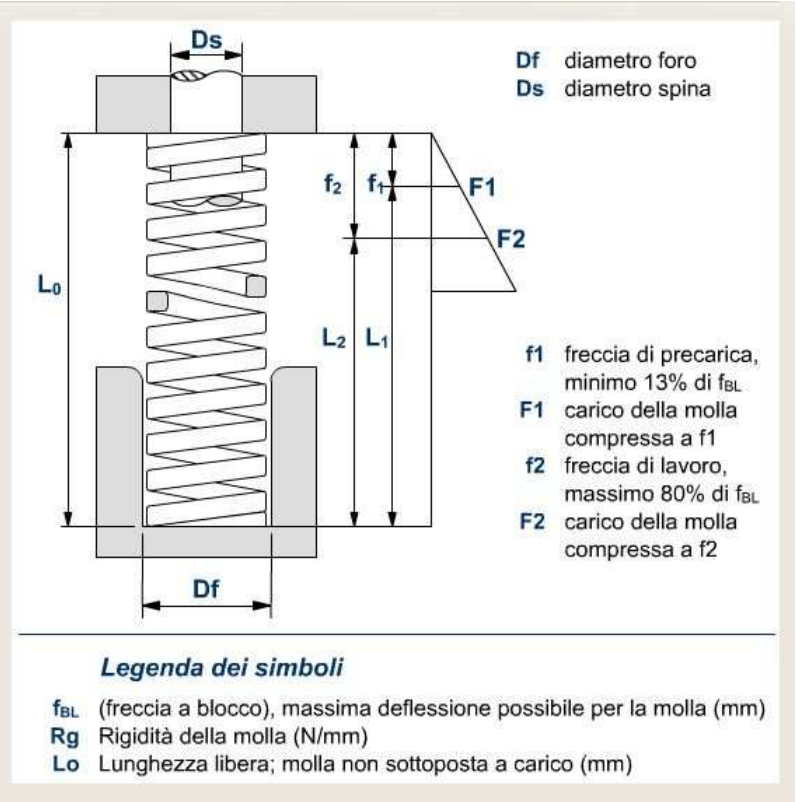

Figure A-10: main parameters which determine the choice of a spring

The spring is chosen from the following catalogue:

Molle per stampi, carichi forti – Df 63 mm

L_0 mm	R_g N/mm	f_{BL} mm	A 13%f_{BL} mm (N)	B 30%f_{BL} mm (N)	C 45%f_{BL} mm (N)	D 62%f_{BL} mm (N)	E 80%f_{BL} mm (N)	Codice	Prezzo
76	618	29	3,7 (2310)	8,6 (5330)	12,9 (7995)	17,8 (11016)	23 (14214)	CF63x76	da 21,32 euro
89	515	34	4,4 (2260)	10,1 (5214)	15,2 (7822)	20,9 (10776)	27 (13905)	CF63x89	da 23,12 euro
102	438	39	5 (2206)	11,6 (5092)	17,4 (7638)	24 (10523)	31 (13578)	CF63x102	da 24,12 euro
115	370	44	5,7 (2104)	13,1 (4856)	19,7 (7284)	27,1 (10036)	35 (12950)	CF63x115	da 25,68 euro
127	333	48	6,2 (2056)	14,3 (4745)	21,4 (7118)	29,4 (9807)	38 (12654)	CF63x127	da 27,92 euro
152	269	58	7,5 (2011)	17,2 (4640)	25,9 (6960)	35,6 (9590)	46 (12374)	CF63x152	da 30,80 euro
178	226	66	8,6 (1946)	19,9 (4492)	29,8 (6738)	41,1 (9283)	53 (11978)	CF63x178	da 34,64 euro
203	198	76	9,9 (1963)	22,9 (4529)	34,3 (6794)	47,3 (9361)	61 (12078)	CF63x203	da 39,60 euro
254	155	95	12,4 (1914)	28,5 (4418)	42,8 (6626)	58,9 (9130)	76 (11780)	CF63x254	da 47,36 euro
305	128	114	14,8 (1893)	34,1 (4368)	51,2 (6552)	70,5 (9027)	91 (11648)	CF63x305	da 56,24 euro

Figure A-11: catalogue from www.prontomolle.it

The fifth spring of the catalogue will be employed. The main characteristics are the following:

- L_0 = 127 mm
- R_g = 333 N/mm
- f_{bl} = 48 mm
- F_1 = 2056 N
- f_1 = 6.2 mm
- F_2 = 12654 N
- f_2 = 38 mm

If the hypothesis to use a couple of springs with these characteristics is respected, the minimal pre-load to apply is:

$$F1 = 2056 \times 2 = 4112\ N$$

This load corresponds to the above reported deformation of 6.2 mm.

Each sample will be subjected to a central force equal to:

$$R = 5000\ N$$

This force represents consequently the compression to which the spring will be subjected.

The lower limit F1 is implicitly verified.

The upper limit in this configuration will be calculated as:

$$F2 = 2 \times 80\% f_{bl} = 2 \times 12654\ N = 25308\ N$$

This means that the system can operate in a range from 4112 N to 25308 N. More likely it will be employed to apply forces in a range from 5000 N to 10000 N,these latter corresponding respectively to the lower limit of the spring F_1 and the average residual load of the tested samples.

It has to be considered that the cracked samples, when subjected to the load, will immediately deform.

Consequently the spring will be subjected to a relaxation. However, the difference between the initial deformation of the spring and its relaxation must be higher than the minimal deformation f_1.

For an applied load of 5000 N the deformation of the couple of springs is:

$$f = \frac{5000\ N}{666 \frac{N}{mm}} = 7.508\ mm$$

The immediate deformation of the samples can be calculated from the average values of CMOD obtained during the unloading: for FRC specimens precracked up to 600 μm it had be obtained, in the Indian experimentation, an average closure at the mouth of the crack of 220 μm.

Due to the impossibility of registering the unloading, it can be considered an elastic behaviour of the sample. This would lead the consider that with the application of 5000 N, the half of the average residual load, the re-opening at the mouth of the crack would be the half of the average closure: 110 μm.

This latter is a value of CMOD, which has to be translated in a value of deflection, following the EN 14651.

The deflection δ can be calculated from the CMOD with the formula:

$$\delta = 0.85 \times \mathrm{CMOD} + 0.04\ [mm]$$

where:

$$\mathrm{CMOD} = \mathrm{CMODy}\ \frac{\mathrm{h}}{\mathrm{h}+\mathrm{y}}\ [mm]$$

- h is the total depth of the sample
- Y is the distance of the measuring clip gauge from the mouth of the crack

In our case:

- CMODy = 110 µm
- h = 150 mm
- y = 2 mm

$$\mathrm{CMOD} = 0.110\ \times 0.9868\ = 0.109\ [mm]$$

$$\delta = 0.85 \times 0.109 + 0.04 = 0.1327\ [mm]$$

The spring is subjected to a relaxation equal to 0.1327 mm per specimen: in total 0.2654 mm.

Consequently, the deformation after loading is:

$$f' = f - 2\delta = 7.243[mm]\ > f_1\ = 6.2\ [mm]$$

Checking of the rods

The goal is to verify whether is possible to convert the compressive setups, with their plates, crosses and rods, to apply a tensile stress.
Due to the geometry of the plates and the position of the holes, it is possible to apply the required force by tightening only two of the four rods initially forecast. Otherwise the samples could not be positioned and a modification of the plates would be needed.
The system is subjected to a maximum force equal to:

$$R = 25308\ N$$

Consequently, according to Fgure1, each couple of rods is subjected to a force:

$$F = \frac{1}{2} \times = 12654\ N$$

This load corresponds to a force per rod of:

$$\frac{F}{2} = \frac{12654}{2} = 6327\ N$$

It had already been calculated that each threaded rod, presenting a diameter of 16mm, could bear a load

$$L = 51025\ kN > F$$

It can be stated that a couple of rods per side abundantly resists to the load we need to apply.

Calculation of the couple of tightening

The couple of forces necessary to tighten the bolt is calculated by imposing an upper limit to the tensile stress applied from the bolt to the threaded rod. This limit corresponds to the 70% of the tensile stress necessary to yield the road:

$$N = 0.7 \times f_y\ \times A_{eff}\ = 0.7 \times 325 \times 157 = 35717.5\ N$$

Being the force to be applied widely lower than the calculated limit, the connection is verified to failure.
The value of the couple of tightening is calculated as:

$$T = k \times N \times d$$

- k is a coefficient depending on the treatment of the surface and its oiling (k=0.17 if oil is employed)
- N is the force to apply
- d is the diameter of the bolt.

Being the diameter of the rods of 16 mm:

$$T = 0.17 \times 1250 \times 16 = 3400\ Nmm = 3.4\ Nm$$

The applied force will be checked after tightening by measuring through LVDTs the deformation of the spring.

A.4 Three point bending test results: 600µm

Plain concrete								
specimen	Fmax [kN]	Fmax [N]	L [mm]	B [mm]	H [mm]	Dnotch [mm]	Hsp [mm]	Stress max [Mpa]
PLAIN5	17.379	17379	500	150	150	30	120	6.03
PLAIN6	15.33	15330	500	150	150	30	120	5.32
PLAIN7	16.027	16027	500	150	150	30	120	5.56
PLAIN8	15.418	15418	500	150	150	30	120	5.35
PLAIN17	16.336	16336	500	150	150	30	120	5.67
PLAIN16	15.621	15621	500	150	150	30	120	5.42
PLAIN	16.163	16163	500	150	150	30	120	5.61
PLAIN12	17.588	17588	500	150	150	30	120	6.11
PLAIN15	16.074	16074	500	150	150	30	120	5.58
AVERAGE								5.63
DEV ST								0.28
STRENGTH								5.17

Table A-7: three point bending test results strength on plain concrete samples: CMOD 600µm

FRC (India)											
specimen	Fl(0.05) [kN]	Fl(0.05) [N]	L [mm]	B [mm]	H [mm]	Dnotch [mm]	Hsp [mm]	LOP [Mpa]	RL [kN]	RL [N]	f,R(0.6) [Mpa]
FRC6	19.24	19240	500	150	150	30	120	6.68	9.86	9860.00	3.42
FRC13	21.289	21289	500	150	150	30	120	7.39	16.36	16360.00	5.68
FRC17	19.741	19741	500	150	150	30	120	6.85	13.40	13400.00	4.65
FRC5	22.003	22003	500	150	150	30	120	7.64	10.81	10810.00	3.75
FRC15	20.668	20668	500	150	150	30	120	7.18	9.38	9380.00	3.26
FRC16	20.536	20536	500	150	150	30	120	7.13	13.29	13290.00	4.61
FRC11	20.715	20715	500	150	150	30	120	7.19	17.11	17110.00	5.94
FRC14	19.16	19160	500	150	150	30	120	6.65	12.39	12390.00	4.30
AVERAGE								7.09			4.45
DEV ST								0.34			0.98
STRENGTH								6.52			2.83

Table A-8: three point bending test results strength on FRC samples (India): CMOD 600µm

FRC+Pen (India)											
specimen	Fl(0.05) [kN]	Fl(0.05) [N]	L [mm]	B [mm]	H [mm]	Dnotch [mm]	Hsp [mm]	LOP [Mpa]	RL [kN]	RL [N]	f,R(0.6) [Mpa]
PEN8	22.268	22268	500	150	150	30	120	7.73	16.36	16360.00	5.68
PEN6	20.457	20457	500	150	150	30	120	7.10	14.45	14450.00	5.02
PEN2	21.472	21472	500	150	150	30	120	7.46	18.96	18960.00	6.58
PEN5	20.962	20962	500	150	150	30	120	7.28	16.05	16050.00	5.57
PEN3	19.761	19761	500	150	150	30	120	6.86	13.70	13700.00	4.76
PEN4	18.222	18222	500	150	150	30	120	6.33	12.94	12940.00	4.49
PEN7	19.552	19552	500	150	150	30	120	6.79	11.63	11630.00	4.04
PEN15	21.105	21105	500	150	150	30	120	7.33	11.39	11390.00	3.95
AVERAGE								7.11			5.01
DEV ST								0.44			0.90
STRENGTH								6.38			3.53

Table A-9: three point bending test results strength on FRC samples containing Penetron (India): CMOD 600µm

FRC+Latex											
specimen	Fl(0.05) [kN]	Fl(0.05) [N]	L [mm]	B [mm]	H [mm]	Dnotch [mm]	Hsp [mm]	LOP [Mpa]	RL [kN]	RL [N]	f,R(0.6) [Mpa]
LAT	15.077	15077	500	150	150	30	120	5.24	9.65	10950.00	3.80
LAT9	15.165	15165	500	150	150	30	120	5.27	10.95	9750.00	3.39
LAT17	15.411	15411	500	150	150	30	120	5.35	9.75	9750.00	3.39
LAT18	14.33	14330	500	150	150	30	120	4.98	8.07	8070.00	2.80
LAT12	14.458	14458	500	150	150	30	120	5.02	9.10	9100.00	3.16
LAT10	14.733	14733	500	150	150	30	120	5.12	8.30	8300.00	2.88
LAT13	14.408	14408	500	150	150	30	120	5.00	6.30	6300.00	2.19
LAT14	15.245	15245	500	150	150	30	120	5.29	12.32	12320.00	4.28
AVERAGE								5.16			3.24
DEV ST								0.15			0.64
STRENGTH								4.91			2.18

Table A-10: three point bending test results strength on latex-modified FRC samples: CMOD 600µm

FRC (Italy)											
specimen	Fl(0.05) [kN]	Fl(0.05) [N]	L [mm]	B [mm]	H [mm]	Dnotch [mm]	Hsp [mm]	LOP [Mpa]	RL [kN]	RL [N]	f,R(0.6) [Mpa]
S1	15.732	15732	500	150	150	30	120	5.46	10.94	10940.00	3.80
S2	16.237	16237	500	150	150	30	120	5.64	10.50	10500.00	3.65
S3	15.41	15410	500	150	150	30	120	5.35	8.44	8440.00	2.93
S4	14.37	14370	500	150	150	30	120	4.99	9.18	9180.00	3.19
S5	13.44	13440	500	150	150	30	120	4.67	10.36	10360.00	3.60
S6	13.22	13220	500	150	150	30	120	4.59	8.44	8440.00	2.93
S7	14.83	14830	500	150	150	30	120	5.15	8.30	8300.00	2.88
S8	12.81	12810	500	150	150	30	120	4.45	9.15	9150.00	3.18
S9	14.36	14360	500	150	150	30	120	4.99	14.88	14880.00	5.17
AVERAGE								5.05			3.48
DEV ST								0.38			0.72
STRENGTH								4.42			2.29

Table A-11: three point bending test results strength on FRC samples (Italy): CMOD 600μm

FRC+Pen (Italy)											
specimen	Fl(0.05) [kN]	Fl(0.05) [N]	L [mm]	B [mm]	H [mm]	Dnotch [mm]	Hsp [mm]	LOP [Mpa]	RL [kN]	RL [N]	f,R(0.6) [Mpa]
C1	12.04	12040	500	150	150	30	120	4.18	8.36	8360.00	2.90
C2	13.11	13110	500	150	150	30	120	4.55	8.25	8250.00	2.86
C3	15.34	15340	500	150	150	30	120	5.33	11.22	11220.00	3.90
C4	13.09	13090	500	150	150	30	120	4.55	10.45	10450.00	3.63
C5	12.66	12660	500	150	150	30	120	4.40	8.87	8870.00	3.08
C6	13.26	13260	500	150	150	30	120	4.60	14.19	14190.00	4.93
C7	13.82	13820	500	150	150	30	120	4.80	14.36	14360.00	4.99
C8	15.34	15340	500	150	150	30	120	5.33	9.57	9570.00	3.32
C9	14.3	14300	500	150	150	30	120	4.97	10.96	10960.00	3.81
AVERAGE								4.72			3.71
DEV ST								0.42			0.80
STRENGTH								4.03			2.40

Table A-12: three point bending test results strength on FRC samples containing Penetron (Italy): CMOD 600μm

A.5 Three point bending test results: 4000µm

FRC (India)											
specimen	Fl(0.05) [kN]	Fl(0.05) [N]	L [mm]	B [mm]	H [mm]	Dnotch [mm]	Hsp [mm]	LOP [Mpa]	RL [kN]	RL [N]	f,R(4) [Mpa]
FRC2	19.474	19474	500	150	150	30	120	6.76	11.24	11238.00	3.90
FRC3	20.209	20209	500	150	150	30	120	7.02	14.43	14430.00	5.01
FRC16	16.1	16100	500	150	150	30	120	5.59	10.98	10984.00	3.81
FRC s4	19.735	19735	500	150	150	30	120	6.85	12.45	12451.00	4.32
FRC s5	19.011	19011	500	150	150	30	120	6.60	10.56	10560.00	3.67
FRC s6	21.299	21299	500	150	150	30	120	7.40	11.37	11374.00	3.95
FRC s7	19.765	19765	500	150	150	30	120	6.86	12.38	12378.00	4.30
FRC s8	18.734	18734	500	150	150	30	120	6.50	10.97	10965.00	3.81
AVERAGE								6.70			4.10
DEV ST								0.52			0.44
STRENGTH								5.83			3.38

Table A-13: three point bending test results strength on FRC samples (India): CMOD 4000µm

FRC+Pen (India)											
specimen	Fl(0.05) [kN]	Fl(0.05) [N]	L [mm]	B [mm]	H [mm]	Dnotch [mm]	Hsp [mm]	LOP [Mpa]	RL [kN]	RL [N]	f,R(4) [Mpa]
PEN9	19.521	19521	500	150	150	30	120	6.78	13.42	13419.00	4.66
PEN11	17.047	17047	500	150	150	30	120	5.92	7.40	7397.00	2.57
PEN12	17.125	17125	500	150	150	30	120	5.95	11.16	11158.00	3.87
PEN13	20.581	20581	500	150	150	30	120	7.15	14.57	14565.00	5.06
PEN14	18.696	18696	500	150	150	30	120	6.49	7.77	7772.00	2.70
PEN1	21.229	21229	500	150	150	30	120	7.37	15.53	15534.00	5.39
PEN10	18.085	18085	500	150	150	30	120	6.28	9.08	9084.00	3.15
PEN16	20.314	20314	500	150	150	30	120	7.05	14.17	14171.00	4.92
AVERAGE								6.62			4.04
DEV ST								0.55			1.12
STRENGTH								5.71			2.19

Table A-14: three point bending test results strength on FRC samples containing Penetron (India): CMOD 4000µm

FRC+Latex											
specimen	Fl(0.05) [kN]	Fl(0.05) [N]	L [mm]	B [mm]	H [mm]	Dnotch [mm]	Hsp [mm]	LOP [Mpa]	RL [kN]	RL [N]	f,R(4) [Mpa]
LAT4	12.632	12632	500	150	150	30	120	4.39	4.36	4355.00	1.51
LAT5	12.541	12541	500	150	150	30	120	4.35			
LAT6	15.01	15010	500	150	150	30	120	5.21	4.87	4870.00	1.69
LAT8	13.633	13633	500	150	150	30	120	4.73	7.19	7188.00	2.50
LAT17	12.632	12632	500	150	150	30	120	4.39	4.36	4355.00	1.51
LAT2	14.326	14326	500	150	150	30	120	4.97	7.46	7460.00	2.59
LAT3	14.945	14945	500	150	150	30	120	5.19	3.82	3819.00	1.33
LAT7	13.512	13512	500	150	150	30	120	4.69	9.25	9248.00	3.21
AVERAGE								4.74	5.90		2.05
DEV ST								0.35	2.06		0.72
STRENGTH								4.16	2.50		0.87

Table A-15: three point bending test results strength on latex-modified FRC samples: CMOD 4000µm

A.6 Converting forces into stress

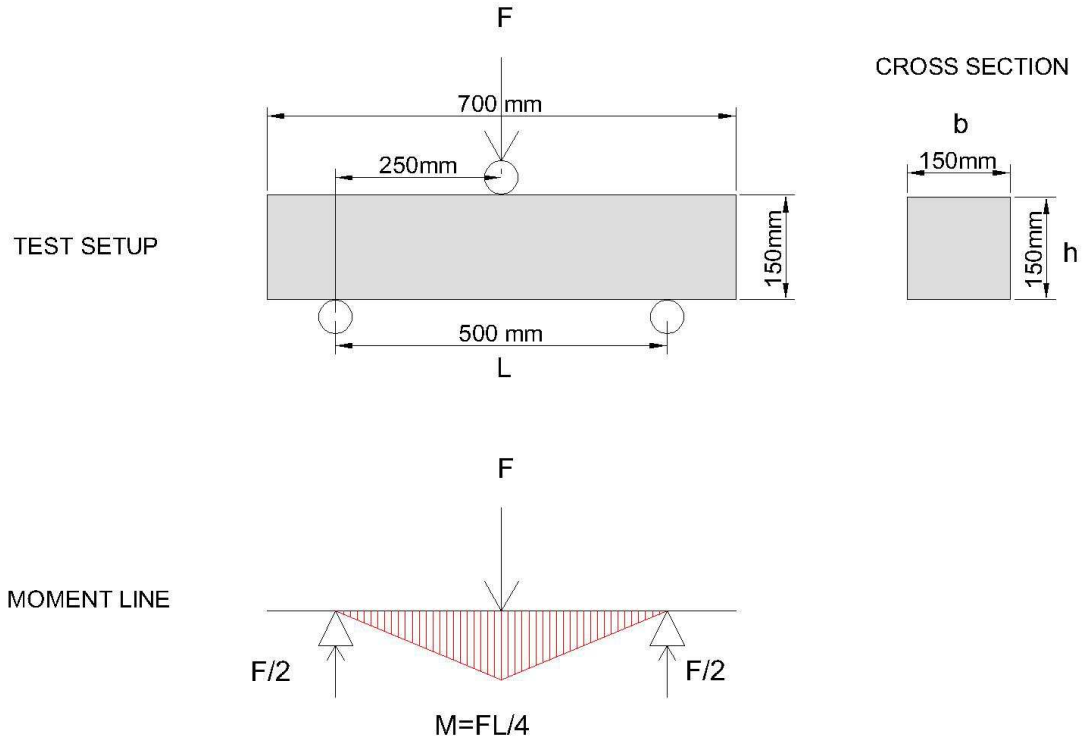

Figure A-12: calculation of the stress induced by three point bending test

$$\sigma = \frac{M}{W} = \frac{\frac{F \times L}{4}}{\frac{b \times h^2}{6}} = \frac{F[N] \times 125[mm]}{562.5[\,mm^3]} = F[N] \times 0.2222[mm^2]^{-1}$$

A.7 Weather conditions in Chennai

2013	Temperature (°C)			Dew point (°C)			Relative humidity (%)			Precipitations (mm)	Events
Dic	high	avg	low	high	avg	low	high	avg	low	sum	
1	28	26	24	25	24	23	94	89	77	4.06	rain, storm
2	28	26	23	25	24	22	100	90	77	0	fog, rain, storm
3	29	26	22	25	22	21	95	80	59	0	fog, rain, storm
4	29	26	22	22	21	18	94	74	51	0	
5	29	26	23	23	21	19	88	73	53	0	rain
6	28	25	22	22	21	18	85	73	60	0	rain
7	27	24	22	23	21	19	96	81	63	9.91	rain
8	27	24	21	21	19	17	88	71	55	0	rain
9	30	25	20	19	17	14	83	63	31	0	
10	32	24	18	21	15	12	74	52	23	0	
11	31	27	22	22	18	13	83	60	31	1.02	
12	29	27	24	25	23	21	94	83	70	0	rain
13	30	27	24	24	23	22	94	83	61	0	rain
14	29	26	23	24	22	21	94	81	59	0	fog, rain
15	29	26	21	22	18	13	94	68	34	0	fog
16	29	23	18	20	18	16	88	69	43	0	
17	29	24	21	20	19	17	88	71	46	0	
18	28	24	19	20	18	16	94	71	44	0	
19	29	24	20	19	17	15	94	67	36	0	
20	29	23	18	19	17	14	94	67	35	0	
21	28	23	18	20	18	16	88	71	37	0	
22	29	24	19	20	18	17	88	69	37	0	
23	30	26	21	22	19	16	94	71	41	0	
24	29	26	23	22	20	19	83	70	53	0	
25	29	25	21	22	19	17	88	69	44	0	
26	28	24	20	21	18	15	88	70	41	0	
27	30	25	20	22	19	14	94	71	32	0	
28	28	24	20	21	18	16	83	67	47	0	
29	29	24	19	21	17	13	92	65	32	0	
30	29	24	19	19	18	17	89	68	48	0	
31	29	24	20	22	19	17	88	71	48	0	

Table A-16: weather conditions in Chennai, December 2013

2014	Temperature (°C)			Dew point (°C)			Relative humidity (%)			Precipitations (mm)	Events
Gen	high	avg	low	high	avg	low	high	avg	low	sum	
1	29	25	21	22	21	19	89	74	61	0.51	rain
2	29	26	23	23	20	18	89	70	52	0	
3	29	26	22	23	21	18	89	75	58	0	
4	29	25	21	22	21	20	94	76	61	0	
5	29	26	22	23	21	19	94	76	52	0	
6	29	25	21	22	21	19	94	77	58	0	fog
7	29	24	20	22	20	18	94	74	48	0	fog
8	29	25	21	22	20	19	90	73	50	0	
9	29	26	21	22	21	19	94	75	50	0	
10	31	26	21	22	19	18	94	74	50	0	fog
11	29	24	19	21	19	18	94	73	47	0	fog
12	30	25	20	21	20	18	94	75	46	0	
13	29	25	21	21	20	18	94	73	48	0	fog
14	29	26	22	22	19	17	94	71	46	0	
15	30	26	21	21	20	18	94	73	45	0	
16	30	26	21	22	20	19	94	73	43	0	
17	29	24	20	21	20	18	91	74	49	0	fog
18	29	24	20	21	19	17	88	70	43	0	
19	30	26	22	23	21	20	94	74	48	0.51	rain
20	29	26	22	22	20	18	94	69	48	0	
21	29	25	21	22	19	17	94	68	48	0	rain
22	29	26	22	19	18	15	73	61	40	0	
23	29	24	20	21	19	17	88	69	46	0	
24	30	25	20	21	19	18	94	71	43	0	
25	30	26	21	21	19	15	88	68	40	0	
26	30	26	21	21	19	16	88	67	40	0	rain
27	30	27	23	22	18	15	79	59	38	0	
28	30	26	21	21	18	17	88	63	38	0	
29	30	25	20	19	18	16	88	63	40	0	
30	29	24	19	19	17	13	88	64	37	0	
31	31	26	20	21	19	18	88	69	41	0	

Table A-17: weather conditions in Chennai, January 2014

2014	Temperature (°C)			Dew point (°C)			Relative humidity (%)			Precipitations (mm)	Events
Feb	high	avg	low	high	avg	low	high	avg	low	sum	
1	30	27	24	22	21	19	88	70	51	0	
2	30	26	22	22	20	19	88	71	47	0	
3	31	26	20	21	18	15	88	68	31	0	
4	31	26	20	20	18	14	88	67	35	0	fog
5	32	26	18	20	18	12	94	69	28	0	fog
6	31	24	18	21	18	15	94	72	29	0	fog
7	32	26	18	20	17	9	94	66	19	0	fog
8	32	25	18	20	17	10	94	66	30	0	
9	32	25	18	21	16	10	94	63	26	0	
10	33	26	19	21	17	9	88	63	19	0	
11	32	26	19	22	17	9	94	63	24	0	
12	31	26	21	21	18	12	94	62	31	0	
13	31	26	20	22	19	17	88	66	42	0	
14	31	26	21	22	20	18	94	70	46	0	
15	31	26	22	22	21	20	94	73	56	0	
16	31	28	24	23	22	21	80	70	55	0	
17	27	26	24	25	23	22	90	81	73	0	rain
18	31	27	23	24	22	20	94	75	48	0	
19	30	27	23	23	21	20	84	71	52	0	rain
20	31	26	21	22	19	17	88	66	45	0	
21	30	26	21	21	18	17	88	67	43	0	fog
22	30	25	20	20	17	15	88	63	34	0	
23	31	25	19	21	18	16	83	65	41	0	
24	28	26	23	23	21	20	89	78	65	0	rain
25	31	27	23	22	21	19	83	69	50	0	
26	31	27	22	22	19	18	94	68	43	0	
27	31	26	20	21	19	17	88	67	42	0	
28	32	27	21	22	19	16	89	64	38	0	

Table A-18: weather conditions in Chennai, February 2014

2014	Temperature (°C)			Dew point (°C)			Relative humidity (%)			Precipitations (mm)	Events
Mar	high	avg	low	high	avg	low	high	avg	low	sum	
1	31	27	23	22	19	18	83	62	40	0	
2	32	27	22	22	21	19	88	67	45	0	
3	31	27	23	23	21	20	83	66	49	0	
4	32	28	24	23	21	19	83	65	44	0	
5	32	27	23	21	21	19	83	65	40	0	
6	31	27	23	22	20	19	83	65	46	0	
7	31	27	23	22	20	19	78	64	45	0	
8	31	27	23	22	20	18	88	66	40	0	
9	31	27	23	21	20	18	83	65	43	0	
10	31	27	23	22	21	19	83	66	40	0	
11	32	28	24	22	21	17	78	64	38	0	
12	32	27	22	22	20	16	88	66	35	0	
13	32	27	22	22	20	17	94	68	33	0	
14	33	27	22	22	18	11	94	62	18	0	fog
15	33	27	21	22	19	16	88	65	35	0	
16	32	27	22	22	20	14	88	66	32	0	
17	34	28	22	23	20	15	94	68	28	0	fog
18	36	29	22	23	19	10	94	64	19	0	
19	35	29	22	24	22	20	89	67	35	0	
20	34	29	24	25	23	22	94	73	44	0	
21	36	31	25	26	23	17	91	70	34	0	
22	36	30	25	26	23	19	91	70	39	0	
23	36	30	24	26	22	12	94	66	24	0	
24	33	28	23	26	23	19	94	70	43	0	
25	34	29	23	24	22	18	97	68	36	0	
26	33	28	23	24	22	19	94	71	45	0	
27	35	29	23	24	21	16	94	66	32	0	
28	37	29	22	25	21	12	94	63	23	0	
29	37	30	24	26	21	14	89	59	25	0	
30	38	31	23	24	18	10	94	55	18	0	
31	39	31	23	25	19	10	89	54	17	0	

Table A-19: weather conditions in Chennai, March 2014

2014	Temperature (°C)			Dew point (°C)			Relative humidity (%)			Precipitations (mm)	Events
Apr	high	avg	low	high	avg	low	high	avg	low	sum	
1	38	31	23	27	19	7	94	57	16	0	
2	36	31	26	26	24	19	93	72	36	0	
3	34	29	25	26	23	20	89	71	46	0	
4	34	30	25	24	22	16	89	67	36	0	
5	36	30	24	27	23	21	89	70	36	0	
6	36	31	26	26	24	21	92	70	43	0	
7	37	31	26	26	23	19	89	66	35	0	
8	37	31	26	26	24	20	89	69	37	0	
9	38	32	27	26	24	19	84	66	32	0	
10	36	31	27	26	23	17	84	63	29	0	
11	37	31	26	26	23	18	84	66	26	0	
12	35	31	27	26	24	23	89	70	43	0	
13	34	31	27	26	24	24	85	72	50	0	
14	34	30	27	25	24	22	84	68	43	0	
15	34	30	26	24	23	22	84	67	45	0	
16	35	30	25	24	23	21	89	66	38	0	
17	37	31	25	26	23	19	89	68	35	0	
18	35	31	26	25	24	21	89	69	41	0	
19	35	30	25	25	23	19	89	66	36	0	
20	35	29	24	24	23	18	89	67	34	0	
21	36	30	25	24	23	20	89	67	41	0	
22	34	30	25	25	23	20	94	65	37	0	
23	35	30	25	25	23	22	89	67	40	0	
24	36	31	26	26	24	21	89	68	40	0	
25	37	31	26	26	24	21	84	68	32	0	
26	38	32	27	26	24	22	85	67	34	0	
27	36	32	27	26	24	22	89	68	38	0	
28	37	32	27	26	24	21	89	67	37	0	
29	37	32	27	26	24	22	89	67	42	0	
30	36	31	27	26	24	21	89	66	42	0	

Table A-20: weather conditions in Chennai, April 2014

A.8 Weather conditions in Milan

2014	Temperature (°C)			Dew point (°C)			Relative humidity (%)			Precipitations (mm)	Events
Sep	high	avg	low	high	avg	low	high	avg	low	sum	
1	26	20	14	14	4	1	88	34	13	0	
2	26	18	11	12	6	1	72	41	20	0	
3	21	16	11	15	12	9	94	72	49	0	rain
4	25	19	13	17	14	12	94	73	50	0	rain
5	22	19	16	18	17	15	94	85	56	0.25	fog, rain
6	27	20	13	17	15	13	100	78	38	0	fog
7	27	21	16	18	17	16	94	75	42	0	
8	27	22	17	19	17	16	94	73	46	0	
9	27	22	17	19	18	16	100	85	53	0.25	fog, rain, storm
10	24	19	14	18	17	14	100	87	64	0	fog
11	24	19	15	16	15	13	100	76	46	0	rain, storm
12	24	18	11	14	12	10	100	69	38	0	rain, storm
13	25	18	10	15	13	9	94	71	43	0	
14	24	18	12	15	14	12	100	76	46	0	fog
15	24	19	14	16	14	13	100	74	42	0	
16	24	20	15	17	16	14	94	80	49	0	rain
17	23	19	15	17	15	13	100	75	47	0	rain
18	18	17	16	16	15	14	100	86	72	0	rain
19	17	16	15	16	16	14	100	92	80	0	rain, storm
20	23	20	16	18	17	16	100	89	58	0	fog
21	25	19	14	18	17	15	100	83	52	0	fog, rain
22	27	19	12	15	7	-2	100	50	11	0	
23	22	16	10	11	6	-2	87	53	18	0	
24	20	14	8	11	8	5	93	66	27	0	
25	23	16	9	12	9	8	94	71	31	0	
26	21	16	10	13	11	10	94	76	48	0	fog
27	24	17	8	15	12	9	100	79	40	0	fog
28	24	18	13	15	14	12	100	79	49	0	fog
29	24	17	11	16	13	10	100	79	44	0	fog
30	21	17	13	17	15	12	100	87	61	0	fog, rain

Table A-21: weather conditions in Milan, September 2014

2014	Temperature (°C)			Dew point (°C)			Relative humidity (%)			Precipitations (mm)	Events
Oct	high	avg	low	high	avg	low	high	avg	low	sum	
1	23	19	14	17	16	14	100	88	52	0	fog, rain
2	23	17	11	17	14	12	100	85	47	0	fog
3	23	17	12	15	13	12	100	77	38	0	fog
4	21	17	12	14	12	10	100	78	41	0	fog
5	21	16	11	13	12	11	100	79	49	0	
6	19	16	12	13	12	11	100	81	56	0	rain
7	15	13	12	14	13	10	100	94	84	0	rain
8	16	14	13	16	15	14	100	98	92	0	fog, rain
9	19	17	14	17	16	14	100	96	86	1.02	fog, rain
10	20	18	16	18	17	16	100	96	83	0.25	fog, rain
11	19	17	15	17	17	15	100	96	86	7.11	fog, rain
12	19	17	14	18	17	15	100	96	88	0.76	fog, rain
13	18	17	16	18	17	15	100	97	93	18.03	rain, storm
14	19	17	14	16	14	13	100	92	77	0.25	rain
15	22	17	13	15	13	12	100	82	49	0	
16	22	16	11	15	13	11	100	86	50	0	
17	23	18	12	15	14	12	100	80	43	0	
18	24	18	12	17	14	12	100	84	54	0	fog
19	23	18	13	18	16	13	100	89	65	0	fog
20	21	16	11	17	14	11	100	90	64	0	fog
21	22	18	13	16	15	13	100	87	62	0	fog
22	16	11	7	15	-3	-7	83	31	15	0	
23	21	12	3	1	-2	-5	65	31	14	0	
24	21	12	4	6	3	1	82	57	19	0	
25	16	11	5	10	8	4	100	83	55	0	
26	16	11	5	10	8	5	100	84	47	0	fog
27	14	8	2	8	6	2	100	78	52	0	fog
28	16	8	1	8	5	0	100	83	52	0	fog
29	14	8	1	7	4	2	100	84	51	0	fog
30	15	7	-1	9	5	0	100	85	54	0	fog
31	17	9	2	9	6	1	100	86	52	0	fog

Table A-22: weather conditions in Milan, October 2014

2014	Temperature (°C)			Dew point (°C)			Relative humidity (%)			Precipitations (mm)	Events
Nov	high	avg	low	high	avg	low	high	avg	low	sum	
1	18	10	2	10	6	2	100	85	45	0	fog
2	18	10	2	10	6	3	100	82	42	0	fog
3	15	9	4	12	10	4	100	90	66	2.03	rain
4	15	13	11	13	11	10	100	93	73	22.1	rain, storm
5	14	13	12	14	13	12	100	99	94	2.03	fog, rain
6	13	9	5	13	9	5	100	98	88	0.25	fog, rain
7	17	10	2	12	8	3	100	90	62	0.51	fog
8	18	12	6	12	9	6	100	85	45	0	fog
9	15	12	10	13	12	10	100	95	80	11.94	rain
10	12	11	10	13	11	10	100	99	94	28.96	rain
11	14	12	11	13	12	11	100	97	92	18.03	rain
12	14	12	10	14	12	10	100	97	93	22.1	rain
13	17	12	6	11	9	6	100	86	56	0	fog, rain
14	16	11	6	12	11	7	100	92	74	8.89	fog, rain
15	12	10	8	12	11	8	100	97	92	50.04	rain
16	16	10	4	10	7	4	100	88	51	0	fog, rain
17	10	8	6	9	8	6	100	97	92	7.11	rain, storm
18	13	7	1	8	5	2	100	88	49	0	fog, rain
19	12	6	0	8	4	0	100	91	60	0	fog
20	13	6	-2	8	3	-1	100	89	57	0	fog
21	11	5	-1	7	3	-1	100	87	62	0	fog
22	13	6	-1	6	3	-1	100	85	49	0	fog
23	13	7	0	7	4	0	100	89	57	0	fog
24	12	8	3	9	7	3	100	90	67	0	fog
25	13	7	2	10	8	0	100	94	77	0.51	fog, rain

Table A-23: weather conditions in Milano, November 2014